



# CLT Rib Panels by Stora Enso

## Structural design manual



|          |  |           |
|----------|--|-----------|
| <b>1</b> | <b>INTRODUCTION .....</b>  | <b>5</b>  |
| <b>2</b> | <b>PRODUCT DESCRIPTION .....</b>   | <b>5</b>  |
| 2.1      | Intended use .....   | 6         |
| 2.2      | Basic product information .....  | 7         |
| 2.3      | Basic dimensions and material .....  | 8         |
| 2.4      | Tolerances of dimensions .....   | 8         |
| 2.4.1    | Skewed end - Layout in plan view .....   | 9         |
| 2.5      | Support types .....  | 10        |
| <b>3</b> | <b>CREEP AND DURATION OF LOAD.....</b>   | <b>12</b> |
| 3.1      | Partial factors for the material properties loads and load combinations and factors for load duration and moisture content ..... | 12        |
| 3.2      | Partial factors for loads and load combinations .....  | 13        |
| 3.3      | Factors accounting for the load duration and moisture content .....  | 13        |
| 3.3.1    | Modification factor $k_{mod}$ .....  | 13        |
| 3.3.2    | Deformation factor $k_{def}$ .....   | 14        |
| 3.4      | Dimensional stability of rib/box panels .....  | 14        |
| 3.5      | Size effect parameter.....   | 15        |
| <b>4</b> | <b>DESIGN PRINCIPLES.....</b>  | <b>16</b> |
| 4.1      | Limit states principle .....   | 16        |
| 4.2      | Design values .....  | 16        |
| 4.3      | Design loads .....   | 16        |
| <b>5</b> | <b>CROSS-SECTION PROPERTIES.....</b>   | <b>17</b> |
| 5.1      | Effective cross section .....  | 17        |
| 5.2      | Definition of the effective width $b_{ef}$ (per rib).....  | 18        |
| 5.3      | Effective width for different loadings.....  | 19        |
| 5.3.1    | Effective width $b_{ef}$ for continuously (uniformly) distributed loads (at midspan) .....                                       | 19        |
| 5.3.2    | Effective width $b_{ef}$ for rib panels under single point loads at the support.....   | 21        |
| 5.3.3    | Effective width for rib panels at a support (Rolling shear) .....  | 22        |
| 5.4      | Effective bending stiffness .....  | 23        |
| 5.5      | Effective shear stiffness.....   | 25        |
| <b>6</b> | <b>ULTIMATE LIMIT STATE (ULS) DESIGN – LOAD COMBINATIONS.....</b>  | <b>27</b> |
| <b>7</b> | <b>BENDING RESISTANCE.....</b>   | <b>28</b> |
| 7.1      | Flexural stresses parallel to grain in the section .....   | 28        |
| 7.2      | Normal stresses from axial force.....  | 31        |
| 7.2.1    | Tension parallel to the grain.....   | 31        |
| 7.2.2    | Compression parallel to the grain.....   | 31        |
| 7.3      | Bending strength parallel to grain.....  | 32        |
| 7.4      | Tensile strength parallel to grain .....   | 32        |
| 7.5      | Compressive strength parallel to grain .....   | 33        |
| 7.6      | Members subjected to combined bending and axial compression or tension .....   | 34        |
| 7.6.1    | Combined bending and axial compression .....   | 34        |
| 7.6.2    | Combined bending and axial tension .....   | 34        |
| 7.7      | Stability of CLT Rib Panels .....  | 35        |
| 7.7.1    | Stability – buckling of columns subjected to either compression or combined compression and bending                              | 35        |



|           |   |           |
|-----------|---|-----------|
| 7.7.2     | Stability – lateral torsional buckling (LTB) of beams subjected to either bending or combined bending and compression ..... | 36        |
| <b>8</b>  | <b>SHEAR RESISTANCE .....</b>   | <b>38</b> |
| 8.1       | Calculation of shear stresses .....   | 39        |
| 8.1.1     | Simplified approximation .....  | 40        |
| 8.2       | Shear stress verification .....   | 41        |
| 8.2.1     | Shear parallel to grain .....   | 41        |
| 8.2.2     | Rolling shear: (shear perpendicular to grain) .....   | 42        |
| 8.3       | Shear of the glue line .....  | 42        |
| 8.4       | In-plane shear stress in CLT panels .....   | 43        |
| 8.4.1     | Representative Volume Element (RVE) .....   | 44        |
| 8.4.2     | ULS verifications for shear force $n_{xy}$ .....  | 45        |
| 8.4.3     | In plane shear in the net section of CLT .....  | 50        |
| 8.4.4     | In plane torsional shear in the glue line of the face gluing of CLT .....   | 50        |
| <b>9</b>  | <b>VOIDS IN THE GLULAM RIB .....</b>  | <b>51</b> |
| 9.1       | Verification of tension force perpendicular to grain (splitting) .....  | 53        |
| 9.2       | Verification of shear stresses for circular and rectangular holes in beams .....  | 55        |
| 9.3       | Verification of longitudinal stresses – Bending .....   | 55        |
| <b>10</b> | <b>VOIDS IN THE CLT PANEL .....</b>   | <b>56</b> |
| <b>11</b> | <b>VERIFICATION AT THE SUPPORTS .....</b>   | <b>57</b> |
| 11.1      | Simple supports with blockings .....  | 57        |
| 11.1.1    | Bearing pressure transferred through the ribs .....   | 57        |
| 11.1.2    | Bearing pressure transferred through the blocking .....   | 59        |
| 11.1.3    | $k_{c,90}$ values for CLT .....   | 61        |
| 11.2      | Supports with ribs supported individually or by mechanical joints .....   | 64        |
| 11.2.1    | End beam support .....  | 64        |
| 11.2.2    | Support with individually supported ribs .....  | 65        |
| 11.2.3    | Support with ribs supported by mechanical joints .....  | 65        |
| 11.3      | Suspended support with cut-back ribs .....  | 66        |
| <b>12</b> | <b>CONNECTION BETWEEN PANELS AND ADJACENT STRUCTURES - STRUCTURAL BEHAVIOR OF CLT RIB PANEL DIAPHRAGMS .....</b>            | <b>69</b> |
| 12.1      | Longitudinal joints of CLT rib panels .....   | 69        |
| 12.1.1    | Ribs at the edges of the plate .....  | 69        |
| 12.1.2    | Stepped profile of the CLT plate .....  | 70        |
| 12.2      | Verification with stepped profile of the plate .....  | 71        |
| 12.3      | Vertical forces at the longitudinal edges .....   | 71        |
| 12.3.1    | Incompatible deformations between CLT rib panels supported on 3 and 2 edges respectively .....                              | 73        |
| 12.3.2    | Comparable specifications .....   | 74        |
| 12.3.3    | Summary .....   | 74        |
| 12.4      | Horizontal forces at the longitudinal edges .....   | 74        |
| 12.4.1    | Horizontal shear along the longitudinal joints .....  | 77        |
| a)        | In-plane shear stress in CLT panels .....   | 77        |
| 12.4.2    | Number of fasteners required to carry the shear force .....   | 77        |
| 12.4.3    | Determination of the limiting moment in a longitudinal joint of a diaphragm .....   | 78        |
| <b>13</b> | <b>SERVICEABILITY LIMIT STATES .....</b>  | <b>82</b> |
| 13.1      | Deformation .....   | 82        |

|           |   |            |
|-----------|---|------------|
| 13.1.1    | Introducing the creep coefficient $k_{def}$ in a hybrid system.....   | 84         |
| 13.2      | Vibration.....  | 86         |
| 13.3      | Vibration - future design method [23] .....   | 89         |
| 13.3.1    | 1 <sup>st</sup> natural frequency $f_1$ .....   | 89         |
| 13.3.2    | Deflection due to 1 kN single load in the most unfavourable position on the floor (stiffness criterion) .   | 89         |
| 13.3.3    | Design procedure for transient floors → when $f_1 \geq 8$ Hz.....   | 90         |
| 13.3.4    | Design procedure for resonant floors → when $f_1 < 8$ Hz.....   | 92         |
| 13.3.5    | Floor damping values .....  | 92         |
| 13.3.6    | Floor performance levels and corresponding vibration criteria .....   | 93         |
| 13.3.7    | Recommendations for the choice of the floor performance level.....  | 93         |
| <b>14</b> | <b>SAFETY IN CASE OF FIRE.....</b>  | <b>94</b>  |
| 14.1      | Reaction to fire .....  | 94         |
| 14.2      | Resistance to fire of CLT Rib Panels based on calculations according to EN 1995-1-2:2011 (Eurocode 5)   | 94         |
| 14.3      | Verification method for actions in the fire situation according to EN 1995-1-2:2011 .....   | 95         |
| 14.4      | Verification method for mechanical resistance in the fire situation according to EN 1995-1-2:2011 ....  | 96         |
| 14.5      | Design stiffness values .....   | 96         |
| 14.6      | Charring rates of CLT Rib Panel by Stora Enso .....   | 96         |
| 14.6.1    | Design value of charring rates for surfaces which are unprotected throughout the time of fire exposure  | 97         |
| 14.6.2    | Design value of charring rates for surfaces which are initially protected from exposure to fire by protective gypsum plasterboard (following the rib section in case of Open type, or mounted on the bottom side of a CLT rib panel in case of Inverted or Closed type) ..... | 98         |
| 14.6.3    | Start of charring on initially protected components .....   | 102        |
| 14.6.4    | Failure time of fire protective claddings .....   | 103        |
| 14.6.5    | Charring for surfaces, initially protected from fire exposure with protective layers, installed horizontally below ribs (void cavities), in case of a CLT Rib Panel Open type.....  | 105        |
| 14.6.6    | Charring for surfaces initially protected from fire exposure with protective layers installed horizontally below ribs (cavities filled with insulation) in case of a CLT Rib Panel Open type .....  | 105        |
| 14.7      | Determining the load-bearing capacity (R) of CLT Rib Panels elements according to EN 1995-1-2:2011  | 106        |
| 14.7.1    | Reduced cross-section method.....   | 106        |
| <b>15</b> | <b>FIRE PERFORMANCE.....</b>  | <b>109</b> |
| <b>16</b> | <b>STRUCTURAL ANALYSIS IN FIRE SITUATION.....</b>   | <b>110</b> |
| 16.1      | Effective bending stiffness after fire.....   | 110        |
| 16.2      | Flexural rigidity in fire situation.....  | 111        |
| 16.3      | Flexural stress parallel to grain in the section.....   | 111        |
| 16.3.1    | Flexural stresses verification in fire situation .....  | 113        |
| 16.4      | Bending strength parallel to grain in fire situation .....  | 115        |
| 16.5      | Tensile strength parallel to grain in fire situation.....   | 116        |
| 16.6      | Compressive strength parallel to grain in fire situation.....   | 117        |
| 16.7      | Shear stresses distribution in the section after fire.....  | 118        |
| 16.7.1    | Point location and width for shear design after charring.....   | 118        |
| 16.8      | Calculation of shear stresses in fire situation.....  | 120        |
| 16.9      | Shear stress verification in fire situation .....   | 120        |
| 16.9.1    | Shear parallel to grain.....  | 120        |
| 16.9.2    | Rolling shear: (shear perpendicular to grain).....  | 121        |
| 16.10     | Load bearing of the CLT section between ribs (spanning in cross direction) .....  | 122        |
| <b>17</b> | <b>FIRE CLASSIFICATIONS.....</b>  | <b>124</b> |



# CLT Rib Panels

**18 ACOUSTIC PERFORMANCE..... 128**

**19 REFERENCES ..... 130**



## 1 Introduction

When using CLT Rib Panels by Stora Enso, an increase in stiffness of roofs and floors is possible with low material consumption and consequently an increase of the spans. The CLT panels are arranged with their outer layers in parallel to the direction of span. The ribs consist of glued-laminated timber and are rigidly connected (structural gluing) with the CLT panel at the factory under controlled conditions by screw-press gluing. Thereby, from a static point of view, each of the ribs forms a T or I-cross-section with its associated effective part of the CLT panel.

Between the ribs, installations can be inserted, or acoustic panels arranged. Mounting of the CLT Rib Panels by Stora Enso is undertaken either by direct positioning of the ribs on a transverse supporting beam or on a wall cut out in the form of the ribbed cross-section, by mounting on transverse end beams or by mounting of the sufficiently dimensioned plate with notched ribs. If the ribs are notched, then detachment of the ribs from the panel shall be avoided by mandatory reinforcement with vertically arranged screws as close to the rib end as possible. The screws shall be designed for end reaction forces with the given guidelines.

With respect to the economic spans, there shall be a differentiation between roofs and floors, since normally higher loads act on floors and, in addition to the deflection requirements, vibration requirements shall also be fulfilled.

## 2 Product description

The present design manual is made to cover the design of three CLT Rib Panel types that Stora Enso provides presented in 2.2 with single span solutions. The document is intended to be used by structural engineers responsible for the task, according to the laws of the Member States (MS).

CLT Rib Panel by Stora Enso is covered by the ETA-20/0893 [1]. CLT Rib Panels by Stora Enso are composite slab elements consisting of Stora Enso Cross Laminated Timber (CLT) according to ETA-14/0349 [2] as panel stiffened out of plane by Glued Laminated Timber (GLT) ribs according to EN 14080 in the direction of the span. These two components are assembled by structural gluing. The cover layers of the CLT shall have same grain orientation as the glulam rib. CLT Rib Panels by Stora Enso contain screws to create gluing pressure or to fix secondary construction elements, but they do not have an influence on the composite effect.

The adhesive used for the interface (connections between CLT-slab and ribs) of CLT rib panels is a one component polyurethane adhesive as defined in EN 15425 or a MUF adhesive according to EN 301 and of type I according to EN 15425 or EN 301. The adhesive is approved for gluing of load-bearing structures.

Glued laminated timber, CLT and LVL may be used for blockings at supports. The materials, dimensions and tolerances are given in Annex 1.

## 2.1 Intended use

CLT Rib Panels by Stora Enso are intended to be used as structural or non-structural elements in buildings. The panels shall have single span supported at the ends.

The panels are intended to be used subject to static or quasi-static actions only. In seismic areas the behavior factor of CLT rib panels used for the design is limited to non-dissipative or low-dissipative structures ( $q \leq 1,5$ ), defined according to Eurocode 8 (EN 1998-1:2004 clauses 1.5.2 and 8.1.3 b) and applicable national rules on construction works.

With regard to moisture behavior of the product, the product shall be used in service classes 1 and 2, according to EN 1995-1-1 [3]. The product shall not be used in use class 3 (3.1 exterior, above ground, protected; occasionally wet).

From the mechanical point of view CLT Rib Panels can be regarded as load-carrying members with a pronounced orthotropic behavior. An overview of the system and the system components is given Figure 2-a. The components in the cross section can be arranged in different ways with the CLT element above and below the ribs as well as on both sides as boxed cross section resp. Figure 2-d.

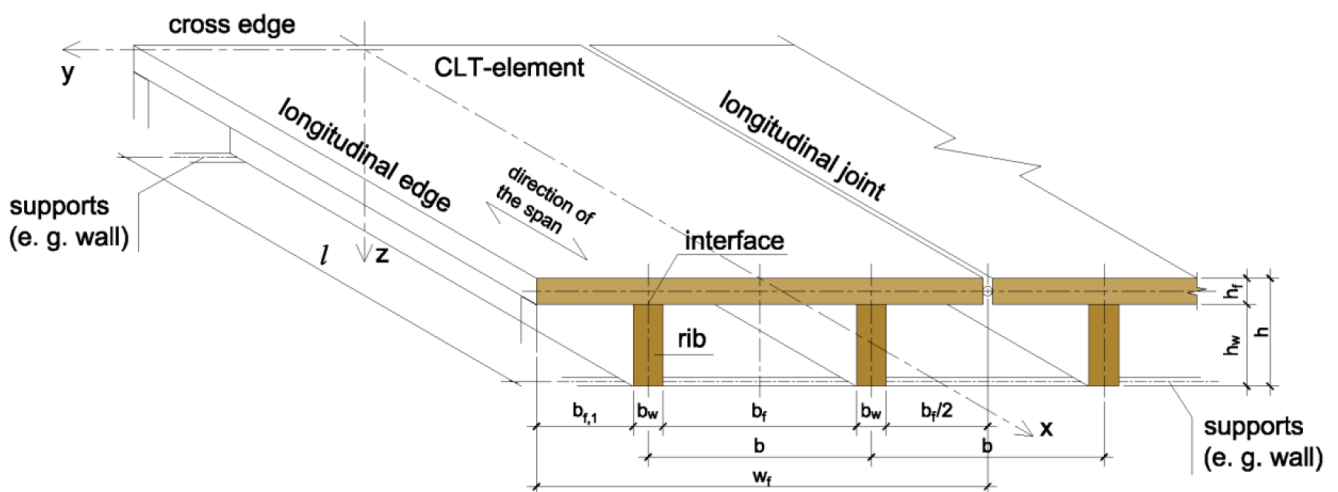


Figure 2-a: Overview of the system components of CLT Rib Panels

## 2.2 Basic product information

CLT rib panels are a factory-made structural component. They are made from a CLT by Stora Enso panel (Cross Laminated Timber) and a glued laminated timber rib. The panel and the rib are glued together, and the pressure is being applied by a screw-glue application. Figure 2-b, Figure 2-c and Figure 2-d show the different options for rib or box panels. Support types are presented in chapter 2.5.

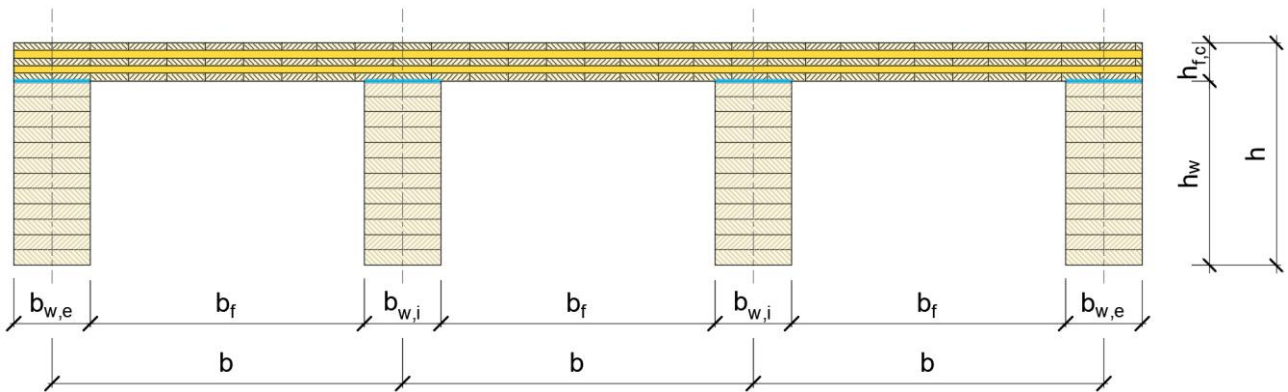


Figure 2-b: Open CLT Rib Panel – CLT above the ribs

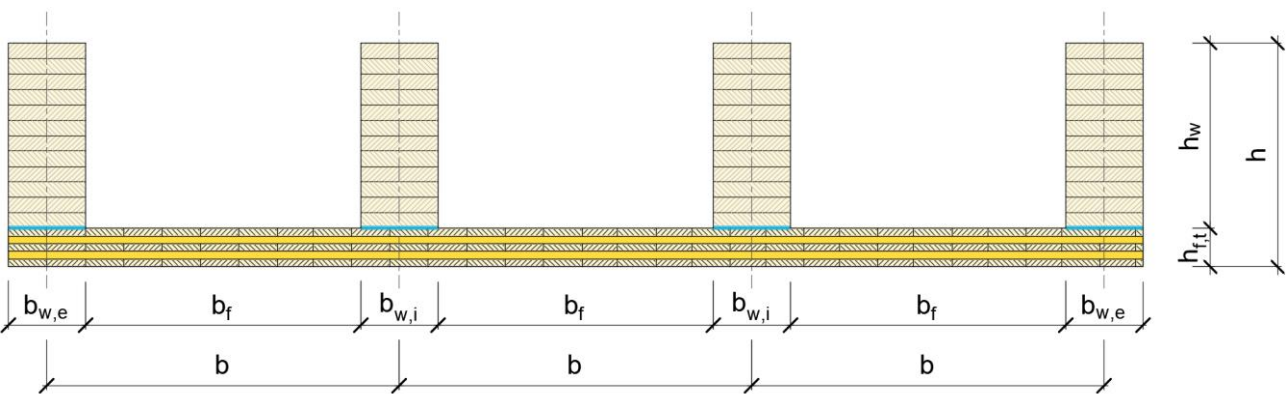


Figure 2-c: Inverted CLT Rib Panel – CLT below the ribs

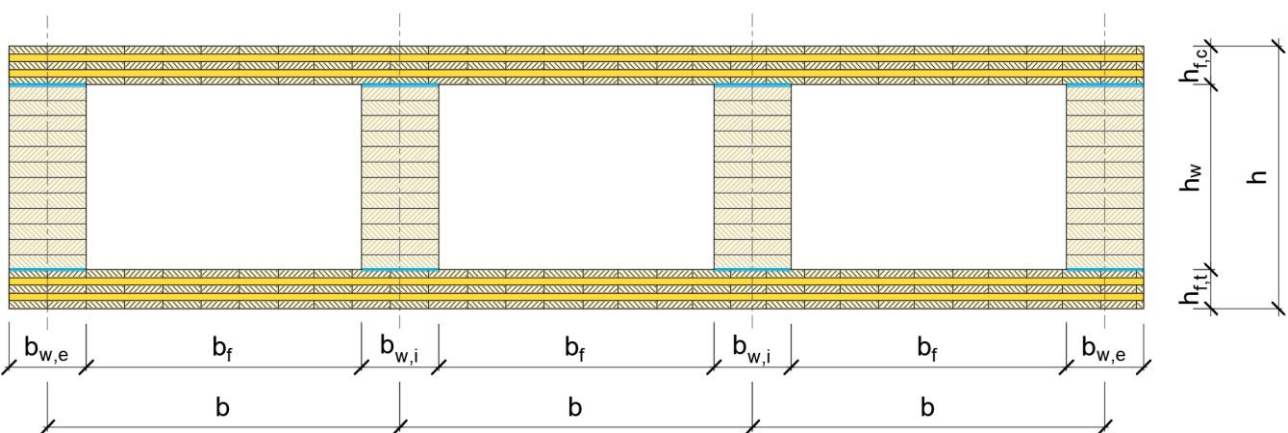


Figure 2-d: Closed CLT Rib Panel – CLT above & below the ribs

## 2.3 Basic dimensions and material

The CLT panels shall be Cross Laminated timber from Stora Enso, according to ETA-14/0349 [2].

All CLT panels that are covered by the ETA shall be a valid component for a CLT Rib Panel.

One CLT Rib Panel element is limited in size by the element size of a Stora Enso CLT panel and the layer composition shall be according to ETA-14/0349.

The thickness of the CLT shall be in a range between 60 mm and 200 mm.

Typical length of the product is 5 m to 16,5 m. The thickness of the CLT panel used for CLT Rib Panel is from 60 mm to 200 mm;

Minimum GLT rib cross section dimensions are a height of 100 mm and width of 60 mm. All other boundary conditions on shape and size are given Table 2-1.

Table 2-1: Standard dimensions of CLT Rib Panel

|  |                                     |
|--|-------------------------------------|
| Span $l$   | 5,0 to 16,5 m                       |
| Width top cord, $b_{f,t,tot}$ / width bottom cord, $b_{f,b,tot}$ | < 3500 mm                           |
| Height top cord, $h_{f,t}$ / height bottom cord, $h_{f,b}$       | 60 – 200 mm                         |
| Material top/bottom cord <sup>1</sup>                            | C16, C24, C30                       |
| Depth rib, $h_w$   | > 100 mm                            |
| Width rib, $b_w$   | > 60 mm                             |
| Material rib <sup>2</sup>  | GL 20h – GL 32h and GL 20c – GL 32c |
| Rib spacing, $b$   | variable                            |

## 2.4 Tolerances of dimensions

Tolerances of dimensions at the reference moisture content of  $10 \pm 2\%$  are presented in Table 2-2.

Table 2-2: Tolerances of CLT Rib Panels by Stora Enso.

| Dimension                   |                                    | Tolerance, mm or % |
|-----------------------------|------------------------------------|--------------------|
| Depth                       | $h_w (=h_{rib}) \leq 400\text{mm}$ | -2 / +4 mm         |
|                             | $h_w (=h_{rib}) > 400\text{mm}$    | -0.5%·h / +1%·h    |
| Width of the CLT Rib Panel  |                                    | -2 / +2 mm         |
| Length of the CLT Rib Panel |                                    | $\pm 5$ mm         |

<sup>1</sup> According to ETA-14/0349 [2]

<sup>2</sup> According to EN 14080 [13]



## 2.4.1 Skewed end - Layout in plan view

All given layout recommendations are only valid for CLT Rib Panels with ribs, oriented parallel to the direction of the CLT cover layer.

CLT Rib Panels may be used in all kinds of plan layouts. Still, they are usually used for rectangular layouts.

If the axis between the longitudinal direction of skewed panels and the supporting line is  $\alpha \geq 70^\circ$  (Figure 2-e), the influence of the skewness can be neglected. The span of the system can be considered as the distance perpendicular to the supporting lines.

In all other cases the influence of the supporting conditions shall be analysed more detailed, by means of special methods (e. g. FEM).

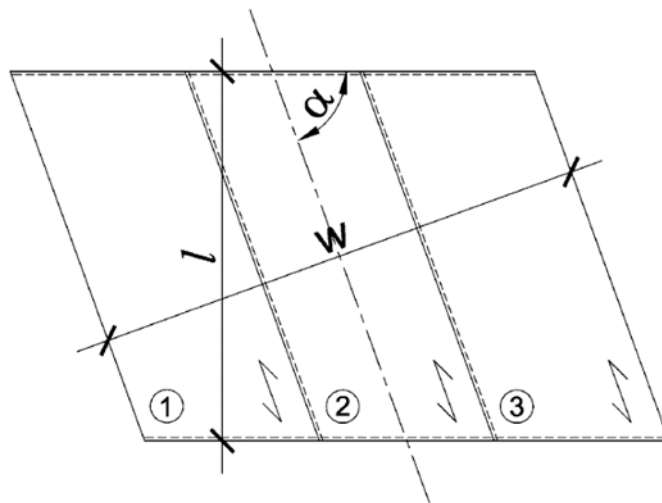


Figure 2-e: CLT rib panels with skew cut layout in plan view

For layouts with an irregular shape, the design shall be done using the longest distance between supporting lines as span. This shall be always measured parallel to the ribs (Figure 2-f). As alternative, the design by means of special methods (e. g. FEM) is recommended.

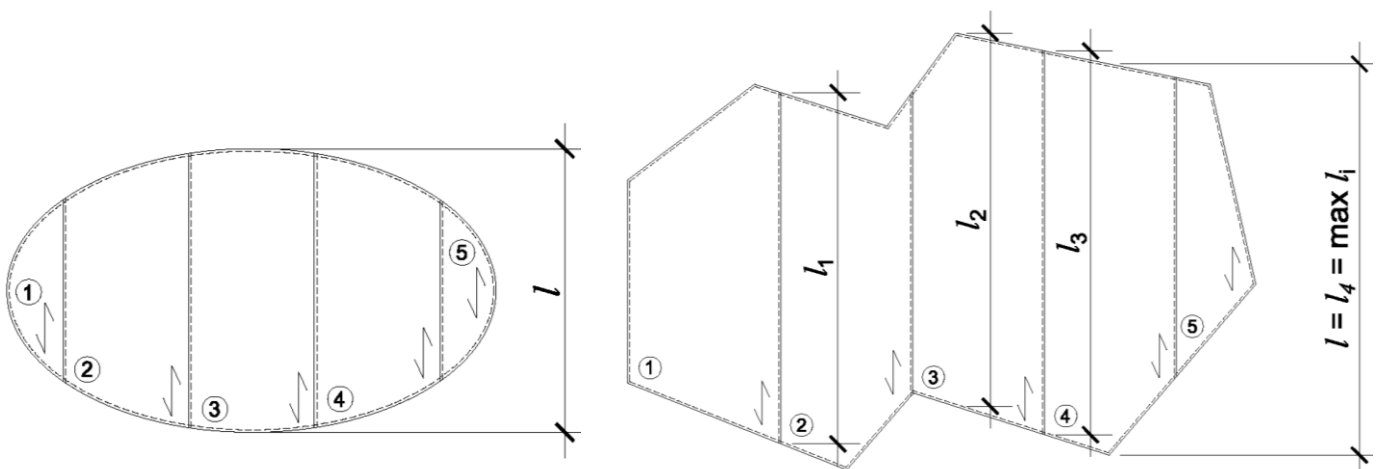


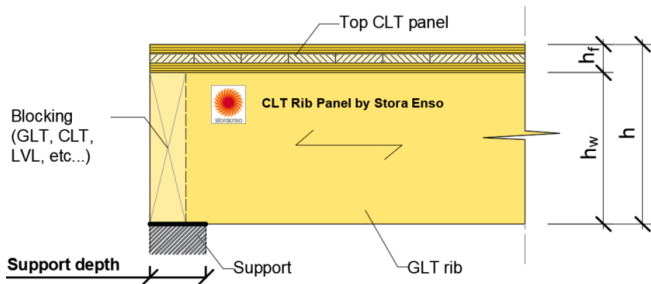
Figure 2-f: Plates with elliptical (left) and irregular shape (right)

## 2.5 Support types

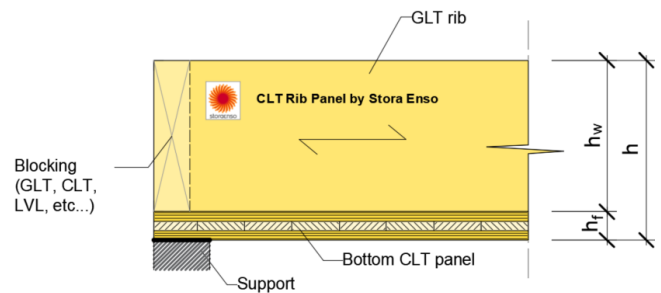
CLT Rib Panels can be supported in different ways depending on the structural detailing which influence the type of verification at the supports.

Basic support types are presented in the Figure 2-g.

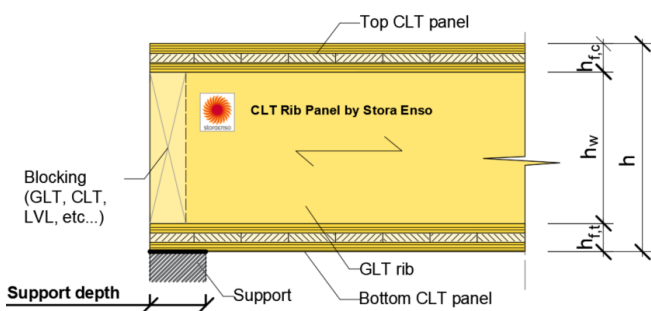
### Open CLT Rib Panel - Simple support



### Inverted CLT Rib Panel - Simple support



### Closed CLT Rib Panel - Simple support



### Open CLT Rib Panel - End beam support

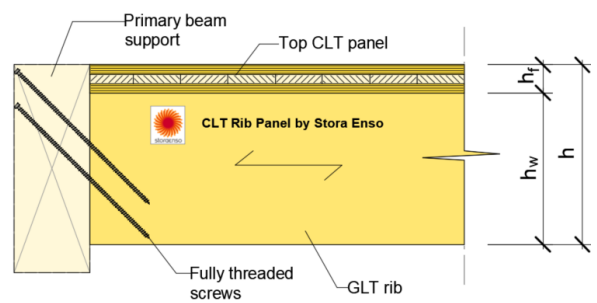


Figure 2-g: Basic support types

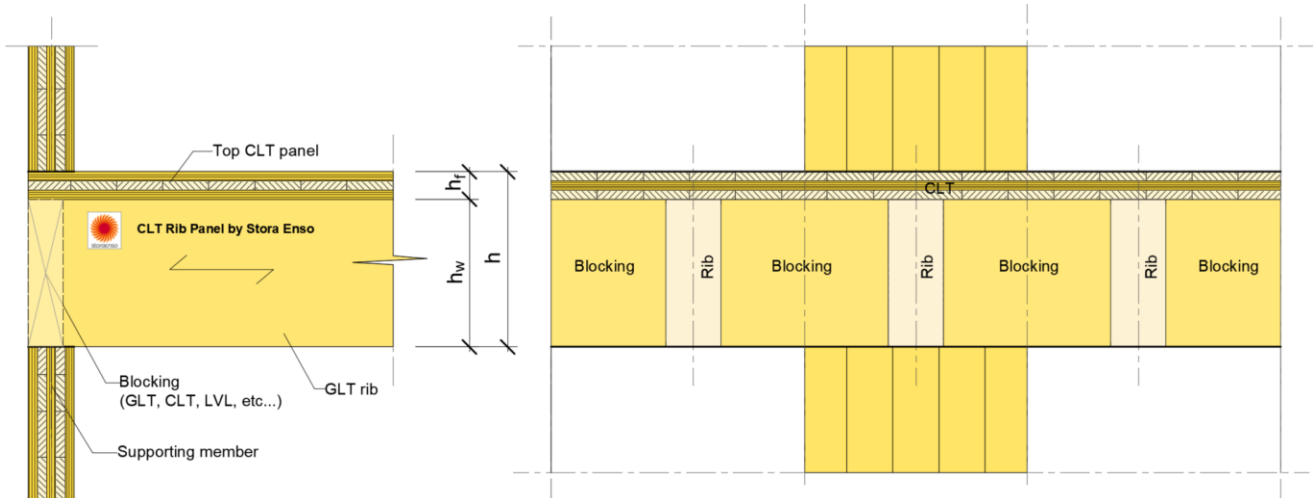


Figure 2-h: Continuous simple support with blockings

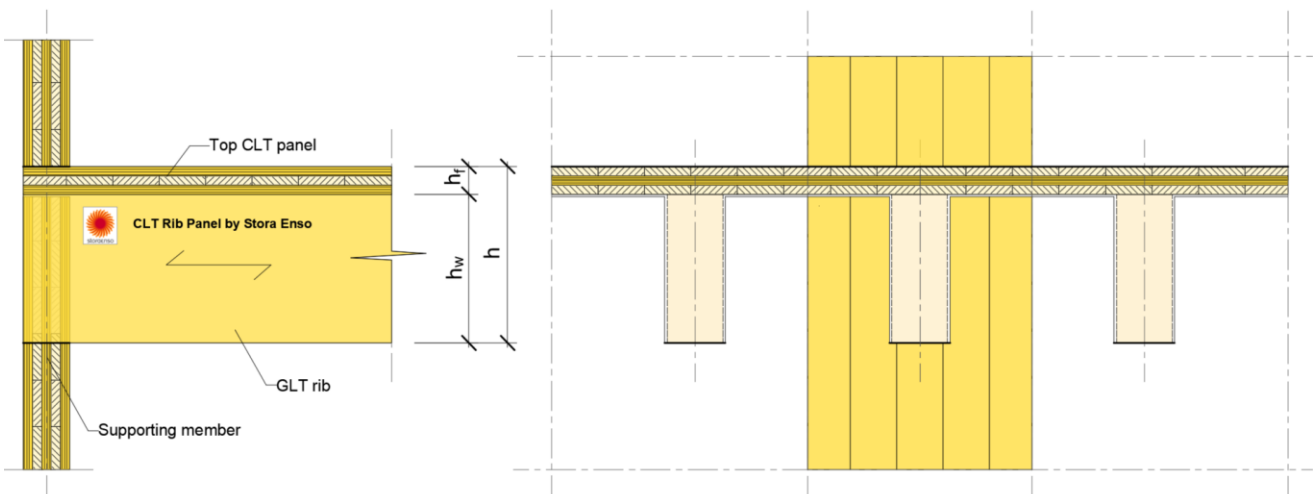


Figure 2-i: Individually supported ribs- Simple support

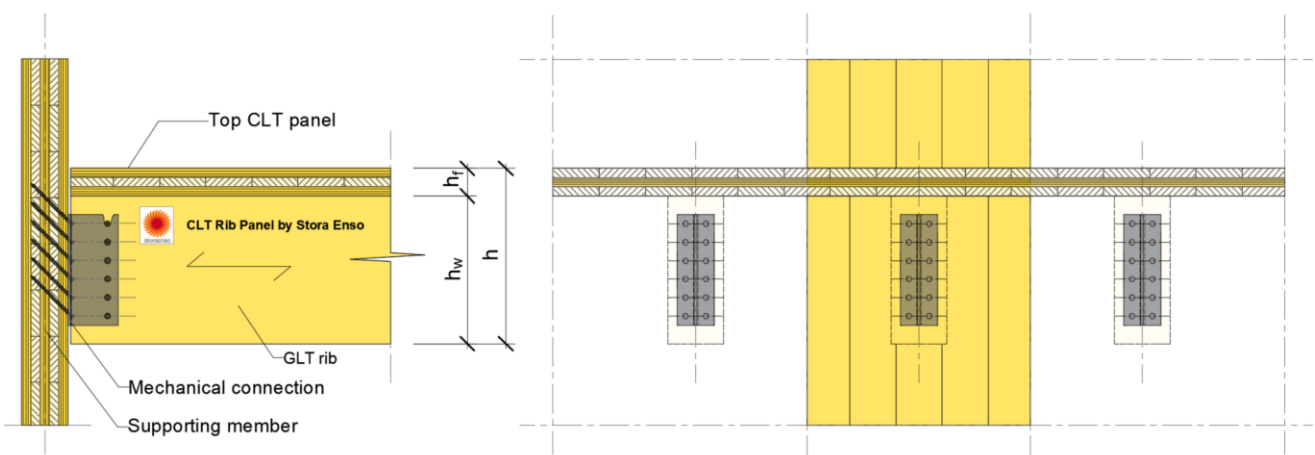


Figure 2-j: Ribs supported by mechanically fixed connection - Concealed bracket connection

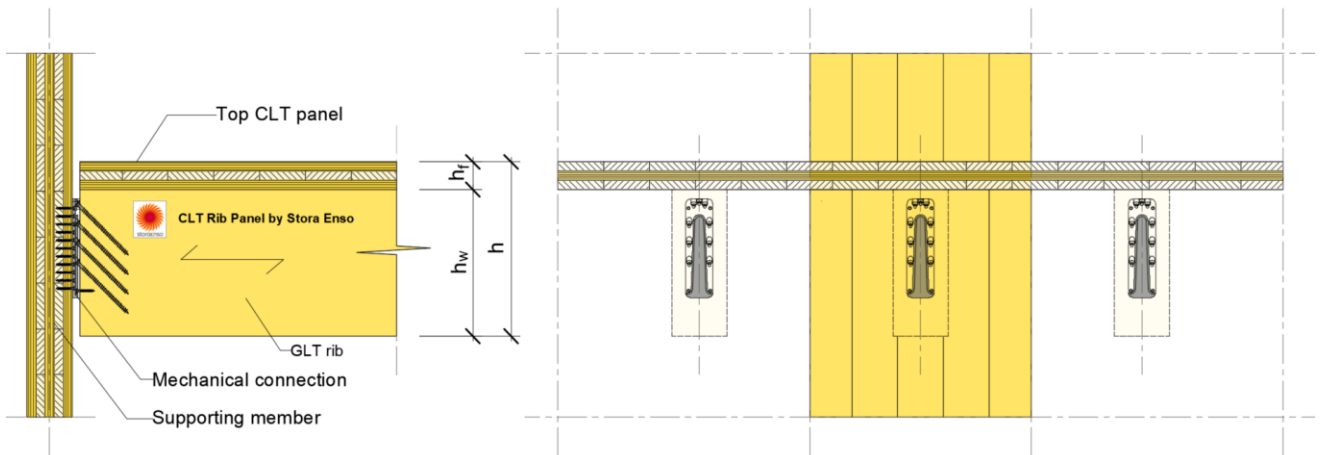


Figure 2-k: Ribs supported by mechanically fixed connection - Concealed hook connection

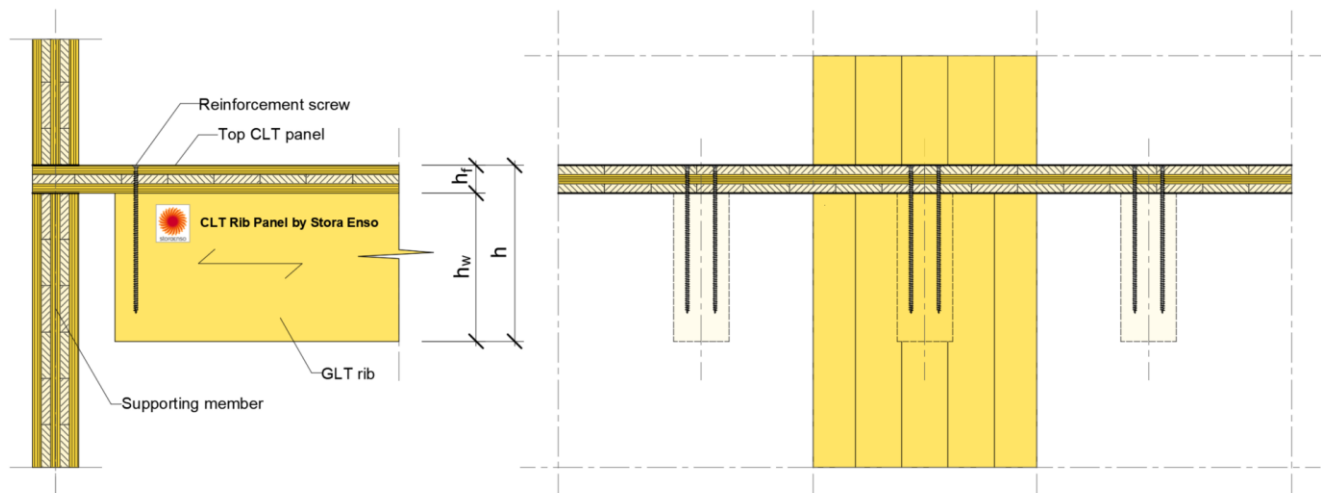


Figure 2-l: Cut-back (notched) ribs – Suspended support

### 3 Creep and duration of load

#### 3.1 Partial factors for the material properties loads and load combinations and factors for load duration and moisture content

The partial factor for CLT and the Glued Laminated Timber for the ribs shall be according to EN1995-1-1 [3] and the applicable NA.

The recommended partial factor for both components of CLT Rib Panels is:

$$\gamma_M = 1.25$$

## 3.2 Partial factors for loads and load combinations

The design value  $E_d$  for the effects of actions shall be calculated using EN 1990 and its national annexes. Partial factors for loads, load combinations and for different consequence classes are taken from the appropriate national annex.

## 3.3 Factors accounting for the load duration and moisture content

The moisture content and the load duration shall be taken according to the appropriate national annex.

The modification factors for strength  $k_{mod}$  and deformation  $k_{def}$  shall be according to EN1995-1-1 [3] and the applicable NA. A recommendation is given in the tables below:

In Table 3-1, values for  $k_{mod}$  and in Table 3-2, values for  $k_{def}$  can be found.

Table 3-1: Load-duration class and load types.

| Load-duration class | Action time of the load | Load                                 |
|---------------------|-------------------------|--------------------------------------|
| Permanent           | More than 6 months      | Self-weight, imposed load Category E |
| Medium-term         | 10 minutes - 6 months   | Imposed floor load, snow             |
| Short term          | Less than 1 week        | Snow                                 |
| Instantaneous       | Below 10 minutes        | Wind, accidental load                |

### 3.3.1 Modification factor $k_{mod}$

Table 3-2: Strength modification factor  $k_{mod}$ .

| Service class | CLT and GLT         |                  |                    |                   |                      |
|---------------|---------------------|------------------|--------------------|-------------------|----------------------|
|               | Load-duration class |                  |                    |                   |                      |
|               | Permanent action    | Long term action | Medium term action | Short term action | Instantaneous action |
| 1             | 0.6                 | 0,70             | 0.8                | 0,90              | 1.10                 |
| 2             | 0.6                 | 0,70             | 0.8                | 0,90              | 1.10                 |
| 3             | -                   | -                | -                  | -                 | -                    |

If a load combination consists of actions belonging to different load-duration classes, a value of  $k_{mod}$  should be chosen which corresponds to the action with the shortest duration.



### 3.3.2 Deformation factor $k_{def}$

Table 3-3: Values of the deformation factor  $k_{def}$  of the components of CLT Rib Panels.

|                        | Service class |      |   |
|------------------------|---------------|------|---|
|                        | 1             | 2    | - |
| CLT                    | 0.80          | 1.00 | - |
| Glued Laminated Timber | 0.60          | 0.80 | - |

Deformation factors  $k_{def}$  consider the influence of load-duration (creep) and moisture influences on deformations.

Recommended values for the components of CLT rib panels are given in Table 3-3.

The majority of the flexural rigidity originates from the Glued Laminated Timber ribs. Therefore, the simplification of applying a uniform  $k_{def}$  to the entire system is allowed. In that case a mean  $k_{def}$  shall be calculated as follows:

$$k_{def} = \sqrt{k_{def,GLT} \cdot k_{def,CLT}} \quad \text{Eq. 3-1}$$

The deformation factors for CLT Rib Panels computed with the simplification are listed in Table 3-4.

Table 3-4: Recommended values for the deformation factor simplified  $k_{def}$  of CLT rib panels

|               | Service class |      |   |
|---------------|---------------|------|---|
|               | 1             | 2    | - |
| CLT Rib Panel | 0.70          | 0.90 | - |

However, a more precise result will be obtained, by applying the  $k_{def}$  factor to each individual layer (section component), as demonstrated in the analysis sample [5]. See chapter 13.1.1 deflection calculations.

The service classes are defined in EN 1995-1-1 [3]. Service class 1 means that the structure is in warmed indoors conditions where the moisture content corresponds mainly to a temperature of 20 ° C and the relative humidity of air exceeds 65 % only for a few weeks per year.

### 3.4 Dimensional stability of rib/box panels

The swelling and shrinkage behavior due to change in moisture content of CLT rib/box panels relates to the swelling and shrinkage behavior of the base material.

When manufactured, the moisture content of the components is below the equilibrium value in use conditions. Due to changing temperature and relative humidity of the surrounding air, the moisture content of CLT Rib Panel by Stora Enso will continuously change.

CLT Rib Panels should not unnecessarily be exposed to climatic conditions (e. g. during the transport and the assembling) which are more severe than those expected in the finished structure.

The swelling and shrinkage values in % per % change of moisture content are given in Table 3-5. They shall be used to determine the dimensional changes of the CLT Rib Panel.

A recommendation is given from EN1995-1-1 [3], Austrian NA (Table NA.3.1-E1):

Table 3-5: Swelling and shrinkage coefficients in different direction of CLT and GLT in % per % change of moisture content.

| Type of timber and species | Swelling and shrinkage in percent per percent change in moisture content |  |
|----------------------------|--|--|
|                            | Perpendicular to the grain or to the panel surface                       | Parallel to the grain or in the plane of a panel |
| GLT (spruce, pine)         | 0,24   | 0,01   |
| CLT (spruce, pine)         | 0,24   | 0,02 – 0,04                                      |

Between production and completion of the structure, CLT rib panels should not unnecessarily be exposed to climatic conditions, more severe than those, expected in the finished structure.

The design rules in EN 1995-1-1 as well as the following design recommendations assume that deviations of members from the straightness, measured between the supports, should be limited to 1/500 times the length of the element. Higher values of deformation must be considered in the structural analysis of the CLT rib elements.

### 3.5 Size effect parameter

The effect of the size for glued laminated timber shall be taken into consideration for the ribs with a height  $h < 600$  mm in the design (EN 1995-1-1, item 3.3) [3].

For member in bending the characteristic value for  $f_{m,0,k}$  and  $f_{t,0,k}$  shall be multiplied by the factor

$$k_h = \min \left\{ \left( \frac{600}{h} \right)^{0,1} \right. \\ \left. 1.1 \right. \quad \text{Eq. 3-2}$$

$h$  is the height of the member [mm]

## 4 Design principles

### 4.1 Limit states principle

The structural performance of CLT rib panels shall be verified in accordance with the limit state design principles and rules specified in the Eurocodes. In general, the calculation method regarding the ultimate limit state (ULS) and serviceability limit state (SLS) shall be used according to EN 1995-1-1 [3].

If rules for the specific design of CLT Rib Panels are missing or are necessary, reference to the present design manual document shall be given.

The consequence class according to EN 1990 [6] for CLT Rib Panels are CC1 and CC2.

According to EN 1990, the following equation for the property under consideration shall be fulfilled:

$$E_d \leq R_d \quad \text{Eq. 4-1}$$

where

$E_d$  is the design value of the effect of actions

$R_d$  is the design value of the corresponding resistance

The slab is bearing dead load, imposed load and snow load. The consequence class could be CC1 and CC2. The slab is designed according to Eurocode 5 [3] and appropriate national annex.

### 4.2 Design values

The design values are calculated as

$$X_d = k_{mod} \cdot \frac{X_k}{\gamma_M} \quad \text{Eq. 4-2}$$

with

$X_d$  design strength

$X_k$  characteristic strength

$k_{mod}$  modification factor

$\gamma_M$  partial safety factor

Note:

The determination of the design value may be complemented by the consideration of other factors (e. g. for the consideration of height  $k_h$  and others). See chapter 3.5.

### 4.3 Design loads

Actions to be used in the design may be obtained from the relevant parts of EN 1991 [7]. CLT rib panels shall be used for static and quasi-static actions only.

Combinations of actions shall be considered acc. to EN 1990.

Assignments to a load-duration class shall be made acc. to EN 1995-1-1 [3], section 2.3.1.2.

## 5 Cross-section properties

Due to shear deformations of the flange, complex and non-linear stresses in the cross-section of CLT Rib Panels occur. Therefore, some assumptions – regarding a plane cross-section don't comply with the commonly used method in practice (Technical Bending Theory (TBT)). To overcome a complex design procedure, the concept of the effective width  $b_{ef}$  can be applied, making the application of the TBT possible.

In this chapter, approximation equations for the determination of the effective width  $b_{ef}$  of CLT Rib Panels are given. These equations were derived by means of data fitting of a more detailed model (See [8]) and lead to conservative results for  $b_{ef}$ .

### 5.1 Effective cross section

The cross-section of Open/Inverted type rib panels is divided into T and L section and for Closed type rib panels into C and I section - see Figure below. Each section should be calculated individually.

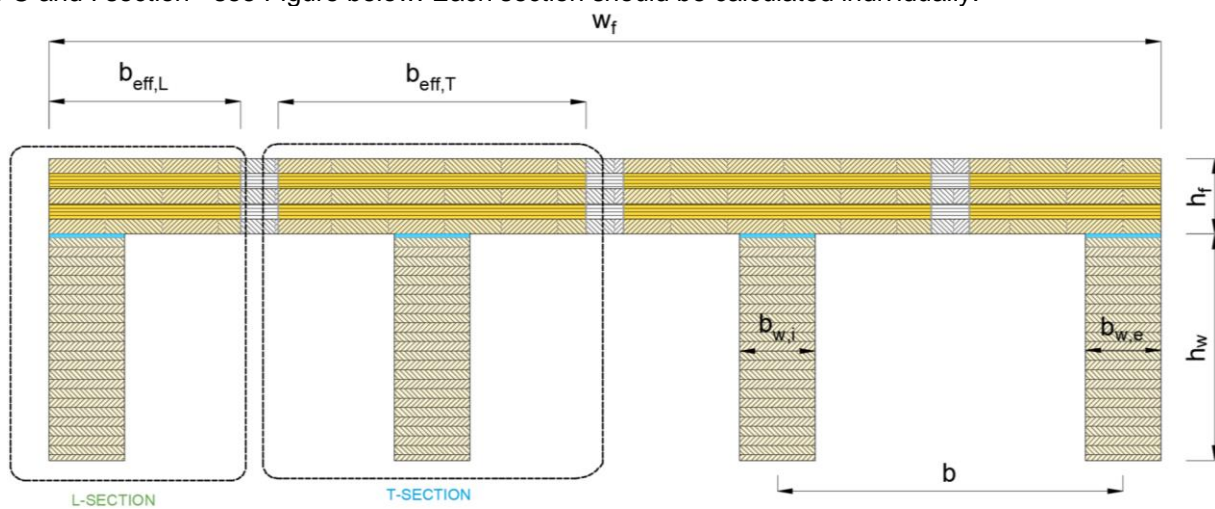


Figure 5-a: Open type CLT Rib Panel effective section

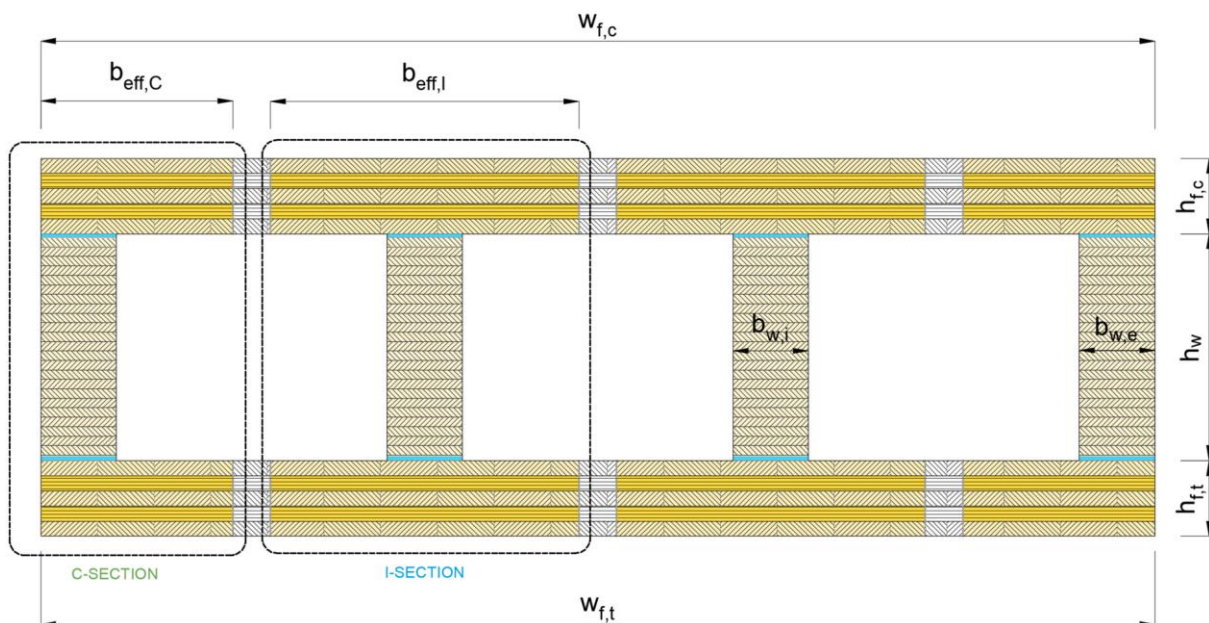


Figure 5-b: Closed type CLT Rib Panel effective section

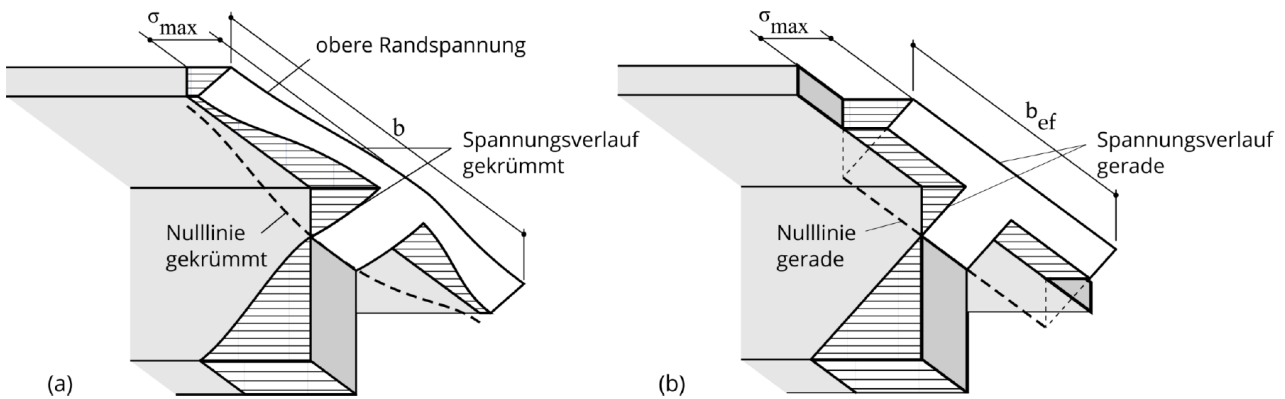


Figure 5-c: Effective width with (a) the actual stress distribution and (b) the linear stress distribution and effective width

Figure 5-c shows the non-linear distribution of the bending stresses in a plate with a rib on the basis of Leonhardt, 1973. In order to attribute the problem to the beam theory with the assumption of a linear distribution of stresses, the effective width  $b_{ef}$  of the panel is determined such that the maximum edge stress in the panel  $\sigma_{max}$  is equal to the non-linear case.

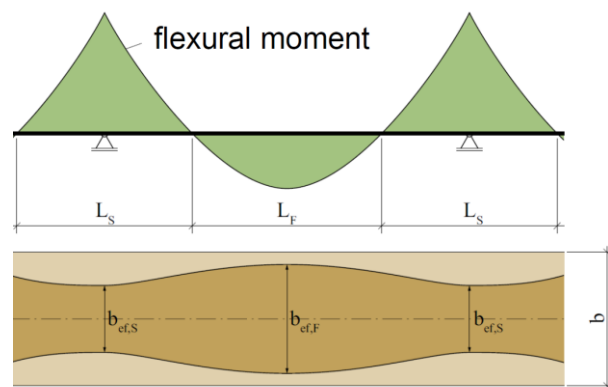


Figure 5-d: Variation of the effective width in the system

## 5.2 Definition of the effective width $b_{ef}$ (per rib)

The effective width for rib panels shall be determined by the fitting function to a theory, elaborated by Holzbau Forschungs GmbH (TU Graz) [9]. Background knowledge on this theory is to be found in [8] and [10].

The effective width  $b_{ef}$  per rib is defined as the sum of the rib width  $b_w$  plus the effective width  $b_{ef,i}$  at each side of the rib.

$$b_{ef} = \min \left\{ b_w + \sum_b b_{ef,i} \right\}$$

Eq. 5-1

with

- $b_{ef}$  Effective width of the CLT Rib Panel [mm]
- $b_{ef,i}$  Effective width at each side of the rib ( $i = 1, 2$ ) [mm]
- $b_w$  Width of the rib [mm]



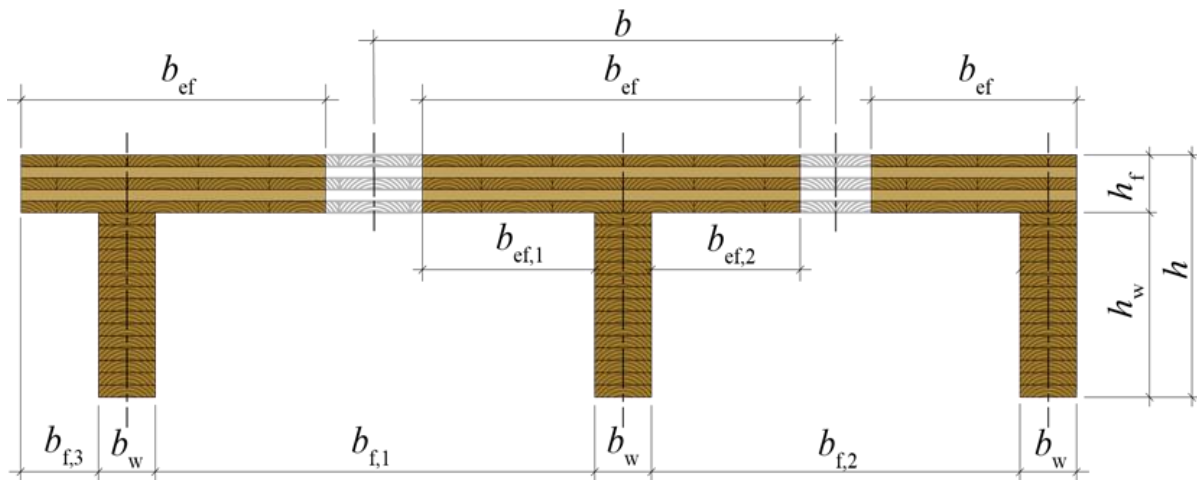


Figure 5-e: Definition of the effective width

### 5.3 Effective width for different loadings

The given equations are valid for a range of applications:

- ratio of the clear distance between the ribs and span

$$0.02 \leq \frac{b_f}{l} \leq 0.25$$

whereas for  $\frac{b_f}{l} \leq 0.02$  :  $b_{ef} = b$

- ratio of the in-plane stiffness in the direction of the span and the (effective) shear stiffness

$$5 \leq \frac{(E \cdot A)_x}{S^*_{xy}} \leq 22$$

- ratio of span and the total height of the member

$$14 \leq \frac{l}{h} \leq 25$$

- For the span  $l$  the distance between zero moments should be used.
- For locally acting loads with a load introduction point  $\leq b$  to a zero moment or if  $c_p < 0,05 \cdot l$  the effective width should be considered as  $b_{ef,i} = 0$  (with  $c_p$  being the length of the distributed load).

#### 5.3.1 Effective width $b_{ef}$ for continuously (uniformly) distributed loads (at midspan)

Eq. 5-2 is valid for the verification of stresses (ULS) in the field (bay) and the serviceability limit state (SLS) of single span as well as continuous rib panels (span = distance between zero moments); both under predominantly uniformly distributed loads.

The effective width shall be determined as follows:

$$b_{ef,i} = b_{f,j} \cdot \min \left\{ 0,5 - 0,35 \cdot \left( \frac{b_{f,j}}{l} \right)^{0,90} \cdot \left( \frac{(E \cdot A)_x}{S^*_{xy}} \right)^{0,45} \right.$$

Eq. 5-2

with

$b_{ef,i}$  Effective width at each side of the rib [mm]  
 $b_{f,j}$  Clear distance between the ribs [mm]  
 $(EA)_x$  In-plane stiffness of the CLT panel in span direction [N/m]  
 $(E \cdot A)_x = \sum E_{i,0,mean} \cdot 1m \cdot t_{i,x}$

$S^*_{xy}$  In-plane shear stiffness of the CLT element [N/m] according to [11] Eq. 5-3

$$S^*_{xy} = \frac{G_{0,mean} \cdot t}{1 + 6 \cdot p_s \cdot \left(\frac{t_{max}}{a}\right)^{q_s}}$$

with

$G_{0,mean}$  mean value of shear modulus parallel to the grain [N/mm<sup>2</sup>]  
 $t$  total thickness of the CLT element [mm]  
 $t_{max}$  maximum thickness of an individual layer [mm]  
 $a$  mean value of the width of the CLT boards

|                               |                              |       |
|-------------------------------|------------------------------|-------|
| Visual quality VI             | <130mm in AU<br><150mm in SE | 100mm |
| Industrial visual quality IVI | <130mm in AU<br><150mm in SE | 100mm |
| Non-visual quality NVI        | <250mm                       | 130mm |

if a value is unknown a width of  $a = 80$  mm should be used

| $p_s ; q_s$ | Parameter        |      |   |
|-------------|------------------|------|---|
|             | Number of layers |      |   |
|             | 3                | 5    | 7 |
| $p_s$       | 0,53             | 0,43 |   |
| $q_s$       | 1,21             |      |   |

Remarks:

- 1) The range of the parameter ( $b_f/l$ ) in practise is approx.:

$Max: (1200 / 5000) = 0.24 ; Min: (600 / 15000) = 0.04 ;$

for the ratio  $(E \cdot A)_x / S^*_{xy} : Min \approx 11, Max \approx 22,$

thus  $b_{ef,i}$  varies between approx.  $Min b_{ef,i} \approx 0.111 \cdot b_f$  and  $Max b_{ef,i} \approx 0.443 \cdot b_f$  (and  $b_{ef,i} \approx 0.500 \cdot b_f$  resp.)

- 2)  $b_{ef}$  influences the width of the CLT element in the determination of cross section values. With a decreasing value a shift of the centre of gravity (COG) is evident. If  $b_{ef}$  is determined with some inaccuracy due to its modelling generally only small differences in the computation of stresses follows.
- 3) Since the ratios of the stiffness values for available CLT layups  $(E \cdot A)_x / S^*_{xy}$  cover a wide range ( $Min \approx 11, Max \approx 22$ ) the stiffness values should be considered – apart from the  $b_f/l$  -ratio – in the model for the effective width  $b_{ef}$ .

This is also a reminder for engineers of the most influencing factors on  $b_{ef}$ , although more efforts are necessary in its determination. The rules given in EN 1995-1-1 are specified on a simpler approach, only depending on the span  $l$ .

The equations Eq. 5-2 apply, regardless, whether the CLT panel is attached to the top of the rib, or to the bottom of the rib.

### 5.3.2 Effective width $b_{ef}$ for rib panels under single point loads at the support

Apart from the influencing factors mentioned in section 5.3.1, the effective width  $b_{ef}$  in the case of single (point) loads is additionally influenced by

- the ratio between the height of the rib and the CLT element  $h_w / h_f$

For the determination of  $b_{ef}$  (see Eq. 5-4 and Eq. 5-5) two cases should be distinguished:

$$2 \leq \frac{h_w}{h_f} < 3 \quad \text{and} \quad 3 \leq \frac{h_w}{h_f} \leq 5$$

Eq. 5-4 and Eq. 5-5 are valid for the verification of stresses (ULS) in the field (bay) of single-span and continuous rib panels with single (point) loads as well as for stresses (ULS) over the supports of continuous rib panels.

The effective width shall be determined as follows:

$$2 \leq \frac{h_w}{h_f} \leq 3: \quad b_{ef,i} = b_{f,j} \cdot \min \left\{ 0,5 - 0,30 \cdot \left( \frac{b_{f,j}}{l} \right)^{0,25} \cdot \left( \frac{(E \cdot A)_x}{S^*_{xy}} \right)^{0,25} \right\} \quad \text{Eq. 5-4}$$

and

$$3 \leq \frac{h_w}{h_f} \leq 5: \quad b_{ef,i} = b_{f,j} \cdot \min \left\{ 0,5 - 0,36 \cdot \left( \frac{b_{f,j}}{l} \right)^{0,40} \cdot \left( \frac{(E \cdot A)_x}{S^*_{xy}} \right)^{0,25} \right\} \quad \text{Eq. 5-5}$$

with

|           |   |
|-----------|---|
| $h_w$     | Height of the web (=rib) $h_w = h_{rib}$ [mm]                 |
| $h_f$     | Height of the flange (=CLT panel(s)) $h_f = t_{CLT,tot}$ [mm] |
| $b_{f,j}$ | Clear distance between the ribs [mm]                          |

It is not recommended to apply this equation for systems with a  $h_w/h_f$  ratio  $>5$ . The equations Eq. 5-4 and Eq. 5-5 apply, regardless, whether the CLT panel is attached to the top of the rib, or to the bottom of the rib.

### 5.3.3 Effective width for rib panels at a support (Rolling shear)

At supports, the shear design will be design governing.

Due to the local effect from the load application problem in the CLT panel, higher shearing stresses occur locally in the CLT plate than those resulting according to the technical bending theory. Therefore, for the determination of the maximum rolling shear stress, a small effective width is applied for the panel. It is suggested to use an effective width in the size of the GLT rib width plus a distribution width of the bottommost outer layer of the CLT panel oriented in parallel to the GLT axis.

Shear stress – rolling shear stress in particular – is spreading out in an angle of 45°, originating from the edge of a rib. This assumption was verified using FE simulations and, compared to more exact models, results in acceptable deviations on the safe side. The first cross layer is reached after penetrating the bottom cover layer (always in span direction).

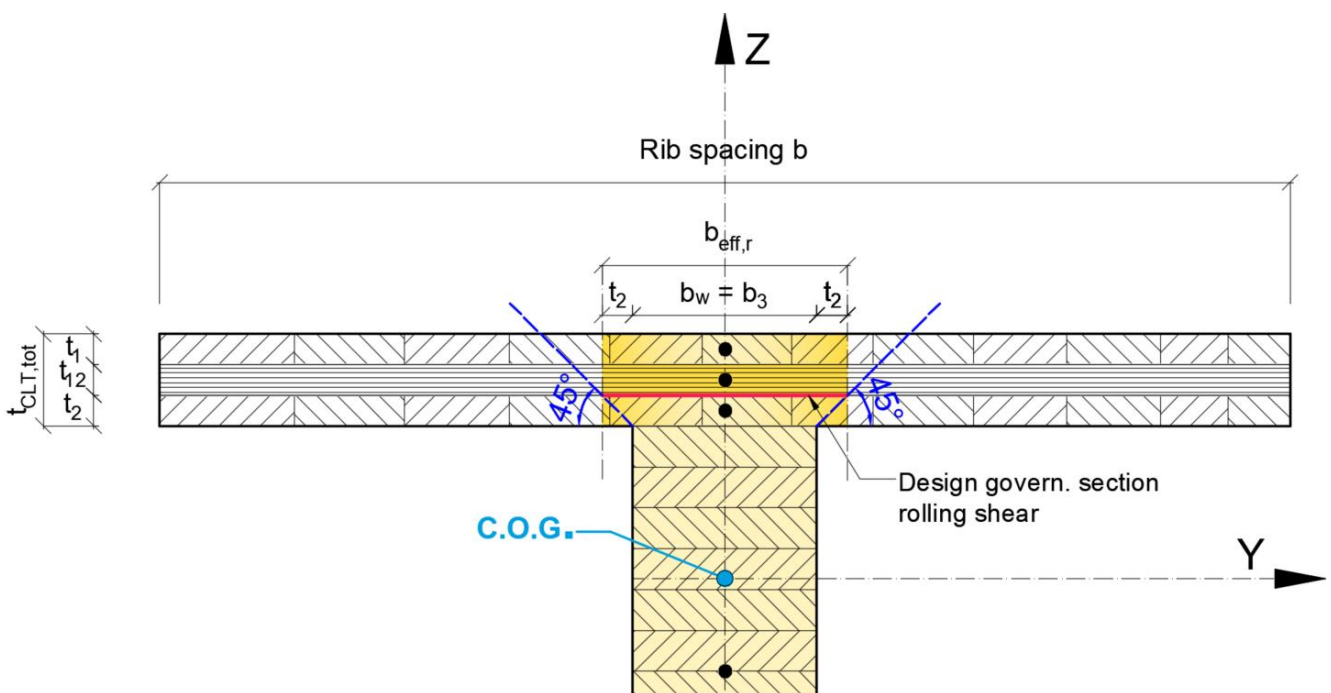


Figure 5-f: Effective width for the determination of the shear or rolling shear stresses, resp.

The effective width for the rolling shear design at the outermost CLT layer close to the glue-line shall be as follows:

$$b_{ef,r} = b_w + 2 \cdot t_n \quad \text{Eq. 5-6}$$

with

|            |  |
|------------|--|
| $b_{ef,r}$ | effective width for the rolling shear design [mm]                |
| $b_w$      | width of the GLT rib [mm]  |
| $t_n$      | thickness of the outermost CLT layer close to the glue-line [mm] |
|            | for a CLT L3s $\rightarrow t_2$                                  |
|            | for a CLT L5s $\rightarrow t_3$                                  |

## 5.4 Effective bending stiffness

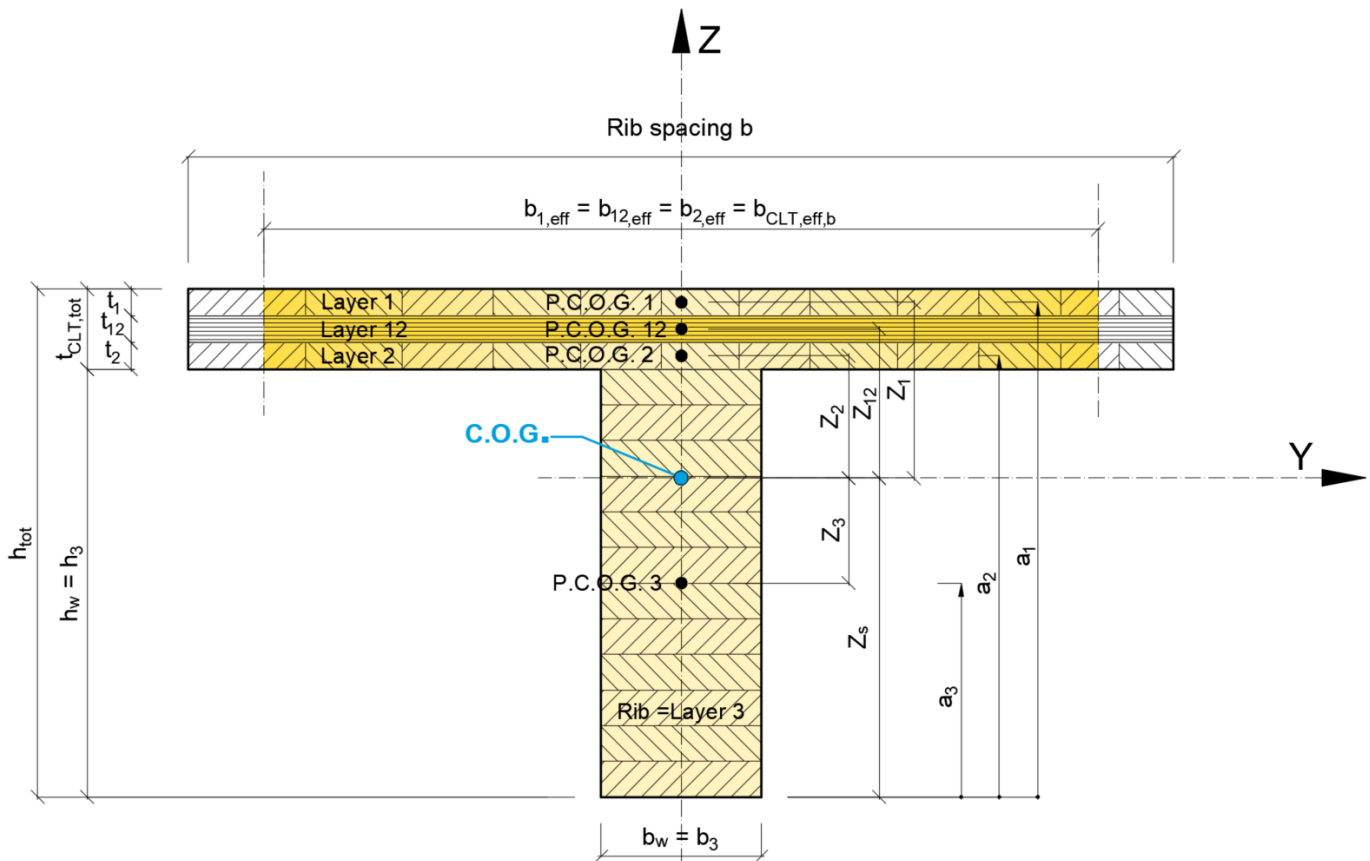


Figure 5-g: Effective cross section (T-section) of a CLT Rib Panel at midspan

### Layer notation:

Layers i, j, ... are layers in principal direction;

note: the rib is considered as a layer in principal direction and follows the same notation pattern (in the figure above, the rib is layer 3)

Layers ij, jk, ... are cross layers (e.g. between the principal layers i and j, j and k, etc.)  
(in the figure above, the CLT cross layer 12 is a cross layer between layer 1 and 2)

For each section (T, L, C or I) the area and the bending stiffness is calculated as follows.

Areas of partial section (e.g. one layer) in the CLT may be calculated as follows:

$$A_i = b_{i,eff} \cdot t_i \quad \text{Eq. 5-7}$$

$b_{i,eff}$  is the effective width of layer i in the CLT section, or the width of the rib

$t_i$  is the thickness of layer i, or the height of the rib

The net cross sectional area of the rib panel is the sum of the partial cross sections in principal direction of the CLT + the sectional area of the rib

$$A_{net} = \sum_i A_i \quad \text{Eq. 5-8}$$

Location of the center of gravity (C.O.G.), about to the bottom of the rib panel section: (Figure 5-g)

$$z_s = \frac{\sum_i E_i \cdot A_i \cdot a_i}{\sum_i E_i \cdot A_i} \quad \text{Eq. 5-9}$$

with

$A_i$  Sectional area of the respective layer/rib

$a_i$  distance from the bottom edge of the rib panel section to the partial center of gravity of the respective layer/rib

$E_i$  Young's modulus of the respective layer/rib. For each situation with different Young's modulus, the C.O.G. needs to be calculated individually (ULS  $t=0$ , ULS  $t=\infty$ , SLS  $t=0$ , SLS creep)

CLT and GLT have almost the same but not the same time-dependent properties (see different  $k_{def}$  values). Due to creep effects, a stress redistribution in the cross-section over service time will take place. Since the stress distribution in the section is influenced by the stiffness and the stiffness is time dependent, consequently the stresses in the ULS have to be determined with the design values of the stiffness. The following cases need to be considered separately:

The following figures are an example and are based on:

- $E_{0,mean,CLT} = 12,000 \text{ N/mm}^2$  (according to ETA-20/0893)
- $E_{0,mean,GLT} = 11,500 \text{ N/mm}^2$  (GL 24h, according to EN14080)

Table 5-1: Young's modulus for different design cases

| Design | Time           | Definition acc.to<br>EN 1995-1-1   | $E_0$ [N/mm <sup>2</sup> ] |        | $G_0$ [N/mm <sup>2</sup> ] |       | $G_r$ [N/mm <sup>2</sup> ] |      |
|--------|----------------|--|----------------------------|--------|----------------------------|-------|----------------------------|------|
|        |                |  | CLT                        | GLT    | CLT                        | GLT   | CLT                        | GLT  |
| ULS    | t = 0          | $X_{fin,d} = \frac{X_{mean}}{\gamma_M}$                                  | 9 600                      | 9 200  | 552                        | 520   | 40.0                       | 52.0 |
|        |                | $n_{inst,d} = X_{inst,CLT}/X_{inst,GLT}$                                 | 1.043                      |        |                            |       |                            |      |
|        | t = ∞          | $X_{fin,d} = \frac{X_{mean}}{\gamma_M \cdot (1 + \psi_2 \cdot k_{def})}$ | 7 742                      | 7 797  | 445                        | 441   | 32.3                       | 44.1 |
|        |                | $n_{fin,d} = X_{fin,CLT}/X_{fin,GLT}$                                    | 0.993                      |        |                            |       |                            |      |
| SLS    | t = 0          | $X_{inst,d} = X_{mean}$  | 12 000                     | 11 500 | 690                        | 650   | 50                         | 65   |
|        |                | $n_{inst,d} = X_{inst,CLT}/X_{inst,GLT}$                                 | 1.043                      |        |                            |       |                            |      |
|        | Creep<br>t = ∞ | $X_{creep} = \frac{X_{mean}}{k_{def}}$                                   | 15 000                     | 19 166 | 863                        | 1 083 | 63                         | 108  |
|        |                | $n_{creep,d} = X_{creep,CLT}/X_{creep,GLT}$                              | 0.783                      |        |                            |       |                            |      |
|        | t = ∞          | $X_{fin,d} = \frac{X_{mean}}{1 + k_{def}}$                               | 6 667                      | 7 188  | 383                        | 406   | 27.8                       | 40.6 |
|        |                | $n_{fin,d} = X_{fin,CLT}/X_{fin,GLT}$                                    | 0.927                      |        |                            |       |                            |      |



$n_{inst}$  and  $n_{fin}$  are ratios of the Young's Modulus of 2 different materials. When calculating the center of gravity, one can either use the Young's modulus in the equation or apply the  $n$  values to increase/decrease the related parts. If nothing else, the  $n$  factors give an idea about the difference in elasticity between 2 materials. Bending stiffness about the Y-axis (Z-direction) of the partial sections shall be

$$EI_i = \frac{E_i \cdot b_{i,eff} \cdot d_i^3}{12} + E_i \cdot A_i \cdot z_i^2 \quad \text{Eq. 5-10}$$

The bending stiffness is dependent on the Young's modulus and C.O.G. and needs to be analyzed for each of the following cases individually:

| Case           | Bending stiffness   |          |
|----------------|---|----------|
| ULS, $t=0$     | $EI_{i,inst,d} = \frac{E_{i,inst,d} \cdot b_{i,eff} \cdot d_i^3}{12} + E_{i,inst,d} \cdot A_i \cdot z_{i,inst,d}^2$ | Eq. 5-11 |
| ULS $t=\infty$ | $EI_{i,fin,d} = \frac{E_{i,fin,d} \cdot b_{i,eff} \cdot d_i^3}{12} + E_{i,fin,d} \cdot A_i \cdot z_{i,fin,d}^2$     | Eq. 5-12 |
| SLS, $t=0$     | $EI_{i,inst} = \frac{E_{i,inst} \cdot b_{i,eff} \cdot d_i^3}{12} + E_{i,inst} \cdot A_i \cdot z_{i,inst}^2$         | Eq. 5-13 |
| SLS creep      | $EI_{i,creep} = \frac{E_{i,creep} \cdot b_{i,eff} \cdot d_i^3}{12} + E_{i,creep} \cdot A_i \cdot z_{i,creep}^2$     | Eq. 5-14 |

Bending stiffness about the Y-axis (Z-direction) of the considered CLT Rib Panel shall be

$$EI_{eff} = \sum_i EI_i \quad \text{Eq. 5-15}$$

## 5.5 Effective shear stiffness

Modelling as a shear-flexible beam is suitable for ribbed cross-sections with a rigid, i.e. glued joint. In the ultimate limit state (ULS), the cross-sectional values for the rigid compound are used. The stress verifications are undertaken with the net cross-sectional values. In the serviceability limit state of (SLS), the portion of shear deformation shall be considered via the shear stiffness and the shear correction factor.

Currently there is no exact analytical solution for a corrective shear coefficient known. An approximate solution is given in the next equation.

If the verification is based on a model considering shear deflection (Timoshenko beam theory) the following approximation equation for the shear correction factor  $\kappa$  may be used. This equation was found within a fitting analysis with the same range of parameters – elaborated with holzbau forschungs GmbH.

**For T shaped section (Open/Inverted types):**

$$\kappa = \frac{1}{1.20} - 0.25 \cdot \frac{\left(\frac{b_{ef}}{b_w}\right)^{0.70}}{\left(\frac{h_w}{h_f}\right)^{0.50}} \quad \text{Eq. 5-16}$$

**For I shaped section (Closed type):**

$$\kappa = \frac{1}{1.20} - 0.25 \cdot \frac{\left(\frac{\min(b_{ef,top}; b_{ef,bottom})}{b_w}\right)^{0.70}}{\left(\frac{h_w}{\min(h_{f,top}; h_{f,bottom})}\right)^{0.50}} \quad \text{Eq. 5-17}$$

with

- $\kappa$  Shear correction factor (a coefficient K is  $1/\kappa$ )
- $b_{ef}$  Effective tributary width of the CLT panel in case of T shaped cross section [mm]
- $b_{ef,top}$  Effective tributary width of the top CLT panel in case of I shaped cross section [mm]
- $b_{ef,bottom}$  Effective tributary width of the bottom CLT panel in case of I shaped cross section [mm]
- $b_w$  Width of the rib [mm]
- $h_w$  Height of the rib [mm]
- $h_f$  Thickness of the CLT panel in case of T shaped cross section [mm]
- $h_{f,top}$  Thickness of the top CLT panel in case of I shaped cross section [mm]
- $h_{f,bottom}$  Thickness of the bottom CLT panel in case of I shaped cross section [mm]

The effective shear stiffness of the considered CLT Rib Panel shall be:

$$(GA)_{eff} = \kappa \cdot \sum_i G_i \cdot A_i \quad \text{Eq. 5-18}$$

The shear stiffness is dependent on the shear modulus and needs to be analyzed for each of the following cases individually:

| Case      | Shear stiffness   |          |
|-----------|---|----------|
| ULS, t=0  | $(GA)_{eff} = \kappa \cdot \sum_i G_{i,inst,d} \cdot A_i$ | Eq. 5-19 |
| ULS t=∞   | $(GA)_{eff} = \kappa \cdot \sum_i G_{i,fin,d} \cdot A_i$  | Eq. 5-20 |
| SLS, t=0  | $(GA)_{eff} = \kappa \cdot \sum_i G_{i,inst} \cdot A_i$   | Eq. 5-21 |
| SLS creep | $(GA)_{eff} = \kappa \cdot \sum_i G_{i,creep} \cdot A_i$  | Eq. 5-22 |

## 6 Ultimate Limit State (ULS) design – load combinations

For ultimate limit state design (ULS design), the applicable load combinations, according to EN1990, item 6.4.3 shall be applied.

The CLT rib panel may only be subject to static loading, such as, but not limited to:

- Dead load
- Live load
- Snow load
- Soil pressure

and to quasi static loading (load that is derived from dynamic actions, but applied to the system as static forces):

- Wind load (according to EN1991-4)
- Seismic load (according to EN1998-1)

In seismic areas the behaviour factor of CLT rib panels used for the design is limited to non-dissipative or low-dissipative structures ( $q \leq 1,5$ ), defined according to Eurocode 8 (EN 1998-1:2004 clauses 1.5.2 and 8.1.3 b), and applicable national rules on works.

Transverse to the direction of span of the ribbed plates, it's the task of the CLT plate, among other things, to distribute concentrated live loads onto the ribs. The static system is a plate strip with orthotropic properties. Upon compliance with the rib distances according to Section 5.1, the load-bearing capacity as well as sufficient stiffness of the plate are normally given for these concentrated loads.

## 7 Bending resistance

Bending stresses shall be verified about the main axis (x- and y-axis) of the CLT element. The verification of the rib shall be done about the y-axis. If the CLT Rib Panel is loaded by negative moments (compression stresses in the rib) buckling of the ribs has to be verified. When the ratio between the width and height of the rib is  $h/b_w \leq 4$  this verification should not be applied. If the CLT rib panels is loaded in compression parallel to the longitudinal axis, the stability of the members (buckling out of the plane) shall be verified.

### 7.1 Flexural stresses parallel to grain in the section

If the section is purely subject to out of plane loading that is causing a bending reaction on the rib panel, the normal stress in the section shall be calculated as follows:

$$\sigma_i(x, z) = \frac{E_i \cdot z_i \cdot M_y(x)}{EI_{y,ef}} \quad \text{Eq. 7-1}$$

|                  |   |
|------------------|---|
| $\sigma_i(x, z)$ | Normal stress at location x of the rib panel at coordinate z in the section [N/mm <sup>2</sup> ]                          |
| $E_i$            | Young's Modulus at coordinate z [N/mm <sup>2</sup> ]  |
| $M_y(x)$         | Bending moment about Y axis at location x of the rib panel [N.mm]   |
| $z_i$            | Coordinate z of the point "i" where the stress is being analyzed (distance to neutral axis [mm])                          |
| $EI_{y,ef}$      | Effective bending stiffness about the Y-axis based on the effective width at midspan (section 5.3.1) [N.mm <sup>2</sup> ] |

#### - Bending stresses at the edges of the rib panel

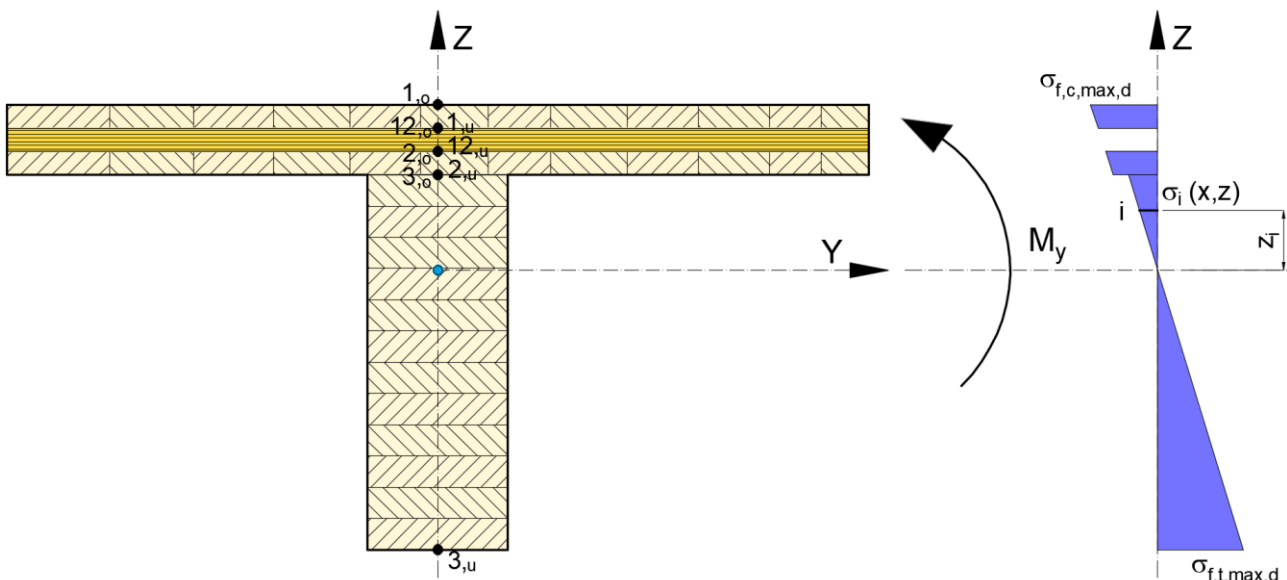


Figure 7-a: Flexural stress distribution [12]

$$\sigma_{m,d;1,o} = E_{d,CLT} \cdot \frac{M_{y,max}}{(E \cdot I)_{ef}} \cdot z_{1,o}$$

$$\sigma_{m,d;1,u} = E_{d,CLT} \cdot \frac{M_{y,max}}{(E \cdot I)_{ef}} \cdot z_{1,u}$$

$$\sigma_{m,d;2,o} = E_{d,CLT} \cdot \frac{M_{y,max}}{(E \cdot I)_{ef}} \cdot z_{2,o}$$

$$\sigma_{m,d;2,u} = E_{d,CLT} \cdot \frac{M_{y,max}}{(E \cdot I)_{ef}} \cdot z_{2,u}$$

$$\sigma_{m,d;3,o} = E_{d,GLT} \cdot \frac{M_{y,max}}{(E \cdot I)_{ef}} \cdot z_{3,o}$$

$$\sigma_{m,d;3,u} = E_{d,GLT} \cdot \frac{M_{y,max}}{(E \cdot I)_{ef}} \cdot z_{3,u}$$

- Normal stresses at the partial centre of gravity of each layer

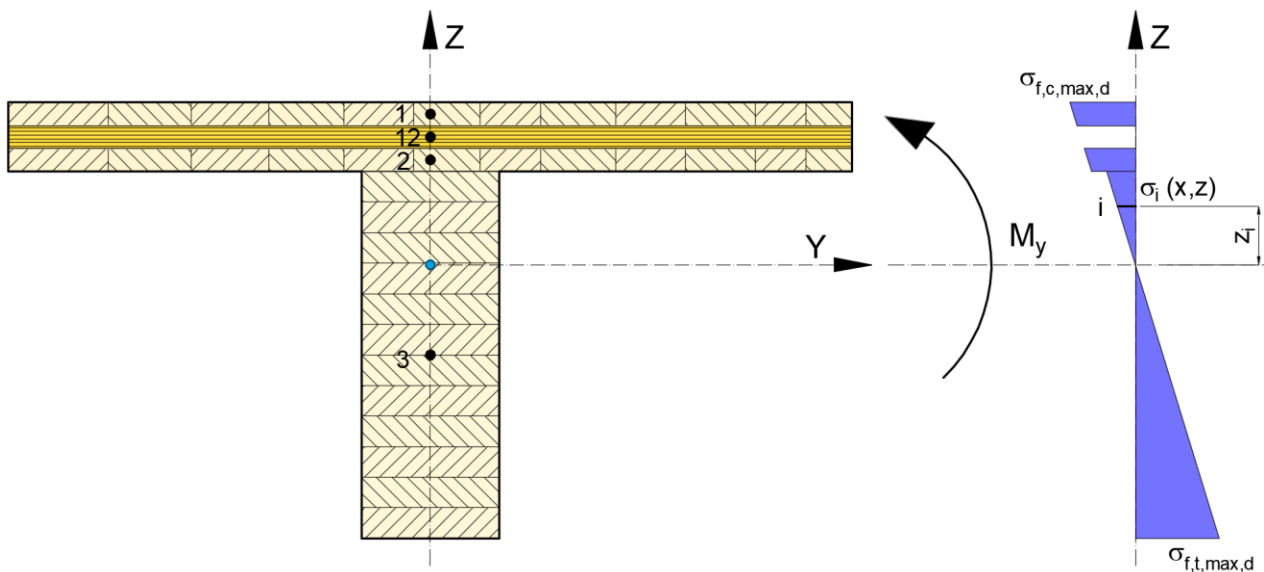


Figure 7-b: Normal stresses in partial centre of gravity of the respective layers

$$\sigma_1 = \frac{1}{2} \cdot (\sigma_{m,d;1,u} + \sigma_{m,d;1,o})$$

$$\sigma_2 = \frac{1}{2} \cdot (\sigma_{m,d;2,u} + \sigma_{m,d;2,o})$$

$$\sigma_3 = \frac{1}{2} \cdot (\sigma_{m,d;3,u} + \sigma_{m,d;3,o})$$

The stress analysis shall be performed at the top and bottom extreme fibre of the CLT and GLT rib. The stress analysis shall be performed according to EN 1995-1-1 [3], item 9.1.1

**Bending stress verification:**

$$\sigma_{f,c,max,d} \leq f_{m,d} \quad \text{Eq. 7-2}$$

$$\sigma_{f,t,max,d} \leq f_{m,d} \quad \text{Eq. 7-3}$$

and consequently

$$\sigma_i(x, z) \leq f_{m,i,d} \quad \text{Eq. 7-4}$$

with

- $\sigma_{f,c,max,d}$  Extreme fiber flange design compressive stress [N/mm<sup>2</sup>]
- $\sigma_{f,t,max,d}$  Extreme fiber flange design tensile stress [N/mm<sup>2</sup>]
- $f_{m,i,d}$  Design bending strength in partial section "i" [N/mm<sup>2</sup>]

**Normal stress verification:**

At the same time the following requirements according to EN 1995-1-1 [3], item 9.1.1 (Glued thin-webbed beams) shall be fulfilled: The requirement is graphically illustrated, using a rib panel section, as indicated in Figure 7-c.

$$\sigma_{f,c,i,d} \leq f_{c,0,i,d} \quad \text{Eq. 7-5}$$

$\sigma_{f,c,i,d}$  Compressive design stress in partial section "i" [N/mm<sup>2</sup>]

$f_{c,0,i,d}$  Compressive design strength parallel to grain in partial section "i" [N/mm<sup>2</sup>]

$$\sigma_{f,t,i,d} \leq f_{t,0,i,d} \quad \text{Eq. 7-6}$$

$\sigma_{f,t,i,d}$  Tensile design stress in partial section "i" [N/mm<sup>2</sup>]

$f_{t,0,i,d}$  Tensile design strength parallel to grain in partial section "i" [N/mm<sup>2</sup>]

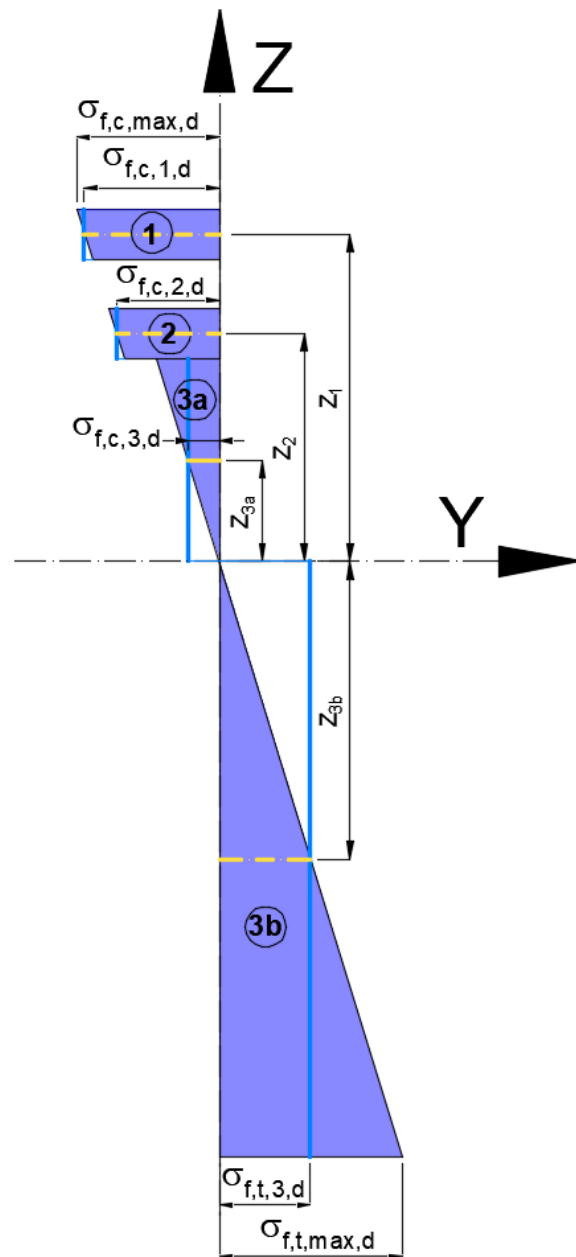


Figure 7-c: Flexural stress distribution

## 7.2 Normal stresses from axial force

The normal stresses in the panels and in the rib shall be executed according to EN 1995-1-1 and should satisfy the following expressions:

### 7.2.1 Tension parallel to the grain

It has to be verified that the following equation is fulfilled

$$\sigma_{t,0,i,d} \leq f_{t,0,i,d} \quad \text{Eq. 7-7}$$

with

$$\begin{aligned} \sigma_{t,0,i,d} & \text{ Design tensile stress parallel to grain at point "i" [N/mm}^2\text{]} \\ f_{t,0,i,d} & \text{ Design tensile strength parallel to grain at point "i" [N/mm}^2\text{]} \end{aligned}$$

whereby

$$\sigma_{t,0,i,d} = \frac{E_i \cdot N_{ed}}{EA_{eff}} \quad \text{Eq. 7-8}$$

$$EA_{eff} = \sum E_i \cdot A_i \quad \text{Eq. 7-9}$$

with

$$\begin{aligned} N_{ed} & \text{ Design tensile force parallel to grain [N]} \\ E_i & \text{ Modulus of elasticity at the point "i" [N/mm}^2\text{]} \\ EA_{eff} & \text{ Effective axial (longitudinal) stiffness [N]} \end{aligned}$$

### 7.2.2 Compression parallel to the grain

It has to be verified that the following equation is fulfilled

$$|\sigma_{c,0,i,d}| \leq k_c \cdot f_{c,0,i,d} \quad \text{Eq. 7-10}$$

with

$$\begin{aligned} \sigma_{c,0,i,d} & \text{ Design compressive stress parallel to grain at point "i" [N/mm}^2\text{]} \\ f_{c,0,i,d} & \text{ Design compressive strength parallel to grain at point "i" [N/mm}^2\text{]} \\ k_c & \text{ Instability buckling coefficient calculated according to the equations above and EN1995-1-1 [8] (6.3.2) and chapter 7.7.1 of this design manual.} \end{aligned}$$

whereby

$$\sigma_{c,0,i,d} = \frac{E_i \cdot N_{ed}}{EA_{eff}} \quad \text{Eq. 7-11}$$

$$EA_{eff} = \sum E_i \cdot A_i \quad \text{Eq. 7-12}$$

with

$$\begin{aligned} N_{ed} & \text{ Design compressive force parallel to grain [N]} \\ E_i & \text{ Modulus of elasticity at the point "i" [N/mm}^2\text{]} \\ EA_{eff} & \text{ Effective axial (longitudinal) stiffness [N]} \end{aligned}$$



## 7.3 Bending strength parallel to grain

### CLT:

$$f_{CLT,m,d} = \frac{k_{sys} \cdot k_{mod} \cdot f_{CLT,m,k}}{\gamma_{m,CLT}} \quad \text{Eq. 7-13}$$

with

|                  |   |
|------------------|---|
| $f_{CLT,m,d}$    | Design bending strength for CLT [N/mm <sup>2</sup> ]  |
| $k_{mod}$        | Factor, according to EN1995-1-1, Table 3.1, taking a load duration (permanent – very short) and the utilization class (1-3) into consideration  |
| $k_{sys}$        | System factor, according to EN1995-1-1 [3], and ETA [2];  |
| $f_{CLT,m,k}$    | Characteristic bending strength of the CLT lamination material, according to ETA [2] [N/mm <sup>2</sup> ]   |
| $\gamma_{m,CLT}$ | Partial safety coefficient, applicable for CLT, according to either EN1995-1-1, Table 2.3, or some local regulations.<br>For Austria: EN1995-1-1 NA, chapter K.2.4 proposes $\gamma_{m,CLT} = 1,25$ |

### GLT:

$$f_{GLT,m,d} = \frac{k_{mod} \cdot f_{GLT,m,k} \cdot k_h}{\gamma_{m,GLT}} \quad \text{Eq. 7-14}$$

with

|                  |  |
|------------------|--|
| $f_{GLT,m,d}$    | Design bending strength for Glued Laminated Timber [N/mm <sup>2</sup> ]  |
| $k_{mod}$        | Factor, according to EN1995-1-1, Table 3.1, taking a load duration (permanent – very short) and the utilization class (1-3) into consideration |
| $f_{GLT,m,k}$    | Characteristic bending strength of Glued Laminated Timber, according to EN 14080 [N/mm <sup>2</sup> ]  |
| $k_h$            | Depth factor according to EN 1995-1-1, item 3.3 (3)  |
| $\gamma_{m,GLT}$ | Partial safety coefficient, applicable for glued laminated timber, according to EN1995-1-1, Table 2.3  |

## 7.4 Tensile strength parallel to grain

### CLT:

$$f_{CLT,t,d} = \frac{k_{mod} \cdot f_{CLT,t,k}}{\gamma_{m,CLT}} \quad \text{Eq. 7-15}$$

with

|                  |   |
|------------------|---|
| $f_{CLT,t,d}$    | Design tensile strength for CLT [N/mm <sup>2</sup> ]  |
| $k_{mod}$        | Factor, according to EN1995-1-1, Table 3.1, taking a load duration (permanent – very short) and the utilization class (1-3) into consideration  |
| $f_{CLT,t,k}$    | Characteristic tensile strength of the CLT lamination material, according to ETA [2] [N/mm <sup>2</sup> ]   |
| $\gamma_{m,CLT}$ | Partial safety coefficient, applicable for CLT, according to either EN1995-1-1, Table 2.3, or some local regulations.<br>For Austria: EN1995-1-1 NA, chapter K.2.4 proposes $\gamma_{m,CLT} = 1,25$ |

**GLT:**

$$f_{GLT,t,0,d} = \frac{k_{mod} \cdot f_{GLT,t,0,k} \cdot k_h}{\gamma_{m,GLT}} \quad \text{Eq. 7-16}$$

with

|                  |  |
|------------------|--|
| $f_{GLT,t,0,d}$  | Design tensile strength for Glued Laminated Timber [N/mm <sup>2</sup> ]  |
| $k_{mod}$        | Factor, according to EN1995-1-1, Table 3.1, taking a load duration (permanent – very short) and the utilization class (1-3) into consideration |
| $f_{GLT,t,0,k}$  | Characteristic tensile strength of Glued Laminated Timber, according to EN 14080 [N/mm <sup>2</sup> ]  |
| $k_h$            | Depth factor according to EN 1995-1-1 [3], item 3.3 (3)  |
| $\gamma_{m,GLT}$ | Partial safety coefficient, applicable for glued laminated timber, according to EN1995-1-1 [3], Table 2.3                                      |

## 7.5 Compressive strength parallel to grain

**CLT:**

$$f_{CLT,c,0,d} = \frac{k_{mod} \cdot f_{CLT,c,0,k}}{\gamma_{m,CLT}} \quad \text{Eq. 7-17}$$

with

|                  |   |
|------------------|---|
| $f_{CLT,c,0,d}$  | Design compressive strength for CLT [N/mm <sup>2</sup> ]  |
| $k_{mod}$        | Factor, according to EN1995-1-1, Table 3.1, taking a load duration (permanent – very short) and the utilization class (1-3) into consideration  |
| $f_{CLT,c,0,k}$  | Characteristic compressive strength of the CLT lamination material, according to ETA [2] [N/mm <sup>2</sup> ]   |
| $\gamma_{m,CLT}$ | Partial safety coefficient, applicable for CLT, according to either EN1995-1-1, Table 2.3, or some local regulations.<br>For Austria: EN1995-1-1 [3] NA, chapter K.2.4 proposes $\gamma_{m,CLT} = 1,25$ |

**GLT:**

$$f_{GLT,c,0,d} = \frac{k_{mod} \cdot f_{GLT,c,0,k}}{\gamma_{m,GLT}} \quad \text{Eq. 7-18}$$

with

|                  |  |
|------------------|--|
| $f_{GLT,c,0,d}$  | Design compressive strength for Glued Laminated Timber [N/mm <sup>2</sup> ]  |
| $k_{mod}$        | Factor, according to EN1995-1-1, Table 3.1, taking a load duration (permanent – very short) and the utilization class (1-3) into consideration |
| $f_{GLT,c,0,k}$  | Characteristic compressive strength of Glued Laminated Timber, according to EN 14080 [13] [N/mm <sup>2</sup> ]                                 |
| $\gamma_{m,GLT}$ | Partial safety coefficient, applicable for glued laminated timber, according to EN1995-1-1 [3], Table 2.3                                      |

## 7.6 Members subjected to combined bending and axial compression or tension

In case of an inclination of the rib panels, an axial load component will appear. These equations apply to the entire section, from top to bottom. For flanges, the axial stress from normal forces are directly added to the mean axial stresses from the bending moment. Therefore, the verification shall be only with the design compressive/tensile strength for the first part.

The stress design then shall be executed according to EN 1995-1-1, items 6.2.3 and 6.2.4:

### 7.6.1 Combined bending and axial compression

**Verification** (acc to EN1995-1-1 item 6.2.4)

For the flanges

$$\left(\frac{\sigma_{c,i,d}}{f_{c,i,d}}\right)^2 + \frac{\sigma_{f,c,max,d}}{f_{f,m,0,d}} \leq 1 \quad \text{Eq. 7-19}$$

For the rib (web)

$$\left(\frac{\sigma_{c,i,d}}{f_{c,i,d}}\right)^2 + \frac{\sigma_{w,c,max,d}}{f_{m,w,0,d}} \leq 1 \quad \text{Eq. 7-20}$$

with

|                      |   |
|----------------------|---|
| $\sigma_{c,i,d}$     | Design compressive stress in the partial section “i” coming from normal force [N/mm <sup>2</sup> ]        |
| $\sigma_{f,c,max,d}$ | Maximum design compressive stress in the upper flange coming from the bending moment [N/mm <sup>2</sup> ] |
| $f_{c,i,d}$          | Design compressive strength of the partial section “i” [N/mm <sup>2</sup> ]                               |
| $f_{f,m,0,d}$        | Design bending strength of the flange [N/mm <sup>2</sup> ]  |
| $\sigma_{w,c,max,d}$ | Maximum design compressive stress of the rib [N/mm <sup>2</sup> ]   |
| $f_{m,w,0,d}$        | Design bending strength of the rib  |

### 7.6.2 Combined bending and axial tension

**Verification** (acc to EN1995-1-1 item 6.2.3)

For the flanges

$$\frac{\sigma_{t,i,d}}{f_{t,i,d}} + \frac{\sigma_{f,t,max,d}}{f_{f,m,0,d}} \leq 1 \quad \text{Eq. 7-21}$$

For the rib (web)

$$\frac{\sigma_{t,i,d}}{f_{t,i,d}} + \frac{\sigma_{w,t,max,d}}{f_{m,w,0,d}} \leq 1 \quad \text{Eq. 7-22}$$

with

|                      |  |
|----------------------|--|
| $\sigma_{t,i,d}$     | Design tensile stress in the partial section “i” coming from normal force [N/mm <sup>2</sup> ]         |
| $\sigma_{f,t,max,d}$ | Maximum design tensile stress in the bottom flange coming from the bending moment [N/mm <sup>2</sup> ] |
| $f_{t,i,d}$          | Design tensile strength of the partial section “i” [N/mm <sup>2</sup> ]                                |
| $f_{f,m,0,d}$        | Design bending strength of the flange [N/mm <sup>2</sup> ]   |

|                      |   |
|----------------------|---|
| $\sigma_{w,t,max,d}$ | Maximum design tensile stress in the rib [N/mm <sup>2</sup> ] |
| $f_{m,w,0,d}$        | Design bending strength of the rib [N/mm <sup>2</sup> ]       |

## 7.7 Stability of CLT Rib Panels

### 7.7.1 Stability – buckling of columns subjected to either compression or combined compression and bending

The verification may be done either

- (1) based on the equivalent members method acc. to EN 1995-1-1 or
- (2) calculations based on a Second-Order Elastic Analysis.

Condition according to EN1995-1-1 [3], item 6.3.2 (3) needs to be fulfilled. Stability and lateral torsional stability shall be verified using the characteristic properties  $E_{0,k}$ . This applies to the CLT as well as to the GLT rib.

**Verification** (acc to EN1995-1-1 clause 6.3.2)

When  $\lambda_{rel} \leq 0,3$  the stresses should satisfy the equations Eq. 7-19 and Eq. 7-20 of combined bending and axial compression, meaning that in this case, buckling will not have any effect.

In all other cases when  $\lambda_{rel} > 0,3$  the stresses, which will be increased due to deflection, should satisfy the following expressions:

$$\left( \frac{\sigma_{c,0,d}}{k_c \cdot f_{c,0,d}} \right) + \frac{\sigma_{m,y,d}}{f_{m,y,d}} \leq 1 \quad \text{Eq. 7-23}$$

with

|                  |  |
|------------------|--|
| $\sigma_{c,0,d}$ | design compressive stress parallel to grain [N/mm <sup>2</sup> ];  |
| $f_{c,0,d}$      | design compressive strength parallel to grain [N/mm <sup>2</sup> ] |
| $k_c$            | instability (buckling) factor [-]                                  |

The verification should be done considering the shear flexibility of the cross section

$$\sigma_{c,0,i,d} = \frac{E_i \cdot N_{ed}}{EA_{0,eff}} \quad \text{Eq. 7-24}$$

$$EA_{0,eff} = \sum E_i \cdot A_{c,0,i} \quad \text{Eq. 7-25}$$

with

|                    |  |
|--------------------|--|
| $N_{ed}$           | Design compressive force parallel to grain [N]   |
| $E_i$              | Modulus of elasticity at the point “i” [N/mm <sup>2</sup> ]  |
| $EA_{0,eff}$       | Effective axial (longitudinal) stiffness [N]   |
| $A_{c,0,eff}$      | effective cross section in compression (areas of cross layers shall be neglected) considering the effective width [mm <sup>2</sup> ]<br>Remark: Unless a more detailed calculation is made the effective width $b_{ef} \leq \min \{20 \cdot h_f; b_f\}$ (according to EN 1995-1-1 for plywood with grain direction of the outer plies parallel to the ribs) may be used. |
| $\sigma_{c,0,i,d}$ | Design compressive stress parallel to grain [N/mm <sup>2</sup> ]   |

The relative slenderness ratio should be calculated as

$$\lambda_{rel,y} = \sqrt{\frac{A_{c,0,ef} \cdot f_{c,0,k}}{n_{cr}}} \quad \text{Eq. 7-26}$$

where

$$n_{cr} = \frac{(EI)_{ef,05} \cdot \pi^2}{l_k^2 \cdot \left(1 + \frac{(EI)_{ef,05} \cdot \pi^2}{S_{05} \cdot l_k^2}\right)} = \frac{(EI)_{ef,05} \cdot \pi^2}{l_k^2} \cdot \frac{1}{1 + k_c} \quad \text{Eq. 7-27}$$

$$k_c = \min \left\{ k + \sqrt{k^2 + \lambda_{rel}^2} \right\} \quad \text{Eq. 7-28}$$

$$k = 0,5 \cdot (1 + \beta_c \cdot (\lambda_{rel,y} - 0,3) + \lambda_{rel}^2) \quad \text{Eq. 7-29}$$

$\beta_c$  is a factor for members within straightness limit

$\beta_c = 0,10$  for GLT within the straightness limit of  $L/500$

The limit is defined in Eurocode5 section 10 as the deviation from straightness measured midway between the supports of members where lateral instability can occur.

with

|                   |  |
|-------------------|--|
| $\lambda_{rel,y}$ | Relative slenderness ratio corresponding to bending about y axis (deflection in the z direction)   |
| $n_{cr}$          | Critical elastic buckling load [N/m]   |
| $E_{0,05}$        | Characteristic value 5% quantile of the modulus of elasticity parallel to the grain. [N/mm <sup>2</sup> ]  |
| $(EI)_{ef,05}$    | Effective bending stiffness of the cross section considering the effective and the 5% quantile of the modulus of elasticity parallel to the grain [N·mm <sup>2</sup> ] |
| $l_k$             | Buckling length [mm]   |
| $S_{05}$          | shear stiffness of the effective cross section considering $b_{ef}$ and the 5% quantile of the shear moduli:<br>$S_{05} = \kappa \cdot \sum_i G_{i,05} \cdot A_i$      |
| $\kappa$          | Corrective shear coefficient (see chapter 5.5)   |
| $k_c$             | instability (buckling) factor [-]  |

## 7.7.2 Stability – lateral torsional buckling (LTB) of beams subjected to either bending or combined bending and compression

In general, no failure of CLT rib panels in lateral torsional stability is expected until the ribs have a ratio of their dimension  $h/w \leq 4$ . If ribs with a higher dimension ratio shall be applied, a detailed analysis of the stability behavior (e. g. with numerical methods) shall be done.

### 7.7.2.1 CLT Rib Panel Open and Closed type

No lateral torsional buckling is possible. The compressions side of the section a CLT panel that is providing stability out of plane.

## 7.7.2.2 CLT Rib Panel Inverted type

In this case the compression zone is in the rib and therefore the rib might be vulnerable to lateral torsional buckling. To account for lateral torsional buckling, it shall be sufficient, to run a buckling analysis (according to EN1995-1-1 [3], item 6.3.2 (3)) for the extreme half of the compression zone (blue), as indicated in the figure below:

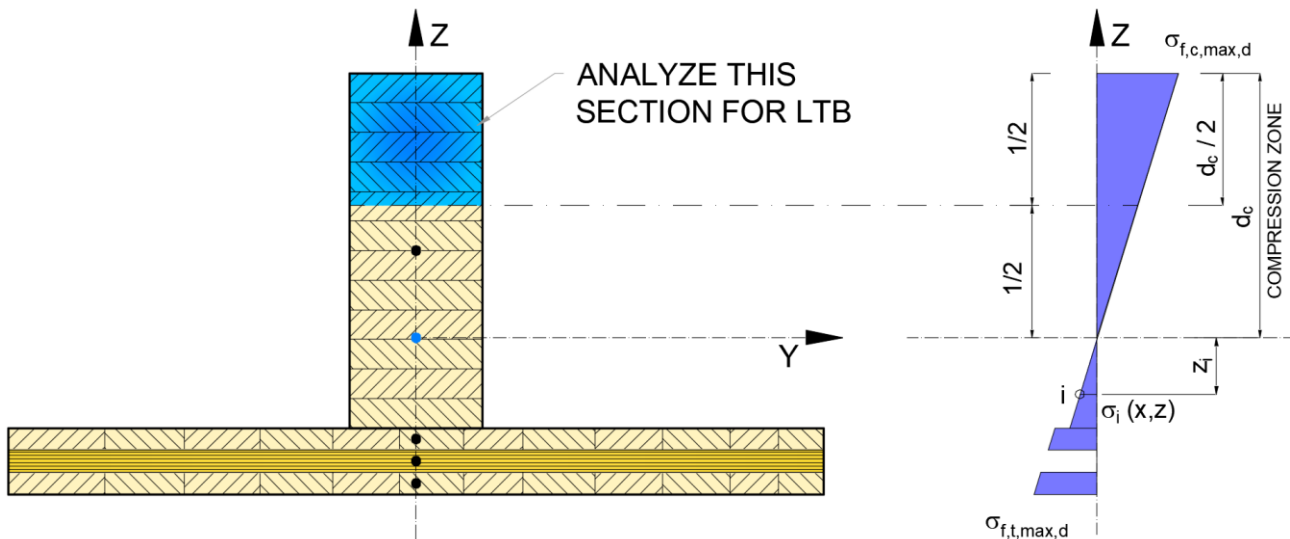


Figure 7-d: Section for lateral torsional buckling analysis

Lateral torsional stability shall be verified both in the case where only a moment  $M_d$  exists about the strong axis and where a combination of moment  $M_{d,b}$  and compressive force  $N_c$  exists.

Table 7-1: Effective length as a ratio of the span

| Beam type        | Loading type                                 | $l_{ef}/l^a$ |
|------------------|--|--------------|
| Simply supported | Constant moment                              | 1,0          |
|                  | Uniformly distributed load                   | 0,9          |
|                  | Concentrated force at the middle of the span | 0,8          |
| Cantilever       | Uniformly distributed load                   | 0,5          |
|                  | Concentrated force at the free end           | 0,8          |

<sup>a</sup> The ratio between effective length  $l_{ef}$  and the span  $l$  is valid for a beam with torsionally restrained supports and loaded at the centre of gravity. If the load is applied at the compression edge of the beam,  $l_{ef}$  should be increased by  $2h$  and may be decreased by  $0.5 h$  for the tension edge of the beam.

If the compressed side of the GLT ribs is laterally blocked with blockings and having a spacing “a” between blockings, that may be used as effective length taking account the note in the

Table 7-1 (usually  $l_{ef} = a + 2h$ ).

If lateral torsional buckling is still critical, the distance between the blockings can be reduced.

## 8 Shear resistance

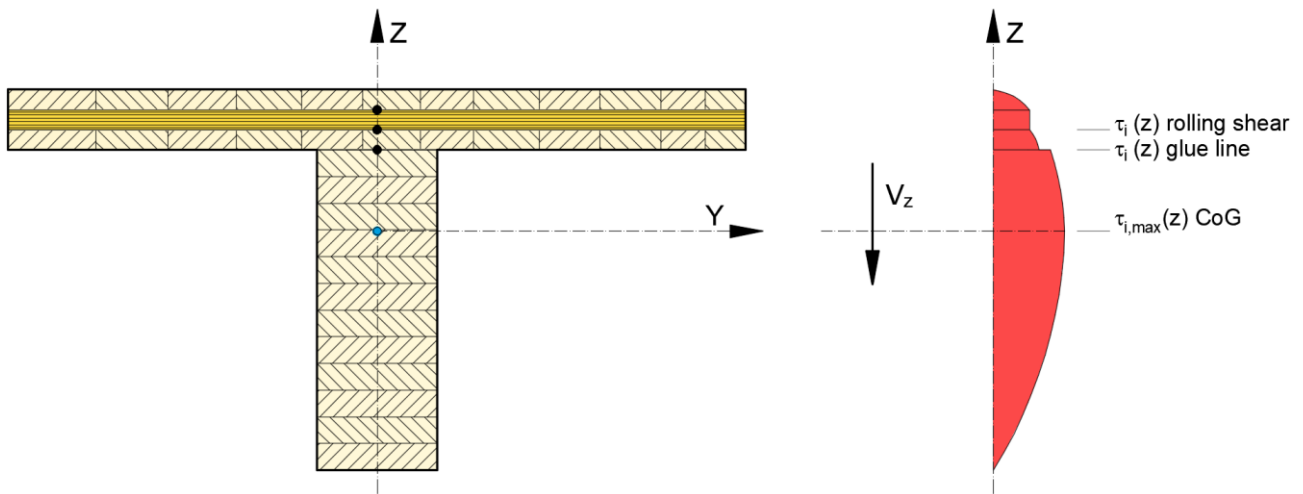


Figure 8-a: Progression of the shear stress

Shear stress of the section needs to be checked in different locations. The most essential points within a section are:

- C.O.G. (center of gravity)
- Glue line between rib and CLT panel
- Glue line within the CLT panel, between the cover layer that is attached to a rib and its cross layer. The applicable tributary width for this the rolling shear design at this point shall be per item 5.3.3.

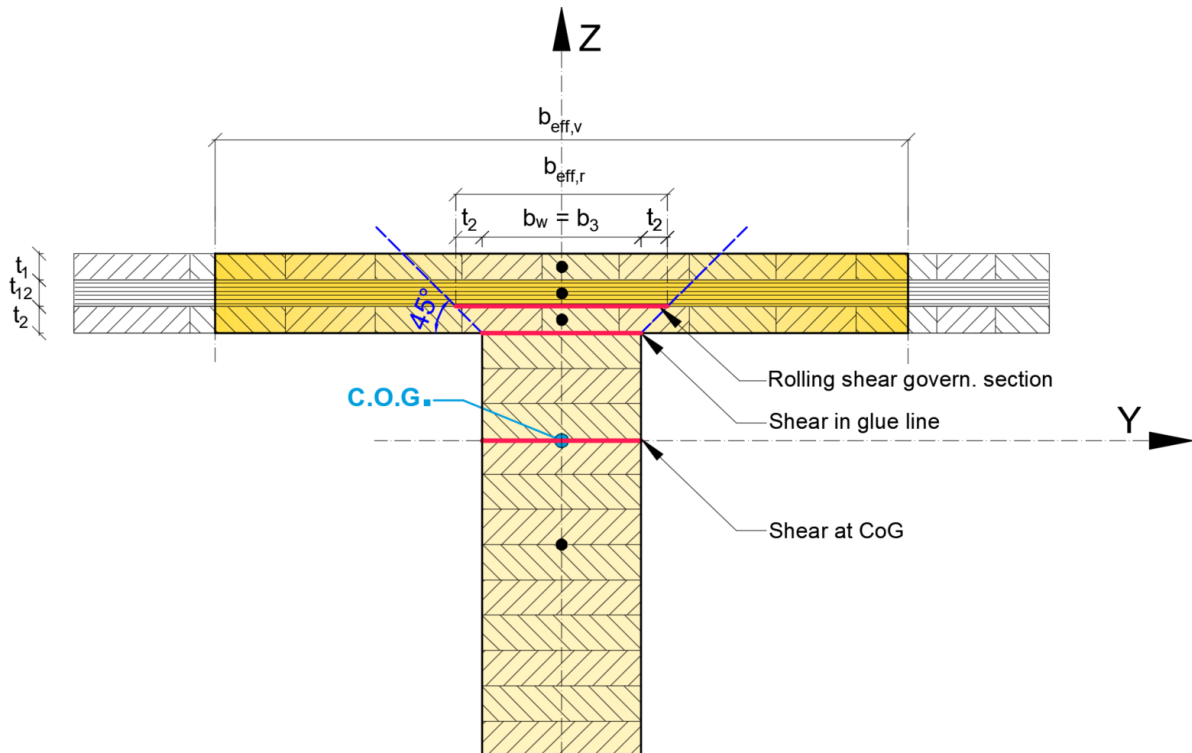


Figure 8-b: locations for shear design at T and L section



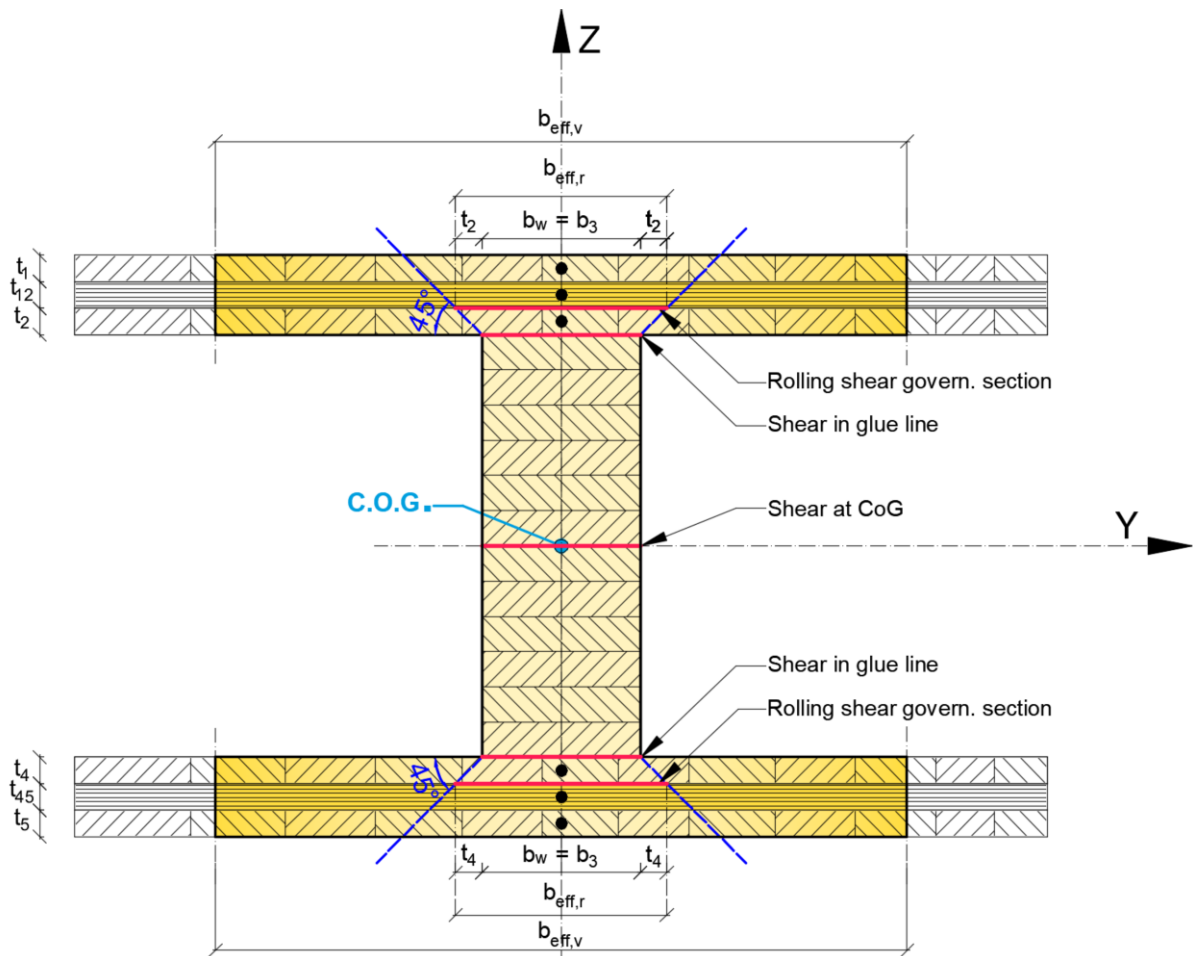


Figure 8-c: locations for shear design at I and C sections

## 8.1 Calculation of shear stresses

Shear stresses should be calculated in points, given in Figure 8-b and Figure 8-c.

$$\tau(z)_d = E_i \cdot \frac{S_y(z) \cdot V_{z,d}}{EI_{y,ef} \cdot b(z)} \quad \text{Eq. 8-1}$$

with

|             |   |
|-------------|---|
| $\tau(z)_d$ | Design shear stress at a given coordinate “z” [N/mm <sup>2</sup> ]  |
| $E_i$       | Young’s modulus of the respective layer/rib – see Table 5-1 [N/mm <sup>2</sup> ]  |
| $S_y(z)$    | Static moment at the coordinate “z”, about the Y-axis [mm <sup>3</sup> ]  |
| $V_{z,d}$   | Design shear force [N]  |
| $I_{y,ef}$  | Effective moment of inertia about the Y-axis [mm <sup>4</sup> ]   |
| $EI_{y,ef}$ | Effective bending stiffness about the Y-axis <u>based on the effective width at the supports</u> (section 5.3.2) [N.mm <sup>2</sup> ] |

$b(z)$  Width of the section at given "z" coordinate

For shear parallel to grain design at the COG and glue line :  $b(z) = b_w$

For rolling shear design:  $b(z) = b_{eff,r}$  → see Eq. 5-6 and Figure 5-f.

$$S_y(z) = \sum_i A_i \cdot e_{z,i} \quad \text{Eq. 8-2}$$

where

$S_y(z)$  Static moment at the coordinate "z", about the Y-axis [mm<sup>3</sup>]  
 $A_i$  Area of the partial surface "i" [mm<sup>2</sup>]  
 $e_{z,i}$  Eccentricity of the partial surface "i" = distance between partial C.O.G. of partial surface "i" and total C.O.G. of the entire section [mm]

### 8.1.1 Simplified approximation

If the cross-section values are calculated by computer, Eq. 8-1 is the clearer and most precise way but if it is done "manually" or for a quick check, the given simplification (which is always conservative) can be used.

Be aware that the effective width at the supports is not valid with this simplified approximation. Also, the cross-section values there are not correct. Directly above the supports, the rib panel is more a "web section".  $b_{ef}$  is first valid in a distance of approx. 1 x h from the support.

Assumption: Directly above the supports the total shear force is carried by a T-formed cross-section.

#### Simplified verification of shear stresses parallel to grain:

A reduction of the design shear force according to EN 1995-1-1, section 6.1.7 (2) may be considered. The shear stresses of the GLT rib and the CLT element (at the glue line) shall be determined with the equations in section 8.1 considering the effective width of the CLT element according to section 5.3.2 Effective width  $b_{ef}$  for rib panels under single point loads at the support as an approximation.

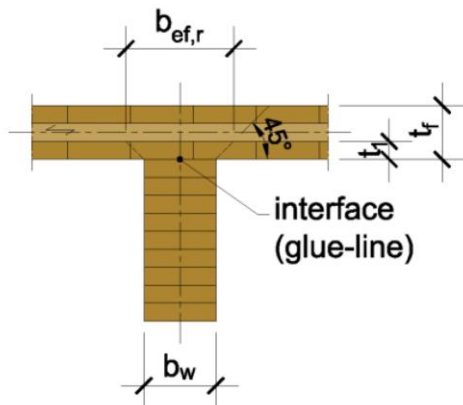
As an approximation the shear stresses of the GLT rib and the CLT panel (glue line) at the support may be determined using the (net) cross section of the rib ( $A_{net,w} = b_w \cdot h_w$ ).

$$\tau_d = 1.20 \cdot \frac{E_i}{E_{ref}} \cdot \frac{V_d}{A_{net,w}} \quad \text{Eq. 8-3}$$

with

$\tau_d$  design value of shear stress in the CoG of the T-shaped cross-section [N/mm<sup>2</sup>]  
 $E_i$  modulus of elasticity in point "i" (for layers parallel to grain) [N/mm<sup>2</sup>]  
 $E_{ref}$  reference modulus of elasticity [N/mm<sup>2</sup>]  
 $V_d$  design value of shear force [N]  
 $A_{net,w}$  net cross section of the rib (web) [mm<sup>2</sup>]

**Simplified verification of rolling shear stresses in the first cross layer closed to the glue-line:**



The shear stresses of the GLT rib and the CLT element shall be determined with the equations given in section 8.1 considering the effective width of the CLT element according to section 5.3.2 Effective width  $b_{ef}$  for rib panels under single point loads at the support as an approximation.

The rolling shear stresses in the CLT element can be computed as a simplification according to the following equation:

$$\tau_{r,d} = \tau_d \cdot \left(1 - \frac{t_n}{t_{CLT}}\right) \cdot \frac{b_w}{b_w + 2 \cdot t_n} \quad \text{Eq. 8-4}$$

with

|              |  |
|--------------|--|
| $\tau_{r,d}$ | design values of rolling shear stress (in the first CLT cross layer close to the glue-line) [N/mm <sup>2</sup> ] |
| $\tau_d$     | design value of shear stress in the CoG of the T-shaped cross-section [N/mm <sup>2</sup> ]                       |
| $t_n$        | thickness of the outermost CLT layer close to the glue-line [mm]   |
| $t_{CLT}$    | (total) thickness of the CLT element [mm]  |
| $b_w$        | width of the rib [mm]  |

## 8.2 Shear stress verification

### 8.2.1 Shear parallel to grain

The shear stresses parallel to grain should satisfy the following requirement in GLT ribs

$$\tau_{i,d} \leq f_{v,0,GLT,d} \quad \text{Eq. 8-5}$$

with

$$f_{v,0,GLT,d} = \frac{k_{mod} \cdot k_{cr} \cdot f_{v,0,GLT,k}}{\gamma_{m,GLT}} \quad \text{Eq. 8-6}$$

where

|                  |  |
|------------------|--|
| $\tau_{i,d}$     | Design shear stress in at a given point “i” in the section, located in the rib (GLT) [N/mm <sup>2</sup> ]  |
| $f_{v,0,GLT,d}$  | Design shear strength parallel to grain for glued laminated timber [13] [N/mm <sup>2</sup> ]   |
| $k_{mod}$        | Factor, according to EN1995-1-1 [3], Table 3.1, taking a load duration (permanent – very short) and the utilization class (1-3) into consideration |
| $k_{cr}$         | Crack coefficient according to EN 1995-1-1 [3], item 6.1.7   |
| $f_{v,0,GLT,k}$  | Characteristic shear strength parallel to gran of the GLT, according to EN 14080 [13] [N/mm <sup>2</sup> ]   |
| $\gamma_{m,GLT}$ | Partial safety coefficient, applicable for GLT, according to EN1995-1-1 [3], Table 2.3, or some local regulations.                                 |

The shear stresses parallel to grain should satisfy the following requirement in CLT panels:

$$\tau_{i,d} \leq f_{v,0,CLT,d} \quad \text{Eq. 8-7}$$

with

$$f_{v,0,CLT,d} = \frac{k_{mod} \cdot f_{v,0,CLT,k}}{\gamma_{m,CLT}} \quad \text{Eq. 8-8}$$

where

- $f_{v,0,CLT,d}$  Design shear strength parallel to grain for CLT [N/mm<sup>2</sup>]
- $k_{mod}$  Factor, according to EN1995-1-1 [3], Table 3.1, taking a load duration (permanent – very short) and the utilization class (1-3) into consideration
- $f_{v,0,CLT,k}$  Characteristic shear strength parallel to grain of the CLT lamination material, according to ETA [2] [N/mm<sup>2</sup>]
- $\gamma_{m,CLT}$  Partial safety coefficient, applicable for CLT, according to either EN1995-1-1, Table 2.3, or some local regulations.  
For Austria: EN1995-1-1 NA [3], chapter K.2.4 proposes  $\gamma_{m,CLT} = 1,25$

## 8.2.2 Rolling shear: (shear perpendicular to grain)

The shear stress perpendicular to grain should satisfy the following requirement in CLT panel:

$$\tau_{i,r,d} \leq f_{r,CLT,d} \quad \text{Eq. 8-9}$$

with

$$f_{r,CLT,d} = \frac{k_{mod} \cdot f_{r,CLT,k}}{\gamma_{m,CLT}} \quad \text{Eq. 8-10}$$

where

- $f_{r,CLT,d}$  Design rolling shear strength for CLT [N/mm<sup>2</sup>]
- $k_{mod}$  Factor, according to EN1995-1-1 [3], Table 3.1, taking a load duration (permanent – very short) and the utilization class (1-3) into consideration
- $f_{r,CLT,k}$  Characteristic rolling shear strength of the CLT lamination material, acc to ETA [2] [N/mm<sup>2</sup>]
- $\gamma_{m,CLT}$  Partial safety coefficient, applicable for CLT, according to EN1995-1-1 [3], Table 2.3, or some local regulations.

## 8.3 Shear of the glue line

As mentioned above in chapter 8, the shear stress in the joint between the GLT rib and CLT panel must be analyzed. Shear tests (large and small scale) have shown that the shear strength of the glue line is higher than the shear strength of the timber parts that are glued to another. The shear failure will not occur directly in the glue joint, but in the timber adjacent to the glue line that will fail in shear parallel to the grain or rolling shear. Therefore, it is assumed that sufficient shear strength in the joint is given, if the design requirements in item 8.2 are met.

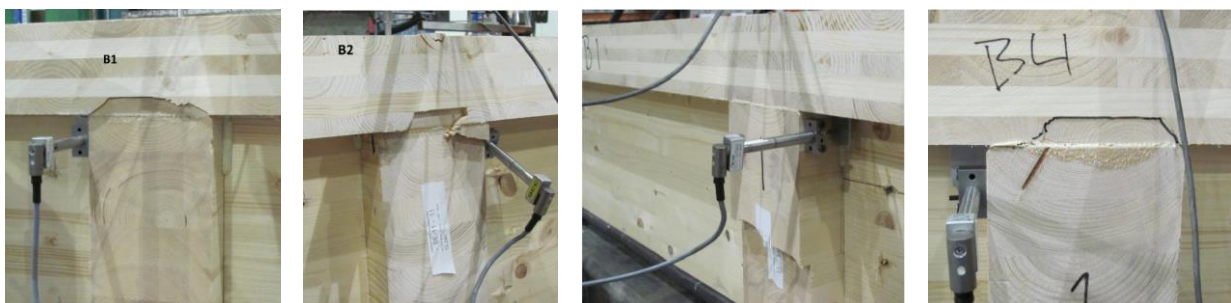


Figure 8-d: shear failure modes with large scale test of CLT Rib Panels

## 8.4 In-plane shear stress in CLT panels

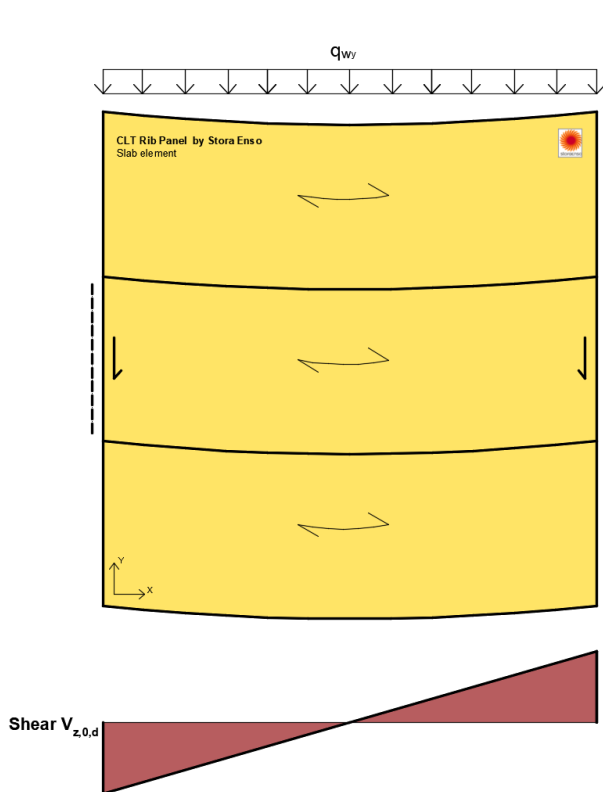


Figure 8-e: In-plane shear in Y direction

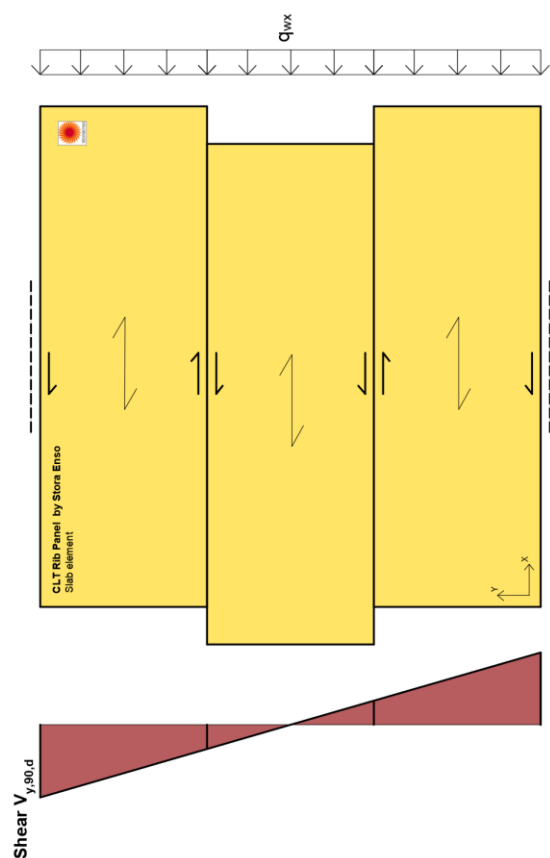


Figure 8-f: Figure 8-g: In-plane shear in X direction

The in-plane shear stress within a CLT panel shall be analyzed for two failure modes:

- Shear in end-grain sections (mechanism I), slightly different from shear in net section method (Figure 8-i)
- Torsional shear in the glue line of the face gluing (mechanism II) (Figure 8-j)
- Shear in the gross section is not relevant (Figure 8-h)

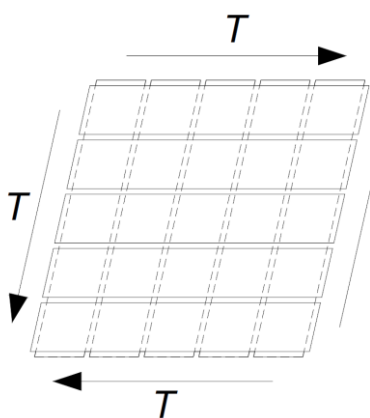


Figure 8-h: Shear of the entire panel (gross section)

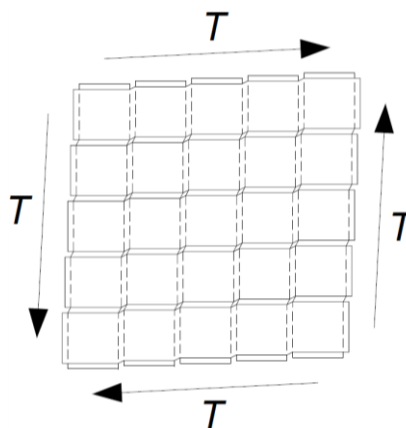


Figure 8-i: Shear failure in the joints between the boards (net section)

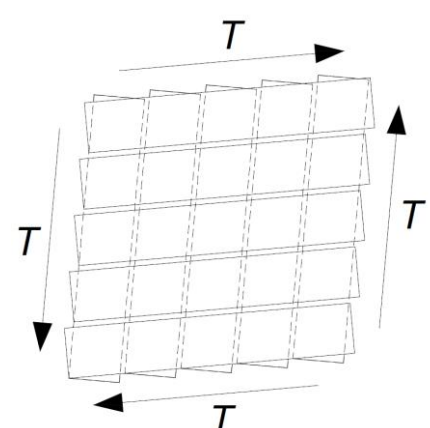


Figure 8-j: Torsional shear failure of the intersection points

Both mechanisms (see Figure 8-k: mechanism I – shear, and see Figure 8-l: mechanism II – torsion) must be verified separately.

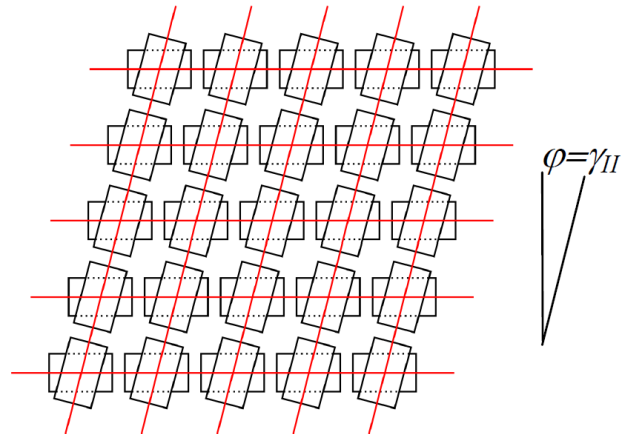
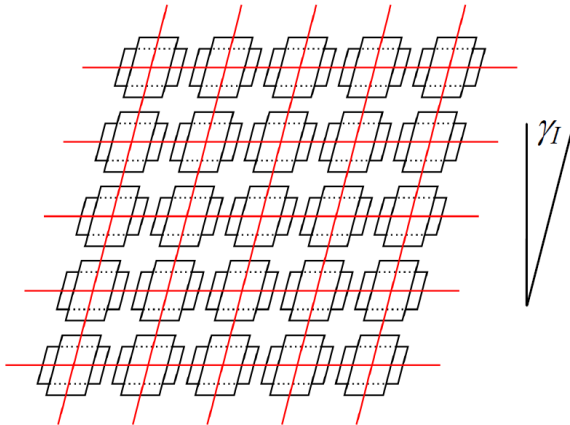


Figure 8-k: Mechanism I “shear” + shear deformation  $\gamma_I$

Figure 8-l: Mechanism II “torsion” + shear deformation  $\gamma_{II}$

In contrast to the following method, in some technical approvals or expertise ([2] or [14]) the verification of mechanism I is based on the net cross section area (Figure 8-i). In case of constant layer thicknesses, both methods produce identical results but, for varying layer thicknesses, differences can occur.

Also, mechanism II is regulated in some technical approvals. However, the specified equations in the approvals are only valid for quadratic rectangular CLT elements, with constant layer thickness, without openings, under constant shear. In that case, the following approach proposed here and that given in the approvals lead to identical results. If there is a large variation in layer thicknesses, significant differences will occur.

The following method shall be followed for in-plane shear design of CLT elements.

## 8.4.1 Representative Volume Element (RVE)

The shear design is being executed on a representative volume element (RVE) that leads to a representative sub-volume element (RSVE) according to method developed in [15] and [16].

The RVE is defined by a thickness equivalent to the CLT element  $t_{CLT}$ , with a square surface equivalent to a node of crossed boards, with lateral length equivalent to the board’s width plus half of the gap width on both sides. This RVE is further subdivided into RVSEs. These have the same square surface and a thickness  $t_i^*$ , which is composed of the minimum of the adjacent halved board thicknesses on both sides of the adhesive layer, as plane of symmetry (see Figure 8-m).

Theoretically, the RVSE is based on the assumption of an infinite number of layers of constant thickness. Thus, boundary effects, as consequence of a finite number of layers, are neglected. These effects must be considered in a separate step, which will be explained later (8.4.2.2).

The RVE is solely stressed in-plane (normal forces  $n_x$  and  $n_y$ , shear force  $n_{xy}$ ), thus stresses and strains are constant over the entire thickness  $t_{CLT}$ . The design method, which is according to [15] is generally applicable for two-dimensional plane CLT elements loaded in-plane (for CLT which is used as linear element (e.g. beams) loaded in-plane, different considerations have to be made).



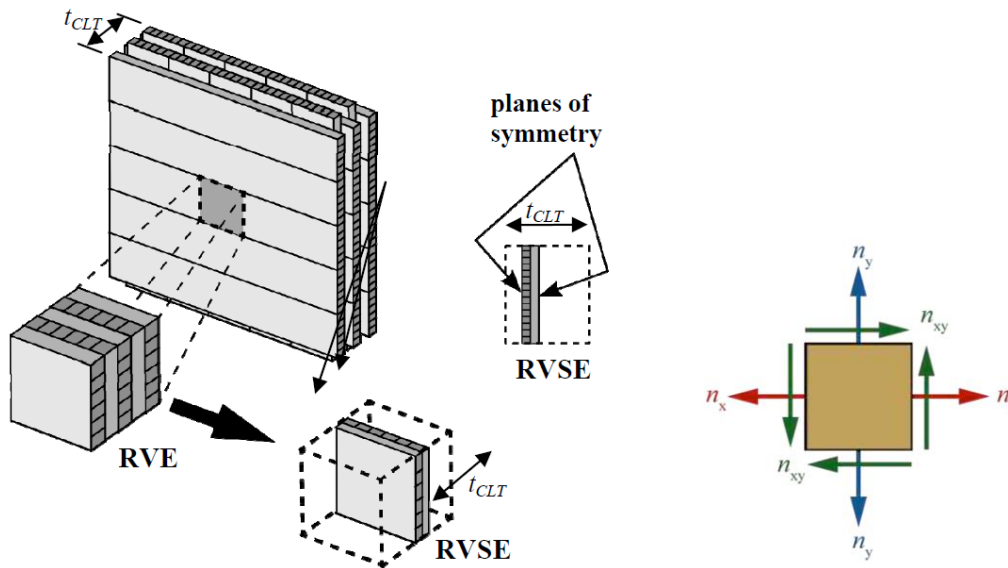


Figure 8-m: Definition of RVE and RVSE on a CLT element (left) and acting forces on a RVE (right)

## 8.4.2 ULS verifications for shear force $n_{xy}$

Calculation of design shear stresses can be divided into two steps. In a first step the situation in the ideal RVSE element, which represents an infinite sequence of layers in thickness direction, is presented in 8.4.2.1. In a second subsequent step an extension to a real CLT element with finite number of layers is carried out (see 8.4.2.2).

### 8.4.2.1 Design stresses for shear force $n_{xy}$ in RVSE

As a single RVSE is part of an infinite sequence of RVSEs, it is not possible to establish an overall shear force  $n_{xy}$  in this theoretical case. It is only possible to calculate a proportional shear force  $n_{xy,RVSE(i)}$  which acts in one single RVSE. The nominal shear stress  $\tau_0$ , associated with this RVSE, can be calculated with Eq. 8-11.

$$\tau_0 = \frac{n_{xy,RVSE}}{a \cdot t} \quad \text{Eq. 8-11}$$

The nominal shear stress  $\tau_0$  does not take into account the internal structure of the CLT-element. Shear stresses  $\tau_0$  act both on the end cross sections and narrow faces of the boards (Figure 8-n). Up to this step, the internal structure of CLT remains unconsidered. In a CLT-element shear forces are only transmitted via cross sections perpendicular to grain from one RVSE to the next as explained previously.

Not all CLT products use boards glued on the narrow faces. Even so, the occurrence of cracks due to swelling and shrinkage cannot be prevented. Thus, shear stresses can only appear in end grain sections (cross sectional areas), narrow faces are free of those stresses. Therefore, shear forces can only be transferred indirectly across the crossing of two boards in adjacent layers. Due to shear forces acting in different planes, torsional stresses in the glued interface occur (see Figure 8-p).

An internal torsional moment, acting on both sides of the gluing interface, vanishes all shear stresses, located at the narrow faces of the boards (Figure 8-p). Simultaneously shear stresses, located in the cross-sectional areas, are doubled. The final stress situation in a CLT-element is shown in Figure 8-o.

The effective shear stresses  $\tau_V$  of a RVSE in the cross-sectional areas can be calculated with:



$$\tau_V = 2 \cdot \tau_0$$

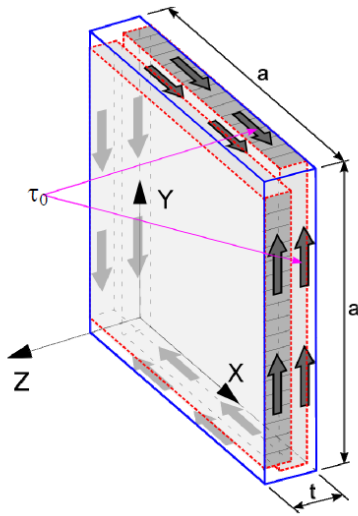


Figure 8-n: nominal shear  $\tau_0$  stress in RSVE glued on narrow faces and completely free from cracks

Eq. 8-12

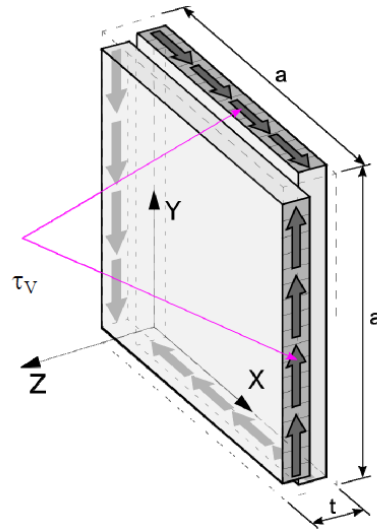


Figure 8-o: Real shear stress distribution  $\tau_V$  in RSVE (mechanism I)

The second verification must be carried out for the torsional stresses in the gluing interface due to Mechanism II (Figure 8-i).

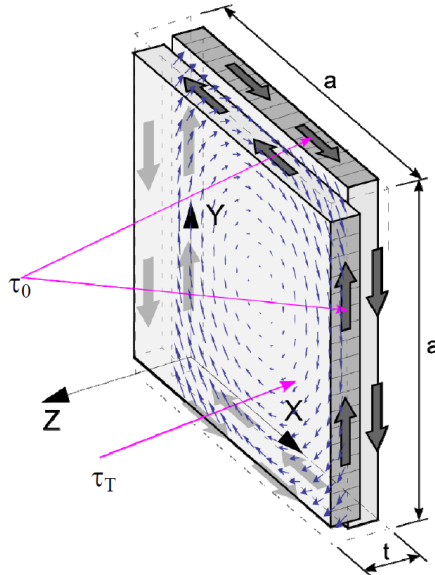


Figure 8-p: torsional shear  $\tau_T$  in glue line of RSVE (mechanism II)

The torsional moment can be calculated by

$$M_T = a^2 \cdot t \cdot \tau_0$$

Eq. 8-13

The maximal torsional stresses are defined by dividing the torsional moment  $M_T$  by the polar moment of inertia  $W_p$ .

$$\tau_T = \frac{M_T}{W_p} = \frac{\tau_0 \cdot t \cdot a^2}{\frac{a^3}{3}} = 3 \cdot \tau_0 \cdot \frac{t}{a} \quad \text{Eq. 8-14}$$

$\tau_V$  and  $\tau_T$  are the two shears stresses, which must be verified.

The design values  $\tau_{v,d}$  and  $\tau_{T,d}$  are calculated by using the design stress  $\tau_{0,d}$ .

As the torsional shear stresses  $\tau_{T,d}$  depend on the ratio  $(t/a)$ , it can be concluded, that the controlling RVSE is the thickest one.

### 8.4.2.2 Design stresses for shear force $n_{xy}$ in a CLT element

When a CLT-element with its limited, odd number of layers is regarded, the following differences to the RVSE will occur:

- number of layers oriented in both main directions of the CLT-element is not the same,
- thickness of layers is not constant,
- plane of symmetry in the middle of the boards is lost due to boundary.

One RVSE has the dimensions of two crossing boards of adjacent layers, with gaps included, times the ideal thickness  $t_i^*$  according to the scheme shown in Table 8-1. With this scheme the edge effect of a finite number of layers and varying thicknesses of layers are also considered. Of course, this approach might give conservative results. This is due to the fact that, in cases of different thicknesses of adjacent layers, only the thinner layer is taken into account.

Verification of the CLT-element shall be carried out by checking a series of ideal RVSEs, which are adjusted to the existing CLT-element. One ideal RVSE matches one gluing interface and both surrounding boards of the CLT-element as shown in Figure 8-q.

Table 8-1: Scheme for the determination of the ideal thickness  $t_i^*$  of a  $n$ -layer CLT element

| Node of RVSE                   | Layer                                  | Ideal thickness                          |
|--------------------------------|--|--|
| node 1 (= node on the top)     | layer 1 (top)<br>layer 2 (core)        | $t_1^* = \min(2 \cdot t_1; t_2)$         |
| node $i$ (= core node)         | layer $i$ (core)<br>layer $i+1$ (core) | $t_i^* = \min(t_i; t_{i+1})$             |
| node $n-1$ (= node on the top) | layer $n-1$ (core)<br>layer $n$ (top)  | $t_{n-1}^* = \min(t_{n-1}; 2 \cdot t_n)$ |

Here a conservative solution is proposed. As explained previously, when checking the  $i^{\text{th}}$  gluing interface of the CLT-element, it will be assumed, that always the thinner thickness of the two attached boards is the controlling thickness for the  $i^{\text{th}}$  RVSE.

One exception can be admitted, with the outer boards, which are connected to the first or last gluing interface and glued to only one board. Therefore, thickness of the first and last ideal RVSE with one outer board is either twice the thickness of the outer board or the ordinary thickness of the inner board, whatever is less.

A 5-layered CLT-element is illustrated in Figure 8-q. Four ideal RVSEs, connected to the gluing interfaces, exist.

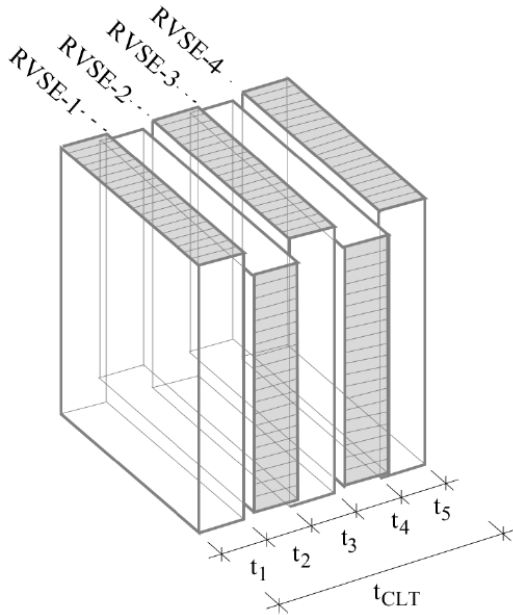


Table 8-2: thickness for ideal RVSE's of a 5 layered CLT element

| i <sup>th</sup> RVSE | Ideal thickness $t_i^*$          |
|----------------------|----------------------------------|
| 1                    | $t_1^* = \min(2 \cdot t_1; t_2)$ |
| 2                    | $t_2^* = \min(t_2; t_3)$         |
| 3                    | $t_3^* = \min(t_3; t_4)$         |
| 4                    | $t_5^* = \min(t_4; 2 \cdot t_5)$ |

Table 8-3: thickness for ideal RVSE's of a 3 layered CLT element

| i <sup>th</sup> RVSE | Ideal thickness $t_i^*$          |
|----------------------|----------------------------------|
| 1                    | $t_1^* = \min(2 \cdot t_1; t_2)$ |
| 2                    | $t_5^* = \min(t_2; 2 \cdot t_3)$ |

Figure 8-q: Ideal RVSE for a CLT-element with 5 layers

The overall thickness of all ideal RVSEs is denoted as the sum of the ideal thicknesses (see Eq. 8-15) and thus is always smaller than or equal to the geometric overall thickness  $t_{CLT}$  of the CLT-element. Usually symmetry is given in thickness direction, resulting in  $t_4=t_2$  and  $t_5=t_1$ .

Determination of ideal RVSEs thickness shall be carried out analogously in case of a 3-, 5-, 7- or more layered CLT elements. Ideal thicknesses of the two RVSE are given exemplary in Table 8-3, for a 3-layered CLT-element.

$$t^* = \sum_{i=1}^{n-1} t_i^* \leq t_{CLT} \tag{Eq. 8-15}$$

$n$  being the number of layers

The proportionate shear force  $n_{xy,RVSE(i)^*}$  of the  $i^{th}$  RVSE in an  $n$ -layered CLT-element can be determined by the following equation, which assumes a thickness-related participation of each RVSE in bearing the shear force  $n_{xy}$ .

$$n_{xy,RVSE(i)^*} = n_{xy} \cdot \frac{t_i^*}{t^*} = n_{xy} \cdot \frac{t_i^*}{\sum_{i=1}^{n-1} t_i^*} \tag{Eq. 8-16}$$

The ideal nominal shear stress  $\tau_{0,RVSE(i)^*}$  can be calculated by dividing the proportionate shear force  $n_{xy,RVSE(i)^*}$  by the thickness  $t_i^*$  of the  $i^{th}$  RVSE. This leads to a constant nominal shear stress  $\tau_0^*$  for all RVSEs (see following Eq. 8-17).

$$\tau_{0,RVSE(i)^*} = \frac{n_{xy} \cdot \frac{t_i^*}{\sum_{i=1}^{n-1} t_i^*}}{t_i^*} = \frac{n_{xy}}{\sum_{i=1}^{n-1} t_i^*} = \frac{n_{xy}}{t^*} = \tau_0^* \tag{Eq. 8-17}$$

Design shear stresses for verification of ULS can be calculated similar to ideal RVSE, given in 8.4.3. As presented below, the nominal shear stress  $\tau_0$  must be replaced by the ideal nominal shear stress  $\tau_0^*$  given in Eq. 8-17.

### For mechanism I:

the size of effective shear stress  $\tau_{v,d}$ , of a RVSE in the cross-sectional area, can be calculated with Eq. 8-18. It is twice the ideal nominal shear stress and equal for all ideal RVSEs.

$$\tau_{v,d} = 2 \cdot \tau_{0,d}^* \quad \text{Eq. 8-18}$$

with

|                |  |
|----------------|--|
| $\tau_{v,d}$   | effective design shear stress of a RVSE in the cross-sectional area [N/mm <sup>2</sup> ] |
| $\tau_{0,d}^*$ | design nominal shear stress for all RVSEs [N/mm <sup>2</sup> ]                           |

### Note:

*For determination of the shear stress, a constant distribution over width of the board, contrary to a quadratic distribution as well-known from rectangular cross sections of a linear element ( $\tau_{max}$  is of a factor 3/2 higher than the constant supposed value), is assumed. This can be expected because the assumptions of the beam theory (constant shear force distribution as well as free shear warping on the boundary) is not satisfied. Instead, it can be assumed that interference by the locked structure of the CLT plate will lead to a rather constant shear stress distribution.*

*In contrast to the previously mentioned method, in some technical approvals (SE ETA as well) the verification of mechanism I is based on the net cross section area. In case of constant layer thicknesses, both methods produce identical results but, for varying layer thicknesses, differences can occur.*

### For mechanism II:

each node (glued interface) of the RVE has to be verified. The RVSE with the largest ideal thickness  $t_i^*$  is decisive, because there the maximum torsional moment,  $M_{T,i}$  appears (see Eq. 9-20).

$$M_{T,i} = a^2 \cdot t_i^* \cdot \tau_{0,d}^* \quad \text{Eq. 8-19}$$

The torsional stress,  $\tau_{T,d}$  (see Eq. 8-20), is defined by dividing the torsional moment  $M_{T,i}$ , by the polar moment of resistance  $W_p$ , (see Eq. 8-21).

$$\tau_{T,d} = \frac{M_{T,i}}{W_p} = \frac{\tau_{0,d}^* \cdot t_i^* \cdot a^2}{\frac{a^3}{3}} = 3 \cdot \tau_{0,d}^* \cdot \frac{t_i^*}{a} \quad \text{Eq. 8-20}$$

$$W_p = \frac{I_p}{\frac{a}{2}} = \frac{a^3}{3} \quad \text{Eq. 8-21}$$

The polar moment of resistance  $W_p$ , is composed of the polar moment of inertia of the glued interface  $I_p$  according to Eq. 8-22, and the edge distance,  $a/2$  (assumption: dimension of the glued interface  $a \cdot a$ ).

$$I_p = I_y + I_z = \frac{a \cdot a^3}{12} + \frac{a^3 \cdot a}{12} = \frac{a^4}{6} \quad \text{Eq. 8-22}$$

with

|                |   |
|----------------|---|
| $M_{T,i}$      | design torsional moment in $i^{\text{th}}$ RVSE [N.mm]                        |
| $a$            | dimension of the gluing interface, which is identical to the board width [mm] |
| $t_i^*$        | largest $i^{\text{th}}$ RVSE ideal thickness [mm]                             |
| $\tau_{0,d}^*$ | design nominal shear stress for all RVSEs [N/mm <sup>2</sup> ]                |
| $\tau_{T,d}$   | maximal design torsional stress [N/mm <sup>2</sup> ]                          |
| $I_P$          | polar moment of inertia of the gluing interface [mm <sup>4</sup> ]            |
| $W_P$          | polar moment of resistance/polar section modulus [mm <sup>3</sup> ]           |

Note:

Also, mechanism II is regulated in some technical approvals. However, the specified equations in the approvals are only valid for rectangular CLT elements, with constant layer thickness, without openings, under constant shear. In that case, the approach proposed here and that given in the approvals lead to identical results. If there is a large variation in layer thicknesses, significant differences will occur.

### 8.4.3 In plane shear in the net section of CLT

The in-plane shear stresses should satisfy the following requirement in CLT panels:

$$\tau_{v,d} \leq f_{v,ip,CLT,d} \quad \text{Eq. 8-23}$$

where

$$f_{v,ip,CLT,d} = \frac{k_{mod} \cdot f_{v,ip,CLT,k}}{\gamma_{m,CLT}} \quad \text{Eq. 8-24}$$

with

|                  |   |
|------------------|---|
| $f_{v,ip,CLT,d}$ | Design in-plane shear strength for CLT  |
| $k_{mod}$        | Factor, according to EN1995-1-1 [3], Table 3.1, taking a load duration (permanent – very short) and the utilization class (1-3) into consideration  |
| $f_{v,ip,CLT,k}$ | Characteristic in-plane shear strength of the CLT lamination material, according to [14]<br>$f_{v,ip,CLT,k} = 8,0 \text{ N/mm}^2$ (For mechanism I – shear)<br>$f_{v,gross,CLT,k} = 3,5 \text{ N/mm}^2$ (For shear of the entire panel (gross section)) |
| $\gamma_{m,CLT}$ | Partial safety coefficient, applicable for CLT, according to either EN1995-1-1, Table 2.3, or some local regulations.<br>For Austria: EN1995-1-1 NA [3], chapter K.2.4 proposes $\gamma_{m,CLT} = 1,25$   |

### 8.4.4 In plane torsional shear in the glue line of the face gluing of CLT

The in-plane torsional shear stresses should satisfy the following requirement in CLT panels:

$$\tau_{T,d} \leq f_{T,ip,CLT,d} \quad \text{Eq. 8-25}$$

where

$$f_{T,ip,CLT,d} = \frac{k_{mod} \cdot f_{T,ip,CLT,k}}{\gamma_{m,CLT}} \quad \text{Eq. 8-26}$$

with

|                  |   |
|------------------|---|
| $f_{T,ip,CLT,d}$ | Design in-plane torsional shear strength for CLT  |
| $k_{mod}$        | Factor, according to EN1995-1-1 [3], Table 3.1, taking a load duration (permanent – very short) and the utilization class (1-3) into consideration  |
| $f_{T,ip,CLT,k}$ | Characteristic in-plane torsional shear strength of the CLT lamination material, according to [14] for mechanism II – torsion<br>Spruce: $f_{T,ip,CLT,k} = 2,5 N/mm^2$<br>Pine: $f_{T,ip,CLT,k} = 3,0 N/mm^2$ |
| $\gamma_{m,CLT}$ | Partial safety coefficient, applicable for CLT, according to either EN1995-1-1, Table 2.3, or some local regulations. For Austria : EN1995-1-1 NA [3], chapter K.2.4 proposes $\gamma_{m,CLT} = 1,25$         |

## 9 Voids in the glulam rib

Holes are openings with a clear dimension  $d \geq h/10$  with  $h$ , being the height of the rib or  $d \geq 80\text{mm}$ . For smaller voids, an analysis as laid out in the following shall not be required, however the opening shall be taken into account in the structural analysis, by using the existing net section (section minus void).

In the current European standard for the design of timber structures EN 1995-1-1 [17] no explicit rules for the verification of holes in beams (loaded in bending) are given. Nevertheless, rules for the handling of this important topic are defined in a few National Annexes of the mentioned standard.

According to ÖNORM B 1995-1-1:2015 [18] the application of unreinforced circular and rectangular holes is restricted to service class 1 and 2.

In general, it is not allowed to carry out on the building site openings not planned in the design.

For the placement of voids and openings of any size, the boundary conditions as indicated in the figure below shall be respected. All corners shall be rounded with a minimum diameter of 15mm.

General boundary condition: Austrian standard ÖNORM B 1995-1-1:2015, Annex F [18]

|                           |                          | <b>Unreinforced</b>  |
|---------------------------|--------------------------|--|
| <b>Minimum distances</b>  | <i>End</i>               | $l_v \geq h$   |
|                           | <i>Spacing</i>           | $l_z \geq \min\left(\frac{1,5 \cdot h}{300\text{mm}}\right)$   |
|                           | <i>Support</i>           | $l_A \geq 0,5 \cdot h$   |
|                           | <i>Edges</i>             | When the hole centre is situated at neutral axis:<br>$h_{ro} \geq 0,425 \cdot h$ and $h_{ru} \geq 0,425 \cdot h$<br><br>When the hole centre is situated eccentrically to the neutral axis (eccentricity) :<br>$h_{ro} \geq 0,35 \cdot h$ and $h_{ru} \geq 0,35 \cdot h$ |
| <b>Maximum dimensions</b> | <i>Rectangular holes</i> | $h_d \leq 0,15 \cdot h$<br>$a \leq 2,5 \cdot h$  |
|                           | <i>Circular holes</i>    | $d \leq 0,15 \cdot h$  |

In Figure 9-a and Figure 9-b, the geometric boundary conditions regarding holes in beams are shown.

### Circular holes:

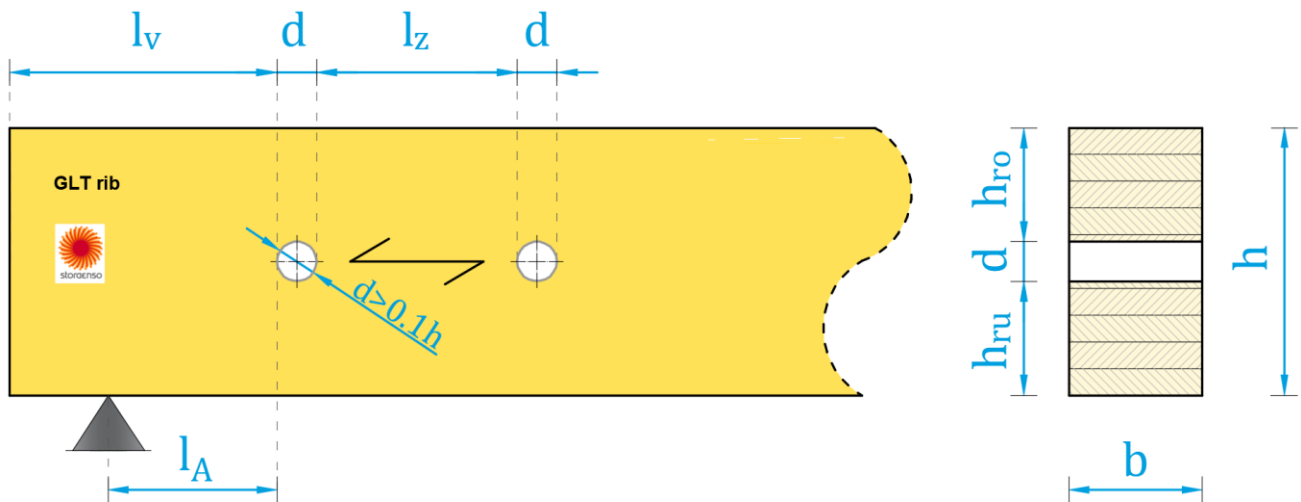


Figure 9-a: Definitions of geometric dimensions related to circular holes

**Rectangular holes:** The radius of curvature at each corner shall be at least 15 mm.

- $a \leq 2.5 \cdot h$

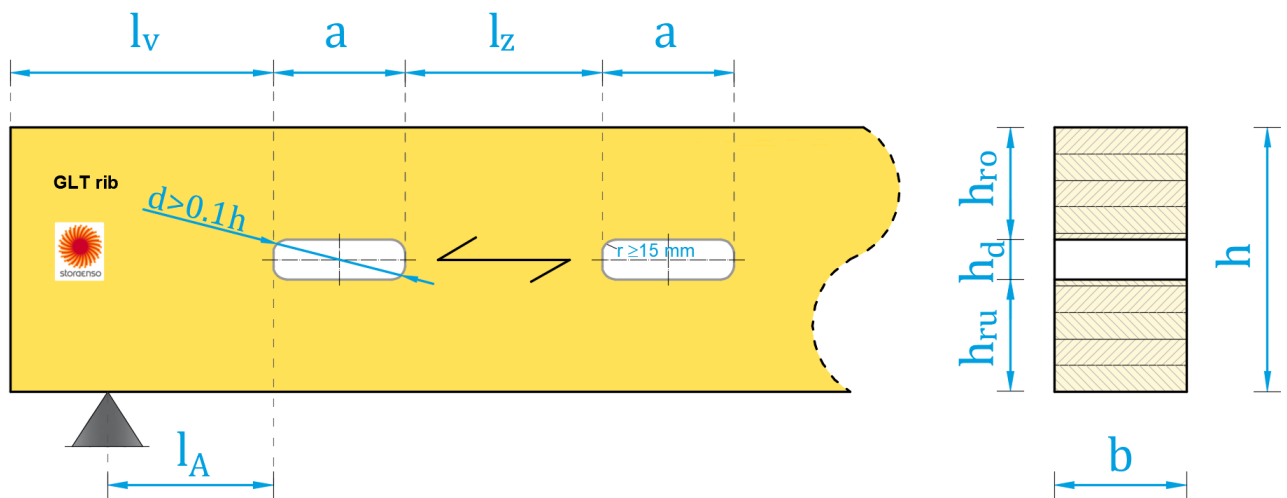


Figure 9-b: Definitions related to rectangular holes

with

- $h$  Depth of the GLT rib [mm];
- $h_d$  Diameter or height of the opening [mm];
- $l_z$  Spacing parallel to grain between holes edge [mm];
- $l_v$  Distance parallel to grain between the end of the beam and the closest hole edge [mm];
- $h_{ro}$  Distance from the upper edge of the hole to the upper edge of the member [mm];
- $h_{ru}$  Distance from the lower edge of the hole to the lower edge of the member
- $a$  Length of the rectangular opening [mm]; for circular holes  $a = h_d$ .

Only unreinforced voids shall be covered within this document.



Extreme climate exposure of the end grain surfaces shall be avoided.

For unreinforced holes, according to [19], the stress components at the corners of the holes in tension perpendicular to grain, shear and bending must be verified.

## 9.1 Verification of tension force perpendicular to grain (splitting)

For the verification of the splitting stress, the following condition shall be fulfilled:

$$\sigma_{t,90,d} = \frac{F_{t,90,d}}{0,5 \cdot l_{t,90} \cdot b_{ef} \cdot k_{t,90}} \leq f_{t,90,d} \quad \text{Eq. 9-1}$$

where

$$k_{t,90} = \min \left\{ \left( \frac{450}{h} \right)^{0,5} \right\} \quad \text{Eq. 9-2}$$

with

|                   |   |
|-------------------|---|
| $\sigma_{t,90,d}$ | Splitting stress design value[N/mm <sup>2</sup> ] |
| $F_{t,90,d}$      | Splitting force design value [N]                  |
| $l_{t,90}$        | Stress distribution length [mm]:                  |

|             |   |         |
|-------------|---|---------|
| rectangular | $l_{t,90} = 0,5 \cdot (h_d + h)$          | Eq. 9-3 |
| circular    | $l_{t,90} = 0,35 \cdot h_d + 0,5 \cdot h$ | Eq. 9-4 |

|                           |         |   |
|---------------------------|---------|---|
| $b_{ef} = k_{cr} \cdot b$ | Eq. 9-5 | Effective width of the glulam rib, see EN1995-1-1, equation (6.13a)                               |
| $f_{t,90,d}$              | $h$     | Tensile design strength perpendicular to the grain [N/mm <sup>2</sup> ]<br>Height of the rib [mm] |

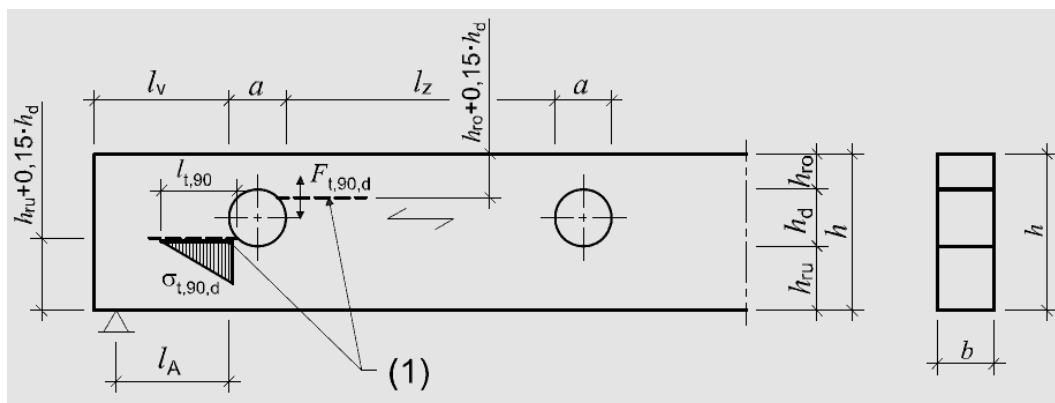


Figure 9-c: Splitting stress distribution with circular holes [18]

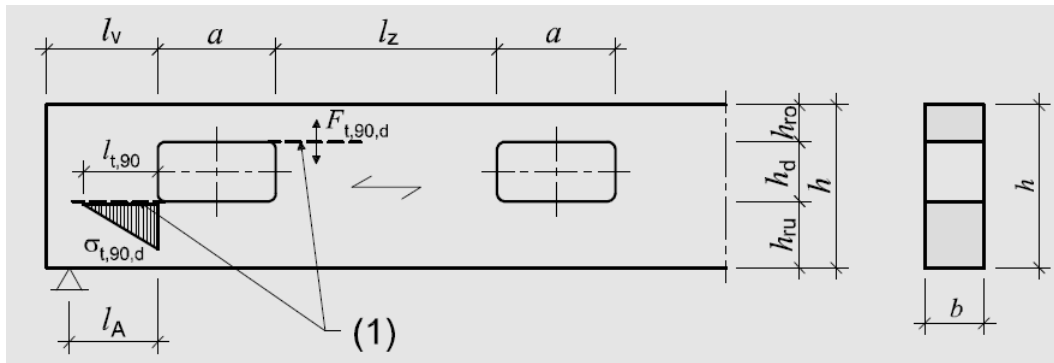


Figure 9-d: Splitting stress distribution with rectangular holes [18]

(1) potential splitting stress crack

The design splitting force shall be

$$F_{t,90,d} = F_{t,V,d} + F_{t,M,d} \quad \text{Eq. 9-6}$$

- for rectangular sections:

$$F_{t,V,d} = \Omega_{shape} \cdot \frac{V_d \cdot h_d}{4 \cdot h} \cdot \left[ 3 - \left( \frac{h_d}{h} \right)^2 \right] \quad \text{Eq. 9-7}$$

- for circular sections:

$$F_{t,V,d} = \Omega_{shape} \cdot \frac{V_d \cdot 0,7 \cdot h_d}{4 \cdot h} \cdot \left[ 3 - \left( \frac{h_d}{h} \right)^2 \right] \quad \text{Eq. 9-8}$$

and

$$F_{t,M,d} = 0,008 \cdot \frac{M_d}{h_r} \quad \text{Eq. 9-9}$$

with

- $F_{t,V,d}$  Splitting force design value, originating from shear force [N]
- $F_{t,M,d}$  Splitting force design value, originating from bending moment [N]
- $M_d$  Bending moment design value at the void limits [N.mm]
- $V_d$  Design shear value at the void limits [N]

|                  |           |             |
|------------------|-----------|-------------|
| $\Omega_{shape}$ | T-section | Box section |
|                  | 1,30      | 1,50        |

$h$  Height of the rib [mm]

$h_r$  Design height [mm]

|   |   |
|---|---|
| Rectangular   | circular  |
| $h_r = \min \left\{ \begin{matrix} h_{ro} \\ h_{ru} \end{matrix} \right.$ | $h_r = \min \left\{ \begin{matrix} h_{ro} + 0,15 \cdot h_d \\ h_{ru} + 0,15 \cdot h_d \end{matrix} \right.$ |
| Eq. 9-10  | Eq. 9-11  |

$h_d$  Height of the void [mm]

## 9.2 Verification of shear stresses for circular and rectangular holes in beams

The shear stress distribution in the section of the beam, in the area of the hole shall be analyzed as follows:

- Splitting the section in an upper T-section (above the opening) and a lower rectangular section below the opening
- Calculate the flexural rigidity  $EI$  of the upper T-section and the lower rectangular section
- Split the shear according to the rigidity to the upper and lower part of the section.
- Calculate the shear distribution over the two partial sections (above and below the void):

$$\tau_d = k_\tau \cdot \frac{V_d \cdot \sum_i (E_i \cdot A_i \cdot e_i)}{(EI)_{ef} \cdot b} \leq f_{v,d} \quad \text{Eq. 9-12}$$

where

$$k_\tau = 1,85 \cdot \left(1 + \frac{a}{h}\right) \cdot \left(\frac{h_d}{h}\right)^{0,2} \quad \text{Eq. 9-13}$$

with

|                                |   |
|--------------------------------|---|
| $\tau_d$                       | Design shear stress for either the section above or below the void [N/mm <sup>2</sup> ]                                   |
| $k_\tau$                       | Coefficient to account for the maximum design shear stress  |
| $V_d$                          | Design shear force at the void location for the section above or below the void [N]                                       |
| $(EI)_{ef}$                    | Effective bending stiffness of the section above/below the void [N.mm <sup>2</sup> ]                                      |
| $E_i$                          | Young's Modulus of the partial section "i" [N/mm <sup>2</sup> ]   |
| $A_i$                          | Area of the partial section "i" [mm <sup>2</sup> ]  |
| $e_i$                          | Eccentricity (distance from the C.O.G. of the section above/below the void to the C.O.G. of the partial section "i") [mm] |
| $\sum_i (A_i \cdot e_i) = S_y$ | Static moment about the Y-axis at the hole edge location [mm <sup>3</sup> ]   |
| $b$                            | Effective width of the rib, see EN1995-1-1 equation (6.13a)   |
| $h$                            | Height of the rib [mm]  |
| $h_d$                          | Height of the void [mm]   |
| $a$                            | Length of the void; for circular voids, $a=h_d$   |
| $f_{v,d}$                      | Design shear strength of the rib [N/mm <sup>2</sup> ]   |

## 9.3 Verification of longitudinal stresses – Bending

Verification at the edges of the hole:

The bending stress at the hole location should satisfy the following expression:

$$\frac{\frac{M_d}{W_n} + \frac{M_{o,d}}{W_o}}{f_{m,d}} \leq 1 \quad \text{Eq. 9-14}$$

and

$$\frac{\frac{M_d}{W_n} + \frac{M_{u,d}}{W_u}}{f_{m,d}} \leq 1 \quad \text{Eq. 9-15}$$

where

$$M_{o,d} = \frac{A_o}{A_u + A_o} \cdot V_d \cdot \frac{a}{2} \quad \text{Eq. 9-16}$$

$$M_{u,d} = \frac{A_u}{A_u + A_o} \cdot V_d \cdot \frac{a}{2} \quad \text{Eq. 9-17}$$

$$A_o = b \cdot h_{ro} \quad \text{Eq. 9-18}$$

$$A_u = b \cdot h_{ru} \quad \text{Eq. 9-19}$$

$$W_o = \frac{b \cdot h_{ro}^2}{6} \quad \text{Eq. 9-20}$$

$$W_u = \frac{b \cdot h_{ru}^2}{6} \quad \text{Eq. 9-21}$$

with

- $M_d$  Design value of the bending moment at the edge of the opening [N.mm];
- $W_n$  Effective cross section modulus of the beam at the position of the opening [mm<sup>3</sup>];
- $f_{m,d}$  Design value for the bending strength of the rib [N/mm<sup>2</sup>];
- $V_d$  Design value of the transversal force at the edge of the opening [N];
- $h_{ro}; h_{ru}$  Remaining heights of the net cross section [mm] According to Figure 9-a and Figure 9-b

For circular holes it is sufficient to verify the bending stresses from the beam theory effect at the edges under consideration of the net cross section (taking the void into account).

The bending stress at the location of a circular hole has to be verified by the equations:

$$\frac{M_d}{W_n} \leq f_{m,d} \quad \text{Eq. 9-22}$$

## 10 Voids in the CLT panel

Any voids and openings in the CLT panel shall be taken into account in the structural analysis, using the available net section for the stress design.

Voids in the CLT panel shall not be wider than the clear distance between the ribs and shall not be located above a rib.

## 11 Verification at the supports

CLT Rib Panels can be supported in different ways depending on the structural detailing which influence the type of verification at the supports.

### 11.1 Simple supports with blockings

This chapter shall explain the bearing pressure design at the supports of rib or box panels.

Due to the rigidity of the rib, all load coming from the rib panel itself (self-weight + all applicable surcharge), shall be led into the support through the load bearing surface of the rib (red arrows). All loading from any given wall, resting on top of the rib panel will be led through blocking between the ribs into the support (blue arrows). In case there is a wall resting on top of the rib panel at the support line, blocking between the ribs shall be mandatory.

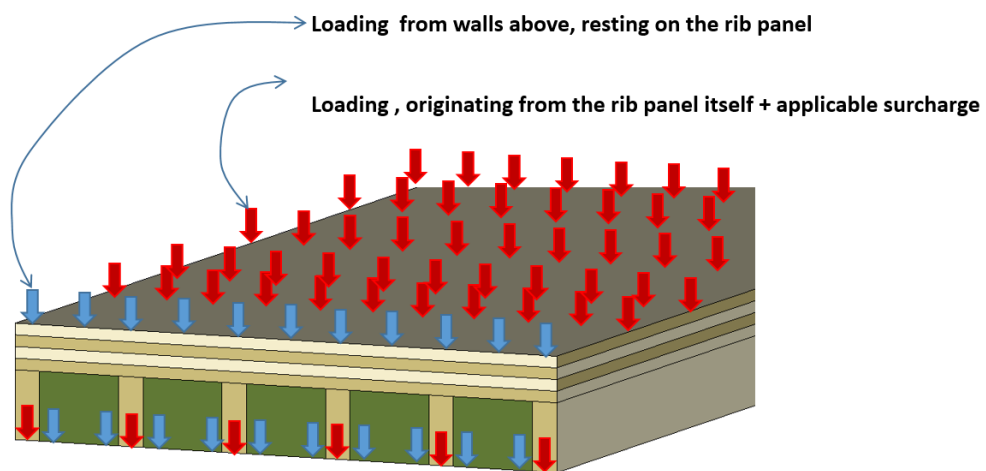


Figure 11-a: Load distribution into supports through blockings (blue) and through ribs (red)

#### 11.1.1 Bearing pressure transferred through the ribs

##### Open type:

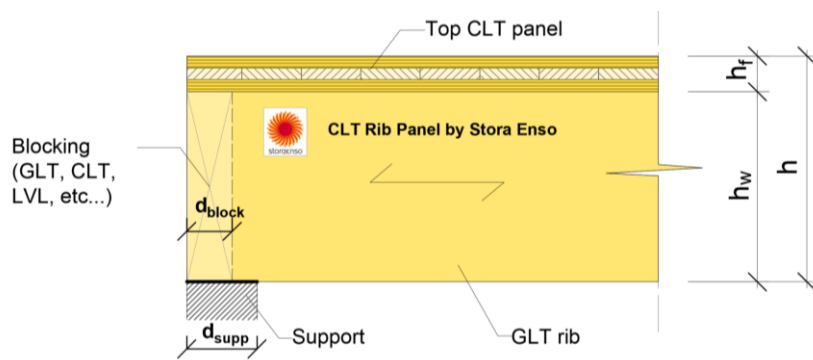


Figure 11-b: Support of a CLT Rib Panel – Open type

For the case of a CLT RP with CLT on top of the rib, the following requirement shall be fulfilled for the rib:

$$\sigma_{c,90,d} \leq k_{c,90} \cdot f_{c,90,GLT,d} \quad \text{Eq. 11-1}$$

with

$$\sigma_{c,90,d} = \frac{F_d}{b_{rib} \cdot (d_{supp} + 30mm)} \quad \text{Eq. 11-2}$$

where

|                     |  |
|---------------------|--|
| $\sigma_{c,90,d}$   | Design compressive stress perpendicular to the grain [N/mm <sup>2</sup> ]  |
| $k_{c,90}$          | Geometry factor to account for the internal stress distribution, according to EN 1995-1-1 [3], item 6.1.5 (4). [-] |
| $f_{c,90,CLT,d}$    | Design compressive strength perpendicular to the grain of the glulam rib [N/mm <sup>2</sup> ]                      |
| $F_d$               | Design support reaction per rib, originating from the rib panel itself and the surcharge applied to it [N]         |
| $b_{rib}$           | Width of the rib [mm]  |
| $(d_{supp} + 30mm)$ | Effective bearing depth of at the rib (in span direction), according to EN 1995-1-1 [3], item 6.1.5 (1). [mm]      |

### Inverted / Closed type:

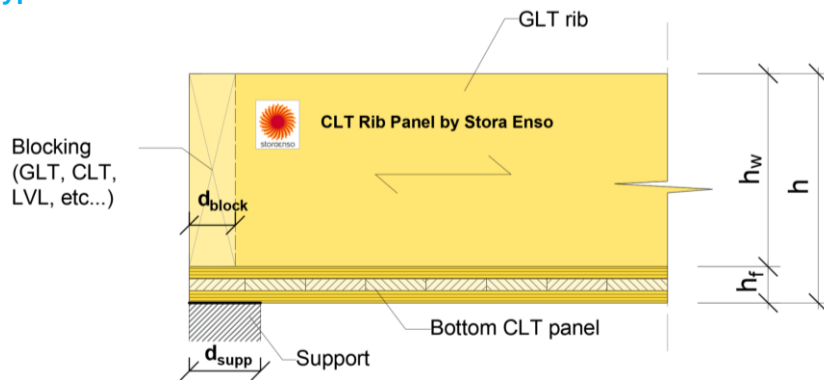


Figure 11-c: Support of a CLT Rib Panel – Inverted type

For the case of a CLT RP with CLT to the bottom of the rib, the following requirement shall be fulfilled for the bottom CLT panel:

$$\sigma_{c,90,d} \leq k_{c,90} \cdot f_{c,90,CLT,d} \quad \text{Eq. 11-3}$$

with

$$\sigma_{c,90,d} = \frac{F_d}{b_{rib} \cdot (d_{supp} + 30mm)} \quad \text{Eq. 11-4}$$

where

|                     |   |
|---------------------|---|
| $\sigma_{c,90,d}$   | Design compressive stress perpendicular to the grain for CLT [N/mm <sup>2</sup> ]   |
| $k_{c,90}$          | Geometry factor to account for the internal stress distribution, according to EN 1995-1-1 [3] and the applicable NA; See chapter 11.1.3 |
| $f_{c,90,CLT,d}$    | Design compressive strength perpendicular to grain of the CLT acc to [4] [N/mm <sup>2</sup> ]   |
| $F_d$               | Design support reaction per rib, originating from the rib panel itself and the surcharge applied to it [N]                              |
| $b_{rib}$           | Width of the rib [mm]   |
| $(d_{supp} + 30mm)$ | Effective bearing depth of at the rib (in span direction), according to EN 1995-1-1 [3], item 6.1.5 (1) [mm]                            |
| $d_{supp}$          | Depth of the support [mm]   |

## 11.1.2 Bearing pressure transferred through the blocking

### Open type:

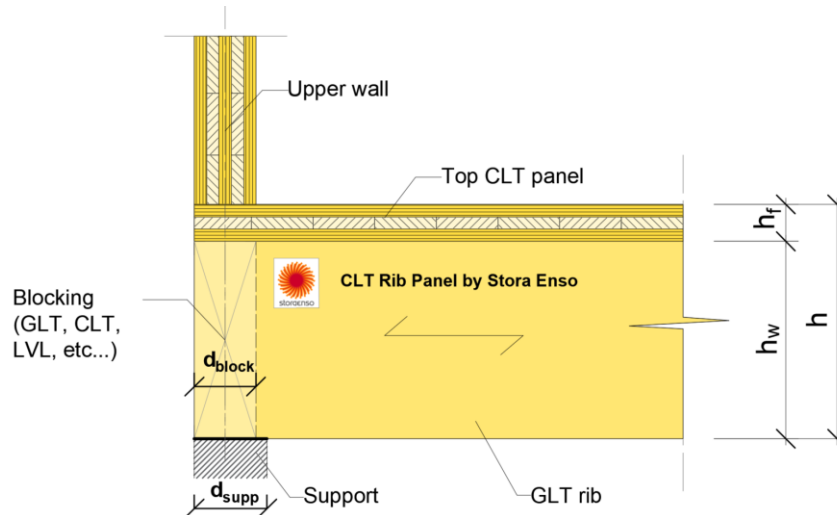


Figure 11-d: Support of a CLT Rib Panel – Open type

For the case of a CLT RP with CLT on top of the rib and compression originating from the wall above (linear load), resting on top of the rib panel, aligned with the support, the following requirement shall be fulfilled for the blocking:

$$\sigma_{c,90,d} \leq k_{c,90} \cdot f_{c,90,block,d} \quad \text{Eq. 11-5}$$

with

$$\sigma_{c,90,d} = \frac{F_{wall,d}}{l_{block} \cdot \min(d_{supp}; d_{block})} \quad \text{Eq. 11-6}$$

where

|                    |  |
|--------------------|--|
| $\sigma_{c,90,d}$  | Design compressive stress perpendicular to the grain for the blocking [N/mm <sup>2</sup> ]   |
| $k_{c,90}$         | Geometry factor to account for the internal stress distribution, according to EN 1995-1-1 [3] and the applicable NA;<br>Recommended for this situation $k_{c,90} = 1,00$ |
| $f_{c,90,block,d}$ | Design compressive strength perpendicular to the grain of the blocking [N/mm <sup>2</sup> ]  |
| $F_{wall,d}$       | Design support reaction per blocking, originating from the wall (linear load), resting on top of the rib panel, aligned with the support [N]                             |
| $l_{block}$        | Length of the blocking [mm]  |
| $d_{block}$        | Thickness of the blocking [mm]   |
| $d_{supp}$         | Depth of the support [mm]  |

In the presented case, the compressive stress perpendicular to grain applied on the top CLT panel should be verified as well:

$$\sigma_{c,90,d} \leq k_{c,90} \cdot f_{c,90,CLT,d} \quad \text{Eq. 11-7}$$

with

$$\sigma_{c,90,d} = \frac{F_{wall,d} [N/m]}{1m \cdot (t_{wall} + 30mm)} \quad \text{Eq. 11-8}$$



## Inverted / Closed type:

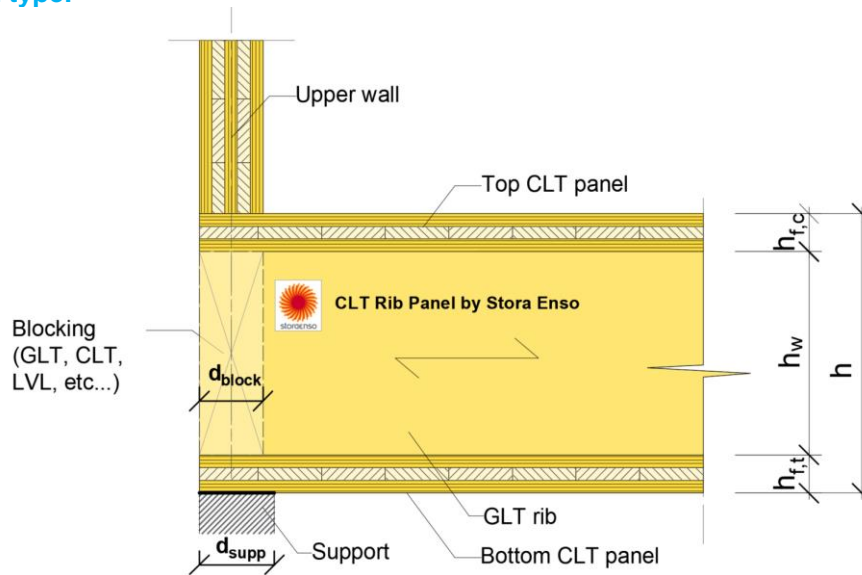


Figure 11-e: Support of a CLT Rib Panel – Closed type

For the case of a CLT RP with CLT at the bottom of the rib and compression originating from the wall above (linear load), resting on top of the rib panel, aligned with the support, the following requirement shall be fulfilled for the bottom CLT panel:

$$\sigma_{c,90,d} \leq k_{c,90} \cdot f_{c,90,CLT,d} \quad \text{Eq. 11-9}$$

with

$$\sigma_{c,90,d} = \frac{F_{wall,d}}{l_{block} \cdot [\min(d_{supp}; d_{block}) + 30\text{mm}]} \quad \text{Eq. 11-10}$$

where

|                   |  |
|-------------------|--|
| $\sigma_{c,90,d}$ | Design compressive stress perpendicular to the grain for CLT [N/mm <sup>2</sup> ]  |
| $k_{c,90}$        | Geometry factor to account for the internal stress distribution, according to EN 1995-1-1 [3] and the applicable NA; See chapter 11.1.3      |
| $f_{c,90,CLT,d}$  | Design compressive strength perpendicular to the grain of the CLT according to [4] [N/mm <sup>2</sup> ]                                      |
| $F_{wall,d}$      | Design support reaction per blocking, originating from the wall (linear load), resting on top of the rib panel, aligned with the support [N] |
| $l_{block}$       | Length of the blockig [mm]   |
| $d_{block}$       | Thickness of the blocking [mm]   |
| $d_{supp}$        | Depth of the support [mm]  |

In the presented case, the compressive stress perpendicular to grain applied on the top CLT panel should be verified as well:

$$\sigma_{c,90,d} \leq k_{c,90} \cdot f_{c,90,CLT,d} \quad \text{Eq. 11-11}$$

with

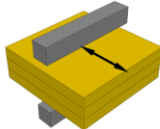
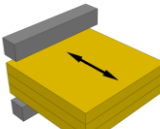
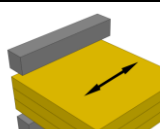
$$\sigma_{c,90,d} = \frac{F_{wall,d} [N/m]}{1\text{m} \cdot (t_{wall} + 30\text{mm})} \quad \text{Eq. 11-12}$$

### 11.1.3 $k_{c,90}$ values for CLT




$k_{c,90} = 1$  when the bearing situation is not clear.

#### 11.1.3.1 *Austrian National Annex K of ÖNORM EN1995-1-1 [11]*

The following values of  $k_{c,90}$  are valid for linear transmission of force to the assembly: according to [11]

| Linear transmission of force to the assembly   |   | $k_{c,90}$ |
|--|---|------------|
| perpendicular to the grain direction of the outer timber layer of continuous support (central) |   | 1,80       |
| perpendicular to the grain direction of the outer timber layer of discrete supports (edge)     |   | 1,50       |
| parallel to the grain direction of the outer timber layer of discrete supports (edge)          |  | 1,50       |

The following values of  $k_{c,90}$  are valid for punctual transmission of force to the assembly: according to [11]

| Punctual transmission of force to the assembly   |  | $k_{c,90}$ |
|--|--|------------|
| for edge distances larger than the thickness of Cross Laminated Timber (Central)   |  | 1,80       |
| on the edge of Cross Laminated Timber, parallel to fibre direction of surface layer, perpendicular to fibre direction of surface layer |  | 1,50       |
| in the corner of Cross Laminated Timber  |  | 1,30       |

## 11.1.3.2 Stress-dispersion model of Van der Put [20] – Alternative approach

Due to its orthogonal layup and the possibility of a two-dimensional load transfer, CLT features some specifics, which differentiate it clearly from structural timber and glulam.

Higher strength and stiffness in CLT in comparison to glulam are found which is dedicated to a “locking effect” caused by alternating reinforcement provided by the orthogonal layering. Consequently, an increase in stiffness and strength with increasing number of layers (decreasing layer thickness) is observed together with a minor reduction in the dispersion.

Applying the two angles  $\alpha_L$  and  $\alpha_T$  in analysing the stress-dispersion from layer to layer and in dependency of the support conditions (see Figure 11-f) allows to explain directly differences between (i) load configurations, (ii) support conditions, (iii) composition and thickness of the CLT elements, and (iv) the edge distances  $a$ .

This by formulating  $A_{ef} = W_{ef} \cdot l_{ef}$

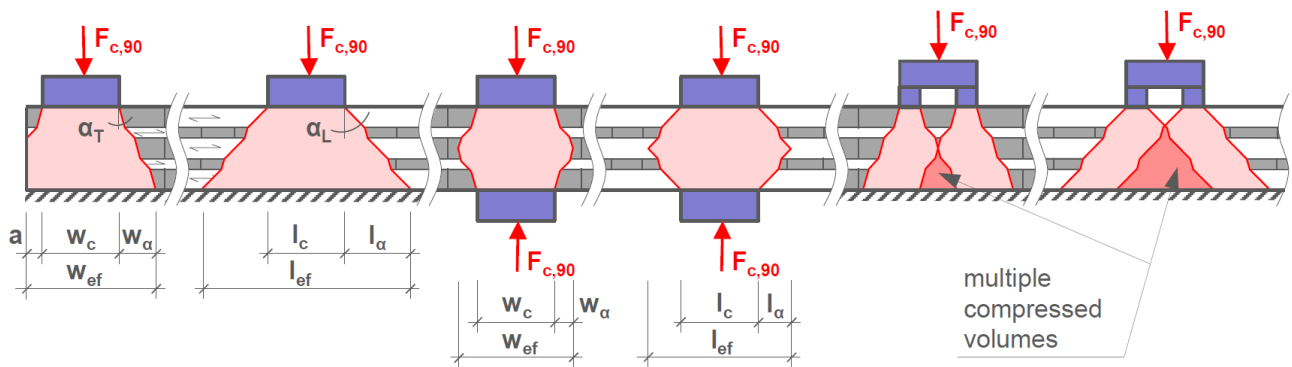


Figure 11-f : Distribution model for compression perpendicular to grain stresses in discrete loaded, continuously or discretely supported CLT-elements [20]

Consequently, an adapted stress dispersion model was formulated:

$$f_{c,90,member} = f_{c,90,prism} \cdot \sqrt{\frac{A_{ef}}{A_c}} = f_{c,90,prism} \cdot \sqrt{\frac{l_{ef} \cdot w_{ef}}{l_c \cdot w_c}} \longrightarrow k_{c,90} = \sqrt{\frac{A_{ef}}{A_c}},$$

Eq. 11-13

with

$$A_{ef} = W_{ef} \cdot l_{ef}$$

$$W_{ef} = 2 \cdot (W_c/2 + \min[a; W_\alpha])$$

$$l_{ef} = 2 \cdot (l_c/2 + \min[a; l_\alpha])$$

$$\alpha_L = 45^\circ \text{ and } \alpha_T = 15^\circ \text{ and with } a \geq (W_{ef}; l_{ef})$$

with

$$\sigma_{c,90,d} \leq k_{c,90} \cdot f_{c,90,CLT,d}$$

Eq. 11-14

$$\sigma_{c,90,d} = \frac{F_{c,90,d}}{A} = \frac{F_{c,90,d}}{W_c \cdot l_c}$$

Eq. 11-15

where



|                   |   |
|-------------------|---|
| $\sigma_{c,90,d}$ | Design compressive stress in the contact area perpendicular to the grain for CLT [N/mm <sup>2</sup> ]                                 |
| $W_{ef}$          | Effective spreading width of the compressive stress in cross direction [mm];  |
| $l_{ef}$          | Effective spreading length of the compressive stress in grain direction [mm];   |
| $k_{c,90}$        | Factor taking into account the load and support configuration and the layup of the cross laminated timber element, according to [20]; |
| $f_{c,90,CLT,d}$  | Design compressive strength perpendicular to the grain of the CLT according to [4] [N/mm <sup>2</sup> ];                              |
| $F_{c,90,d}$      | Design compressive force perpendicular to grain [N];  |
| $l_c$             | Length of the applied force in grain direction [mm];  |
| $W_c$             | Width of the applied force in cross direction [mm];   |
| $A$               | Area of the applied force perpendicular to the grain [mm <sup>2</sup> ].  |

For modelling the resistance of discrete loaded and discretely or continuously supported CLT elements against compression perpendicular to grain, the stress-dispersion model of van der Put (1988, 2008, 2012), defined for linear, unidirectional timber members, is adapted for two-dimensional load transfer in the orthogonal structure of CLT. The model presented in Eq. 11-13 and verified in [20] is successfully verified and further proposed for the design of CLT in compression perpendicular to grain using two different stress dispersion angles  $\alpha_L = 45^\circ$  and  $\alpha_T = 15^\circ$  for longitudinal and transverse direction, respectively, as already anchored in EN 1995-2:2004.

The model allows to explain directly differences between (i) load configurations, (ii) support conditions, (iii) composition and thickness of the CLT elements, and (iv) the edge distance  $a$ .

The formulation for  $k_{c,90}$  makes the consideration of the layup mandatory for an economical design of CLT structures in compression perpendicular to grain.

Overall, the outcome of this study is seen as worthwhile for regulations on test data evaluation (EN 408:2012), for anchoring basic properties of CLT stressed in compression perpendicular to grain (EN 16351:2012) and for the design of point and line loaded and continuously or discretely supported CLT elements (EN 1995-1-1:2008 and EN 1995-2:2004).

## 11.2 Supports with ribs supported individually or by mechanical joints

### 11.2.1 End beam support

In end beam support the rib panel or the box panel is supported by end beam. Figure 11-g is giving a possible solution for a rib panel with CLT on top of the beam. The system is analogous for rib panels with the CLT below the rib and for box panels. The rib or box panel is supported off the glued laminated rib. If necessary, the screw can be embedded in the CLT as well. The rib or box panel shall be hung off the end beam by the use of fully threaded screws, in an angle of 45°, so the screws are in tension. Embedment in the rib is mandatory, additional embedment in the CLT is optional. The fully threaded screw can be inserted from the side of the rib/box panel or from the side of the end beam. The embedment at both ends needs to be sufficient for the given purpose and needs to be designed accordingly.

#### Open CLT Rib Panel - End beam support

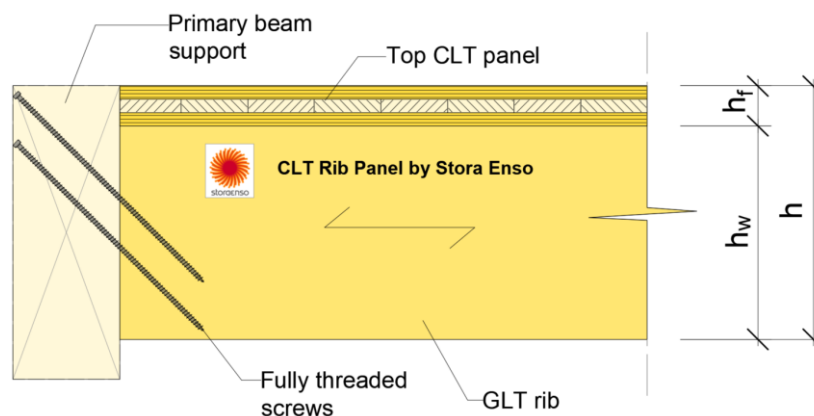


Figure 11-g: End beam support

The design of the screw shall not be treated in this document, since the axial withdrawal capacity of screws is regulated in the related ETA. All applicable spacing and edge distance needs to be executed according to the related ETA.

In case of an end beam support, if the fully threaded screw is not reaching all the way to the bottom of the beam section, a splitting stress design is required. See EN 1995-1-1, chapter 6.5 [3].

## 11.2.2 Support with individually supported ribs

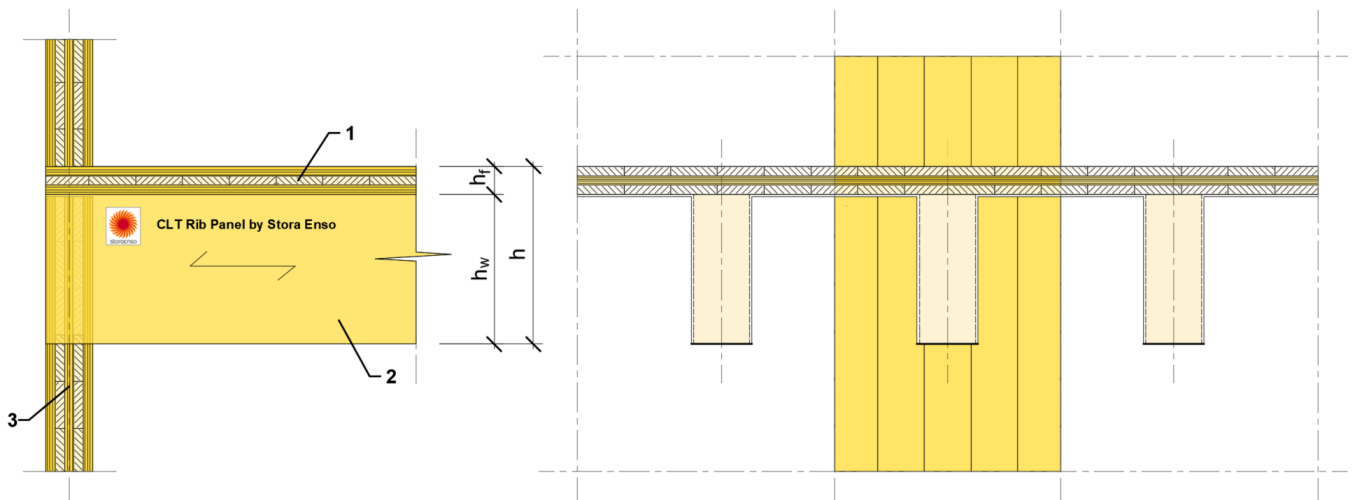


Figure 11-h: Individually supported ribs (1 ... CLT panel, 2 ... rib, 3 ... supporting member)

The vertical load of the CLT Rib Panel members is transferred by the ribs to the supports and the ribs are loaded in compression perpendicular to grain.

Remark: To avoid loadings with tensile stresses perpendicular to the grain and to the gluing-line, it has to be ensured, that the CLT top panel is not loaded by supporting elements below (e.g. walls, blockings, etc.) through rotation of the support and/or swelling/shrinkage of the timber elements.

## 11.2.3 Support with ribs supported by mechanical joints

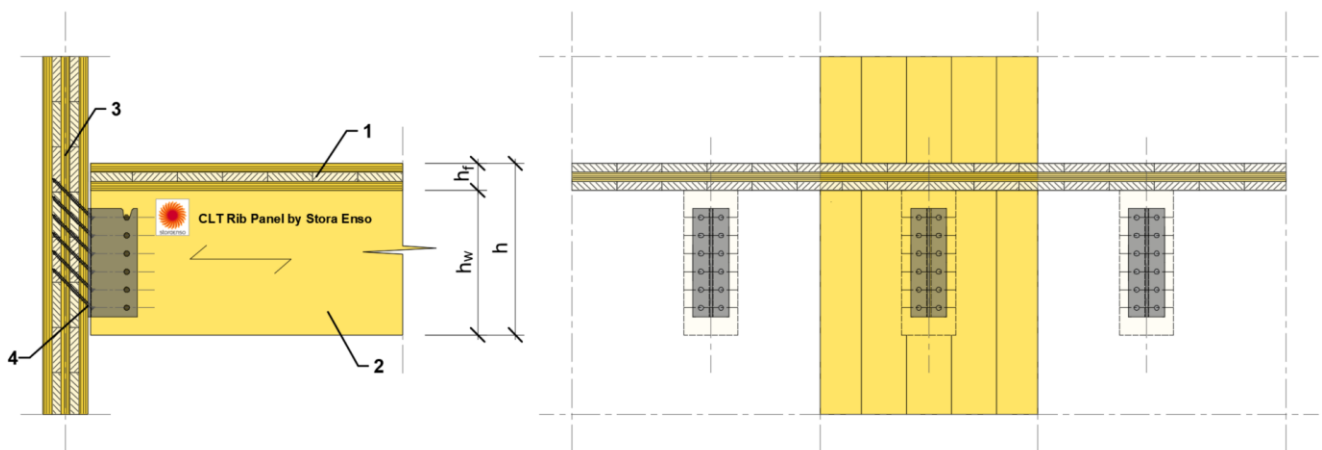


Figure 11-i: Ribs supported by mechanically fixed connections (1 ... CLT panel, 2 ... rib, 3 ... supporting member, 4 ... concealed bracket connection)

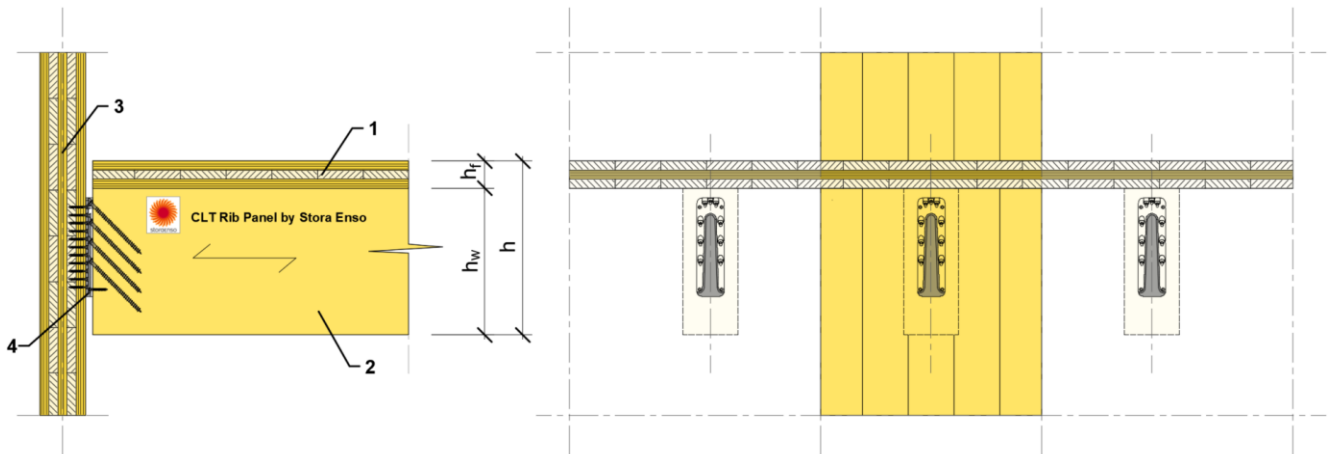


Figure 11-j: Ribs supported by mechanically fixed connections (1 ... CLT panel, 2 ... rib, 3 ... supporting member, 4 ... concealed hook connection)

The vertical load of the CLT Rib Panel members is transferred by appropriate connections (e. g. main and secondary connectors) to the supports. The verification of the joints shall be done in accordance to EN 1995-1-1 [3], chapter 8 and/or specific technical approvals of the connector.

### 11.3 Suspended support with cut-back ribs

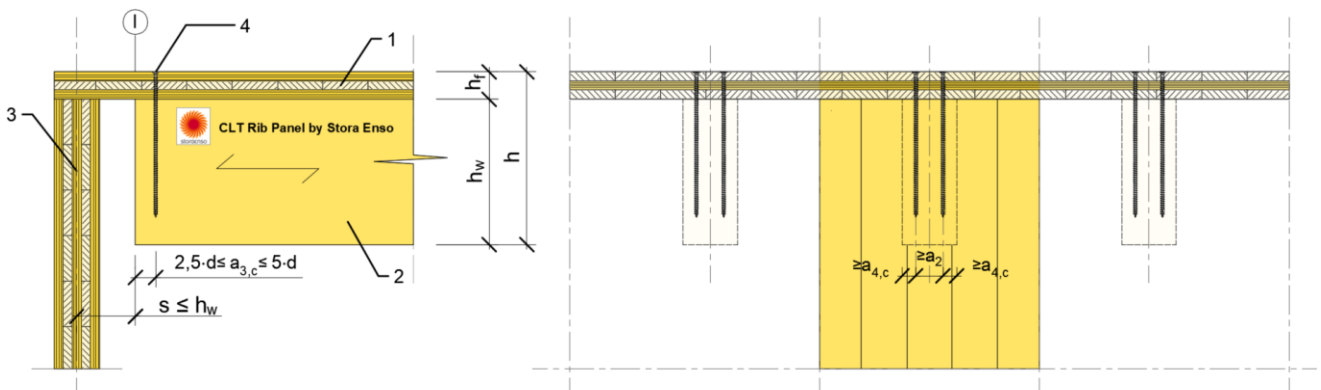


Figure 11-k: Cut-back (notched) ribs (1 ... CLT panel, 2 ... rib, 3 ... supporting member, 4 ... reinforcement)

The following conditions shall to be fulfilled:

1. The maximum distance between the supporting line and the face side of the rib shall be  $s \leq h_w$ .
2. Cut back (notched) ribs must be reinforced by using adequate fasteners (e.g. glued-in rods, self-tapping screws, etc.) and/or other possibilities avoiding a failure in the interface between the CLT element and the glulam rib.

The end distance  $a_{3,c}$  of the fasteners shall be  $2.5 \cdot d \leq a_{3,c} \leq 5 \cdot d$ .

$d$  diameter of the fastener [mm].

In the longitudinal axis of the slab the application of only one fastener is allowed, while in the perpendicular direction more fasteners (depending on the distances  $a_2$  and  $a_{4,c}$ ) may be applied as presented in Figure 11-k . The tip of the fasteners should be positioned as close as possible to the lower edge of the rib.

## General preliminaries

For CLT Rib Panels, some specific points must be considered in the design.

From conducted FEM analysis [9], it was deduced that depending on certain parameters, a considerable part of the vertical forces per rib is carried by the CLT element. It can be assumed that this portion of the vertical load depends mainly on the following parameters:

- ratio between the bending stiffness of the CLT element and the GLT rib,
- ratio between the span and the axis distance of the rib,
- distance of the cut-back to the supporting line of the CLT Rib Panel.

To enable a flexible design, a two-step design approach shall be followed:

A part of the total vertical force  $V_{tot,d}$  per rib is carried directly by the CLT element to the supports.

In a first step, the portion of the total vertical force carried by the rib without the cut-back ( $V_{red,0,d}$ ) shall be determined. For the calculation, the bending stiffness ratio between the CLT panel and the GLT rib  $(E \cdot I)_{rib}/(E \cdot I)_{CLT,y}$  and the ratio between the span and axis distance per rib  $l/b$  are considered.

In the second step, beside the stiffness ratios of the components, the influence of the distance  $s$  between the supporting line and the cut-back (end of the rib) on the vertical force in the rib ( $V_{red,0,d}$ ) is taken into consideration by a reduction factor  $k_s$  for the determination of the relevant force in the cut-back.

## Verification

The following verifications shall be done (according to [9]) :

1. Compression perpendicular to grain at the support on the CLT face

For this part of the design, see chapter 11.

$$\sigma_{c,90,d} \leq k_{c,90} \cdot f_{c,90,CLT,d} \quad \text{Eq. 11-16}$$

with

$$\sigma_{c,90,d} = \frac{F_d}{b \cdot [d_{supp} + 30mm]} \quad \text{Eq. 11-17}$$

|            |  |
|------------|--|
| $b$        | Length of support considered = rib spacing [mm]  |
| $d_{supp}$ | Support member depth (e.g. CLT wall thickness) [mm]  |
| $F_d$      | Design support reaction per rib, originating from the rib panel itself and the surcharge applied to it [N] |

2. The bending as well as the shear and rolling shear stresses of the CLT element must be verified at the position (**section I** in Figure 11-k) of the cut-back of the ribs.  
For this part of the design, see chapter 7 and chapter 8.
3. The reinforcement at the cut-back (notch) of the ribs shall be designed for a load perpendicular to the axis of the rib and CLT element as follows:

$$F_{t,90,d} = V_{red,0,d} \cdot k_s = V_{red,0,d} \cdot \frac{1}{1.0 + \frac{0.3}{\sqrt{Y_{rib}}} - 0.35 \cdot \sqrt{\frac{s}{h}}} \quad \text{Eq. 11-18}$$



valid for  $1.5 \leq Y_{rib} \leq 150$  and  $0.10 \leq \frac{s}{h} \leq 1.0$

with

$F_{t,90,d}$  design force value for the design of the reinforcement [N]

$V_{red,0,d}$  design shear force in the rib without cut-back [N]

$k_s$  reduction factor considering the distance of the cut-back to the supporting line [-]

$$k_s = \frac{1}{1.0 + \frac{0.3}{\sqrt{Y_{rib}}} - 0.35 \cdot \sqrt{\frac{s}{h}}}$$

$s$  distance of the cut-back to the supporting line [mm]

$h$  height of the CLT Rib Panel [mm]

$Y_{rib}$  characteristic rib value in bending about Y axis

$$Y_{rib} = \frac{(E \cdot I)_{rib}}{(E \cdot I)_{CLT,y}}$$

with

$$(E \cdot I)_{rib} = E_{0,w} \cdot \frac{b_w \cdot h_w^3}{12}$$

$$(E \cdot I)_{CLT,y} = \sum_{i=0}^n E_{0,i} \cdot \frac{b \cdot h_i^3}{12} + \sum_{i=0}^n E_{0,i} \cdot b \cdot h_i \cdot z_i^2$$

$n$  number of layers of the CLT-element

$z_i$  distance of the COG of the  $i$ -th layer to the COG of the CLT-element)

## Design value of the shear force in the rib without cut-back

$$V_{red,0,d} = V_{tot,d} \cdot \left( 1.20 - 0.05 \cdot \sqrt{\frac{l}{b} - \frac{0.50}{\sqrt{Y_{rib}}}} \right) \quad \text{Eq. 11-19}$$

valid for  $5 \leq \frac{l}{b} \leq 32$  and  $1.5 \leq Y_{rib} \leq 150$

with

$V_{tot,d}$  total design value of the shear force per rib [N]  
e. g. for continuously distributed load:

$$V_{tot,d} = q_d \cdot \frac{b \cdot l}{2}$$

$q_d$  design value of the continuously distributed load [N/mm<sup>2</sup>]

$l$  span of the CLT Rib Panel [mm]

$b$  rib spacing [mm]

Note:

The verification of the above given design recommendations was carried out by means of a parametric study using FEM.

## 12 Connection between panels and adjacent structures - Structural behavior of CLT Rib Panel diaphragms

The figures below show typical joint connections between two CLT rib panels. The connection shall be made between the CLT panels and designed in a way that all applicable shear forces, in the plane of the CLT and/or out of the plane of CLT can be transferred.

The design of the screws shall be done according to the applicable ETA.

### 12.1 Longitudinal joints of CLT rib panels

CLT rib panels can be joined in the longitudinal direction by means of

- (a) ribs at the edges of the plate or
- (b) stepped profile of the plate.

#### 12.1.1 Ribs at the edges of the plate

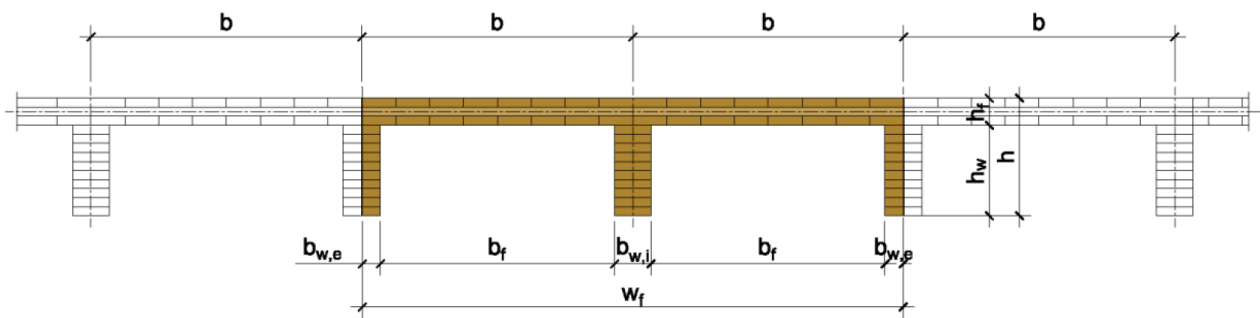


Figure 12-a: CLT Rib Panel longitudinal joints with ribs at the edges of the plate

The edge ribs are usually designed with half of the inner rib width (Figure 12-a), so that the double ribs at the longitudinal joints keep the same geometry as the inner ribs. The connection shall be done with fully threaded screws. The screwed connection shall be executed crossed, with screws coming from either side of the joint.

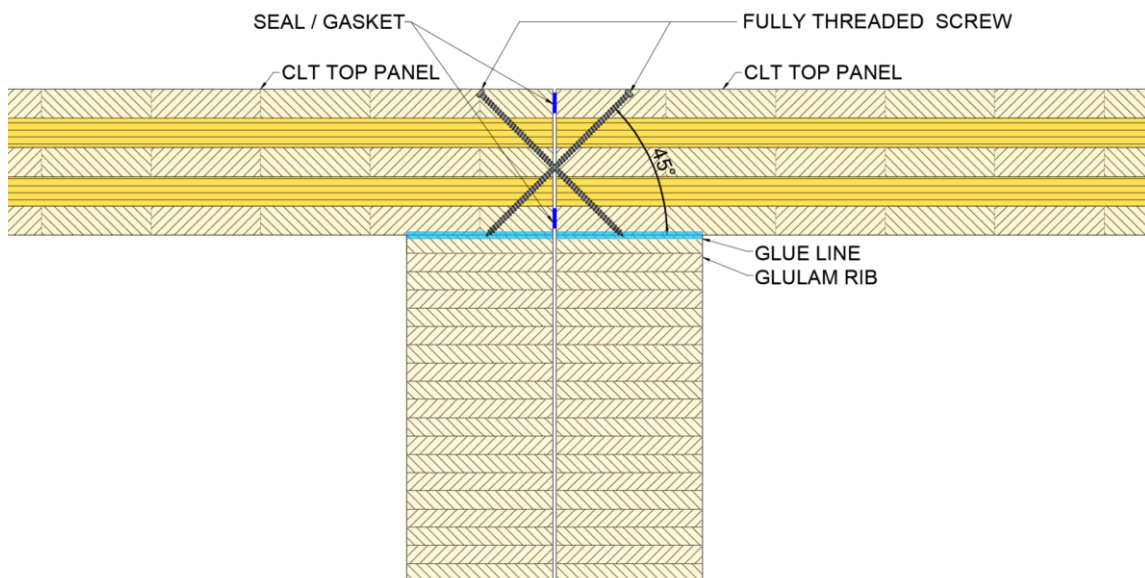


Figure 12-b: Joint connection with ribs at the edges of the plates

## 12.1.2 Stepped profile of the CLT plate

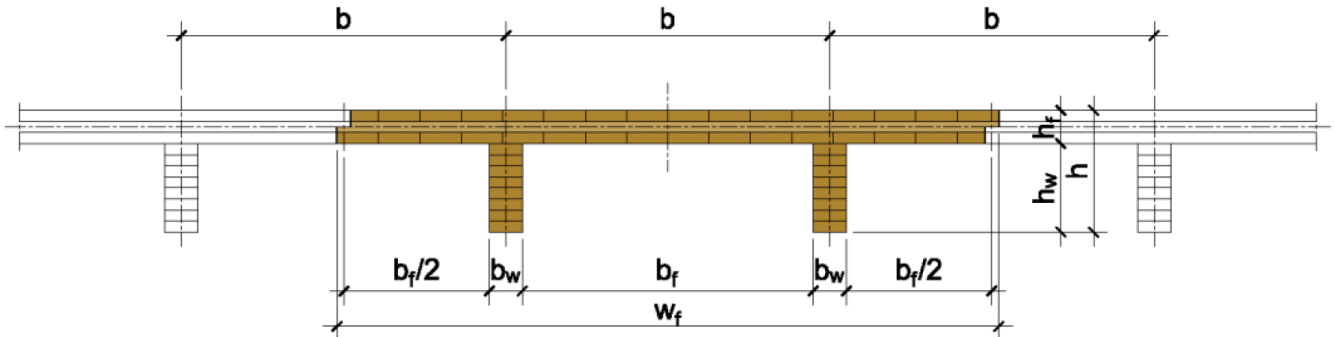


Figure 12-c: CLT Rib Panel with longitudinal joints as stepped profile of the plate

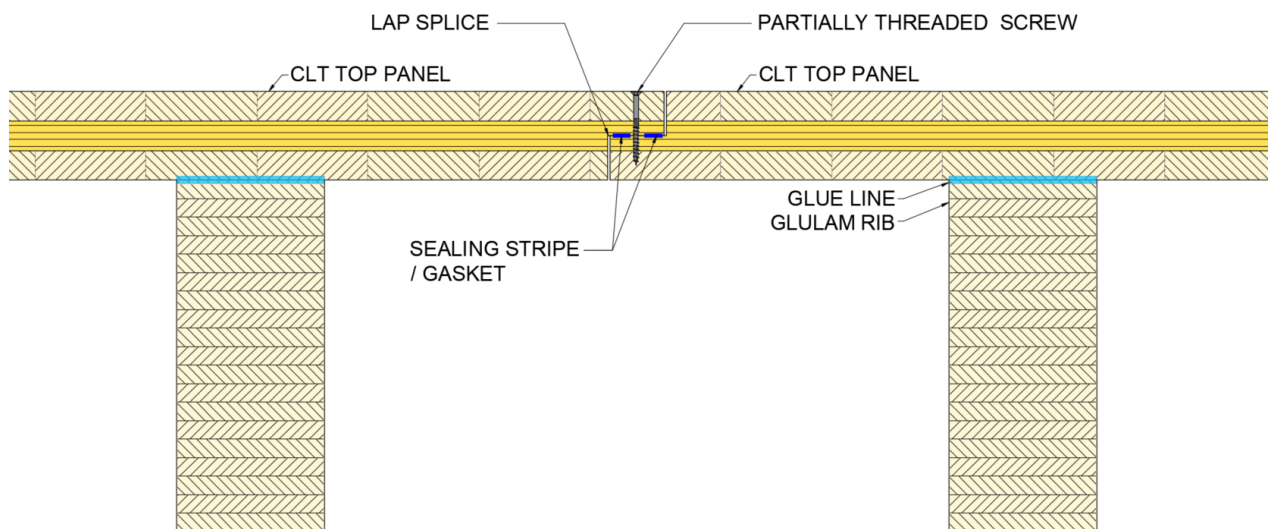


Figure 12-d: Joint connection at the edges of the stepped profile of the plate

## 12.2 Verification with stepped profile of the plate

In EN 1995-1-1 no specification or rule for the vertical loads to be transferred by the longitudinal joint of slabs is given. Thus, an engineering judgement has to be applied for its determination. Since the stiffness of CLT rib panels in the cross direction is much smaller than in the longitudinal (rib) direction  $(E \cdot I)_x \gg (E \cdot I)_y$  and the twisting stiffness is also small  $(\ll (G \cdot I)_{xy})$  only a small portion of the load is carried in the cross direction.

Nevertheless, forces at the coupling edges of adjacent elements should be considered based on experience.

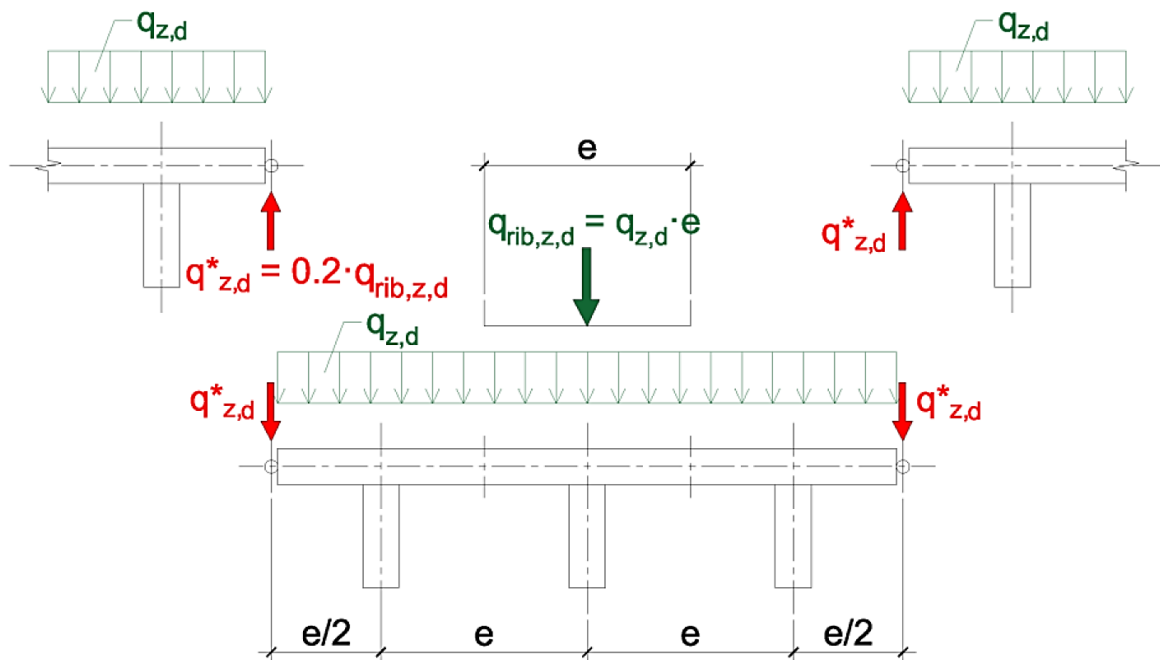


Figure 12-e : Design load  $q^*_{z,d}$  for longitudinal joints

- 1) If the ribbed plate is loaded by dominant continuously distributed loads the longitudinal joints and its fasteners respectively shall be designed (in addition to the forces from the structural analysis) for a line load of 20% of the aliquot line load per rib.
- 2) Individual line (e. g. eccentrically (regarding the rib) situated walls) and single loads (e. g. due to machines) shall be considered using appropriate structural models. If up-lifting forces may occur the corresponding forces shall be transferred by reinforcements of the contact line between plate and rib.
- 3) The edges of all elements must be anchored to the walls and supporting elements respectively. (e.g. lintel beams) below.
- 4) If the ribbed plate is used as diaphragm, the relevant combined vertical and horizontal loads and combinations must be considered in the design of the joint by appropriate models.

## 12.3 Vertical forces at the longitudinal edges

The following arguments can be quoted for the determination of the force to be taken into consideration:

### Different loadings of adjacent elements

This effect will be demonstrated by means of a calculation example given below.

**Example:**

$l = 10.0 \text{ m}$ , CLT element: 5 layered-CLT,  $h_f = t_{CLT} = 140 \text{ mm}$  (40-20-20-20-40 mm); Rib: Glulam GL24h,

$$\frac{b_w}{h_w} = \frac{140}{400}$$

$$b = 800 \text{ mm} \quad , \quad b_{ef} = 422 \text{ mm}, \quad EI_{x,ef} = 3.01 \cdot 10^4 \text{ kNm}^2$$

Actions :

$$\gamma_G = 1.35 \quad | \quad \gamma_Q = 1.50 \quad | \quad G_k = 2.00 \text{ kN/m}^2 \quad | \quad P_k = 3.00 \text{ kN/m}^2$$

Element 1:

$$E_{d,1} = \gamma_G \cdot G_k + \gamma_Q \cdot P_k = 1.35 \cdot 2.00 + 1.50 \cdot 3.00 = 7.20 \text{ kN/m}^2$$

Element 2:

$$E_{d,2} = \gamma_G \cdot G_k + \gamma_Q \cdot P_k = 1.35 \cdot 2.00 + 1.50 \cdot 0 = 2.70 \text{ kN/m}^2$$

Analysis is worked out for a 1.00 m wide stripe on a 1-D structural system. The ribs are simulated as springs with stiffness in the middle of the bay. The step joints are modelled as ideal hinge.

**Stiffness of springs (ribs):**

$$k = \frac{1}{w} = \frac{48 \cdot EI}{l^3} = \frac{48 \cdot 3.01 \cdot 10^4}{1^3} = 1.45 \cdot 10^3 \text{ kN/m/m}$$

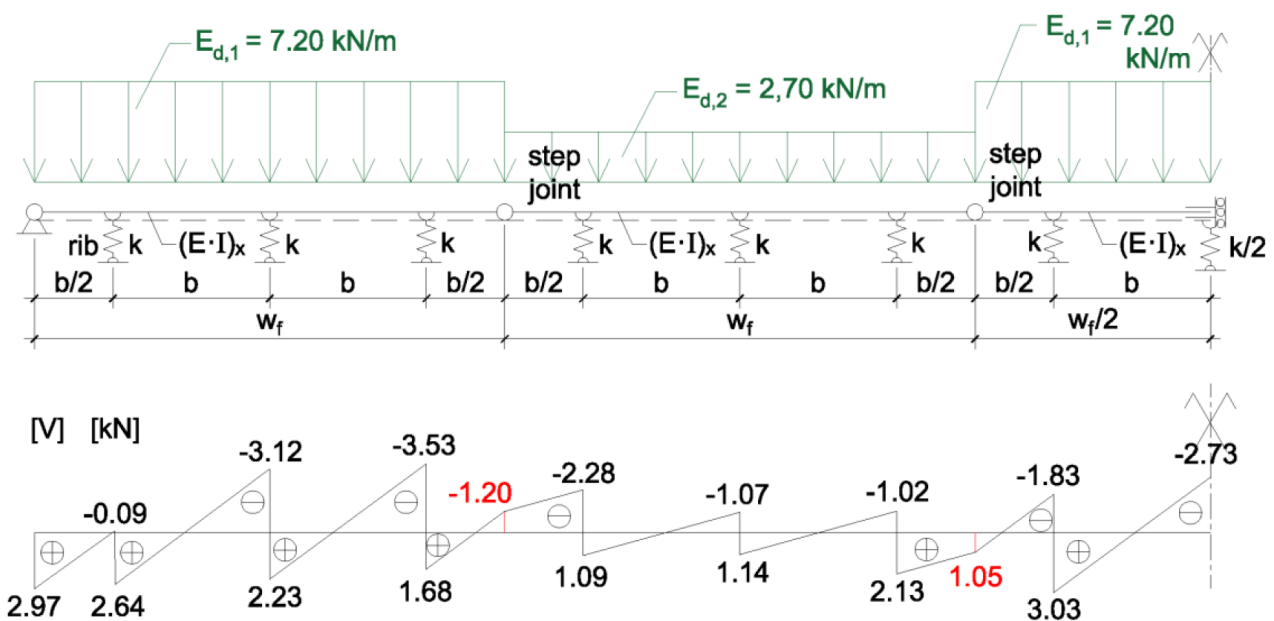


Figure 12-f: Analysed model and distribution of vertical forces

**Result**

The (maximum) shear force at the hinge (in the middle of the field) is  $v_{x,d} = 1.20 \text{ kN/m}$ .

According to the proposed rule the (vertical) load would be:

$$q_d^* = 20\% \cdot (E_{d,1} \cdot b) = 0.20 \cdot (7.20 \cdot 0.80) = 1.15 \text{ kN/m}$$

### 12.3.1 Incompatible deformations between CLT rib panels supported on 3 and 2 edges respectively.

The elements at the start and end (each side) of a floor system are usually supported on 3 sides, while the next ones (in the middle) are supported on 2 edges only. Due to the different stiffness of the elements a difference of deformations between both elements occurs. To avoid a gap between both elements they must be connected by appropriate connections.

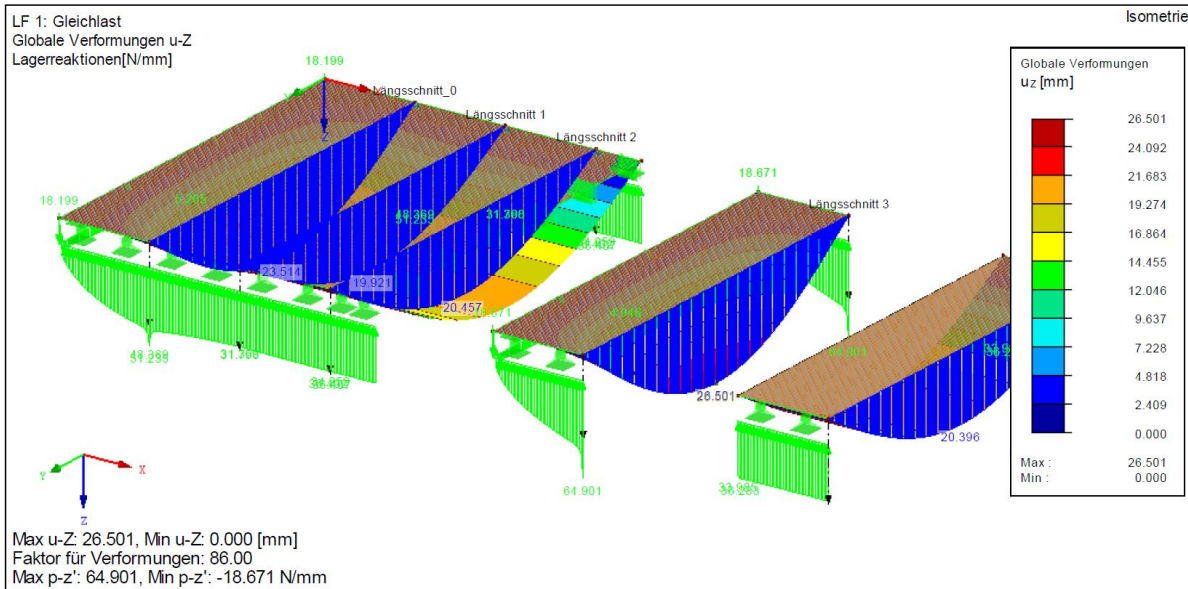


Figure 12-g: Difference of vertical deflections between CLT rib panels elements supported on 3 and 2-sides: System of rib panels coupled with hinges at the longitudinal edges

(left: max. deflection at the first longitudinal joint: 23.514 mm), first rib panel supported on 3 edges (max. deflection: 26.501 mm) and “regular” rib panel supported at 2-sides (right: max. deflection: 20.396 mm)

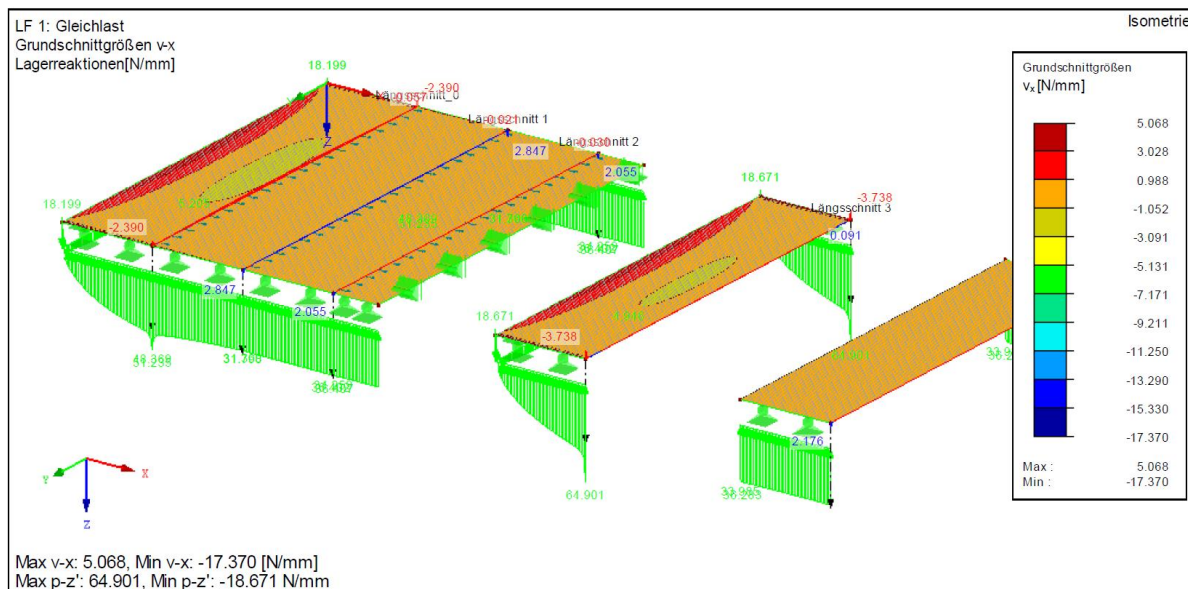


Figure 12-h: Shear forces  $v_x$  of the system of rib panels coupled with hinges at the longitudinal edges; the first rib panel is supported on 3-sides and the “regular” rib panel is supported on 2-sides



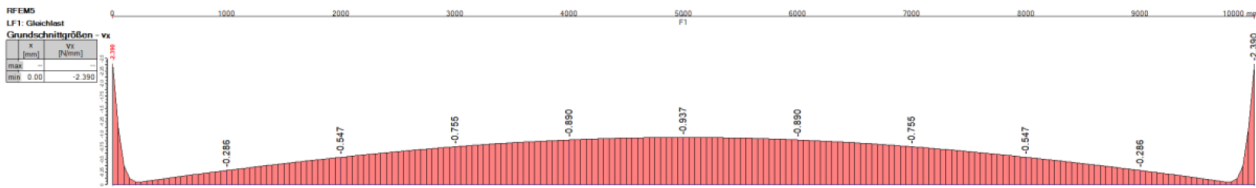


Figure 12-i: Distribution of the shear force  $v_x$  in the first hinged longitudinal edge ( $\max v_x = 0.937 \text{ kN/m}$ )

## Result

According to the FE analysis, the max. shear force in the first longitudinal joint is  $V_x = q_d^* = 0.937 \text{ kN/m}$ .

According to the proposed rule the (vertical) load would be:

$$q_d^* = 20\% \cdot (E_{d,1} \cdot b) = 0.20 \cdot (7.20 \cdot 0.80) = 1.15 \text{ kN/m}$$

### 12.3.2 Comparable specifications

In addition to the already mentioned arguments, a look on specifications for other building materials is expedient.

For example:

#### Rules for solid slabs in EN 1992-1-1

Excerpt from EN 1992-1-1, Clause 9.3.1.1 (2)

“Secondary transverse reinforcement of not less than 20% of the principal reinforcement should be provided in one way slabs.”

### 12.3.3 Summary

As shown, it is arguable that longitudinal joints of CLT rib panels shall be designed for a certain load transfer in the vertical direction, although there are no rules given in standards. The two examples in this chapter demonstrate the effects and are non-exhaustive.

The vertical shear forces in the longitudinal hinge are approximately distributed in a sinusoidal form and the given values are the maximum in the middle of the longitudinal joint. It is recommended to define the vertical load to be transferred by the fasteners of the longitudinal joint with 20% of the total load per rib.

This is in a comparable range as it is specified for concrete slabs in the cross direction. The proposed rule allows a pragmatic, simple and quick estimation of the vertical force in the joint.

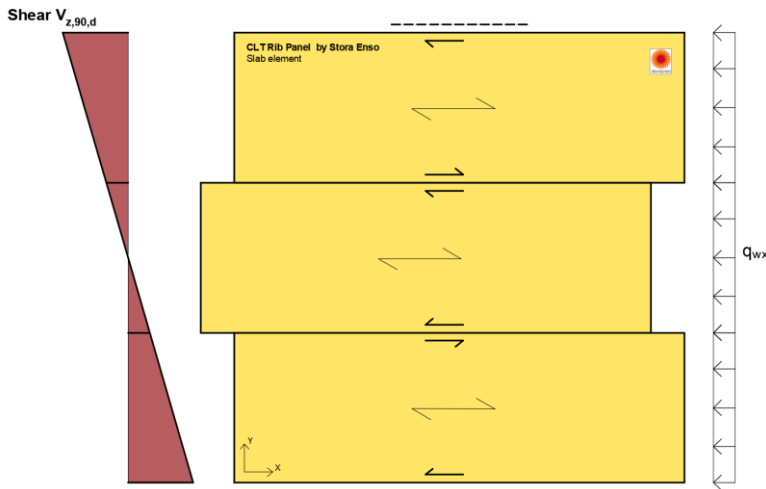
## 12.4 Horizontal forces at the longitudinal edges

In addition to the load transfer in the vertical direction CLT rib panels are also able to carry loads in the horizontal (in-plane) directions. These actions result from e. g. wind and/or earthquake loadings on the global load-carrying structure and occur in two directions: Perpendicular and in the direction of the span (see Figure 12-j). The load transfer perpendicular to the span is often unproblematic. The first and the last CLT rib panel element transfer the load as a horizontal beam into the stabilizing (e.g. walls) structure below.

The load-carrying function parallel to the span requires some additional efforts in the design of the connection at the longitudinal edges of the elements. Due to the horizontal loading of the CLT rib panels, shear forces as well as compression and tensile forces in the longitudinal edges of the elements appear. A model for the determination of the relevant forces is derived in the subsequent sections of this chapter.

Finally, it should be mentioned that for the design of the fasteners and connection system the load-carrying capacity at the longitudinal edge of the elements, the vertical and horizontal forces from the different loadings must be combined.

**a) Shear along the joints**

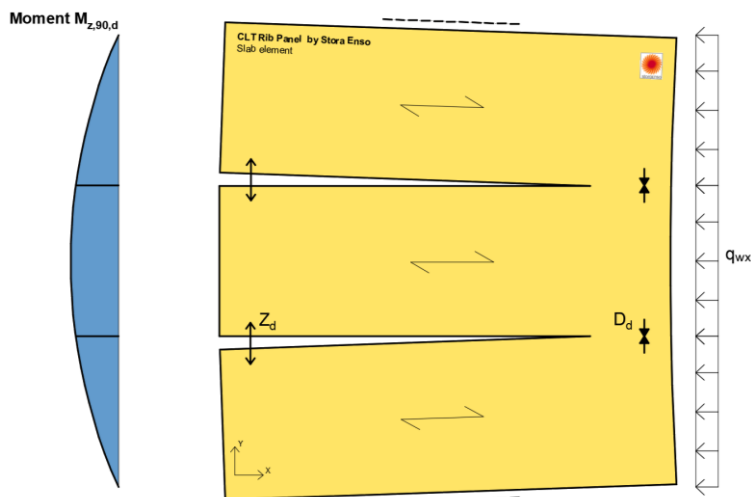


Impacts in the direction of the longitudinal joints between the panels result in:

- a)** shear forces along the joints;
- b)** flange forces composed of tensile forces  $Z_d$ , and compression forces  $D_d$  caused by the bending perpendicular to grain of the diaphragm will occur at the same time at the intermediate joint edges.

The shear forces in the intermediate joints between the panels shall be taken by the respective fasteners designed accordingly.

**b) Flange forces (tension and compression) due to bending perpendicular to grain at the panel edges**



**c) Bending and shear due to bending parallel to grain as a horizontal girder**

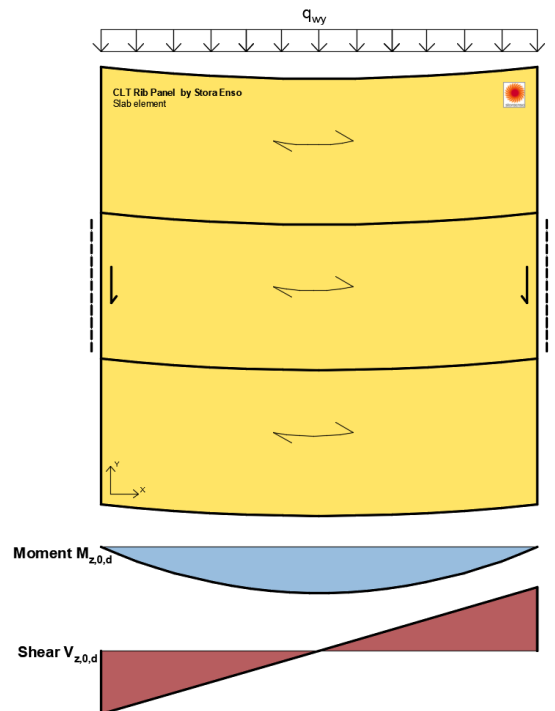


Figure 12-j: Failure mechanisms of diaphragms

Considering a beam with continuously distributed load:



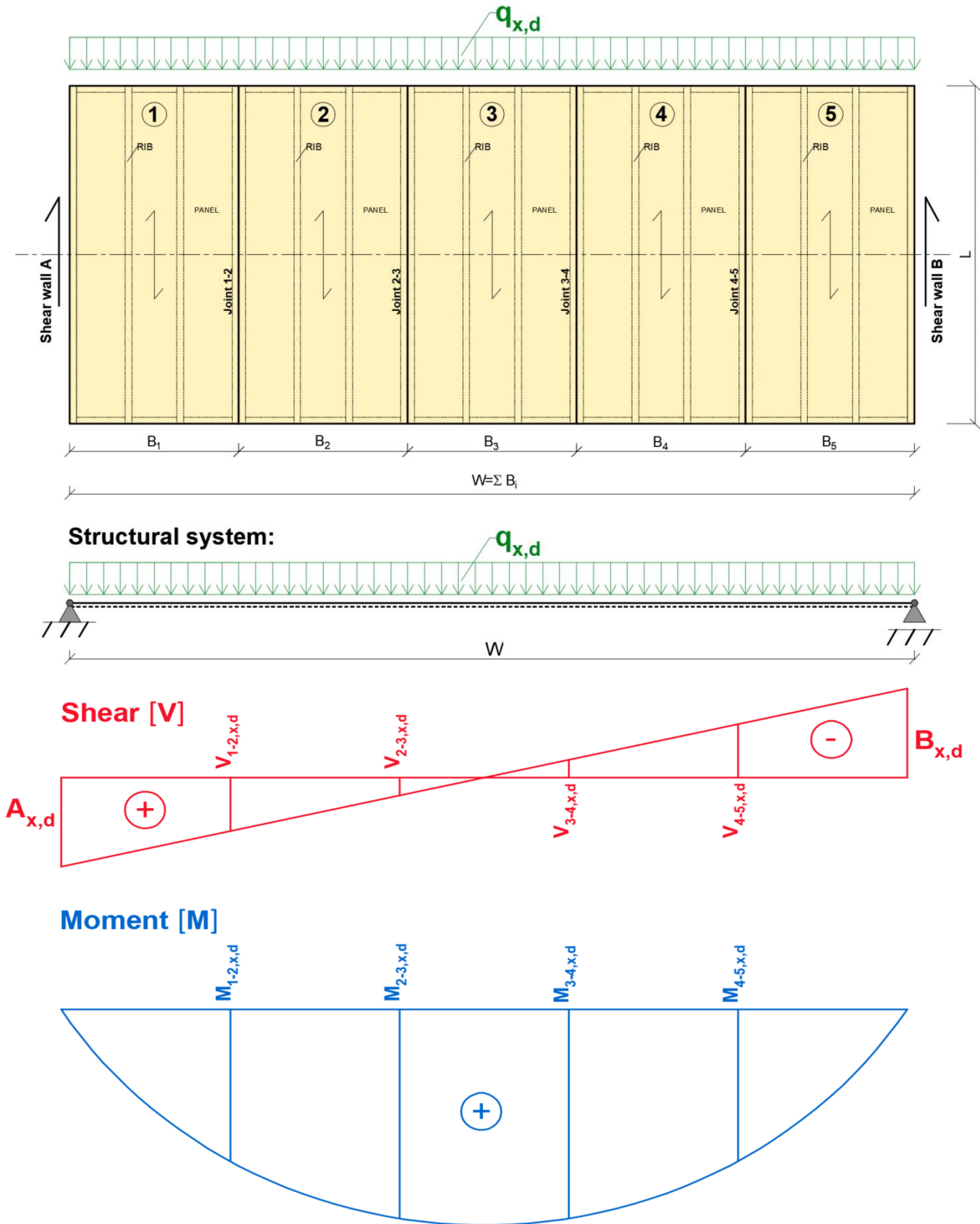


Figure 12-k: Modelling of CLT rib panels diaphragm in the direction of the span

## 12.4.1 Horizontal shear along the longitudinal joints

### a) In-plane shear stress in CLT panels

The in-plane shear stress in the CLT panels shall be analyzed for 2 failure modes:

- Shear in the net section
- Torsional shear in the glue line of the face gluing

See **chapter 8.4** for the design steps.

with the linear design shear force in [N/mm]

$$n_{xy} = \frac{V_{x,d}}{L} \quad \text{Eq. 12-1}$$

$V_{x,d}$  is the design shear force in the respective longitudinal joint [N]

$L$  is the length of the longitudinal joint (span) [mm]

## 12.4.2 Number of fasteners required to carry the shear force

$$n_{req,d} = \frac{F_{V,ed}}{F_{V,Rd}} \quad \text{Eq. 12-2}$$

$$F_{V,Rd} = \frac{k_{mod} \cdot F_{V,Rk}}{\gamma_M} \quad \text{Eq. 12-3}$$

$F_{V,ed} = V_{x,d}$  is the design shear force in the respective longitudinal joint [N]

$F_{V,Rk}$  is the characteristic load-carrying capacity per shear plane per fastener [N], according to Johansen equations in EN1995-1-1, equations (8.6) [3]

$F_{V,Rd}$  is the design load-carrying capacity per shear plane per fastener [N],

$k_{mod}$  is the factor, according to EN1995-1-1, Table 3.1, taking a load duration (permanent – very short) and the service class (1-3) into consideration

$\gamma_M$  is the partial safety coefficient, applicable for CLT

The connection forces to the shear walls must be transferred with respective fasteners designed accordingly.

### 12.4.3 Determination of the limiting moment in a longitudinal joint of a diaphragm

The maximum moment of the longitudinal joint occurs when the maximum compression stress at the edge of the joint and the load carrying capacity of the outermost lying fastener is reached (Figure 12-m and Figure 12-n).

#### Equilibrium

$$\sum F_x = 0 : \frac{1}{2} \cdot f_{c,0,d} \cdot \sum t_{90} \cdot X - \sum_{i=1}^n F_i = 0 \quad \text{Eq. 12-4}$$

with

$$\frac{1}{2} \cdot f_{c,0,d} \cdot \sum t_{90} \cdot X \rightarrow \text{being the compression force area in [N]}$$

the compression will be carried by the cross layer of the CLT panel.

with

$$F_i = K_{ser} \cdot \varphi \cdot (X_i - X) \quad \text{Eq. 12-5}$$

For the outermost lying fastener respectively:

$$F_n = K_{ser} \cdot \varphi \cdot (X_n - X) = F_d \quad \text{Eq. 12-6}$$

$$K_{ser} \cdot \varphi = \frac{F_d}{(X_n - X)}$$

$F_n = F_d = R_d = n_{end} \cdot R_{d,i}$  is the total design carrying capacity of the outermost lying fasteners in [N] with  $n_{end}$  being the number of fasteners connecting the joint at the panel end.

$\varphi$  is the angle of the strain plane

$$\varphi = \frac{F_d}{K_{ser} \cdot (X_n - X)} \quad \text{Eq. 12-7}$$

$$\sum F_x = 0 :$$

$$\frac{1}{2} \cdot f_{c,0,d} \cdot \sum t_{90} \cdot X - \sum_{i=1}^n K_{ser} \cdot \varphi \cdot (X_i - X) = 0$$

$$\frac{1}{2} \cdot f_{c,0,d} \cdot \sum t_{90} \cdot X - \frac{F_d}{(X_n - X)} \cdot \sum_{i=1}^n (X_i - X) = 0 \quad \text{Eq. 12-8}$$

Quadratic equation for the distance  $X$  of the neutral axis from the edge loaded in compression

$$X^2 - \left( X_n + 2 \cdot \frac{n \cdot F_d}{f_{c,0,d} \cdot \sum t_{90}} \right) \cdot X + 2 \cdot \frac{F_d}{f_{c,0,d} \cdot \sum t_{90}} \cdot \sum_{i=1}^n X_i = 0$$

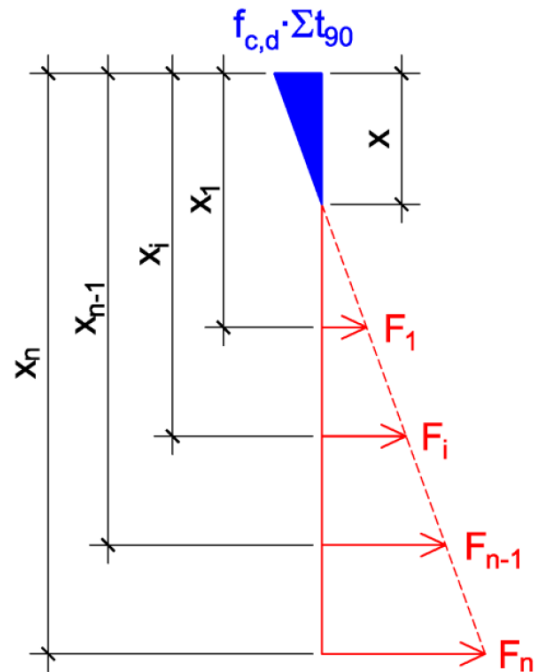


Figure 12-l: Compression perpendicular to grain at the edge of the joint and the load carrying capacity of the outermost lying fastener

## Distance X of the neutral axis from the edge loaded in compression

$$X_{1,2} = \left( \frac{X_n}{2} + \frac{n \cdot F_d}{f_{c,0,d} \cdot \sum t_{90}} \right) \pm \sqrt{\left( \frac{X_n}{2} + \frac{n \cdot F_d}{f_{c,0,d} \cdot \sum t_{90}} \right)^2 - 2 \cdot \frac{F_d}{f_{c,0,d} \cdot \sum t_{90}} \cdot \sum_{i=1}^n X_i}$$

Eq. 12-9

$n$  is the number of fasteners along the longitudinal joint.

$X_n$  is the distance of the outermost lying fastener from the panel extremity where the actions are applied [mm].

$X_i$  is the distance of the  $i^{\text{th}}$  fastener [mm].

$f_{c,0,d}$  is the design compressive strength parallel to grain of the CLT [N/mm<sup>2</sup>].

$t_{90}$  is the thickness of the CLT panel cross layers [mm].

$K_{ser}$  is the slip modulus of the fastener [N/mm].

Since the “fastener springs” are weak, the neutral axis is close to the upper edge. The distance X can also degenerate to  $X = 0$  which is a conservative approach.

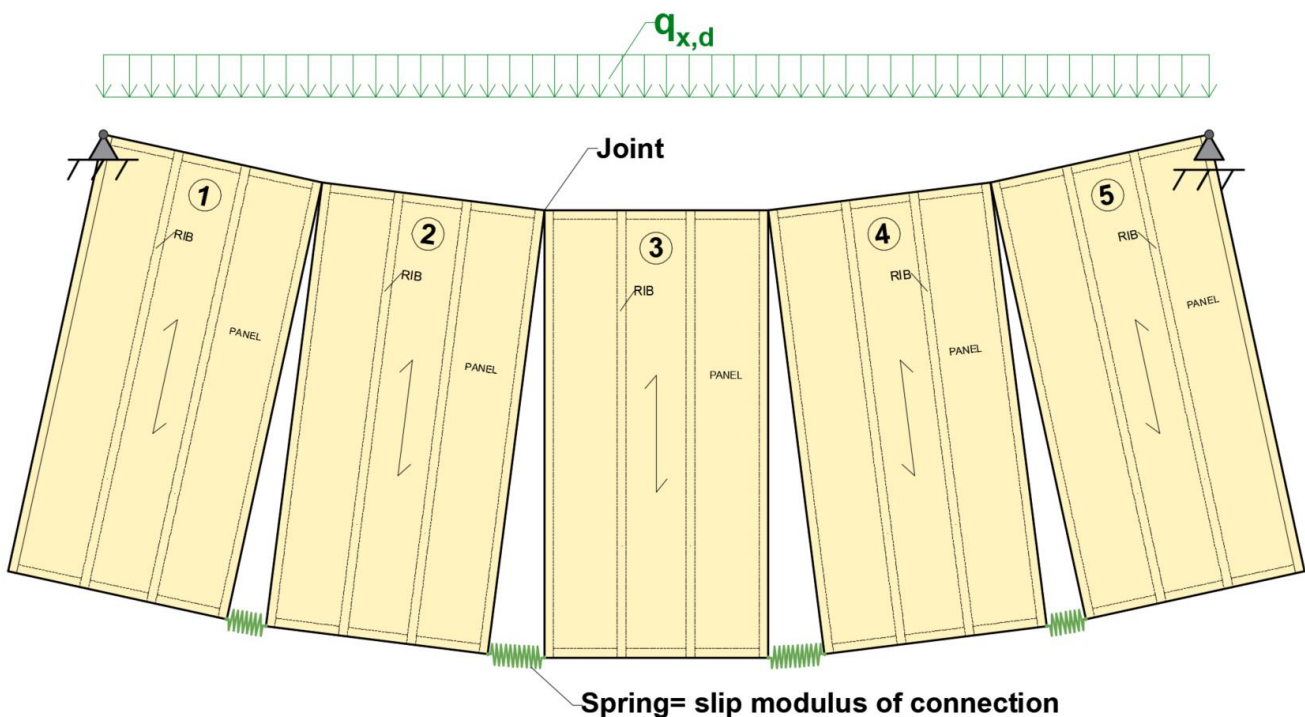


Figure 12-m: Diaphragm behaviour in longitudinal direction with springs in longitudinal joints at the end of the panels.

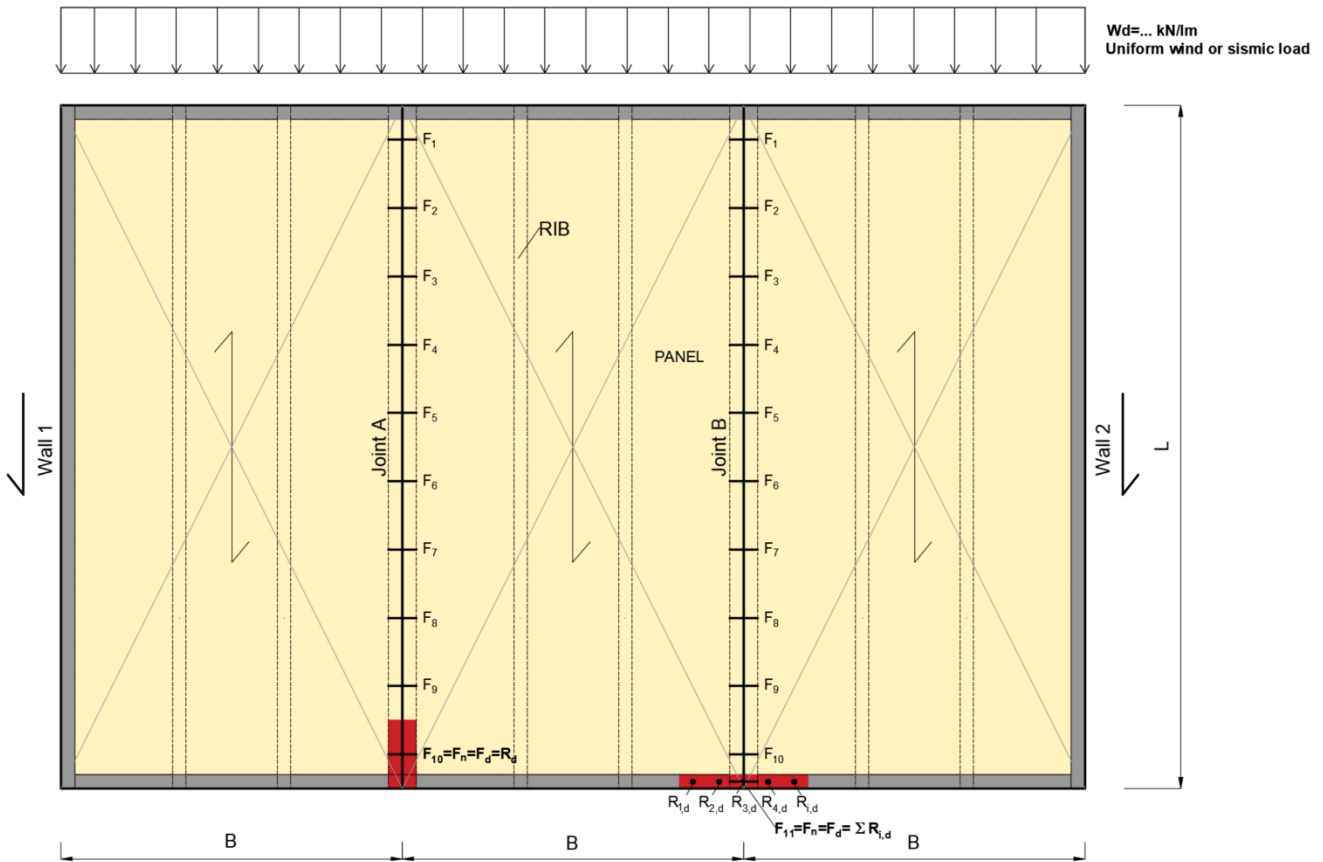


Figure 12-n: Fasteners placed in longitudinal joints and determination of the design carrying capacity of the outermost lying fastener  $F_d$  – Left (Joint A): Single fastener at the end; Right (Joint B): Multiple fasteners at the end .

**Remark:** We assume in this model that all joints have the same slip modulus. Meaning that the same fasteners should be used in the longitudinal joints, which is most often the case.

### Limiting moment

$$\sum M = 0 : -\frac{1}{2} \cdot f_{c,0,d} \cdot \sum t_{90} \cdot X \cdot \frac{X}{3} + K_{ser} \cdot \varphi \cdot \sum_{i=1}^n (X_i - X) \cdot X_i - M = 0$$

$$M_{limit} = \frac{F_d}{(X_n - X)} \cdot \left( \sum_{i=1}^n (X_i^2) - X \cdot \sum_{i=1}^n X_i \right) - \frac{X^2}{6} \cdot f_{c,0,d} \cdot \sum t_{90}$$

Eq. 12-10

### Verification:

For each longitudinal joint present in the floor diaphragm shown in **Figure 12-k**, the respective design bending moment shall be compared with the limiting design moment  $M_{limit}$  calculated for the given joint:

$$\begin{aligned} M_{1,2,x} &\leq M_{limit,1,2} \\ M_{2,3,x} &\leq M_{limit,2,3} \\ M_{3,4,x} &\leq M_{limit,3,4} \\ M_{4,5,x} &\leq M_{limit,4,5} \\ M_{... ,x} &\leq M_{limit,...} \end{aligned}$$

Eq. 12-11

## Resulting compression force

$$\rightarrow C = F_{c,d} = \frac{1}{2} \cdot f_{c,0,d} \cdot \sum t_{90} \cdot X \quad \text{Eq. 12-12}$$

## Force in the i<sup>th</sup> fastener

$$\rightarrow F_i = K_{ser} \cdot \varphi \cdot (X_i - X) = F_d \cdot \frac{(X_i - X)}{(X_n - X)} \quad \text{Eq. 12-13}$$

It is a simple elastic model, not able to consider non-linear behavior which occurs. But valid approach which allows the verification.

## Summary:

- Start by defining the design capacity of the outmost lying fastener at the end of the panel, where most of the tension will occur.
- If there is a single fastener at the end connected in the joint (see Figure 12-n -Joint A): we consider the total design capacity at the outermost lying fastener

$$R_d = F_n = F_d$$

- If there are multiple fasteners at the end connected in the joint (see Figure 12-n -Joint B) then we consider the total design capacity at the outermost lying fasteners

$$R_d = n_{end} \cdot R_{i,d} = \sum R_{i,d} = F_n = F_d$$

→  $F_d$  is the maximum force that can be applied on the outermost connection in [N].

→  $R_{i,d}$  values are the values in [N], calculated from Johansen equations in EN 1995-1-1. The tension is taken in shear by the connectors.

When having the value  $F_d$  and the  $K_{ser}$  of the connectors placed in the longitudinal joint, the forces  $F_i$  that will occur in each fastener depending on their distance from the extremity of the panel where the actions (like wind) are applied can be calculated.

The goal here is to calculate the maximum moment  $M_{limit}$  that can be applied on the floor in longitudinal direction, based on the design capacity at the outermost lying fastener.

The compression zone shall be also verified (on the cross layers of the CLT edge) if it occurs, with the distance  $X$  that was calculated previously.

## 13 Serviceability Limit States

### 13.1 Deformation

The deformation of a structure resulting from the effects of actions (such as axial and shear forces, bending moments and joint slip) and from moisture shall remain within appropriate limits, having regard to the possibility of damage to surfacing materials, ceilings, floors, partitions and finishes, and to the functional needs as well as any appearance requirements.

Limiting values for deformation are taken from EN1995-1-1 [3] and the applicable national annex.

Deformation need to be also limited so that action of the adjacent structures and the intended operation of the building is not disturbed.

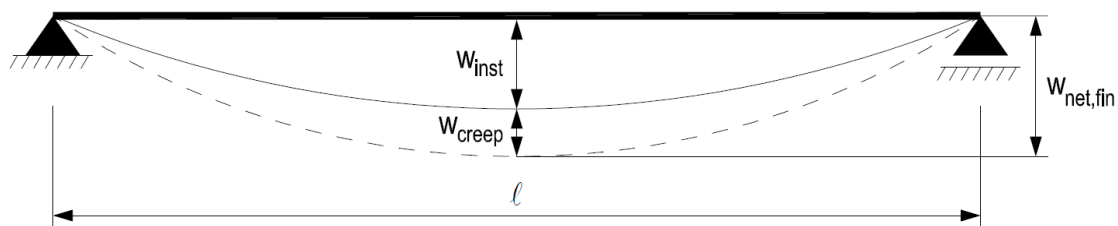


Figure 13-a: Components of deflection

Normally limiting deflections for the beams are according to the table below.

Table 13-1: Proposed deflection limits for CLT Rib Panels from EN 1995-1-1

|                  | $w_{inst}$                                       | $w_{fin}$                                       | $w_{net,fin}$                                       |
|------------------|--|---|---|
| between supports | $w_{inst} \leq \frac{L}{300}$ to $\frac{L}{500}$ | $w_{fin} \leq \frac{L}{150}$ to $\frac{L}{300}$ | $w_{net,fin} \leq \frac{L}{250}$ to $\frac{L}{350}$ |
| for cantilevers  | $w_{inst} \leq \frac{L}{150}$ to $\frac{L}{250}$ | $w_{fin} \leq \frac{L}{75}$ to $\frac{L}{150}$  | $w_{net,fin} \leq \frac{L}{125}$ to $\frac{L}{250}$ |

$L$  is span of the beam

The final net deflection limit for slab between the ribs

$$w_{net,fin} \leq \frac{L}{200} \quad \text{Eq. 13-1}$$

When calculating instantaneous deformations of the CLT Rib Panel, shear deformation shall be taken into account (Timoshenko beam theory) and mean values of stiffness properties and the effective cross-section should be used in the analysis. The combination service limit state is used.

The instantaneous deflection  $w_{inst}$  may be calculated as:

$$w_{inst} = \underbrace{\sum_{j \geq 1} w_{inst,G,j} + w_{inst,Q1}}_{\text{characteristic load combination}} + \sum_{i > 1} \psi_{0,i} \cdot w_{inst,Q,i} \quad \text{Eq. 13-2}$$

The final deflection  $w_{fin}$  may be calculated as:

$$w_{fin} = \underbrace{w_{inst}}_{\text{characteristic load combination}} + \underbrace{w_{creep}}_{\text{quasi permanent load combination}} \quad \text{Eq. 13-3}$$

$$w_{fin} = \underbrace{\sum_{j \geq 1} w_{inst,G,j} + w_{inst,Q1} + \sum_{i > 1} \psi_{0,i} \cdot w_{inst,Q,i}}_{\text{characteristic load combination}} + \underbrace{\left[ \sum_{j \geq 1} w_{inst,G,j} + \sum_{i \geq 1} \psi_{2,i} \cdot w_{inst,Q,i} \right]}_{\text{quasi permanent load combination}} \cdot k_{def,i}$$

$$w_{fin} = w_{fin,G} + w_{fin,Q,1} + \sum w_{fin,Q,i}$$

The creep deformation should be calculated using mean values of the appropriate moduli of elasticity, shear moduli and slip moduli and the relevant values of  $k_{def}$  given in Table 3-3.

with:

Final deflection caused by permanent action

$$w_{fin,G} = w_{inst,G}(1 + k_{def}) \quad \text{Eq. 13-4}$$

Final deflection caused by the leading variable action

$$w_{fin,Q,1} = w_{inst,Q,1}(1 + \psi_{2,1} \cdot k_{def}) \quad \text{Eq. 13-5}$$

Final deflection caused by the accompanying variable action

$$w_{fin,Q,i} = w_{inst,Q,i}(\psi_{0,i} + \psi_{2,i} \cdot k_{def}) \quad \text{Eq. 13-6}$$

The net final deflection  $w_{net,fin}$  may be calculated as:

General:

$$w_{net,fin} = \underbrace{w_{inst}}_{\text{characteristic load combination}} + \underbrace{w_{creep}}_{\text{quasi permanent load combination}} - \underbrace{w_c}_{\text{camber}} = \quad \text{Eq. 13-7}$$

$$w_{net,fin} = \underbrace{\sum_{j \geq 1} w_{inst,G,j} + w_{inst,Q1} + \sum_{i > 1} \psi_{0,i} \cdot w_{inst,Q,i}}_{\text{characteristic load combination}} + \underbrace{\left[ \sum_{j \geq 1} w_{inst,G,j} + \sum_{i \geq 1} \psi_{2,i} \cdot w_{inst,Q,i} \right]}_{\text{quasi permanent load combination}} \cdot k_{def,i} - \underbrace{w_c}_{\text{camber}}$$

In Austria:

$$w_{net,fin} = \underbrace{w_{inst,2} + w_{creep}}_{\text{quasi permanent load combination}} - \underbrace{w_c}_{\text{camber}} = \quad \text{Eq. 13-8}$$

$$w_{net,fin} = \left[ \sum_{j \geq 1} w_{inst,G,j} + \sum_{i \geq 1} \psi_{2,i} \cdot w_{inst,Q,i} \right] + \left[ \sum_{j \geq 1} w_{inst,G,j} + \sum_{i \geq 1} \psi_{2,i} \cdot w_{inst,Q,i} \right] \cdot k_{def,i} - w_c$$

Remark: Eq. 13-8 applies, if  $k_{def}$  is assumed to be constant over the entire section – see item 3.1.

$w_{inst,G}$  is instantaneous deformation for action G



$w_{inst,Q,1}$  is instantaneous deformation for action  $Q_1$

$w_{inst,Q,i}$  is instantaneous deformation for action  $Q_i$

## 13.1.1 Introducing the creep coefficient $k_{def}$ in a hybrid system

### 13.1.1.1 Precise method

The most precise method is to integrate the  $k_{def}$  factor in the bending stiffness (and shear stiffness) for each individual partial section/material.

The bending stiffness is defined in chapter 5.4.

The figure/equations below shall illustrate the method, given the following boundary conditions: single span beam, pin-pin support, continuous loading for quasi-permanent loading (for  $w_{net,fin}$  analysis), shear deformation).

Hybrid/mixed system:

$$w_{inst} = w_{1,inst} \cdot (g_{1,k} + g_{2,k} + q_k) \cdot b$$

$$w_{net,fin} = \left\{ w_{1,inst} \cdot \underbrace{[g_{1,k} + g_{2,k} + q_{1,k}]}_{\text{characteristic loading}} + w_{1,creep} \cdot \underbrace{[g_{1,k} + g_{2,k} + \psi_2 \cdot q_{1,k}]}_{\text{quasi permanent loading}} \right\} \cdot b$$

$$w_{fin} = \left\{ w_{1,inst} \cdot \underbrace{[g_{1,k} + g_{2,k} + q_{1,k}]}_{\text{characteristic loading}} + w_{1,creep} \cdot \underbrace{[g_{1,k} + g_{2,k} + \psi_2 \cdot q_{1,k}]}_{\text{quasi permanent loading}} \right\} \cdot b$$

with

$$w_{1,inst} = \underbrace{\frac{5 \cdot "1" \cdot L^4}{384 \cdot (EI)_{y,ef}}}_{\text{Deformation due to bending moment}} + \underbrace{\frac{"1" \cdot L^2}{8 \cdot (GA)_{y,ef}}}_{\text{Deformation due to shear}} \quad \text{Eq. 13-9}$$

$$w_{1,creep} = \underbrace{\frac{5 \cdot "1" \cdot L^4}{384 \cdot (EI)_{y,creep,ef}}}_{\text{Deformation due to bending moment}} + \underbrace{\frac{"1" \cdot L^2}{8 \cdot (GA)_{y,creep,ef}}}_{\text{Deformation due to shear}} \quad \text{Eq. 13-10}$$

considering:

$$(EI)_{y,ef} = \sum_i E_i \cdot I_{y,i} + \sum_i E_i \cdot A_i \cdot e_i^2 \quad \text{Eq. 13-11}$$

$$(EI)_{y,creep,ef} = \sum_i E_{i,creep} \cdot I_{y,i} + \sum_i E_{i,creep} \cdot A_i \cdot e_i^2 \quad \text{Eq. 13-12}$$

and

$$(GA)_{y,ef} = \sum_i (G_{i,inst} \cdot A_i) \cdot \kappa \quad \text{Eq. 13-13}$$

$$(GA)_{y,creep,ef} = \sum_i (G_{i,creep} \cdot A_i) \cdot \kappa \quad \text{Eq. 13-14}$$

$\kappa$  : Shear corrective factor (see chapter 5.5)

For the calculation of the cross-section values, the effective width  $b_{ef}$  shall be determined with the rules for the uniformly distributed load. Due to the fact, that no constricting effect due to single (point) loads (bearing loads) occurs, the so determined width is more or less constant over the total length of the beam.

with (See Table 5-1)

$$E_{CLT,creep} = \frac{E_{0,mean,CLT}}{K_{def,CLT}} \quad G_{CLT,creep} = \frac{G_{0,mean,CLT}}{K_{def,CLT}} \quad \text{Eq. 13-15}$$

$$E_{GLT,creep} = \frac{E_{0,mean,GLT}}{K_{def,GLT}} \quad G_{GLT,creep} = \frac{G_{0,mean,GLT}}{K_{def,GLT}} \quad \text{Eq. 13-16}$$

Deformation due to bending moment:

$$w_{net,fin} = \frac{5 \cdot q_{inst} \cdot L^4}{384 \cdot (EI)_{y,ef}} + \frac{5 \cdot q_{creep} \cdot L^4}{384 \cdot (EI)_{y,creep,ef}} \quad \text{Eq. 13-17}$$

Deformation due to shear:

$$w_{net,fin} = \frac{q_{inst} \cdot L^2}{8 \cdot (GA)_{y,ef}} + \frac{q_{creep} \cdot L^2}{8 \cdot (GA)_{y,creep,ef}} \quad \text{Eq. 13-18}$$

### 13.1.1.2 Simplified method

Most of the flexural rigidity is provided by the rib in the rib panel system. Therefore, it shall be sufficient to apply a uniform  $k_{def}$  to the entire system.

In that case a mean  $k_{def}$  shall be calculated as given in equation Eq. 3-1.

The figure/equations below shall illustrate the method, given the following boundary conditions: single span beam, pin-pin support, continuous loading for quasi-permanent loading (for  $w_{net,fin}$  analysis), no shear deformation (for shear this would be analogous).

$$w_{1,inst} = \underbrace{\frac{5 \cdot "1" \cdot L^4}{384 \cdot (EI)_{y,ef}}}_{\text{Deformation due to bending moment}} + \underbrace{\frac{"1" \cdot L^2}{8 \cdot (GA)_{y,ef}}}_{\text{Deformation due to shear}} \quad \text{Eq. 13-19}$$

$$w_{1,creep} = \left( \underbrace{\frac{5 \cdot "1" \cdot L^4}{384 \cdot (EI)_{y,ef}}}_{\text{Deformation due to bending moment}} + \underbrace{\frac{"1" \cdot L^2}{8 \cdot (GA)_{y,ef}}}_{\text{Deformation due to shear}} \right) \cdot K_{def} \quad \text{Eq. 13-20}$$

## 13.2 Vibration

The vibration control is made by setting limits to the natural frequency and on the stiffness. In the calculation the average values are used.

The vibration analysis shall be executed according to EN1995-1-1 [3] and the applicable national annex.

In case an applicable national annex to a Eurocode standard is deviating from given recommendations in this document, automatically the national annex is governing.

In the basic edition of EN 1995-1-1 [3], the vibration design is very poorly regulated. Currently the **Austrian national annex** of EN1995-1-1 contains the most extensive vibration design guide lines, which are closely related to the research findings by Patricia Richter and Antje Hamm [21]. Their research is among timber construction experts considered state of the art.

The following criterions on vibration design are available – most of them being mandatory to meet – others only optional:

- Class criterion:

| Floor class I  | Floor class II   |
|--|--|
| One floor element spanning across different occupancy units (apartments with different owners) on the same level | One floor element spanning within the same occupancy unit (apartments with same owner) on the same level |
| Wet floating screed installed on top of light or heavy granular fill.  | Wet screed installed with or without granular fill below   |
| Dry screed installed on top of heavy granular fill (> 60 kg/m <sup>2</sup> )                                     |  |

- Frequency Criterion:

| Floor class I  | Floor class II   |
|--|--|
| One floor element spanning across different occupancy units (apartments with different owners) on the same level | One floor element spanning within the same occupancy unit (apartments with same owner) on the same level |
| $f_1 \geq 8$ Hz  | $f_1 \geq 6$ Hz  |

Fundamental frequency  $f_1$  of the section may be calculated as:

$$f_1 = \frac{\pi}{2 \cdot l^2} \sqrt{\frac{(EI)_{l,eff}}{m}} \cdot \sqrt{1 + \left(\frac{l}{b_R}\right)^4 \cdot \frac{(EI)_{b,eff,1m}}{(EI)_{l,eff,1m}}} \quad \text{Eq. 13-21}$$

*accounting for rigidity in cross direction*

$f_1$  First fundamental frequency [Hz]

$(EI)_{l,eff,1m}$  Flexural rigidity in longitudinal direction for 1m wide (if spacing is not exactly 1m → extrapolation to a 1m wide element) in Nm<sup>2</sup>/m. The flexural rigidity is based on the mean value of the Young's modulus and the effective moment of inertia. If a floating screed is present in the floor layup, the rigidity of the screed  $EI_{screed}$  can be added too.

$(EI)_{b,eff,1m}$  Analogous to  $(EI)_{l,eff,1m}$ , only in cross direction (perpendicular to the span direction) [Nm<sup>2</sup>/m]. In case of CLT RP, this is the flexural rigidity in cross direction of the horizontal structural CLT floor + the screed rigidity, if any.

$m$  Mass of the structure (Self-weight) in kg/m<sup>2</sup> =  $\sum_{i \geq 1} G_{k,i}$  [kg/m<sup>2</sup>]

$b_R$  Width of the floor disregarding panel joints (Width of the room perpendicular to the span)

$l$  Span [m]



- Acceleration criterion (optional, if frequency criterion is not met):

| Floor class I   | Floor class II   |
|---|--|
| One floor element spanning across different occupancy units (apartments with different owners) on the same level  | One floor element spanning within the same occupancy unit (apartments with same owner) on the same level |
| $f_1 \geq 4,5 \text{ Hz}$   | $f_1 \geq 4,5 \text{ Hz}$  |
| $a_{rms} \leq 0,05 \text{ m/s}^2$   | $a_{rms} \leq 0,10 \text{ m/s}^2$  |
| $a_{rms} = \frac{0,4 \cdot e^{-0,47 \cdot f_1} \cdot F_0}{2 \cdot \zeta \cdot \underbrace{\left[ \frac{m \cdot l \cdot b_R}{2} \right]}_{\text{modal mass } M^*}}$ <p style="text-align: right;">Eq. 13-22</p>  |  |
| <p><math>f_1</math> First fundamental frequency [Hz]<br/> <math>F_0</math> Weight of 700N (defined in [22], Austrian NA, ...related to the average weight of a human)<br/> <math>\zeta</math> Damping ratio. For CLT floors and for rib panels, a damping ratio of 4% shall be assumed (0,04)<br/> <math>m</math> Mass of the structure in kg/m<sup>2</sup> = <math>\sum_{i \geq 1} G_{k,i}</math> [kg/m<sup>2</sup>]<br/> <math>b_R</math> Width of the floor disregarding panel joints (Width of the room perpendicular to the span)<br/> <math>l</math> Span [m]</p> |  |

- Stiffness criterion:

| Floor class I   | Floor class II   |
|---|--|
| One floor element spanning across different occupancy units (apartments with different owners) on the same level  | One floor element spanning within the same occupancy unit (apartments with same owner) on the same level |
| $w_{1kN} \leq 0,25 \text{ mm}$  | $w_{1kN} \leq 0,50 \text{ mm}$   |
| $w_{1kN} = \frac{F \cdot l^3}{48 \cdot (EI)_{l,eff,1m} \cdot \left[ \frac{l}{1,1} \cdot \sqrt[4]{\frac{(EI)_{b,eff,1m}}{(EI)_{l,eff,1m}}} \right]} + \frac{F \cdot l}{4 \cdot (GA)_{l,eff,1m} \cdot \left[ \frac{l}{1,1} \cdot \sqrt[4]{\frac{(EI)_{b,eff,1m}}{(EI)_{l,eff,1m}}} \right]}$ <p style="text-align: right;">Eq. 13-23</p>  |  |
| <p><math>f_1</math> First fundamental frequency [Hz]<br/> <math>(EI)_{l,eff,1m}</math> Flexural rigidity in longitudinal direction for 1m wide (if spacing is not exactly 1m → extrapolation to a 1m wide element) in Nm<sup>2</sup>/m. The flexural rigidity is based on the mean value of the Young's modulus and the effective moment of inertia. If a floating screed is present in the floor layup, the rigidity of the screed <math>EI_{screed}</math> can be added too.<br/> <math>(EI)_{b,eff,1m}</math> Analogous to <math>(EI)_{l,eff,1m}</math>, only in cross direction (perpendicular to the span direction) [Nm<sup>2</sup>/m]. In case of CLT RP, this is the flexural rigidity in cross direction of the horizontal structural CLT floor + the screed rigidity, if any.<br/> <math>F</math> for 1 section Point load of 1 kN<br/> <math>(GA)_{l,eff,1m}</math> Shear stiffness of the rib panel in longitudinal direction for a 1m wide rib panel (if rib spacing is not exactly 1m → extrapolation to a 1m wide element) [N/m].<br/> <math>l</math> Span [m]</p> |  |

The vibration design shall be summarized in the following flow chart:

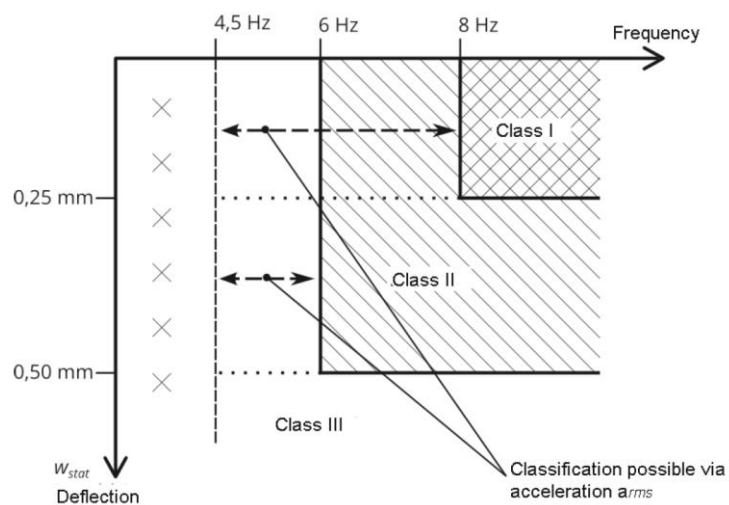
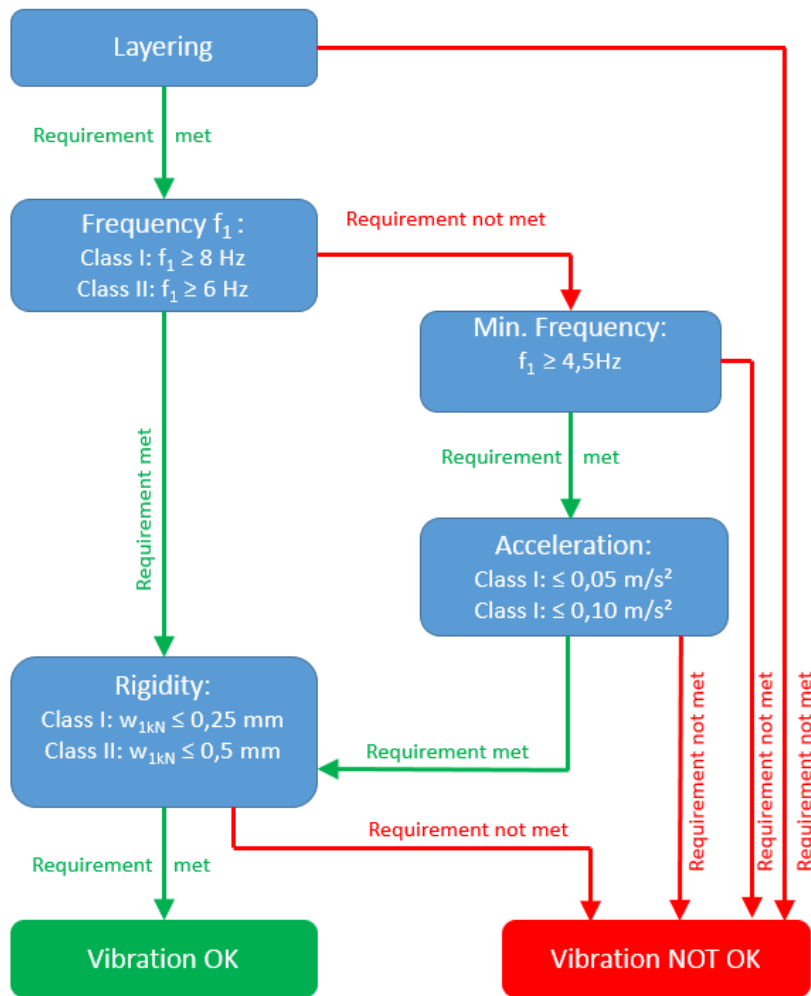


Figure 13-b: Vibration design flow chart

## 13.3 Vibration - future design method [23]

It is recommended to calculate the floor vibration according to proposal [23]. The following equations are valid for floors with approximately rectangular plan views.

### 13.3.1 1<sup>st</sup> natural frequency $f_1$

$$f_1 = \frac{\pi}{2 \cdot l^2} \sqrt{\frac{(EI)_{y,ef}}{m}} \cdot \sqrt{1 + \frac{(EI)_{x,ef}}{(EI)_{y,ef}} \cdot \left(\frac{l}{w}\right)^4} \quad \text{Eq. 13-24}$$

*accounting for rigidity in cross direction*

|               |  |
|---------------|--|
| $f_1$         | First fundamental frequency [Hz]   |
| $(EI)_{y,ef}$ | Effective bending stiffness about the y-axis [kN·m <sup>2</sup> /m]  |
| $(EI)_{x,ef}$ | Effective bending stiffness about the x-axis (perpendicular to span) [kN·m <sup>2</sup> /m]<br>In case of CLT RP, this is the flexural rigidity in cross direction of the horizontal structural CLT floor + the screed rigidity, if any. |
| $m$           | Mass of the structure (Self-weight) in kg/m <sup>2</sup> = $\sum_{i \geq 1} G_{k,i}$ [kg/m <sup>2</sup> ]  |
| $w$           | Width of the floor disregarding panel joints (Width of the room perpendicular to the span) [m]   |
| $l$           | Span [m]   |

Note:

The modulus of elasticity shall be taken as mean value ( $E_{0,mean}$ ). In general, the influence of shear deformations on the 1st natural frequency  $f_1$  can be neglected.

### 13.3.2 Deflection due to 1 kN single load in the most unfavourable position on the floor (stiffness criterion)

$$w_{1kN} = \frac{F(= 1kN) \cdot l^3}{48 \cdot (EI)_{y,ef} \cdot \left[ \frac{l}{1,1} \cdot \sqrt{\frac{(EI)_{x,ef}}{(EI)_{y,ef}}} \right]} + \frac{F(= 1kN) \cdot l}{4 \cdot (GA)_{y,ef} \cdot \left[ \frac{l}{1,1} \cdot \sqrt{\frac{(EI)_{x,ef}}{(EI)_{y,ef}}} \right]} \quad \text{Eq. 13-25}$$

|               |  |
|---------------|--|
| $w_{1kN}$     | Deflection through to a single load of 1 kN in the most unfavorable position on the floor [m]  |
| $(EI)_{y,ef}$ | Effective bending stiffness about the y-axis [kN·m <sup>2</sup> /m]  |
| $(EI)_{x,ef}$ | Effective bending stiffness about the x-axis (perpendicular to span) [kN·m <sup>2</sup> /m]<br>In case of CLT RP, this is the flexural rigidity in cross direction of the horizontal structural CLT floor + the screed rigidity, if any. |
| $b_F$         | Contribution width for vibration [m]   |
|               | $b_F = \left[ \frac{l}{1,1} \cdot \sqrt{\frac{(EI)_{x,ef}}{(EI)_{y,ef}}} \right]$  |
| $(GA)_{y,ef}$ | Shear stiffness of the rib panel in longitudinal direction [kN/m].   |
| $l$           | Span [m]   |

Perception is frequency dependent, people being most sensitive to vibration between 4 and 8 Hz. Below a floor frequency of 8 Hz an acceleration criterion can be applied and above 8 Hz a velocity criterion can be applied.

### 13.3.3 Design procedure for transient floors → when $f_1 \geq 8$ Hz

when  $f_1 \geq 8$  Hz

$$v_{rms}[m/s] < \text{Response factor} \cdot v_{rms,base} = R \cdot 0.0001 [m/s]$$

To predict the response of a floor it is necessary to have an agreed footfall loading model. When the floor frequency is much higher than the walking frequency, the floor response dies out in between footfalls (known as transient response). Hence footfall loading can be idealized as a mean impulsive load (Wilford et al) by:

#### Mean modal impulse I

The mean modal impulse of the floor shall be calculated based on a suitable walking frequency:

$$I = 42 \cdot \frac{f_w^{1.43}}{f_n^{1.3}} \quad \text{Eq. 13-26}$$

$f_w$  walking frequency (e. g.  $f_w = 1.5$  Hz) [Hz]

$f_n$  modal frequency of the floor [Hz] Eq. 13-27

$$f_n = \frac{18}{\sqrt{\delta}} \cdot \sqrt{\frac{(EI)_{x,ef} \cdot l^4}{(EI)_{y,ef} \cdot w^4} + 1}$$

Calculate frequency of 1st mode of the floor using the standard formula above, where delta  $\delta$  is the deflection of the floor assuming one-way span and pinned supports,  $(EI)_{x,ef}/(EI)_{y,ef}$  is the ratio of transverse to longitudinal stiffness,  $l$  is the span of the floor and  $w$  is the width.

#### Peak velocity response of the first mode $v_{1,peak}$ [m/s]

The peak velocity response of the first mode using the standard equation below shall be calculated, assuming a modal mass ( $M^*$ ) of 25% of the floor mass including a realistic proportion of live load, which is based on the assumption that floor behaves like a pin supported plate. It is well known that the ratio of modal mass to total mass of the 1st mode of a plate is 25%.

$$v_{1,peak} = \frac{I}{M^*} \quad \text{Eq. 13-28}$$

$M^*$  modal mass [kg] assuming that the floor is rectangular, and pin supported on all 4 sides.

$$M^* = \frac{m \cdot l \cdot w}{4}$$

$w$  width of the floor [m]

$l$  span [m]

## **Total peak response** $v_{tot,peak}$ [m/s]

$v_{1,peak}$  shall be multiplied by a factor  $K_{imp}$  to account for the contribution of higher modes. The number of higher modes that contribute to the response and therefore  $K_{imp}$  is a function of the ratio of the stiffnesses of the floor in the two directions and is therefore a function of  $w$ ,  $l$ ,  $(EI)_{x,ef}$  and  $(EI)_{y,ef}$ . The equation for  $K_{imp}$  below has been obtained from a parametric analysis accounting for variations of  $w/l$  from 1 to 10 and  $(EI)_{x,ef}/(EI)_{y,ef}$  from 0,05 to 1.

$$v_{tot,peak} = v_{1,peak} \cdot K_{imp} = v_{1,peak} \cdot \max \left[ 0.48 \cdot \left( \frac{w}{l} \right) \cdot \left( \frac{(EI)_{x,ef}}{(EI)_{y,ef}} \right)^{0.25}, 1.0 \right] \quad \text{Eq. 13-29}$$

with

- $w$  Width of the floor [m]
- $l$  Span [m]
- $K_{imp}$  Factor considering the contribution of higher modes [-]

## **Root mean square velocity** $v_{rms}$ [m/s]

Finally, to obtain a  $v_{rms}$  value of velocity between footfalls it is necessary to multiply the total peak by a reduction factor again obtained from a parametric analysis:

$$v_{rms} = \beta \cdot v_{tot,peak} \quad \text{Eq. 13-30}$$

with

$$\beta = (0.65 - 0.01 \cdot f_n) \cdot (1.22 - 0.11 \cdot \zeta) \cdot \eta$$

- $\beta$  Reduction factor (from a parametric analysis) [-]
- $\zeta$  Damping ratio [-]
- $\eta$  Factor
 
$$\eta = \begin{cases} 1.52 - 0.55 \cdot K_{imp} & \text{if } 1.0 \leq K_{imp} \leq 1.5 \\ 0.69 & \text{else} \end{cases}$$

## **Response factor R** [-]

$$R = \frac{v_{rms}}{v_{perception}} = \frac{v_{rms} [m/s]}{0.0001[m/s]} \quad \text{Eq. 13-31}$$

with

- $v_{perception}$  Perceptible vibration velocity (vpercep. = 0.0001 m/s)



### 13.3.4 Design procedure for resonant floors → when $f_1 < 8$ Hz

when  $f_1 < 8$  Hz

$$a_{rms}[m/s^2] < \text{Response factor} \cdot a_{rms,base} = R \cdot 0.005 [m/s^2]$$

The equation to calculate the full build up rms-acceleration from 1st principles (if only one mode governs) is given as follows:

#### **Root mean square acceleration $a_{rms}$ [m/s<sup>2</sup>]**

$$a_{rms} = \frac{F_{dyn}}{v_{perception}} = \frac{F_{dyn}}{2\sqrt{2} \cdot \zeta \cdot M^*} \quad \text{Eq. 13-32}$$

with

$M^*$  modal mass [kg] assuming that the floor is rectangular, and pin supported on all 4 sides.

$$M^* = \frac{m \cdot l \cdot w}{4}$$

$F_{dyn}$  dynamic force amplitude calculated as dynamic load factor times weight of a walking person [N]

$$F_{dyn} = 0.4 \cdot \alpha \cdot F_0 ; F_0 = 700N ; \alpha = e^{-0.4 \cdot f_1}$$

$l$  span [m]

#### **Response factor R [-]**

$$R = \frac{a_{rms}}{a_{perception}} = \frac{a_{rms} [m/s]}{0.005[m/s]} \quad \text{Eq. 13-33}$$

with

$a_{perception}$  Perceptible vibration acceleration ( $a_{perception} = 0.005m/s^2$ )

### 13.3.5 Floor damping values

For CLT rib panels the following floor damping values should be applied

$\zeta = 0.03$  for mass timber floors without a floating layer (screed)

$\zeta = 0.04$  for mass timber floors with a floating layer (screed)

Note:

The given values were taken from NA of Austria (ÖNORM B 1995-1-1:2019). In publication [23] slightly different (lower) values are mentioned.

### 13.3.6 Floor performance levels and corresponding vibration criteria

Six different floor performance levels and respective floor vibration criteria have been proposed by CEN/TC250/SC5/WG3/SG4 as shown in Table 13-2. It is intended that for different use categories, the floor performance level will either be specified in national annexes or by the client or structural designer.

Table 13-2: Floor performance levels and corresponding vibration criteria

| Criteria   | Floor performance levels |          |             |             |             |             |
|--|--------------------------|----------|-------------|-------------|-------------|-------------|
|  | Level I                  | Level II | Level III   | Level IV    | Level V     | Level VI    |
| Frequency $f_1$ [Hz]   | $\geq 4.5$               |          |             |             |             |             |
| Stiffness criteria $w_{1kN}$ [mm]                              | $\leq 0.25$              |          | $\leq 0.50$ | $\leq 0.80$ | $\leq 1.20$ | $\leq 1.60$ |
| Response factor R  | 4                        | 8        | 12          | 16          | 20          | 24          |
| Acceleration criteria if $f_1 < 8$ Hz<br>$a_{rms}$ [ $m/s^2$ ] | $R \cdot 0.005$          |          |             |             |             |             |
| Velocity criteria if $f_1 \geq 8$ Hz<br>$v_{rms}$ [ $m/s^2$ ]  | $R \cdot 0.0001$         |          |             |             |             |             |

Note:

The current requirements of EN 1995-1-1, Austrian NA match approximately the floor performance levels II (NA-AT: class 1) and III (NA-AT: class 2). Table 13-2 is currently under discussion to be implemented in a new draft of EN 1995-1-1

### 13.3.7 Recommendations for the choice of the floor performance level

Depending on the desired quality of the floors system and the given use categories, different floor performance levels can be recommended.

Table 13-3: Floor performance levels depending on quality class and use category

| Use category           | Quality choice | Base choice | Economy choice |
|------------------------|----------------|-------------|----------------|
| <b>A (residential)</b> | Level III      | Level IV    | Level V        |
| <b>B (office)</b>      | Level II       | Level III   | Level IV       |

## 14 Safety in case of fire

### 14.1 Reaction to fire

Reaction to fire requirements are specified for wood surfaces to control the risk of flame spread in buildings. They set boundary conditions for the use of visible wood in claddings and structures. In some cases, fire retardant treatments or sprinkler systems can allow more visible wood structures to be used in architectural design.

CLT Rib Panels by Stora Enso in relation to its reaction to fire behaviour is classified as D-s2, d0 according to the European classification system defined in EN 13501-1:2018 [24].

The format of the reaction to fire classification is:

| Fire behaviour |   | Smoke production |   |   | Flaming droplets |   |
|----------------|---|------------------|---|---|------------------|---|
| D              | - | S                | 2 | , | d                | 0 |

The reaction to fire classification can be improved by fire retardant treatments or with inorganic surface laminates which can delay the combustion of derived timber products and reduce the subsequent release of energy. Depending on the retardant used, the product can be classified up to a class B-s1,d0, which is the highest class for combustible materials.

- Euro classes: A1, A2, B, C, D, E, F (Criteria: ignitability, flame propagation, heat release)
- Smoke classes: s1, s2, s3 (s1 => lowest smoke production)
- Burning droplets classes: d0, d1, d2 (d0 => no flaming droplets)

### 14.2 Resistance to fire of CLT Rib Panels based on calculations according to EN 1995-1-2:2011 (Eurocode 5)

The R (resistance) criterion in the fire design is evaluating the load bearing capacity of a structure or structural component after a certain minimum required fire duration, at the time  $t$  (=time of exposure to fire).

Within the scope of the CLT Rib Panel by Stora Enso ETA, the fire design shall be executed according to EN1995-1-1 [3], EN1995-1-2 [25] and the applicable national annexes of these standards.

As an alternative, the verification of fire resistance can be based on classification reports (see chapter 17) in accordance with EN 13501-2 based on large-scale fire tests.

It is possible to protect the CLT Rib Panels to a certain extent by protecting layers, e.g.: gypsum plaster boards. These delay the start of charring and increase the fire resistance of the element.

Generally, it shall be assumed that the fire is acting on the rib/box panel from the bottom.

For resistance to fire, load-bearing performance (R criterion) can be determined in accordance with EN 1995-1-2 as a part of design of works.

For the required time of fire exposure  $t$ , the following condition shall be fulfilled:

$$E_{d,fi} \leq R_{d,t,fi} \quad \text{Eq. 14-1}$$

where

$E_{d,fi}$  Design value of the most critical effect of actions for the fire situation (= load effect)  
(With materials other than wood, thermal expansion must also be taken into account.)

$R_{d,t,fi}$  Design strength value in case of fire at time  $t$  using the reduced cross-section (= resistance)

## 14.3 Verification method for actions in the fire situation according to EN 1995-1-2:2011

The design value for actions in the fire situation should be determined for time  $t = 0$  using combination factors  $\psi_{1,1}$  or  $\psi_{2,1}$  according to EN 1991-1-2:2002, clause 4.3.1. (See also EN 1990-1-1, clause 6.4.3.3.)

$$E_{d,A,fi} = \sum G_{k,j} + "P" + "A_d" + "Q_{k,1} \cdot (\psi_{1,1} \text{ or } \psi_{2,1})" + \sum \psi_{2,1} \cdot Q_{k,i} \quad \text{Eq. 14-2}$$

where

|           |  |
|-----------|--|
| $G_{k,j}$ | is the characteristic value of a permanent action $j$                    |
| $P$       | is the decisive representative value of a pre-load                       |
| $A_d$     | is the design value of an exceptional action                             |
| $Q_{k,1}$ | is the characteristic value of a decisive variable action 1              |
| $Q_{k,i}$ | is the characteristic value of a decisive variable action $i$            |
| $\psi_1$  | is the combination factor for frequent values of variable actions        |
| $\psi_2$  | is the combination factor for quasi-permanent values of variable actions |

It is up to the engineer to choose/use  $\psi_{1,1}$  (when leading action is snow, ice and wind) or  $\psi_{2,1}$  (leading action not snow, ice and wind).

For simplicity, the design value for actions in the fire situation  $E_{d,fi}$  from the calculation of the design value for actions at normal temperature  $E_d$  may be determined thus:

$$E_{d,fi} = \eta_{fi} \cdot E_d \quad \text{Eq. 14-3}$$

where

|             |  |
|-------------|--|
| $E_{d,fi}$  | is the design value of actions for the fire situation  |
| $\eta_{fi}$ | is the reduction factor for the design value of actions in the fire situation                    |
| $E_d$       | is the design value for actions at normal temperature for the fundamental combination of actions |

For the load combination in accordance with EN 1990-1-1, the reduction factor  $\eta_{fi}$  should be taken as follows, whereby the smallest value is given by the following two equations:

$$\eta_{fi} = \frac{G_k + \psi_{fi} \cdot Q_{k,1}}{Y_G \cdot G_k + Y_{Q,1} \cdot Q_{k,1}}$$

Eq. 14-4

$$\eta_{fi} = \frac{G_k + \psi_{fi} \cdot Q_{k,1}}{\xi \cdot Y_G \cdot G_k + Y_{Q,1} \cdot Q_{k,1}}$$

Eq. 14-5

where

|             |   |
|-------------|---|
| $G_k$       | is the characteristic value of a permanent action   |
| $Q_{k,1}$   | is the characteristic value of the leading variable action 1  |
| $Y_G$       | is the partial safety factor for permanent actions  |
| $Y_{Q,1}$   | is the partial safety factor for the leading variable action  |
| $\psi_{fi}$ | is the combination factor for frequent values of variable actions in the fire situation, given either by $\psi_{1,1}$ or $\psi_{2,1}$ , see EN 1991-1-1 |
| $\xi$       | is a reduction factor for unfavorable permanent actions G (see EN 1990-1-1, clause A.1.3.1)   |

As a simplification, for the reduction factor  $\eta_{fi}$ , as an alternative to the above equation, the recommended value is

$\eta_{fi} = 0.6$  according to EN 1995-1-2:2011, clause 2.4.2. Exceptions here are areas with larger imposed loads according to category E given in EN 1991-1-2:2002, where the recommended value is  $\eta_{fi} = 0.7$ .

When comparing the options for determining actions, it is clear that the simplified assumption with the action  $E_{d,fi}$  results in a greater load than the actions in the exceptional design situation  $E_{d,A}$ .

## 14.4 Verification method for mechanical resistance in the fire situation according to EN 1995-1-2:2011

For verification of mechanical resistance, the design values of strength and stiffness properties shall be determined from:

$$X_{d,fi} = k_{mod,fi} \cdot \frac{X_{k,20}}{\gamma_{M,fi}}$$

$$f_{d,fi} = K_{mod,fi} \cdot \frac{f_{20}}{\gamma_{M,fi}} \quad \text{Eq. 14-6}$$

where

- $f_{d,fi}$  is the design strength value in fire
- $K_{mod,fi}$  is the modification factor in the fire situation for the reduced cross-section method: (same for each part)  
 $K_{mod,fi} = 1,0$  (as per EN 1995-1-2) in most cases, except when the method of annex C of EN 1995-1-2 is used
- $f_{20}$  is the 20% fractile value of a strength property at normal temperature; the 20 % fractile of a strength property may be calculated as:  
 $f_{20} = K_{fi} \cdot f_k$
- $f_k$  is the 5% fractile value of a strength property
- $K_{fi}$  is the coefficient for converting 5% to 20% fractile values;  
 $K_{fi} = 1.15$  (as per EN 1995-1-2)
- $\gamma_{M,fi}$  is the partial safety factor for timber in fire. For CLT and Glued Laminated Timber the partial factor in fire design is  $\gamma_{M,fi} = 1,0$  (as per EN 1995-1-2)  
 Information on national choice may be found in the national annex.

For the calculation in the fire situation, instead of the 5% fractile values, the 20% fractiles are used. The reason for this assumption lies in the extremely low probability of occurrence of a fully developed fire during the lifetime of a supporting structure and does not depend on the material.

For stability calculations, the characteristic values of stiffness properties at normal temperature are used.

## 14.5 Design stiffness values

For fire design, the mean values of stiffness at time  $T=0$  ( $E_{mean}$ ,  $G_{mean}$  and  $G_{r,mean}$ ) shall be used. (see EN1995-1-2, item 2.3 (1) and 2.4.2 (1)).

## 14.6 Charring rates of CLT Rib Panel by Stora Enso

There are two different types of charring rates  $\beta_0$  and  $\beta_n$ . For panels and wide cross sections one-dimensional charring rate  $\beta_0$  is used in the calculations. This is also used as the basis value in some more advanced calculation methods.

When the characteristic density of GLT is  $\rho_k \geq 290 \text{ kg/m}^3$ , under standard fire exposure, the one-dimensional charring rate  $\beta_0$  is 0,65 mm/min and the notional design charring rate  $\beta_n$  is 0,70 mm/min.

In the CLT, the charring rates shall be used in the simplified bilinear model of clause 3.4.3 (Surface of beams and columns initially protected from fire exposure) of EN 1995-1-2:2004 including the tabulated multiplication

factors of the clause to determine the charring depth according to time requirements, considering clause 4.2.2 (Residual cross section method) of EN 1995-1-2:2004. For the application of the simplified bilinear method, it should be highlighted that the fire exposed lamella shall be considered as a protective cladding of the subsequent lamella.

During exposure to fire and to the resulting effect of temperature on the CLT cross-section, the use of polyurethane (PUR) adhesives between individual layers can lead to softening. A possible consequence of this may be that small sections of the heat-insulating char layer fall off, and the protective function of this layer may be lost at certain points.

Therefore, possible delamination must be taken into account, and, for the subsequent fire-exposed layers, it is necessary to mathematically estimate an increased charring rate until the formation of a new 25 mm-thick char layer (see Figure 14-b).

### 14.6.1 Design value of charring rates for surfaces which are unprotected throughout the time of fire exposure

According to Statement No. VTT-S-05640-17 [26], following design values for charring rate  $\beta$  for GLT and CLT must be used for surfaces/members of CLT rib decks which are unprotected throughout the duration of the fire exposure as well as for surfaces being initially protected from fire exposure.

Further rules for surfaces initially protected from fire exposure are given in chapters 14.6.5 and 14.6.6.

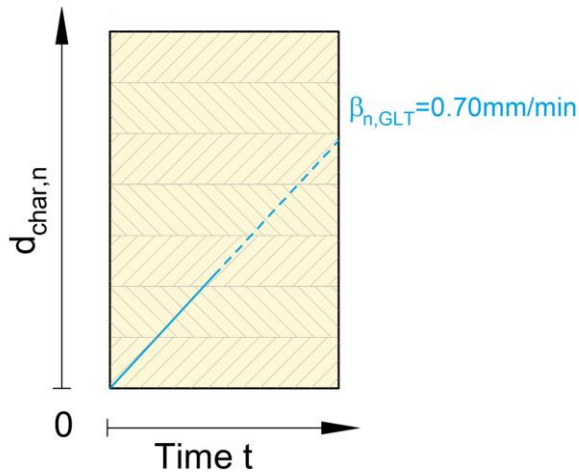


Figure 14-a: Linear notional charring rate of GLT rib

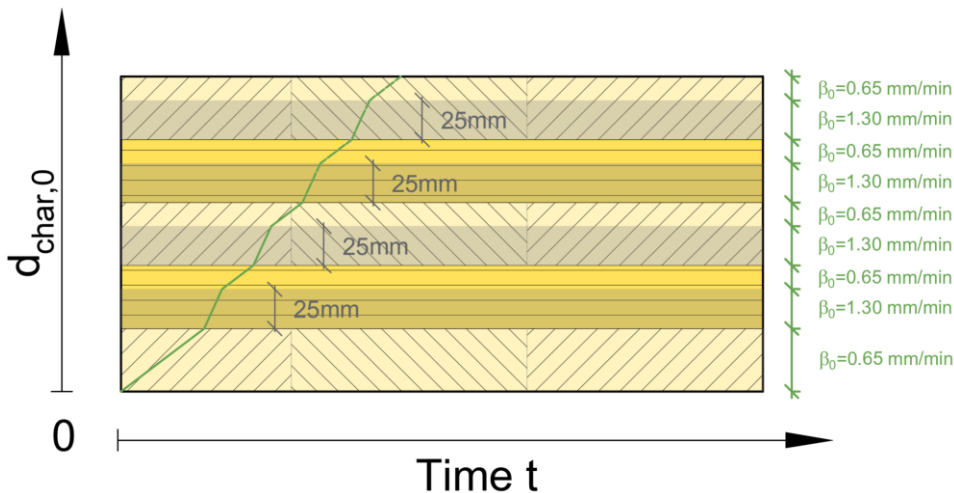


Figure 14-b : Variation of charring depth as a function of time for a horizontal 5-layered CLT

Table 14-1: Charring rates of CLT and GLT

|  | Design charring rate for one-dimensional charring $\beta_0$ | Design notional charring rate $\beta_n$ |
|--|---|---|
| GLT with characteristic density of $\geq 290 \text{ kg/m}^3$ | 0,65 mm/min [25]  | 0,70 mm/min [25]                        |
| CLT according to ETA-14/0349                                 | 0,65 mm/min [26]  | -                                       |

**14.6.2 Design value of charring rates for surfaces which are initially protected from exposure to fire by protective gypsum plasterboard (following the rib section in case of Open type, or mounted on the bottom side of a CLT rib panel in case of Inverted or Closed type)**

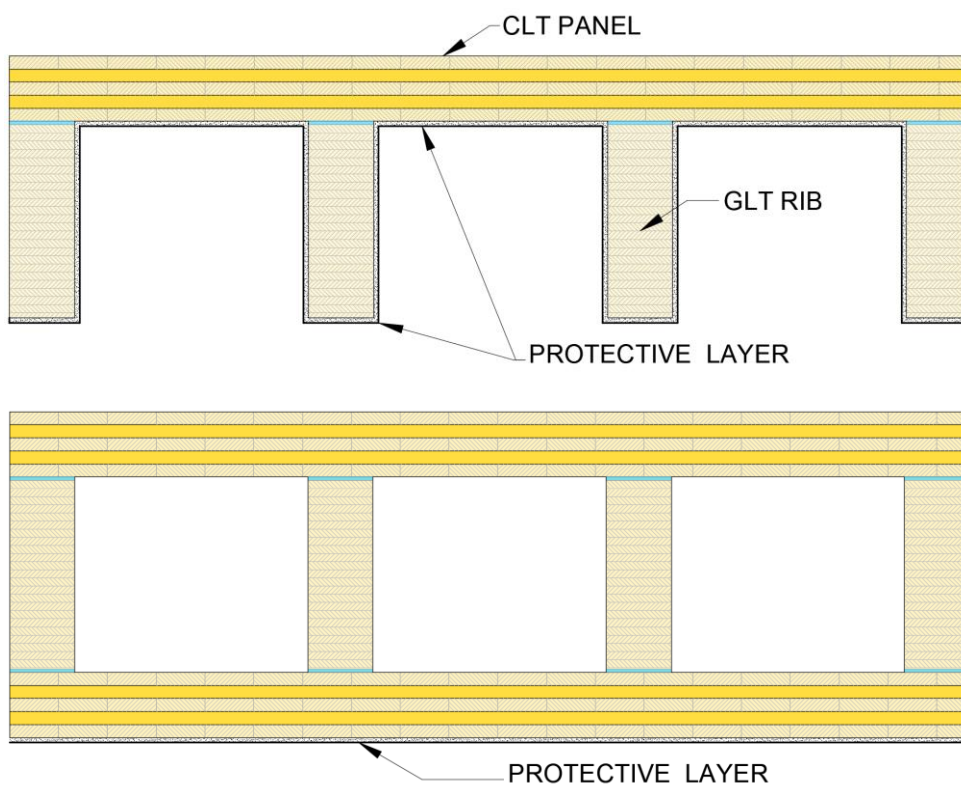


Figure 14-c: CLT Rib Panel with protective layer, following the outline of the soffit

Fire resistance rating of components is determined during exposure to fire on the inside of a room predominantly by interior cladding. To increase the fire resistance of structures such as wall, ceiling, roof or beam elements, plaster building materials/gypsum plasterboards are generally used as, even if they are not very thick, they provide effective protection.

Effective protection is based particularly on the combined crystal water in the panels' gypsum core which has a concentration of approx. 20%. Energy is consumed by the evaporation of this crystal water, and a protective steam curtain is also formed on the fire-exposed side of the component. In addition to delaying the spread of fire, the dehydrated gypsum layer also acts as insulation through the declining thermal conductivity. Fire protection plasterboard also contains glass fibre which reinforces the gypsum core and ensures structural cohesion when exposed to fire.



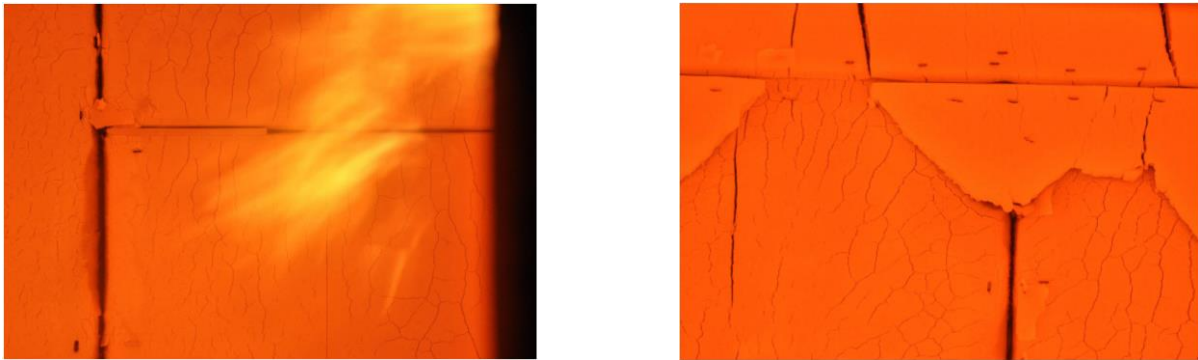


Figure 14-d: Two-ply fire protection plasterboard cladding exposed to fire during a large-scale fire test

Figure 14-d illustrates the behavior of fire protection plasterboard when exposed to fire; in this case there are two layers of cladding.

As it can be seen, after crazing and detaching of the char layer, as time progresses, large gaps appear between the joints, the joint plaster compound fails, and the first section of the first plasterboard layer falls off. If larger panel sections fall away from the first layer, crazing also occurs in the second layer. After gaps appear in this layer's joints, the flames spread through the increasing gaps in the joints towards the underlying timber member which leads to the production and emission of wood gas. Charring starts on the initially protected CLT Rib Panel element.

In the case of initially protected members, the time of start of charring behind the protective layer or cladding  $t_{ch}$  and the failure time of the protective cladding  $t_f$  is essential. According to EN 1995-1-2:2011, the following must be taken into account:

- The start of charring is delayed until time  $t_{ch}$  ;
- Charring can occur before failure of the fire protective cladding, however until the failure time  $t_f$ , the charring rate is lower than the value according to [27], table 3.1 concerning GLT and the value according to [28] for CLT;
- The charring rate after the failure time  $t_f$  of the fire protective cladding until time  $t_a$  is greater than the value according to [27] table 3.1 concerning GLT and the value according to [28] for CLT;
- The charring rate from time  $t_a$ , where the charring depth corresponds to the lowest value – either the charring depth of a similar component without fire protective cladding or 25 mm – again takes the values according to [27], table 3.1 concerning GLT and the values according to [28] for CLT.



The following diagrams from EN 1995-1-2 [29] are provided to support the understanding of the points above (Those diagrams might be updated in the next version of the EN 1995-1-2):

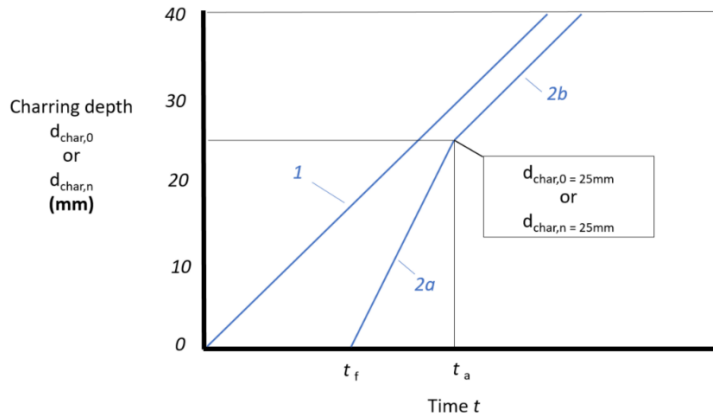


Figure 14-e: Charring depth depending on the time for  $t_{ch} = t_f$  and a charring depth of 25 mm at time  $t_a$

- 1: Relationship for components which are unprotected throughout the time of fire exposure with the notional charring rate  $\beta_n$  (or  $\beta_0$ )

- 2: Relationship for initially protected components after failure of the fire protective cladding

2a: After the fire protective cladding has fallen off, charring starts at an increased rate

2b: After the charring depth exceeds 25 mm or the time  $t_a$  is exceeded, the charring rate reduces to the normal rate.

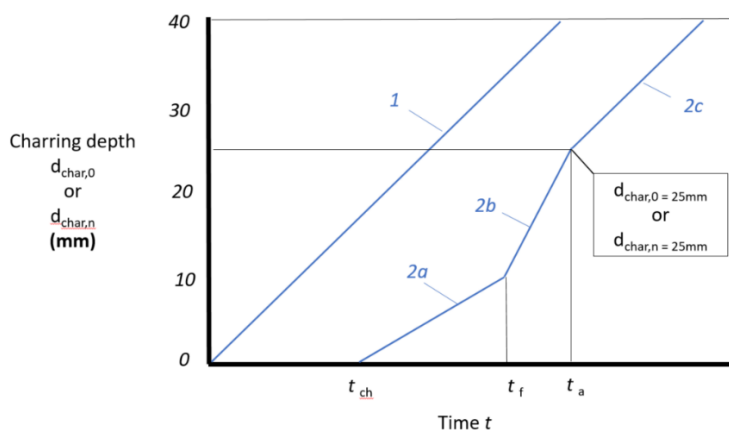


Figure 14-f: Charring depth depending on the time for  $t_{ch} < t_f$

- 1: Relationship for components which are unprotected throughout the time of fire exposure with the notional charring rate  $\beta_n$  (or  $\beta_0$ )

- 2: Relationship for initially protected components on which charring starts before failure of the fire protective cladding

2a: Charring starts at  $t_{ch}$ , at a reduced rate for as long as the fire protective cladding remains intact

2b: After the fire protective cladding falls off, charring starts at an increased rate

2c: After the charring depth exceeds 25 mm or the time  $t_a$  is exceeded, the charring rate reduces to the normal value.

A design for initially protected CLT Rib Panels with, protective layers following the outline of the soffit of a rib panel, are to be executed according to rules of chapter 3.4.3 in EN 1995-1-2:2004 [25].

## Charring rates for initially protected components

For time  $t_{ch} \leq t \leq t_f$ , the charring rates given in EN 1995-1-2 [29], table 3.1 should be multiplied by a factor  $k_2$ ; for single layer gypsum plasterboard, type F, this is calculated as:

$$k_2 = 1 - 0,018 \cdot h_p \quad \text{Eq. 14-7}$$

where:

$h_p$  is the thickness of the layer in mm

For several layers of gypsum plasterboard, type F,  $h_p$  should be taken as the thickness of the inner layer.

If the timber component is protected by rock wool batts (thickness:  $\geq 20$  mm, bulk density:  $\geq 26$  kg/m<sup>3</sup>, melting point:  $\geq 1000$  °C), the factor  $k_2$  may be taken from Table 14-2. For thicknesses between 20 and 45 mm, linear interpolation may be applied.

Table 14-2: values of  $k_2$  for timber components protected by rock fibre batts

| Thickness<br>$h_{ins}$<br>mm | $k_2$ |
|------------------------------|-------|
| 20                           | 1     |
| $\geq 45$                    | 0,6   |

For the stage after failure of the fire protective cladding given by  $t_f \leq t \leq t_a$ , according to [29], the charring rates given in EN 1995-1-2, table 3.1 should be multiplied by a post-protection factor  $k_3 = 2$ .

For  $t \geq t_a$ , the charring rates should be applied without multiplication by the factor  $k_3$ .

The time limit  $t_a$  (see Figure 14-e) should for  $t_{ch} = t_f$ , in accordance with [29], be taken as:

$$t_a = \min \left\{ \begin{array}{l} 2 \cdot t_f \\ \frac{25}{k_3 \cdot \beta_n} + t_f \end{array} \right. \quad \text{Eq. 14-8}$$

Or for  $t_{ch} < t_f$ : (see Figure 14-f)

$$t_a = \frac{25 - (t_f - t_{ch}) \cdot k_2 \cdot \beta_n}{k_3 \cdot \beta_n} + t_f \quad \text{Eq. 14-9}$$

where:

$\beta_n$  is the design value of the notional charring rate in mm/min.  
(In the case of one-dimensional charring,  $\beta_n$  is replaced by  $\beta_0$ .)

## 14.6.3 Start of charring on initially protected components

- **Single layer gypsum plasterboard, type A, F or H:**

For claddings consisting of one layer of gypsum plasterboard, type A, F or H, according to EN 520, outside of joints or at locations adjacent to filled joints, or unfilled gaps with a width of 2 mm or less, in accordance with [29], the start of charring  $t_{ch}$  should be taken as:

$$t_{ch} = 2,8 \cdot h_p - 14 \quad \text{Eq. 14-10}$$

In locations adjacent to joints with unfilled gaps with a width of more than 2 mm, the time of start of charring should be calculated as:

$$t_{ch} = 2,8 \cdot h_p - 23 \quad \text{Eq. 14-11}$$

where:

|          |  |
|----------|--|
| $t_{ch}$ | is the time of start of charring of a protected component in minutes |
| $h_p$    | is the thickness of the fire protective cladding in mm               |

- **Two-layer gypsum plasterboard, type A or H:**

For claddings consisting of two layers of gypsum plasterboard, type A or H in accordance with EN 520, according to [29], the time of start of charring  $t_{ch}$  should be determined according to the equations above, where the thickness  $h_p$  is taken as the thickness of the outer layer and 50% of the thickness of the inner layer. This is subject to the condition that the spacing of fasteners in the inner layer is not greater than the spacing of fasteners in the outer layer.

- **Claddings consisting of two layers of gypsum plasterboard, type F:**

For claddings consisting of two layers of gypsum plasterboard, type F in accordance with EN 520, according to [29], the time of start of charring  $t_{ch}$  should be determined according to the equations above, where the thickness  $h_p$  is taken as the thickness of the outer layer and 80% of the thickness of the inner layer. This is subject to the condition that the spacing of fasteners in the inner layer is not greater than the spacing of fasteners in the outer layer.

- **Beams protected by rock fibre batts (Cavity insulation material):**

If the timber component is protected by rock fibre batts (thickness:  $\geq 20$  mm, bulk density:  $\geq 26$  kg/m<sup>3</sup>, melting point:  $\geq 1000$  °C), for the time of start of charring  $t_{ch}$ , the following equation must also be taken into account:

$$t_{ch} = 0,07 \cdot (h_{ins} - 20) \cdot \sqrt{\rho_{ins}} \quad \text{Eq. 14-12}$$

where:

|              |   |
|--------------|---|
| $t_{ch}$     | is the time until the start of charring of a protected component in minutes |
| $h_{ins}$    | is the insulation material thickness in mm                                  |
| $\rho_{ins}$ | is the insulation material bulk density in kg/m <sup>3</sup>                |

## 14.6.4 Failure time of fire protective claddings

The charring or mechanical degradation of the cladding material, the spacing of, and distances between, fasteners and/or a possible insufficient penetration length of fasteners into the uncharred cross-section could be responsible for the failure of the fire protective cladding.

- **Cladding consisting of gypsum plasterboard, type A or H:**

For gypsum plasterboard, type A or H in accordance with EN 520, according to [30], the failure time  $t_f$  is equal to the time at the start of charring  $t_{ch}$ .

For gypsum plasterboard, type A or H, after the start of charring and after the cladding simultaneously falls off, charring occurs at an increased rate until time  $t_a$ . After formation of a 25 mm-thick char layer, the charring rate reduces to the normal rate – see Figure 14-e.

$$t_f = t_{ch} \quad \text{Eq. 14-13}$$

- **Cladding consisting of gypsum plasterboard, type F:**

However, in the case of gypsum plasterboard, type F or fire protection plasterboard, according to [29], there is less charring from the start of charring  $t_{ch}$  to the time  $t_f$ . Until the subsequent formation of a 25 mm-thick char layer, charring occurs at double the rate, after which, the charring rate reduces to the normal rate – see Figure 14-f.

EN 1995-1-2:2011 [29] does not provide any information regarding the failure time of gypsum plasterboard, type F or fire protection plasterboard.

The failure time of claddings made of gypsum plasterboards type F (according to EN 520) should be determined with respect to the thermal degradation of the cladding and with respect to pull-out failure of fasteners due to insufficient penetration length into the uncharred wood.

The failure time due to thermal degradation of the cladding should be assessed on the basis of tests or may be taken from a National Annex to EN 1995-1-2:2011 [29] containing all Nationally Determined Parameters to be used for the design of buildings and civil engineering works to be constructed in the relevant country. (According to [29], more information on test methods is given in EN 1363-1, EN 1365-1 and EN 1365-2.)

According to ÖNORM B 1995-1-2:2011 (Austrian national specifications), the failure times  $t_f$  for cladding consisting of fire protection plasterboard in accordance with ÖNORM B 3410 or gypsum plasterboards, type DF according to EN 520 and gypsum fibreboard GF-C1-W2 according to EN 15283-2 can be determined as follows:

Wall components:

$$t_f = 2,2 \cdot h_p + 4 \quad \text{Eq. 14-14}$$

Ceiling components:

$$t_f = 1,4 \cdot h_p + 6 \quad \text{Eq. 14-15}$$

where:

|       |  |
|-------|--|
| $t_f$ | is the failure time of the fire protective cladding in minutes |
| $h_p$ | is the thickness of the fire protective cladding in mm         |

In determining the failure time of multiple-layer cladding consisting of gypsum plasterboard, type F, the rules specified in section 14.6.3 apply correspondingly, according to which, the thickness  $h_p$  corresponds to the thickness of the outer layer and to 80% of the thickness of the inner layer.

- **Penetration length of fasteners for gypsum plasterboard**

In addition to thermal degradation of the cladding material, the fire protective cladding can also fall off due to the pull-out failure of fasteners.

According to [29], the required minimum length of the fasteners should also be determined in order to eliminate the fact that pull-out of the fasteners is a relevant factor for the failure of the fire protective cladding.

The minimum penetration length of the fastener  $l_a$  into the uncharred cross-section should be taken as 10 mm at least. The required penetration length of the fastener  $l_{af,req}$  is calculated as follows:

$$l_{f,req} = h_p + d_{char,0} + l_a \quad \text{Eq. 14-16}$$

where:

|              |   |
|--------------|---|
| $h_p$        | is the panel thickness in mm  |
| $d_{char,0}$ | is the charring depth in the timber component                             |
| $l_a$        | is the minimum penetration length of the fastener into the uncharred wood |

For more information on cladding fasteners/penetration lengths, see [29], section 7.1.2.

**14.6.5 Charring for surfaces, initially protected from fire exposure with protective layers, installed horizontally below ribs (void cavities), in case of a CLT Rib Panel Open type**

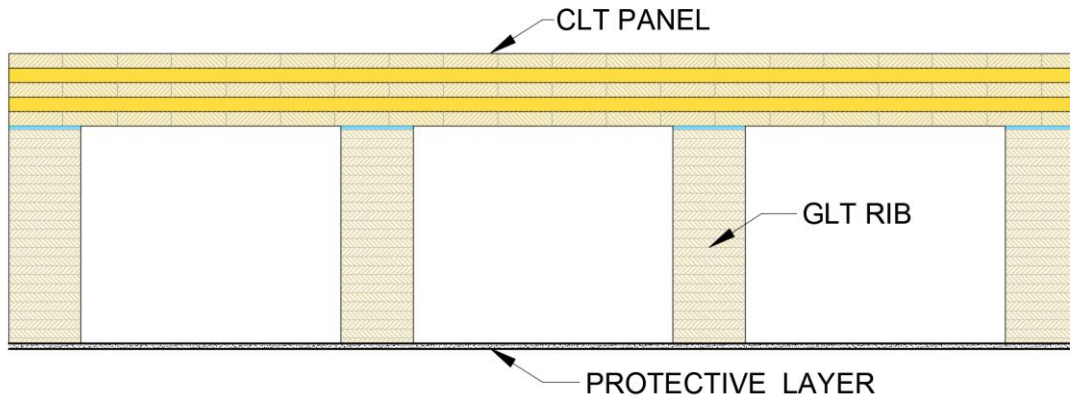


Figure 14-g: CLT Rib Panel with straight protective layer to the soffit of the ribs, creating voids

Analysis for initially protected CLT Rib Panels with protective layers installed horizontally below the ribs (with void cavities between ribs) are to execute according to rules of annex D in EN1995-1-2 [29] and applicable national annex.

**14.6.6 Charring for surfaces initially protected from fire exposure with protective layers installed horizontally below ribs (cavities filled with insulation) in case of a CLT Rib Panel Open type**

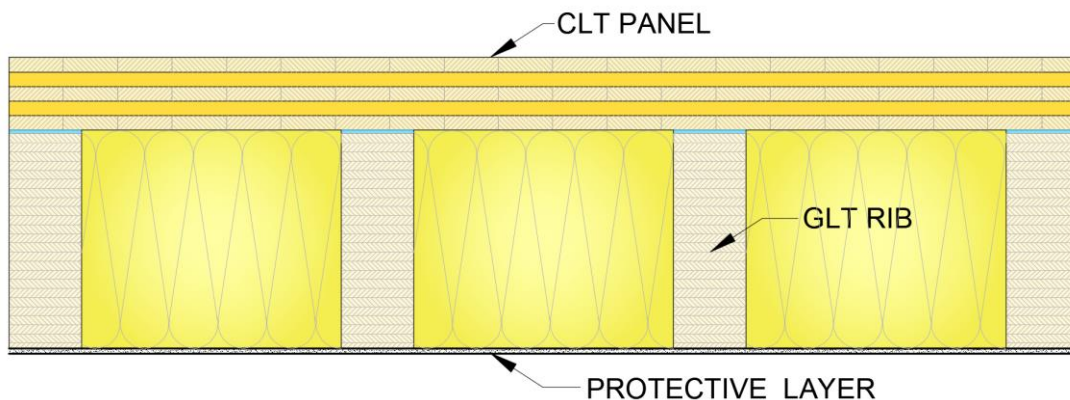


Figure 14-h: CLT Rib Panel with straight protective layer to the soffit of the ribs and filled with insulation

Analysis for initially protected CLT Rib Panels with protective layers installed horizontally below ribs (with cavities between ribs being completely filled with insulation) are to execute according to rules of annex C in EN1995-1-2 [29] and applicable national annex.

## 14.7 Determining the load-bearing capacity (R) of CLT Rib Panels elements according to EN 1995-1-2:2011

When determining the load-bearing capacity (R criterion) of timber components exposed to fire, or when calculating cross sectional values, in addition to determining the charring area, the underlying area affected by temperature must also be taken into account because the wood's strength and stiffness properties decrease as the temperature rises.

As an alternative to the calculation option specified in EN 1995-1-2, annex B, the cross-sectional values can also be calculated using two simplified methods. We recommend the first method:

- **Reduced cross-section method**

For verification in the fire situation, this method uses a reduced cross-section or residual cross-section, calculated on the basis of increased charring (roundings or corner charring), and an additional area affected by temperature (reduction of mechanical properties due to the effect of temperature).

- **Reduced properties method**

As an alternative to the reduced cross-section method – calculated with charring rate and corner charring, this method takes into account the reduction of mechanical properties depending on the type of load and cross-section.

The verification of load-bearing capacity in the fire situation shall be performed for CLT Rib Panel on the basis of the reduced cross-section method.

### 14.7.1 Reduced cross-section method

The cross-section which is reduced by the charring depth (residual cross section) is further reduced by removing a layer with zero strength and stiffness  $k_0 \cdot d_0$ . Thus, the residual cross-section is calculated by deducting the effective charring depth  $d_{ef}$  from the original cross-section as presented in Figure 14-i.

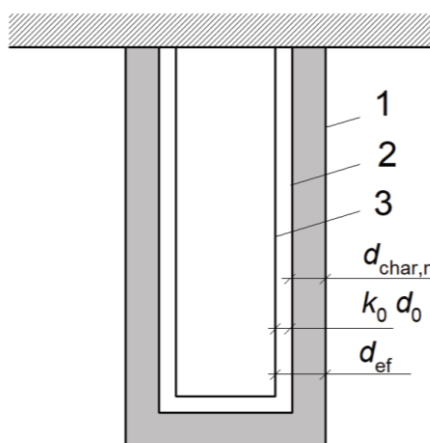


Figure 14-i: Definition of residual cross section and effective cross section.

1. Initial surface of member,
2. Border of residual cross section,
3. Border of effective cross section.

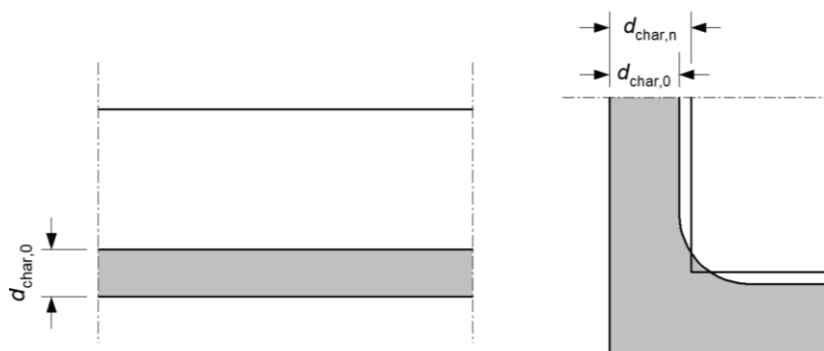


Figure 14-j: Left: One-dimensional charring of panel or wide cross section when fire exposure is below on one side,

Right: Charring depth  $d_{char,0}$  for one-dimensional charring and notional charring depth  $d_{char,n}$  which takes into account the rounding of corners.



$$d_{ef} = d_{char} + k_0 \cdot d_0 \quad \text{Eq. 14-17}$$

$d_{ef}$  is the effective charring depth  
 $d_{char}$  is the notional design charring depth:

| CLT panels                                    | GLT   |
|---|---|
| $d_{char,CLT} = d_{char,0} = \beta_0 \cdot t$ | $d_{char,GLT} = d_{char,n} = \beta_n \cdot t$ |

$\beta_0$  is the design value of the one-dimensional charring rate under standard fire exposure  
 $\beta_n$  is the design notional charring rate under standard fire exposure  
 $t$  is the time under fire exposure

| $k_0$ | CLT panels  | GLT  |
|-------|-------------|--|
|       | $k_0 = 1,0$ | $t < 20 \text{ min.}: k_0 = t / 20$<br>$t \geq 20 \text{ min.}: k_0 = 1.0$ |

$d_0$  is the depth of a layer (close to the char line) with assumed zero strength and stiffness.  
 $d_0 = 7 \text{ mm}$

Note: The value  $d_0$  of 7 mm (for the simplified calculation method of the reduced cross-section method) is currently being discussed by scientists around the world, however no unified opinion has been established. Possible national regulations on  $d_0$  must be taken into account.

For protected surfaces with a start of charring time of  $t_{ch} > 20$  minutes,  $k_0$  is assumed to vary linearly from 0 to 1 during the time interval from  $t = 0$  to  $t = t_{ch}$ , see Figure 14-k (b). For protected surfaces with  $t_{ch} \leq 20$  minutes  $k_0$  is  $t/20$ .

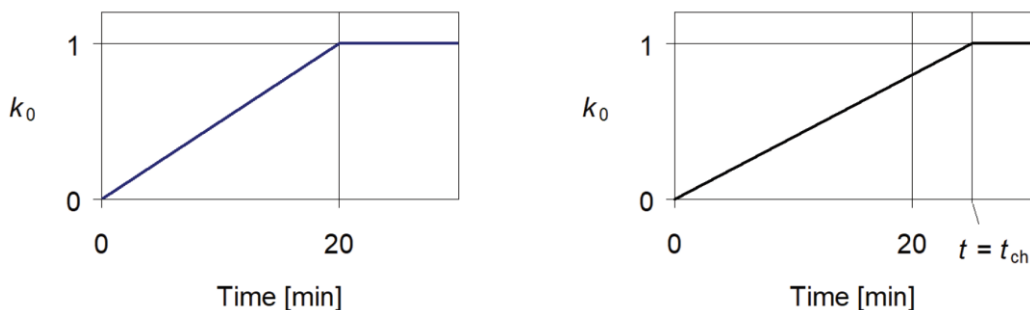


Figure 14-k:(a) Variation of  $k_0$  for unprotected members and protected members where  $t_{ch} \leq 20$  minutes and (b) for protected members where  $t_{ch} > 20$  minutes.

For timber surfaces facing a void cavity in a floor or wall assembly (normally the wide sides of a stud or a joist), the following applies:

- Where the fire protective cladding consists of one or two layers of gypsum plasterboard type A, wood paneling or wood-based panels, at the time of failure  $t_f$  of the cladding,  $k_0$  should be taken as 0,3. Thereafter  $k_0$  should be assumed to increase linearly to 1,0 during the following 15 minutes;
- Where the fire protective cladding consists of one or two layers of gypsum plasterboard type F, at the time of start of charring  $t_{ch}$ ,  $k_0$  is 1. For times  $t < t_{ch}$ , linear interpolation should be applied, see Figure 14-k (b).

The effective (reduced) cross section should be used for the calculation of the stiffness and fire resistance of an CLT Rib Panel element.



Residual cross-sections of layers  $\leq 3$  mm are not used in the remaining calculations. (This assumption takes into account the generally non-linear nature of the char line.)

The remaining analysis steps are performed in the same way as these for cold condition.

## Summarized design process:

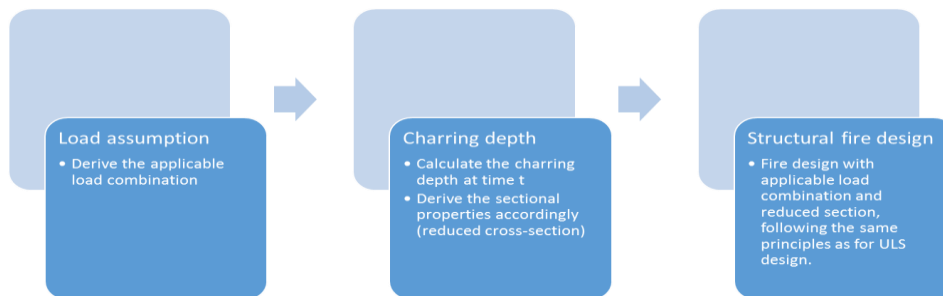


Figure 14-1: Summarized design process

## 15 Fire performance

- Fire design according to EN1995-1-2 (no limits)
- Force can be transferred through glue joint during fire – full composite action [31]
- 4 fire classification reports available

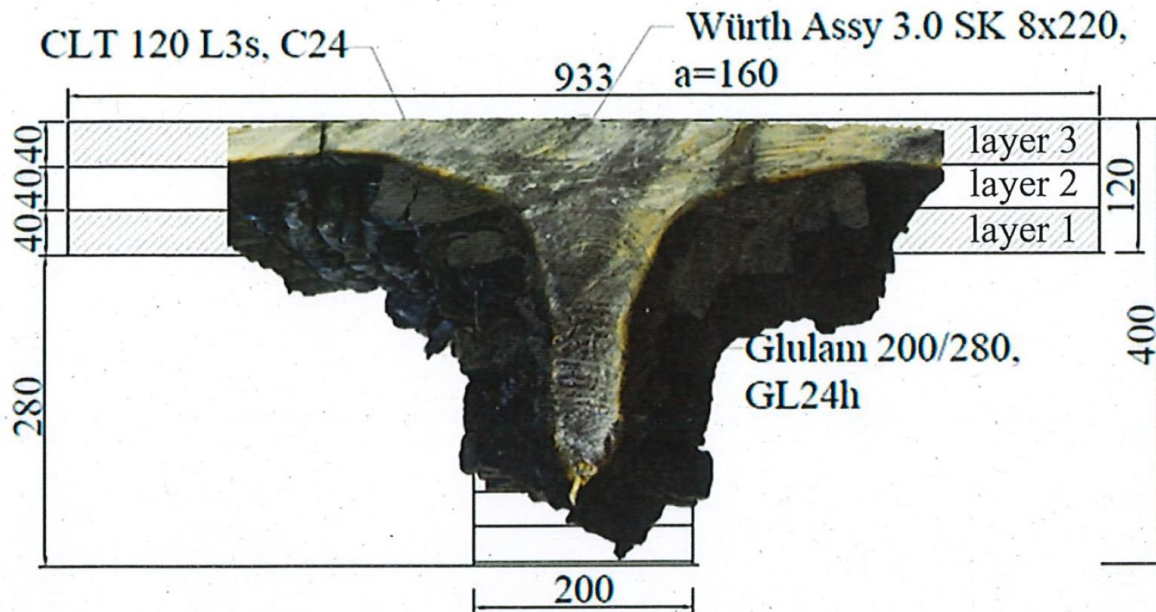


Figure 15-a: Fire test - Remaining cross-section of cross-section A after extinguishment of the test specimen (91+25) minutes

For the analysis of the composite action in fire of CLT Rib Panels manufactured by Stora Enso, the following results of four fire resistance tests were analyzed:

- Horizontal slip measured between CLT plates and glulam ribs
- Temperatures measured in the glue line between CLT plates and glulam ribs
- Residual cross-section documented after the tests (see Figure 15-a example)

After extinguishment of test specimens, residual cross-sections were cut out at quarter points of the total length (see Figure 15-a). In the glue line, no cracks or distortions were visible. The four test reports state the observation taken by the fire lab that "no visible damage was observed in the glue joint between CLT and rib."

The four fire resistance tests showed measurements of horizontal slip < 0.1 mm. Only in case of fall-off of the bottom CLT plate, the slip increases 0.1 mm and goes linearly up to < 0.25 mm. Furthermore, no sudden strong increase could be observed which would indicate a failure of the glue line.

The temperatures in the glue line slowly increase according to the increasing process of thermal degradation starting at the outer edge of the rib ( $T > 300^{\circ}\text{C}$ ). The temperatures in the centre of the rib stay at  $20^{\circ}\text{C}$ . The glue line does not influence the fire behavior of the composite cross-section.

A failure of the glue line due to high temperatures would result in large horizontal slip and vertical deformation as well as cracks. None of it is visible or occurs. The glue line is intact and shows the same quality as the glue lines within CLT and glulam. Furthermore, the residual cross-section corresponds well with the measured temperatures as well as predicted charring depths according to Eurocode 5.

All fire tests conducted confirm that the fire design of CLT Rib Panel can be performed according to Eurocode 5 (EN 1995-1-2 and EN 1995-1-1) and the National Annexes used in the relevant country. Further, it is recommended that the fire design can be performed considering the composite action of the cross-section, with full shear transfer across the glue line. Therefore, no shear connector design is required in fire situation.

## 16 Structural analysis in fire situation

The remaining calculation steps and verifications are performed in the same way as the cold state calculations (but with the effective cross section after charring).

### 16.1 Effective bending stiffness after fire

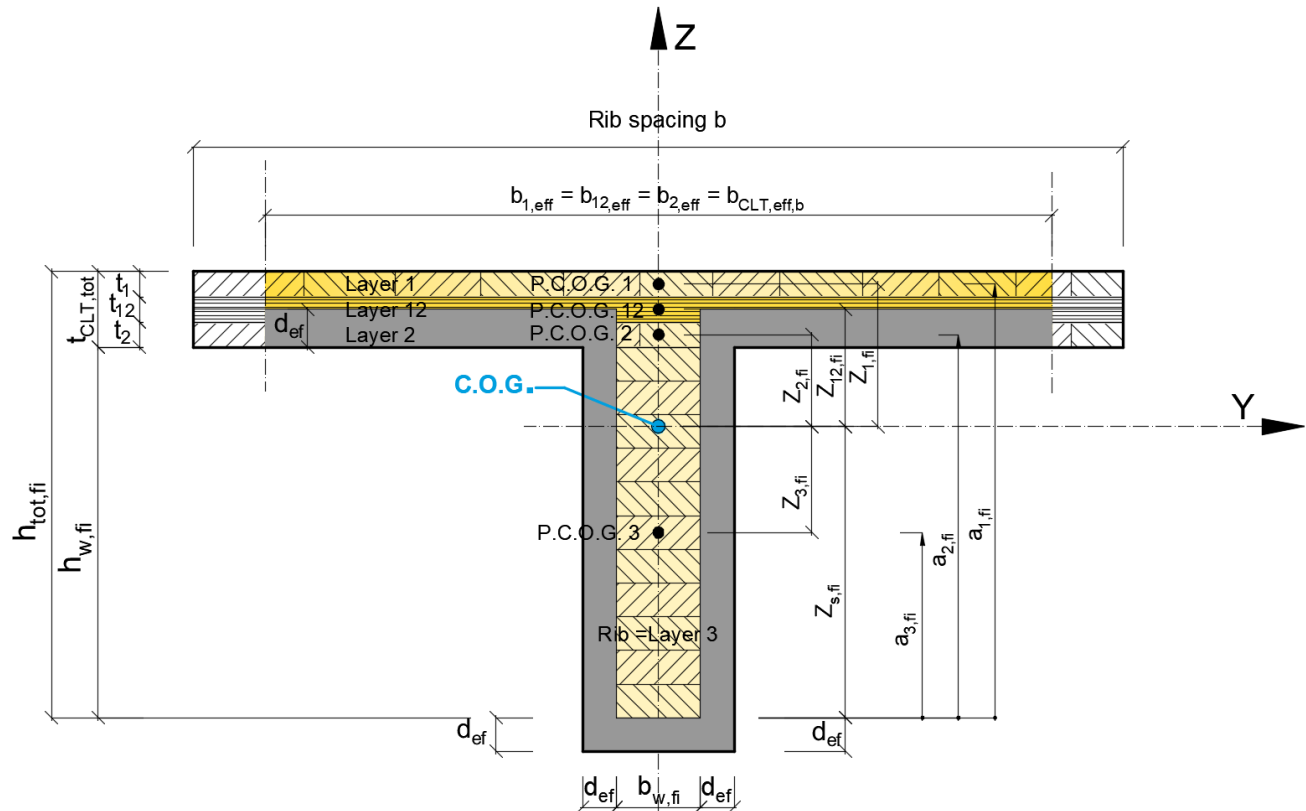


Figure 16-a: Effective cross section (T-section) of a CLT Rib Panel at midspan after charring

#### Layer notation:

Layers  $i, j, \dots$  are layers in principal direction;

note: the rib is considered as a layer in principal direction and follows the same notation pattern (in the figure above, the rib is layer 3)

Layers  $ij, jk, \dots$  are cross layers (e.g. between the principal layers  $i$  and  $j$ ,  $j$  and  $k$ , etc.) (in the figure above, the CLT cross layer 12 is a cross layer between layer 1 and 2)

For each section (T, L, C or I) the area and the bending stiffness is calculated as follows.

Areas of partial section after fire (e.g. one layer in the CLT) may be calculated as follows:

$$A_{i,fi} = b_{i,eff,fi} \cdot t_{i,fi} \quad \text{Eq. 16-1}$$

with

$b_{i,eff,fi}$  is the effective width of layer  $i$  in the CLT section, or the width of the rib after fire

$t_{i,fi}$  is the thickness of layer  $i$ , or the height of the rib after fire

The net cross sectional area of the rib panel is the sum of the partial cross sections in principal direction of the CLT + the sectional area of the rib after charring

$$A_{net,fi} = \sum_i A_{i,fi} \quad \text{Eq. 16-2}$$

Location of the new center of gravity (C.O.G.) after charring, about to the bottom of the rib panel section: (Figure 5-g)

$$z_{s,fi} = \frac{\sum_i E_i \cdot A_{i,fi} \cdot a_{i,fi}}{\sum_i E_i \cdot A_{i,fi}} \quad \text{Eq. 16-3}$$

with

- $A_{i,fi}$  Remaining sectional area of the respective layer/rib after charring [mm<sup>2</sup>]
- $a_{i,fi}$  distance from the bottom edge of the rib panel charred section to the partial center of gravity of the respective layer/rib after fire [mm]
- $E_i$  Young's modulus of the respective layer/rib. For each situation with different Young's modulus, the C.O.G. needs to be calculated individually (Mean values shall be used) [N/mm<sup>2</sup>]

## 16.2 Flexural rigidity in fire situation

All sectional properties need to be derived, using the remaining cross section after charring.

$$E \cdot I_{eff,fi} = \sum E_i \cdot I_{i,fi} + E_i \cdot A_{i,fi} \cdot z_{i,fi}^2 \quad \text{Eq. 16-4}$$

|            |  |
|------------|--|
| $E_i$      | Young's modulus (mean values) of the partial section "i" after charring [N/mm <sup>2</sup> ]                                 |
| $I_{i,fi}$ | Moment of inertia of partial section "i" after charring [mm <sup>4</sup> ]   |
| $A_{i,fi}$ | Surface of the partial section "i" after charring [mm <sup>2</sup> ]   |
| $z_{i,fi}$ | Distance between the general centre of gravity and the partial centre of gravity, of partial section "i" after charring [mm] |

## 16.3 Flexural stress parallel to grain in the section

The calculation of normal stress is analogous to section 7 in this manual.

$$\sigma_{i,fi}(x, z) = \frac{E_i \cdot z_{i,fi} \cdot M_{y,fi}(x)}{EI_{eff,fi}} \quad \text{Eq. 16-5}$$

with

|                       |  |
|-----------------------|--|
| $\sigma_{i,fi}(x, z)$ | Normal stress at location x in a rib panel beam at coordinate z in the section "i" after charring [N/mm <sup>2</sup> ]   |
| $EI_{eff,fi}$         | Effective bending stiffness about the Y-axis based on the effective width at midspan (section 5.3.1), calculated according to section 16.2 after charring [N.mm <sup>2</sup> ] |
| $M_{y,fi}(x)$         | Design moment in fire situation at the most governing location x [N.mm]  |
| $z_{i,fi}$            | Distance between the general centre of gravity and the partial centre of gravity, of partial section "i" after charring [mm]   |
| $E_i$                 | Young's modulus of the partial section "i" [N/mm <sup>2</sup> ]  |

The stress analysis shall be performed at the top and bottom extreme fibre of the CLT and the rib.  
The stress analysis shall be performed according to EN 1995-1-1 [3], item 9.1.1

- Bending stresses parallel to grain at the edges of the rib panel

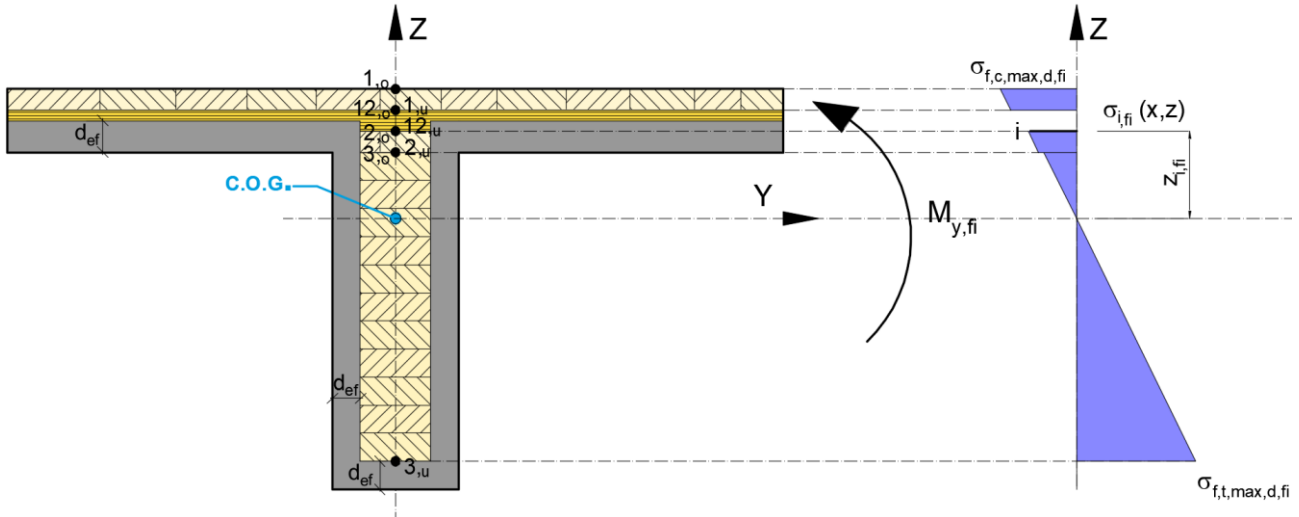


Figure 16-b: Flexural stress distribution in effective cross section after charring [12]

$$\sigma_{m,d;1,o,fi} = E_{d,CLT} \cdot \frac{M_{y,max,fi}}{(E \cdot I)_{eff,fi}} \cdot Z_{1,o,fi}$$

$$\sigma_{m,d;1,u,fi} = E_{d,CLT} \cdot \frac{M_{y,max,fi}}{(E \cdot I)_{eff,fi}} \cdot Z_{1,u,fi}$$

$$\sigma_{m,d;2,o,fi} = E_{d,CLT} \cdot \frac{M_{y,max,fi}}{(E \cdot I)_{eff,fi}} \cdot Z_{2,o,fi}$$

$$\sigma_{m,d;2,u,fi} = E_{d,CLT} \cdot \frac{M_{y,max,fi}}{(E \cdot I)_{eff,fi}} \cdot Z_{2,u,fi}$$

$$\sigma_{m,d;3,o,fi} = E_{d,CLT} \cdot \frac{M_{y,max,fi}}{(E \cdot I)_{eff,fi}} \cdot Z_{3,o,fi}$$

$$\sigma_{m,d;3,u,fi} = E_{d,CLT} \cdot \frac{M_{y,max,fi}}{(E \cdot I)_{eff,fi}} \cdot Z_{3,u,fi}$$

- Normal stresses at the partial centre of gravity of each layer

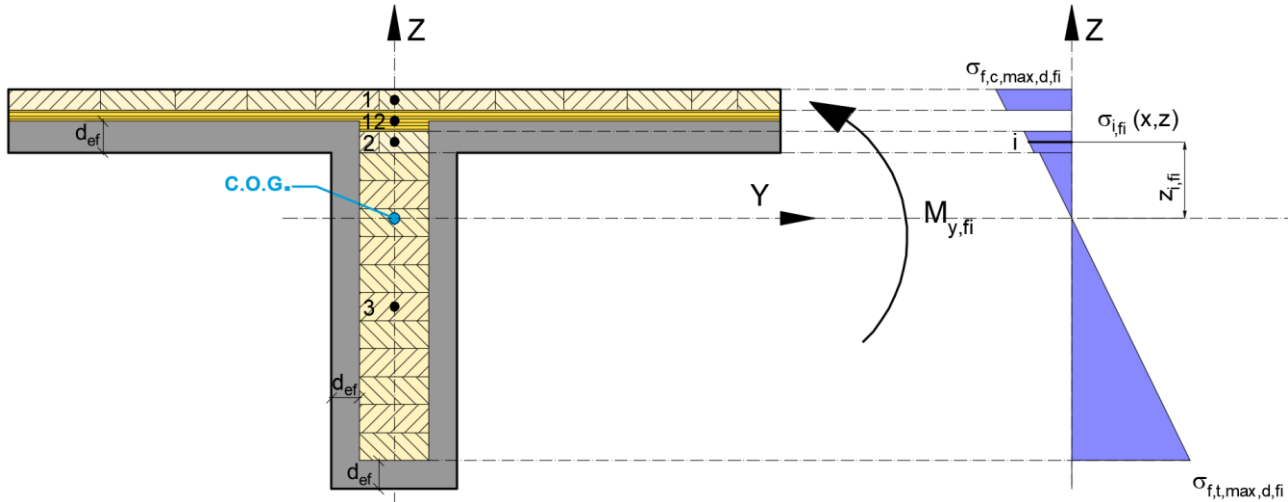


Figure 16-c: Normal stresses in the respective layers of the effective cross section after charring

$$\sigma_{1,fi} = \frac{1}{2} \cdot (\sigma_{m,d;1,u,fi} + \sigma_{m,d;1,o,fi})$$

$$\sigma_{2,fi} = \frac{1}{2} \cdot (\sigma_{m,d;2,u,fi} + \sigma_{m,d;2,o,fi})$$

$$\sigma_{3,fi} = \frac{1}{2} \cdot (\sigma_{m,d;3,u,fi} + \sigma_{m,d;3,o,fi})$$

The stress analysis shall be performed at partial centres of gravity of the longitudinal layers in CLT and GLT rib. At the same time the stress analysis shall be performed according to EN 1995-1-1 [3], item 9.1.1 (Glued thin-webbed beams) shall be fulfilled:

### 16.3.1 Flexural stresses verification in fire situation

**Bending stress verification:**

$$\sigma_{f,c,max,d,fi} \leq f_{m,d,fi} \quad \text{Eq. 16-6}$$

$$\sigma_{f,t,max,d,fi} \leq f_{m,d,fi} \quad \text{Eq. 16-7}$$

and consequently

$$\sigma_{i,fi}(x, z) \leq f_{m,i,d,fi} \quad \text{Eq. 16-8}$$

with

$\sigma_{f,c,max,d,fi}$  Extreme fiber flange design compressive stress after fire [N/mm<sup>2</sup>]

$\sigma_{f,t,max,d,fi}$  Extreme fiber flange design tensile stress after fire [N/mm<sup>2</sup>]

$f_{m,i,d,fi}$  Design bending strength in partial section “i” in fire situation [N/mm<sup>2</sup>]

## Normal stress verification:

Normal stress design requirement (combination of pure normal stress component and flexural stress component) shall be fulfilled for the CLT and GLT:

$$\sigma_{f,c,i,d,fi} \leq f_{c,0,i,d,fi} \quad \text{Eq. 16-9}$$

$\sigma_{f,c,i,d,fi}$  Compressive design stress in partial section "i" after fire [N/mm<sup>2</sup>]

$f_{c,0,i,d,fi}$  Compressive design strength parallel to grain in partial section "i" in fire situation [N/mm<sup>2</sup>]

$$\sigma_{f,t,i,d,fi} \leq f_{t,0,i,d,fi} \quad \text{Eq. 16-10}$$

$\sigma_{f,t,i,d,fi}$  Tensile design stress in partial section "i" after fire [N/mm<sup>2</sup>]

$f_{t,0,i,d,fi}$  Tensile design strength parallel to grain in partial section "i" in fire situation [N/mm<sup>2</sup>]

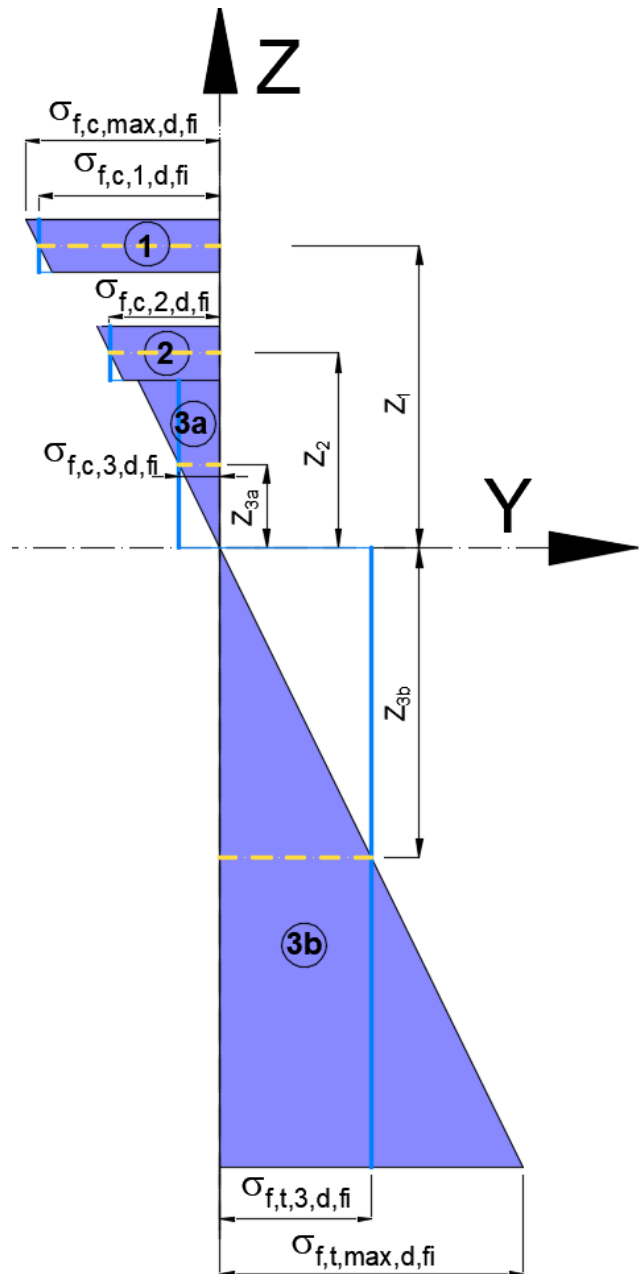


Figure 16-d: Flexural stress distribution in fire situation

## 16.4 Bending strength parallel to grain in fire situation

### **CLT:**

$$f_{CLT,m,d,fi} = \frac{k_{mod,fi} \cdot k_{sys} \cdot k_{fi} \cdot f_{CLT,m,k}}{\gamma_{M,fi}} \quad \text{Eq. 16-11}$$

with

|                  |  |
|------------------|--|
| $f_{CLT,m,d,fi}$ | Design bending strength of CLT in fire situation [N/mm <sup>2</sup> ]  |
| $K_{mod,fi}$     | is the modification factor in the fire situation for the reduced cross-section method: (same for each part)<br>$K_{mod,fi} = 1,0$ (as per EN 1995-1-2) in most cases, except when the method of annex C of EN 1995-1-2 is used |
| $k_{fi}$         | Coefficient for converting 5% to 20% fractile values;<br>$k_{fi} = 1.15$ according to EN1995-1-2, Table 2.1 [25]   |
| $k_{sys}$        | System factor, according to EN1995-1-1 [3], and ETA [2]  |
| $f_{CLT,m,k}$    | Characteristic bending strength of CLT, according to ETA [2] [N/mm <sup>2</sup> ]  |
| $\gamma_{M,fi}$  | Partial safety coefficient for fire design, according to EN1995-1-2 [25], and applicable national annex.   |

### **GLT:**

$$f_{GLT,m,d,fi} = \frac{k_{mod,fi} \cdot k_h \cdot k_{fi} \cdot f_{GLT,m,k}}{\gamma_{M,fi}} \quad \text{Eq. 16-12}$$

with

|                  |  |
|------------------|--|
| $f_{GLT,m,d,fi}$ | Design bending strength of GLT in fire situation [N/mm <sup>2</sup> ]  |
| $K_{mod,fi}$     | is the modification factor in the fire situation for the reduced cross-section method: (same for each part)<br>$K_{mod,fi} = 1,0$ (as per EN 1995-1-2) in most cases, except when the method of annex C of EN 1995-1-2 is used |
| $k_{fi}$         | Coefficient for converting 5% to 20% fractile values;<br>$k_{fi} = 1.15$ according to EN1995-1-2, Table 2.1 [25]   |
| $k_h$            | Depth factor in bending, according to EN1995-1-1 [3] item 3.3  |
| $f_{GLT,m,k}$    | Characteristic bending strength of GLT, according to EN14080 [13] [N/mm <sup>2</sup> ]   |
| $\gamma_{M,fi}$  | Partial safety coefficient for fire design, according to EN1995-1-2 [25], and applicable national annex.   |



## 16.5 Tensile strength parallel to grain in fire situation

### CLT:

$$f_{CLT,t,0,d,fi} = \frac{k_{mod,fi} \cdot k_{fi} \cdot f_{CLT,t,0,k}}{\gamma_{M,fi}} \quad \text{Eq. 16-13}$$

with

- $f_{CLT,t,0,d,fi}$  Design tensile strength parallel to grain of CLT in fire situation [N/mm<sup>2</sup>]  
 $K_{mod,fi}$  is the modification factor in the fire situation for the reduced cross-section method: (same for each part)  
 $K_{mod,fi} = 1,0$  (as per EN 1995-1-2) in most cases, except when the method of annex C of EN 1995-1-2 is used
- $k_{fi}$  Coefficient for converting 5% to 20% fractile values;  $K_{fi} = 1.15$  according to EN1995-1-2, Table 2.1 [25]
- $f_{CLT,t,0,k}$  Characteristic tensile strength parallel to grain of CLT, according to EN14080 [13] [N/mm<sup>2</sup>]  
 $\gamma_{M,fi}$  Partial safety coefficient for fire design, according to EN1995-1-2 [25], and applicable national annex.

### GLT:

$$f_{GLT,t,0,d,fi} = \frac{k_{mod,fi} \cdot k_{fi} \cdot k_h \cdot f_{GLT,t,0,k}}{\gamma_{M,fi}} \quad \text{Eq. 16-14}$$

with

- $f_{GLT,t,0,d,fi}$  Design tensile strength parallel to grain of GLT in fire situation [N/mm<sup>2</sup>]  
 $K_{mod,fi}$  is the modification factor in the fire situation for the reduced cross-section method: (same for each part)  
 $K_{mod,fi} = 1,0$  (as per EN 1995-1-2) in most cases, except when the method of annex C of EN 1995-1-2 is used
- $k_{fi}$  Coefficient for converting 5% to 20% fractile values;  $K_{fi} = 1.15$  according to EN1995-1-2, Table 2.1 [25]
- $k_h$  Depth factor according to EN 1995-1-1 [3], item 3.3 (3)
- $f_{GLT,t,0,k}$  Characteristic tensile strength parallel to grain of GLT, according to EN14080 [13] [N/mm<sup>2</sup>]  
 $\gamma_{M,fi}$  Partial safety coefficient for fire design, according to EN1995-1-2 [25], and applicable national annex.

## 16.6 Compressive strength parallel to grain in fire situation

### CLT:

$$f_{CLT,c,0,d,fi} = \frac{k_{mod,fi} \cdot k_{fi} \cdot f_{CLT,c,0,k}}{\gamma_{M,fi}} \quad \text{Eq. 16-15}$$

with

- $f_{CLT,c,0,d,fi}$  Design compressive strength parallel to grain of CLT in fire situation [N/mm<sup>2</sup>]  
 $K_{mod,fi}$  is the modification factor in the fire situation for the reduced cross-section method: (same for each part)  
 $K_{mod,fi} = 1,0$  (as per EN 1995-1-2) in most cases, except when the method of annex C of EN 1995-1-2 is used
- $k_{fi}$  Coefficient for converting 5% to 20% fractile values;  $K_{fi} = 1.15$  according to EN1995-1-2, Table 2.1 [25]
- $f_{CLTc,0,k}$  Characteristic compressive strength parallel to grain of CLT, according to ETA [2] [N/mm<sup>2</sup>]  
 $\gamma_{M,fi}$  Partial safety coefficient for fire design, according to EN1995-1-2 [25], and applicable national annex.

### GLT:

$$f_{GLT,c,0,d,fi} = \frac{k_{mod,fi} \cdot k_{fi} \cdot f_{GLTc,0,k}}{\gamma_{M,fi}} \quad \text{Eq. 16-16}$$

with

- $f_{GLT,c,0,d,fi}$  Design compressive strength parallel to grain of GLT in fire situation [N/mm<sup>2</sup>]  
 $K_{mod,fi}$  is the modification factor in the fire situation for the reduced cross-section method: (same for each part)  
 $K_{mod,fi} = 1,0$  (as per EN 1995-1-2) in most cases, except when the method of annex C of EN 1995-1-2 is used
- $k_{fi}$  Coefficient for converting 5% to 20% fractile values;  $K_{fi} = 1.15$  according to EN1995-1-2, Table 2.1 [25]
- $f_{GLTc,0,k}$  Characteristic compressive strength parallel to grain of GLT, according to EN14080 [13] [N/mm<sup>2</sup>]  
 $\gamma_{M,fi}$  Partial safety coefficient for fire design, according to EN1995-1-2 [25], and applicable national annex.

## 16.7 Shear stresses distribution in the section after fire

Section properties according to chapter 5 (mean values).

Shear stresses should be calculated in points, given in Figure 16-e and Figure 16-f.

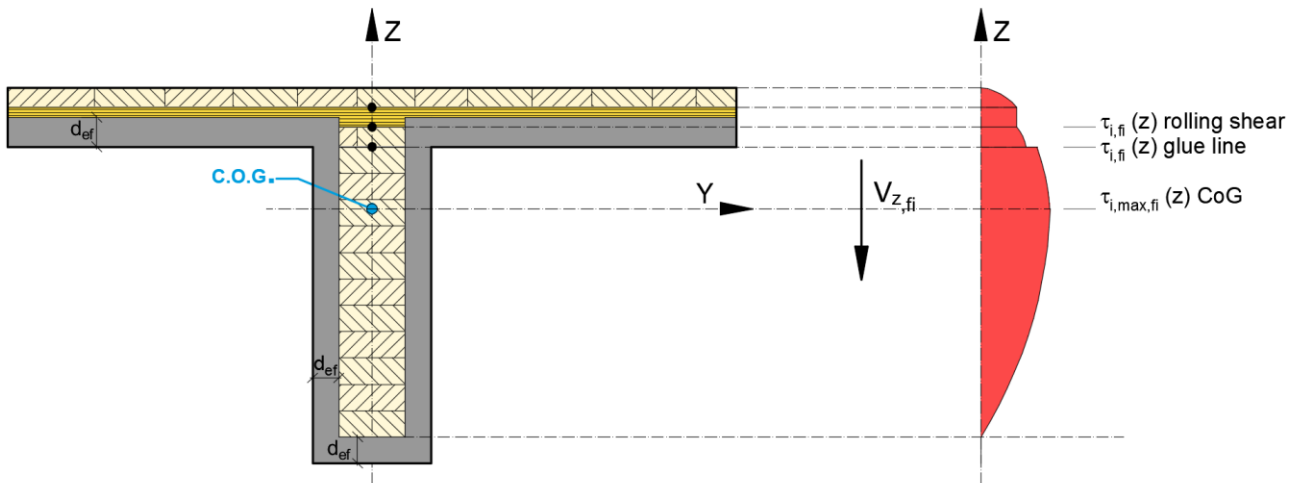


Figure 16-e: Shear stress distribution after charring

Shear stress of the section needs to be checked in different locations. The most essential points within a section are:

- C.O.G. (center of gravity)
- Glue line between rib and CLT panel
- Glue line within the CLT panel, between the cover layer that is attached to a rib and its cross layer. The applicable tributary width for this the rolling shear design at this point shall be per item 16.7.1.

Shear stress – rolling shear stress in particular – is spreading out in an angle of 45°, originating from the edge of a rib effective section. The first cross layer is reached after penetrating the bottom cover layer (always in span direction).

### 16.7.1 Point location and width for shear design after charring

After charring, the effective cross section of the CLT Rib panel doesn't allow the rolling shear transfer at 45° in the same way and needs to be adapted from the charred corner between the CLT panel and the GLT rib ( see Figure 16-f and Figure 16-g)

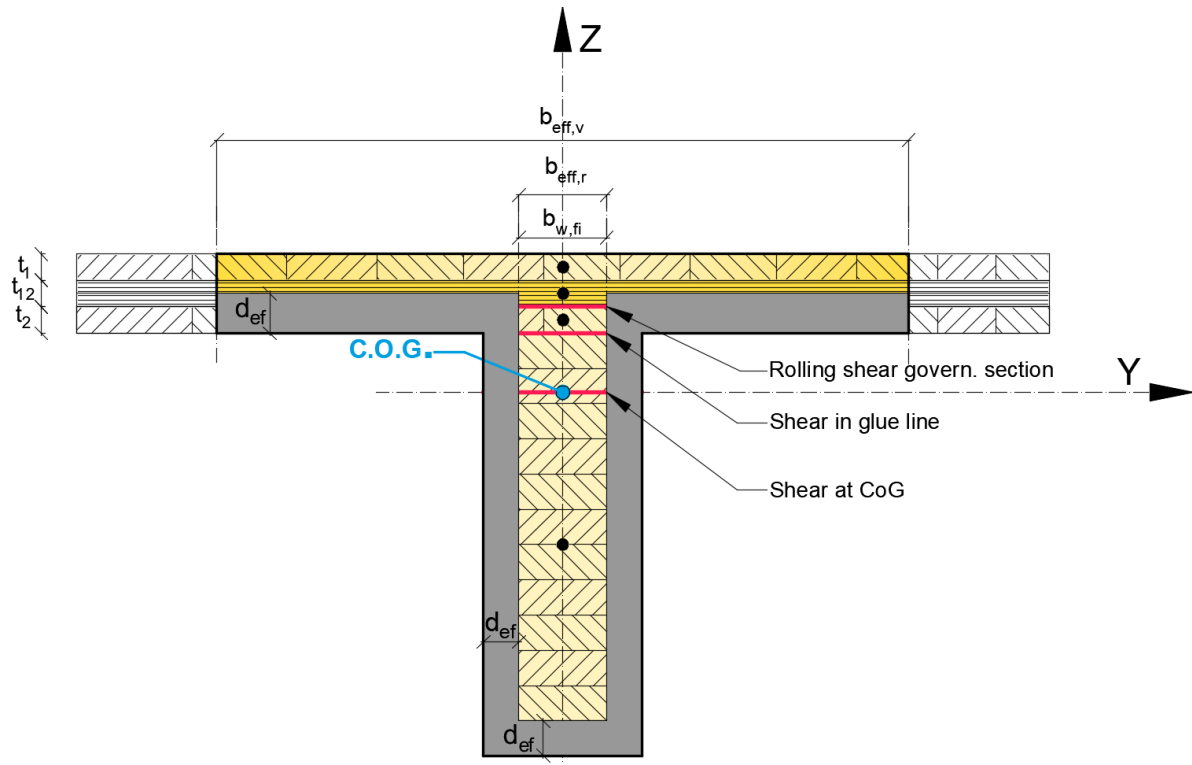


Figure 16-f: Locations for shear design at T and L section when charring reached first CLT cross layer:  $b_{eff,r} = b_{w,fi}$

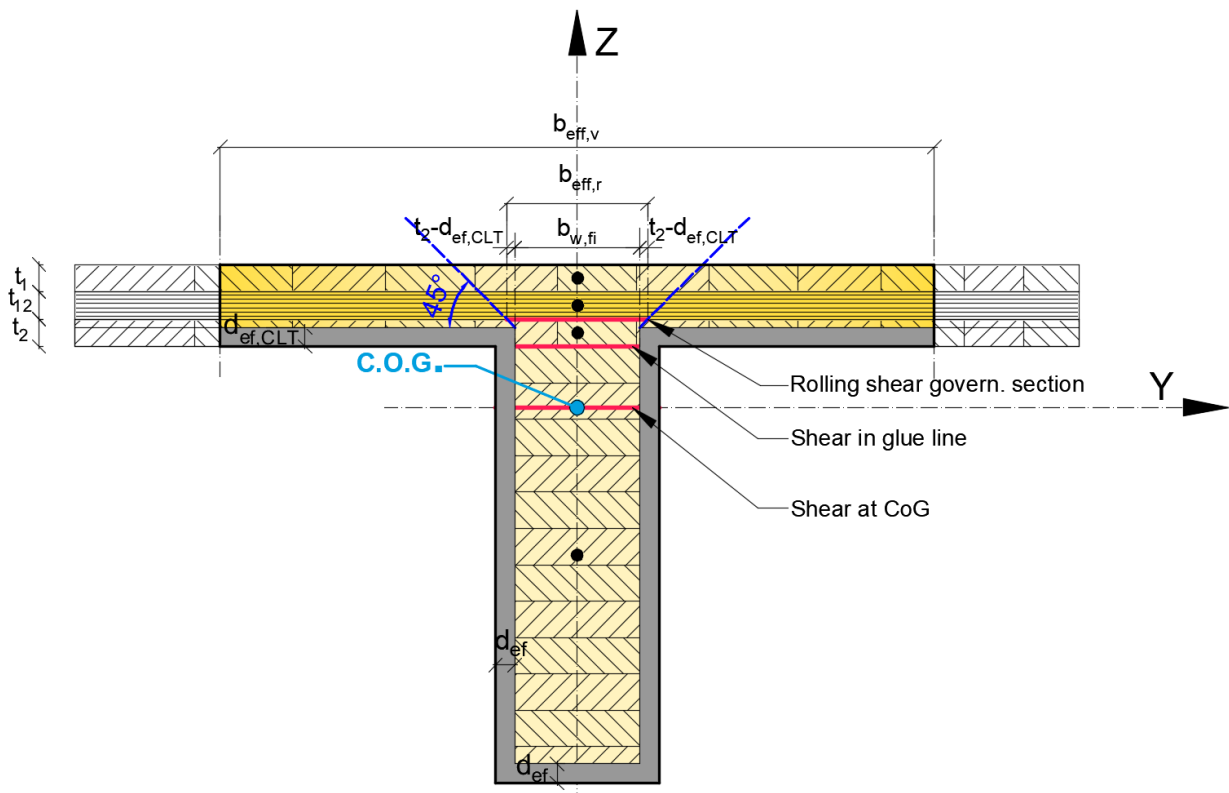


Figure 16-g: Locations for shear design at T and L section when charring did not reach first CLT cross layer (Starting from charred corner):  $b_{eff,r} = b_{w,fi} + 2(t_{2or3} - d_{ef,CLT})$

## 16.8 Calculation of shear stresses in fire situation

Shear stresses should be calculated in points, given in Figure 16-e.

$$\tau(z)_{d,fi} = E_i \cdot \frac{S_y(z) \cdot V_{z,d,fi}}{EI_{y,eff,fi} \cdot b(z)} \quad \text{Eq. 16-17}$$

with

|                  |  |
|------------------|--|
| $\tau(z)_{d,fi}$ | Design shear stress at a given coordinate “z” in fire situation [N/mm <sup>2</sup> ]   |
| $E_i$            | Young’s modulus of the respective layer/rib – see Table 5-1 [N/mm <sup>2</sup> ]   |
| $S_y(z)$         | Static moment at the coordinate “z”, about the Y-axis [mm <sup>3</sup> ]   |
| $V_{z,d,fi}$     | Design shear force in fire situation [N]   |
| $EI_{y,eff,fi}$  | Effective bending stiffness about the Y-axis <u>based on the effective width at the supports</u> (section 5.3.2) after charring [N.mm <sup>2</sup> ] |
| $b(z)$           | Width of the section at given “z” coordinate after charring  |

For shear parallel to grain design at the COG and glue line :  $b(z) = b_{w,fi}$

For rolling shear design:  $b(z) = b_{ef,r} \rightarrow$  see item 16.7.1.

$$S_y(z) = \sum_i A_{i,fi} \cdot e_{z,i,fi} \quad \text{Eq. 16-18}$$

where

|            |   |
|------------|---|
| $S_y(z)$   | Static moment at the coordinate “z”, about the Y-axis [mm <sup>3</sup> ]  |
| $A_{i,fi}$ | Area of the partial surface “i” after charring [mm <sup>2</sup> ]   |
| $e_{z,i}$  | Eccentricity of the partial surface “i” = distance between partial C.O.G. of partial surface “i” and total C.O.G. of the entire section after charring [mm] |

## 16.9 Shear stress verification in fire situation

### 16.9.1 Shear parallel to grain

The shear stresses parallel to grain should satisfy the following requirement in GLT ribs

$$\tau(z)_{d,fi} \leq f_{v,0,GLT,d,fi} \quad \text{Eq. 16-19}$$

with

$$f_{v,0,GLT,d,fi} = \frac{k_{mod,fi} \cdot k_{cr} \cdot k_{fi} \cdot f_{v,0,GLT,k}}{\gamma_{M,fi}} \quad \text{Eq. 16-20}$$

where

|                    |   |
|--------------------|---|
| $\tau_{i,d,fi}$    | Design shear stress in at a given point “i” in the section, located in the rib (GLT) in fire situation [N/mm <sup>2</sup> ]   |
| $f_{v,0,GLT,d,fi}$ | Design shear strength parallel to grain for glued laminated timber [13] in fire situation [N/mm <sup>2</sup> ]  |
| $k_{mod,fi}$       | Modification factor in the fire situation for the reduced cross-section method: (same for each part)<br>$K_{mod,fi} = 1,0$ (as per EN 1995-1-2) in most cases, except when the method of annex C of EN 1995-1-2 is used |

|                 |   |
|-----------------|---|
| $k_{fi}$        | Coefficient for converting 5% to 20% fractile values; $K_{fi} = 1.15$ according to EN1995-1-2, Table 2.1 [25] |
| $k_{cr}$        | Crack coefficient according to EN 1995-1-1 [3], item 6.1.7  |
| $f_{v,0,CLT,k}$ | Characteristic shear strength parallel to grain of the GLT, according to EN 14080 [13] [N/mm <sup>2</sup> ]   |
| $\gamma_{M,fi}$ | Partial safety coefficient for fire design, according to EN1995-1-2 [25], and applicable national annex.      |

The shear stresses parallel to grain should satisfy the following requirement in CLT panels:

$$\tau(z)_{d,fi} \leq f_{v,0,CLT,d,fi} \quad \text{Eq. 16-21}$$

with

$$f_{v,0,CLT,d,fi} = \frac{k_{mod,fi} \cdot k_{fi} \cdot f_{v,0,CLT,k}}{\gamma_{M,fi}} \quad \text{Eq. 16-22}$$

where

|                    |   |
|--------------------|---|
| $f_{v,0,CLT,d,fi}$ | Design shear strength parallel to grain for CLT in fire situation [N/mm <sup>2</sup> ]  |
| $k_{mod,fi}$       | Modification factor in the fire situation for the reduced cross-section method: (same for each part)<br>$K_{mod,fi} = 1,0$ (as per EN 1995-1-2) in most cases, except when the method of annex C of EN 1995-1-2 is used |
| $f_{v,0,CLT,k}$    | Characteristic shear strength parallel to grain of the CLT lamination material, according to ETA [2] [N/mm <sup>2</sup> ]   |
| $\gamma_{M,fi}$    | Partial safety coefficient for fire design, according to EN1995-1-2 [25], and applicable national annex.  |

## 16.9.2 Rolling shear: (shear perpendicular to grain)

The shear stress perpendicular to grain should satisfy the following requirement in CLT panel:

$$\tau(z)_{r,d,fi} \leq f_{r,CLT,d,fi} \quad \text{Eq. 16-23}$$

with

$$f_{r,CLT,d,fi} = \frac{k_{mod,fi} \cdot k_{fi} \cdot f_{r,CLT,k}}{\gamma_{M,fi}} \quad \text{Eq. 16-24}$$

where

|                  |   |
|------------------|---|
| $f_{r,CLT,d,fi}$ | Design rolling shear strength for CLT in fire situation [N/mm <sup>2</sup> ]  |
| $k_{mod,fi}$     | Modification factor in the fire situation for the reduced cross-section method: (same for each part)<br>$K_{mod,fi} = 1,0$ (as per EN 1995-1-2) in most cases, except when the method of annex C of EN 1995-1-2 is used |
| $k_{fi}$         | Coefficient for converting 5% to 20% fractile values; $K_{fi} = 1.15$ according to EN1995-1-2, Table 2.1 [25]   |
| $f_{r,CLT,k}$    | Characteristic rolling shear strength of the CLT lamination material, acc to ETA [2] [N/mm <sup>2</sup> ]   |
| $\gamma_{M,fi}$  | Partial safety coefficient for fire design, according to EN1995-1-2 [25], and applicable national annex.  |

## 16.10 Load bearing of the CLT section between ribs (spanning in cross direction)

The remaining cross section of the CLT panel, which is connected to the ribs, needs to bridge between two adjacent ribs. For simplicity, a single span system can be assumed.

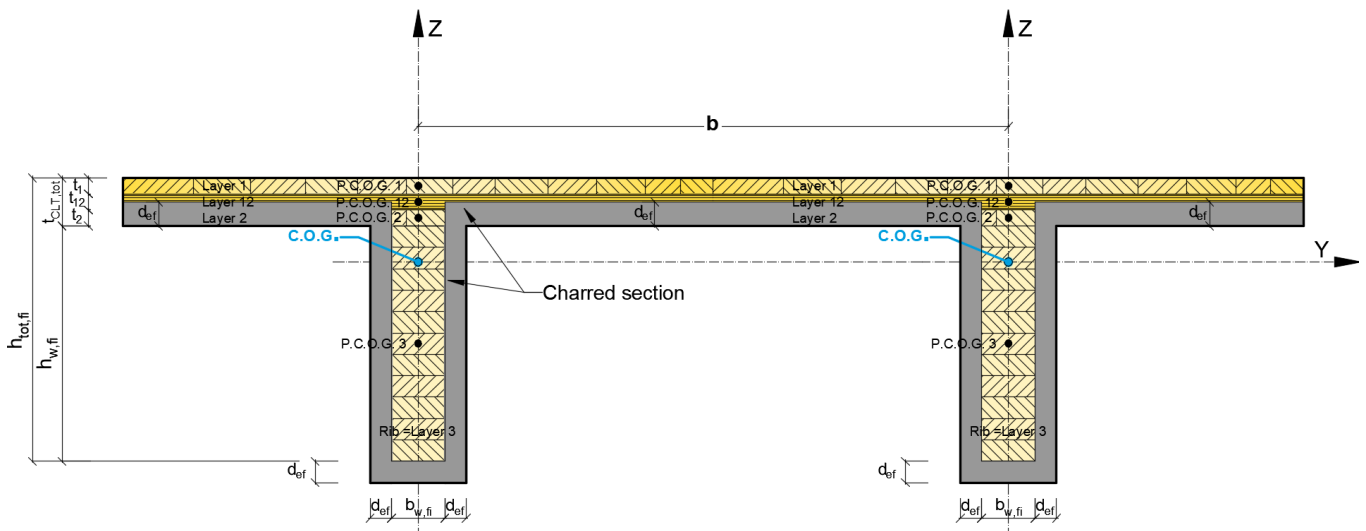


Figure 16-h: Charred cross section of a CLT Rib Panel (CLT L3s) with remaining CLT layers spanning between ribs

The stress calculation shall to be carried out in the same way as described previously but considering the CLT remaining cross layers ( $t_{12}, t_{23}$ ) only.

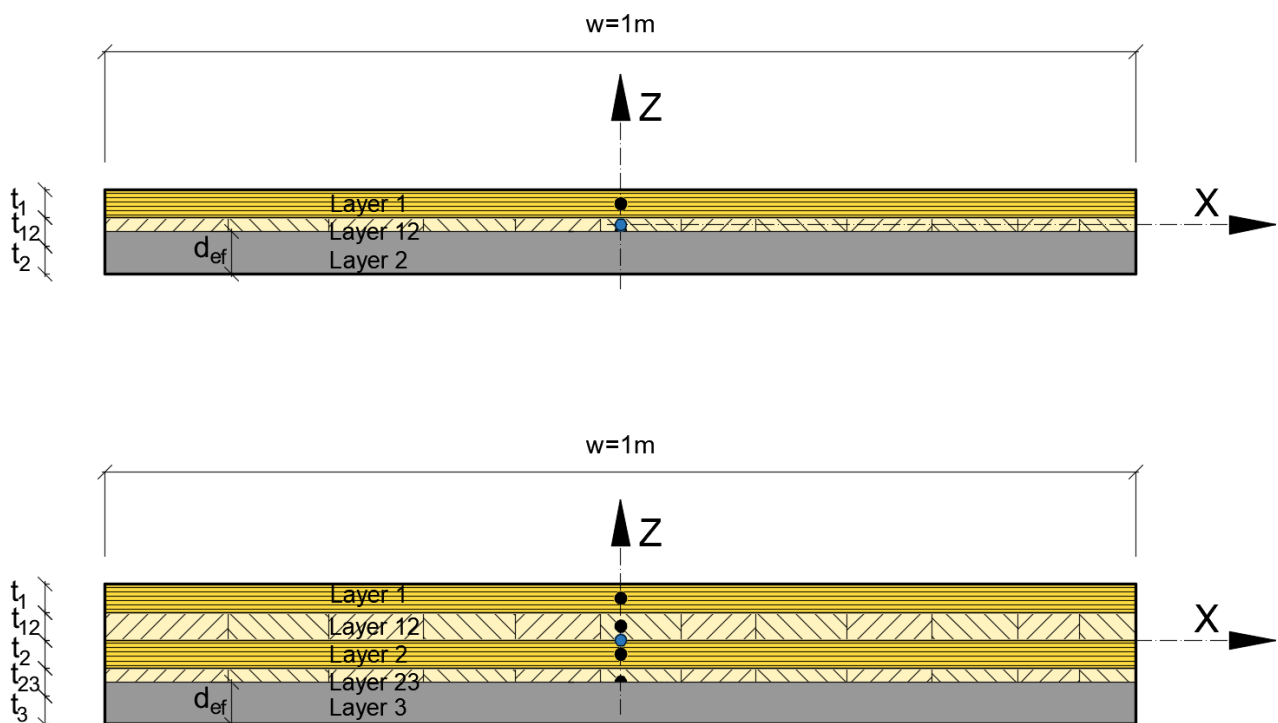


Figure 16-i: Effective cross section of CLT L3s (top) and L5s (bottom) spanning between ribs in transversal Y direction

**Bending moment in cross direction is:**

$$M_{x,d} = \frac{q_d \cdot b^2}{8}$$

$M_{x,d}$  Design bending moment about X axis due to vertical loading  $q$  for 1000mm wide [kN.m/m]

$q_d$  Uniform design load [kN/m<sup>2</sup>]

$b$  Spacing between supports (ribs) in cross direction [m]

## Verification:

$$\sigma_{m,i,d,fi} \leq f_{m,CLT,d,fi}$$

Eq. 16-25

with

$\sigma_{m,x,d,fi}$  Design bending stress about X axis in the CLT after fire [N/mm<sup>2</sup>]

$f_{CLT,m,d,fi}$  Design bending strength of the CLT in fire situation [N/mm<sup>2</sup>]

**Shear force in cross direction is**

$$V_{Ed,x} = \frac{q_d \cdot b}{2}$$

$V_{Ed,x}$  Design shear force with uniform loading [kN/m]

$q_d$  Uniform design load [kN/m<sup>2</sup>]

$b$  Spacing between supports (ribs) in cross direction [m]

## Verification:

$$\tau_{(z)x,d,fi} \leq f_{v,0,CLT,d,fi}$$

Eq 1

With

$f_{v,0,CLT,d,fi}$  Design shear strength parallel to grain for CLT in fire situation [N/mm<sup>2</sup>]

$\tau_{(z)x,d,fi}$  Design shear stress about X axis in the CLT after fire [N/mm<sup>2</sup>]



## 17 Fire classifications

The fire performance was tested on the flowing buildups.

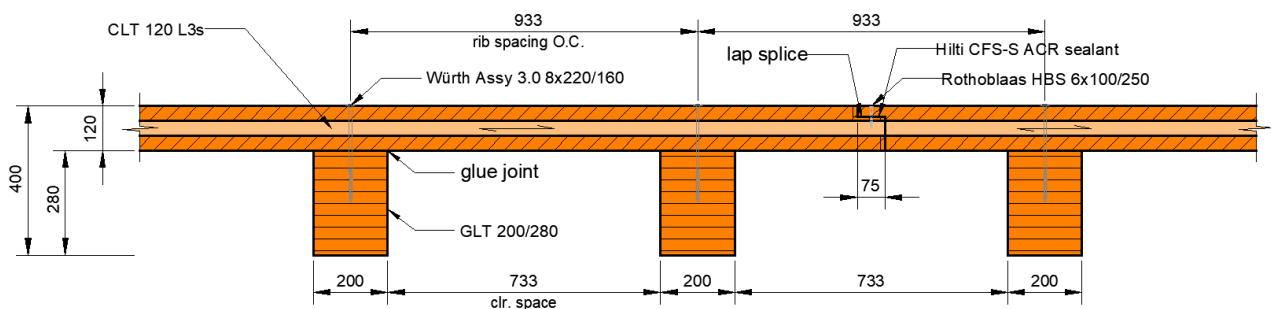
### 1. CLT Rib Panel – Open type; no ceiling structure

**Fire classification [32]: REI 90, RE 90 and R 90 at a bending moment of  $M_{d,fi} = 46.47$  kNm/m**

CLT Rib Panels were made of 120 mm thick CLT 120 L3s panels and GLT 200/280 ribs (b x h = 200 mm x 280 mm, grade GL 24h) glued and screwed together (Würth Assy 3.0 SK 8x220, c/c 160mm). There were two ribs on 2004 mm wide element and one rib on 1071 mm wide element. There were a non-loadbearing GLT 100/180 ribs, cut every 300 mm (b x h = 100 mm x 280 mm, grade GL 24h) on the both long edges of the specimen.

The size of the construction was 3000 mm x 5300 mm and the span was 5200 mm.

The two elements were connected together by screwing the CLT 120 L3s cover boards at the joint (HBS 6X100, c/c 250mm). The width of the joint was 77mm and the joint was sealed with two lines of Fire stop sealant (Hilti CFS-S ACR).



The following classes are applicable for floor construction when the maximum bending moment of 46.47 kNm/m of the floor is not exceeded.

The CLT Rib Panel – Open type; no ceiling structure is classified as **REI 90, RE 90 and R 90** in accordance with EN 13501-2.

The applicable field of application is:

- The maximum moments and shear forces, which when calculated on the same basis as the test load, shall not be greater than those tested.
- The size of panels of the ceiling lining may be increased by a maximum of 5 % but limited to a maximum of 50 mm. The length of the grid members can be increased accordingly.
- The total area occupied by fixtures and fittings relative to the area of the ceiling lining is not increased and the maximum tested opening in the lining is not exceeded.
- The height of the cavity (h) and the minimum distance (d) between the ceiling and the structural members are equal to or greater than those tested.
- No material is added to the cavity.

## 2. CLT Rib Panel – Open type; with a gypsum board ceiling structure

**Fire classification [33]: REI 90, RE 90 and R 90 at a bending moment of  $M_{d,fi} = 48.80$  kNm/m**

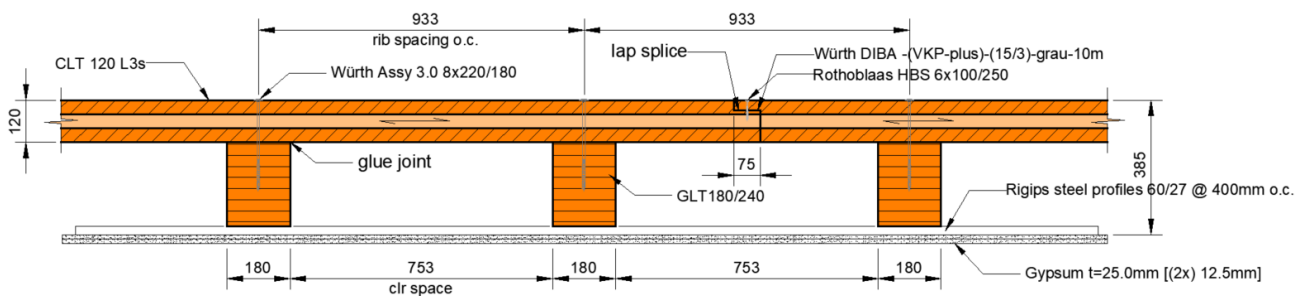
CLT Rib Panels were made of 120 mm thick CLT 120 L3s panels and GLT 180/240 ribs ( $b \times h = 180$  mm x 240 mm, grade GL 24h) glued and screwed together (Würth Assy 3.0 SK 8x220, c/c 180mm). There were two ribs on 2004 mm wide element and one rib on 1071 mm wide element. There were non-loadbearing GLT 100/240 ribs, cut every 300 mm ( $b \times h = 100$  mm x 240 mm, grade GL 24h) on the both long edges of the specimen.

The two elements were connected together by screwing the CLT 120 L3s cover boards at the joint (HBS 6X100, c/c 250mm). The width of the lap joint was 77mm and the joint was sealed with two lines of sealing strip (Würth DIBA-(VKP-PLUS)-(15/3)-Grau-10m).

The size of the construction was 3000 mm x 5300 mm and the span was 5200 mm.

Rigips steel profiles (Hut federschiene 60/27) c/c 400 mm were fixed under the ribs. Two layers of Rigips RF gypsum boards (nominal thickness 12.5 mm, measured weight 10.5 kg/m<sup>2</sup>) were fixed underneath the steel profiles with joints staggered.

The joint between the gypsum boards and frame was sealed with (Hilti CFS-S ACR) Fire Stop Sealant.



The following classes are applicable for floor construction when the maximum bending moment of 48.80 kNm/m of the floor is not exceeded.

The CLT Rib Panel – Open type; with a gypsum board ceiling structure is classified as **REI 90, RE 90 and R 90** in accordance with EN 13501-2.

The applicable field of application is:

- The maximum moments and shear forces, which when calculated on the same basis as the test load shall not be greater than those tested.
- The size of panels of the ceiling lining may be increased by a maximum of 5 % but limited to a maximum of 50 mm. The length of the grid members can be increased accordingly.
- The total area occupied by fixtures and fittings relative to the area of the ceiling lining is not increased and the maximum tested opening in the lining is not exceeded.
- The height of the cavity ( $h$ ) and the minimum distance ( $d$ ) between the ceiling and the structural members are equal to or greater than those tested.
- No material is added to the cavity.

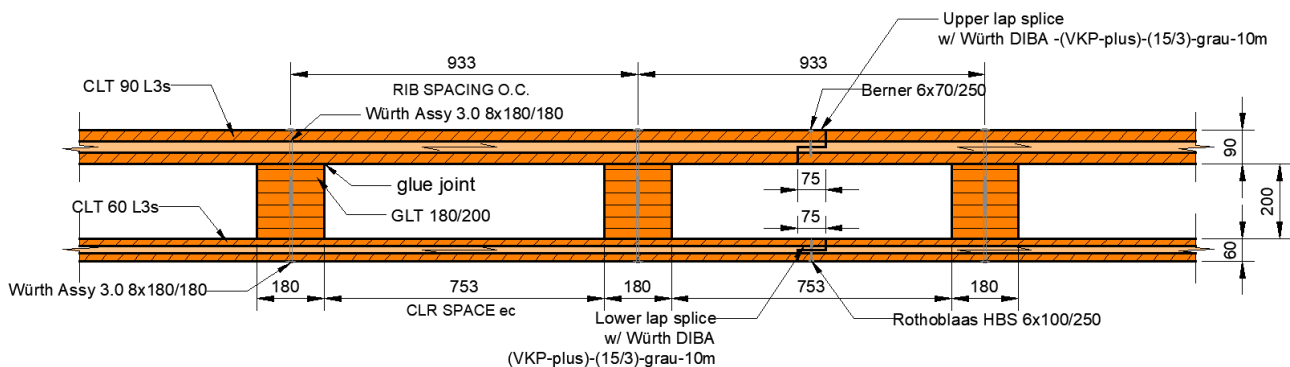
### 3. CLT Rib Panel – Closed type; no ceiling structure

**Fire classification [34]: REI 90, RE 90 and R 90 at a bending moment of  $M_{d,fi} = 48.64 \text{ kNm/m}$**

CLT Rib Panels were made of 90 mm thick CLT 90 L3s panels on the top side and 60 mm thick CLT 60 L3s panels on the bottom side of the GLT 180/200 ribs ( $b \times h = 180 \text{ mm} \times 200 \text{ mm}$ , grade GL 24h) glued and screwed together (Würth Assy 3.0 SK 8x180, c/c 180mm). There were two ribs on 2004 mm wide element and one rib on 1071 mm wide element. There were non-loadbearing GLT 100/200 ribs, cut every 300 mm ( $b \times h = 100 \text{ mm} \times 200 \text{ mm}$ , grade GL 24h) on the both long edges of the specimen.

The two elements were connected together by screwing the CLT 90 L3s cover boards at the joint (Berner 6X70, c/c 250mm) and the CLT 60 L3s cover boards at the joint (HBS 6X60, c/c 250mm). The width of the joint was 75mm and the joint was sealed with one line of sealing strip (Würth DIBA-(VKP-PLUS)-(15/3)-Grau-10m).

The size of the construction was 3000 mm x 5300 mm and the span was 5200 mm.



The following classes are applicable for floor construction when the maximum bending moment of 48.64 kNm/m of the floor is not exceeded.

The CLT Rib Panel – Closed type; no ceiling structure is classified as **REI 90, RE 90 and R 90** in accordance with EN 13501-2.

The applicable field of application is:

- The maximum moments and shear forces, which when calculated on the same basis as the test load, shall not be greater than those tested.
- The size of panels of the ceiling lining may be increased by a maximum of 5 % but limited to a maximum of 50 mm. The length of the grid members can be increased accordingly.
- The total area occupied by fixtures and fittings relative to the area of the ceiling lining is not increased and the maximum tested opening in the lining is not exceeded.
- The height of the cavity ( $h$ ) and the minimum distance ( $d$ ) between the ceiling and the structural members are equal to or greater than those tested.
- No material is added to the cavity.

## 4. CLT Rib Panel – Closed type; with a gypsum board ceiling structure

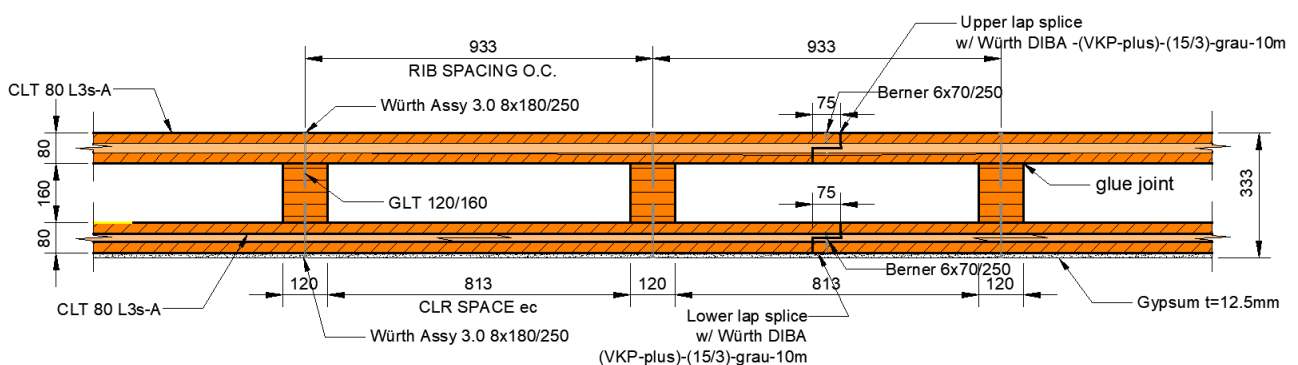
**Fire classification [35]: REI 120, RE 120 and R 120 at a bending moment of  $M_{d,fi} = 48.88 \text{ kNm/m}$**

CLT Rib Panels were made of 80 mm thick CLT 80 L3s panels on both sides of the GLT 120/160 ribs ( $b \times h = 120 \text{ mm} \times 160 \text{ mm}$ , grade GL 24h) glued and screwed together (Würth Assy 3.0 SK 8x180, c/c 250mm). There were two ribs on 2004 mm wide element and one rib on 1071 mm wide element. There were non-loadbearing GLT 100/160 ribs, cut every 300 mm ( $b \times h = 100 \text{ mm} \times 160 \text{ mm}$ , grade GL 24h) on the both long edges of the specimen.

The two elements were connected together by screwing the CLT 80 L3s-A cover boards at the joint (Berner 7X700, c/c 250mm). The width of the joint was 77mm and the lap joints were sealed with one line of sealing strip (Würth DIBA-(VKP-PLUS) -(15/3)-Grau-10m).

The size of the construction was 3000 mm x 5300 mm and the span was 5200 mm.

A layer of Rigips RF gypsum boards (nominal thickness 12.5 mm, measured weight 10.5 kg/m<sup>2</sup>) was fixed underneath the lower CLT 80 L3s-A cover board. The joint between the gypsum boards and frame was sealed with (Hilti CFS-S ACR) Fire Stop Sealant.



The following classes are applicable for floor construction when the maximum moment of 48.88 kNm/m of the floor is not exceeded.

The CLT Rib Panel – Closed type; with a gypsum board ceiling structure is classified as **REI 120, RE 120 and R 120** in accordance with EN 13501-2.

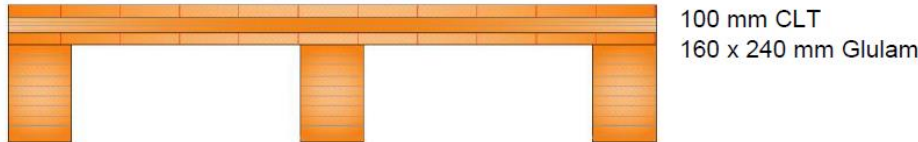
The applicable field of application is:

- The maximum moments and shear forces, which when calculated on the same basis as the test load, shall not be greater than those tested.
- The size of panels of the ceiling lining may be increased by a maximum of 5 % but limited to a maximum of 50 mm. The length of the grid members can be increased accordingly.
- The total area occupied by fixtures and fittings relative to the area of the ceiling lining is not increased and the maximum tested opening in the lining is not exceeded.
- The height of the cavity (h) and the minimum distance (d) between the ceiling and the structural members are equal to or greater than those tested.
- No material is added to the cavity.

## 18 Acoustic performance

The acoustic performance for airborne and impact sound was tested on the following buildups.

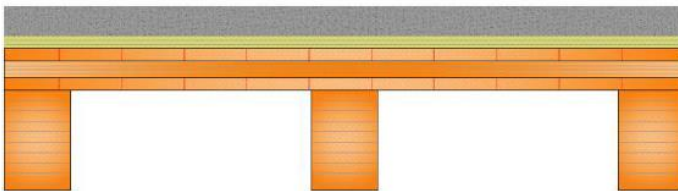
### 1. CLT Rib Panel – Open type; no floor buildup, no ceiling structure



100 mm CLT  
160 x 240 mm Glulam

|          |    |            |    |
|----------|----|------------|----|
| $R_w$    | 36 | $L_{n,w}$  | 91 |
| $C$      | -1 | $C_l$      | -6 |
| $C_{tr}$ | -4 | $C_{l,50}$ | -6 |

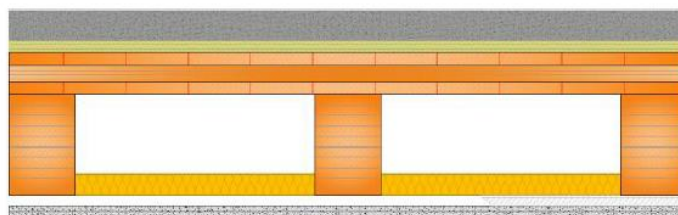
### 2. CLT Rib Panel – Open type; floating wet screed, no ceiling structure



70 mm Wet screed  
30 mm Impact sound insulation, mineral wool  
100 mm CLT  
160 x 240 mm Glulam

|          |    |            |    |
|----------|----|------------|----|
| $R_w$    | 60 | $L_{n,w}$  | 65 |
| $C$      | -2 | $C_l$      | -5 |
| $C_{tr}$ | -5 | $C_{l,50}$ | -2 |

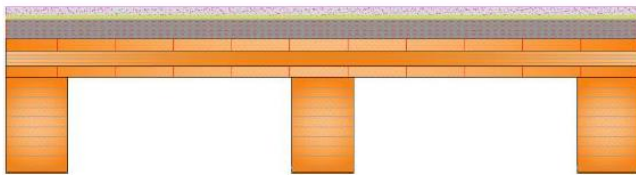
### 3. CLT Rib Panel – Open type; floating wet screed, suspended ceiling structure



70mm Wet screed  
30 mm Impact sound insulation, mineral wool  
100 mm CLT  
160 x 240 mm Glulam  
50 mm Mineral wool  
27 mm Resilient metal channel  
10 mm Gypsum plasterboard  
10 mm Gypsum plasterboard

|          |    |            |    |
|----------|----|------------|----|
| $R_w$    | 75 | $L_{n,w}$  | 47 |
| $C$      | -1 | $C_l$      | -3 |
| $C_{tr}$ | -6 | $C_{l,50}$ | 7  |

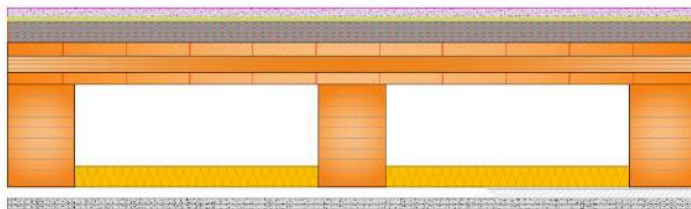
## 4. CLT Rib Panel – Open type; dry screed, no ceiling structure



20 mm Dry screed  
 10 mm Impact sound insulation, wood fibre board  
 50 mm Gravel  
 100 mm CLT  
 160 x 240 mm Glulam

|          |     |            |    |
|----------|-----|------------|----|
| $R_w$    | 58  | $L_{n,w}$  | 60 |
| $C$      | -4  | $C_i$      | 1  |
| $C_{tr}$ | -11 | $C_{i,50}$ | 1  |

## 5. CLT Rib Panel – Open type; dry screed, suspended ceiling structure



20 mm Dry screed  
 10 mm Impact sound insulation, mineral wool  
 50 mm Gravel  
 100 mm CLT  
 160 x 240 mm Glulam  
 50 mm Mineral wool  
 27 mm Resilient metal channel  
 10 mm Gypsum plasterboard  
 10 mm Gypsum plasterboard

|          |     |            |    |
|----------|-----|------------|----|
| $R_w$    | 69  | $L_{n,w}$  | 45 |
| $C$      | -6  | $C_i$      | 3  |
| $C_{tr}$ | -14 | $C_{i,50}$ | 9  |



## 19 References

- [1] ETA-Danmark A/S, "ETA-20/0893 - CLT Rib Panels by Stora Enso," 2020.
- [2] OIB- Austrian Institute of Construction Engineering, "ETA-14/0349- CLT- Cross Laminated Timber by Stora Enso," OIB- Austrian Institute of Construction Engineering, 06.04.2020.
- [3] CEN European Committee for Standardization, EN 1995-1-1 - Eurocode 5: Design of timber structures - Part 1-1: General - Common rules and rules for buildings, Brussels: CEN European Committee for Standardization, 2004.
- [4] OIB- Austrian Institute of Construction Engineering, ETA-14/0349 (02.10.2014) CLT - Cross Laminated Timber, Wien: OIB Austrian Institute of Construction Engineering, 2014.
- [5] Stora Enso Wood Products, "CLT Rib Panels - Analysis sample," Stora Enso Wood Products, Ybbs an der Donau, 2017.
- [6] CEN European Committee for Standardization, "EN 1990:2002+A1 Eurocode - Basis of structural design," 2002.
- [7] CEN European Committee for Standardization, "EN 1991: Eurocode 1: Actions on structures-Part 1-4: General actions — Wind actions," 2011-05-15.
- [8] Bogensperger, Thomas, "focus\_sts 2.2.3\_1 Darstellung und praxistaugliche Aufbereitung für die Ermittlung mitwirkender Plattenbreiten von BSP-Elementen," Holzbau Forschungs GmbH, Graz, 2013.
- [9] holz.bau forschungs GmbH, "Research report- Recommendations regarding the design of CLT rib panels," Graz, August 2020.
- [10] Augustin, Manfred, "Report on the determination of the effective width and verification of rib panels for Stora Enso Timber Wood Products," holz.bau forschungs GmbH, Graz, 2017.
- [11] Austrian Standardization Institute, "ÖNORM B 1995-1-1 Annex K- Cross laminated timber (X-Lam)," 2016.
- [12] Gerhard Schickhofer, Gregor Silly, Thomas Bogensperger, "Comparison of Methods of Approximate Verification Procedures for Cross Laminated Timber," Graz, 2012.
- [13] CEN European Committee for Standardization, "EN 14080 - Timber structures - glued laminated timber and glued solid timber - requirements," CEN European Committee for Standardization, Brussels, 2013.
- [14] Univ.-Prof. Dr. Ing. Hans Joachim. Blaß, "Expert opinion\_CLT - shear in CLT elements," H.J. Blass, Karlsruhe, 2010.
- [15] Thomas Bogensperger, Thomas Moosbrugger, Gregor Silly, "Verification of CLT-plates under loads in plane," in *WCTE 2010*, 2010.
- [16] Richard Harris, Andreas Ringhofer, Gerhard Schickhofer, "COST Action FP1004-European Conference on Cross Laminated Timber (CLT)," Graz University of Technology, Austria, April 2014.
- [17] Austrian Standardization Institute, "ÖNORM EN 1995-1-1: Edition: 2006-01-01 (Identical with EN 1995-1-1:2004), Eurocode 5: Design of Timber Structures, Part 1-1: General – Common Rules and rules for buildings".
- [18] Austrian Standardization Institute, "ÖNORM B 1995-1-1:2015 "Eurocode 5: Design of Timber Structures, Part 1-1: General – Common Rules and rules for buildings. National specifications for the implementation of ÖNORM EN 1995-1-1, national comments and national supplements", Vienna.
- [19] "ÖNORM EN 1995-1-1: Edition: 2006-01-01 (Identical with EN 1995-1-1:2004), Eurocode 5: Design of Timber Structures, Part 1-1: General – Common Rules and rules for buildings".
- [20] R BRANDNER, G SCHICKHOFER, "Properties of Cross Laminated Timber (CLT) in Compression Perpendicular to Grain," Graz University of Technology, Institute of Timber Engineering and Wood Technology 1), Competence Centre holz.bau forschungs gmbh 2), 2014.
- [21] Richter, Patricia Hamm & Antje, "BEMESSUNGS- UND KONSTRUKTIONSREGELN ZUM SCHWINGUNGSNACHWEIS VON HOLZDECKEN," Biberach, 2009.

- [22] CEN European Committee for Standardization, EN 1995-1-1 - Eurocode 5: Design of timber structures - Part 1-1: General - Common rules and rules for buildings, Brussels: CEN European Committee for Standardization, 2004.
- [23] I.K. Abeysekera, Patricia. Hamm, T. Toratti, A. Lawrence, "Development of a Floor Design Method for Eurocode 5 - Paper 51-20-2, Proceedings INTER Meeting 2018," Tallinn/Estonia, 2018.
- [24] CEN European Committee for Standardization, "EN 13501-1:2018 Fire classification of construction products and building elements."
- [25] CEN European Committee for Standardization, EN 1995-1-2 - Eurocode 5: Design of timber structures - Part 1-2: General - Structural fire design, Brussels: CEN European Committee for Standardization, 2004.
- [26] Tuuli Oksanen, "Statement NO VTT-S-05640-17," VTT Expert Services Ltd, Espoo, Finland, 2017.
- [27] C. E. C. f. Standardization, EN 1995-1-2 - Eurocode 5: Design of timber structures - Part 1-2: General - Structural fire design, Brussels: CEN European Committee for Standardization, 2004.
- [28] T. O. VTT Expert Services Ltd, "Statement NO VTT-S-05640-17," VTT Expert Services Ltd, Espoo, Finland, 2017.
- [29] Austrian Standardization Institute, "ÖNORM EN1995-1-2 - Eurocode 5: Design of timber structures – Part 1–2: General – Structural fire design, 2011-09-01 edition," 2011.
- [30] Standardization, CEN European Committee for Standardization, EN 1995-1-2 - Eurocode 5: Design of timber structures - Part 1-2: General - Structural fire design, Brussels: CEN European Committee for Standardization, 2004.
- [31] Institute of Structural Engineering (IBK), ETH Zurich, "Fire design of CLT Rib Panels for the revision of the European Technical Assessment (ETA-17/0911)," ETH Zürich, Zürich, 13th October 2020.
- [32] Eurofins Expert Services Oy, "EUF129-20000133-T1- CLASSIFICATION OF FIRE RESISTANCE IN ACCORDANCE WITH EN 13501-2:2016," April 29, 2020.
- [33] Eurofins Expert Services Oy, "EUF129-20000133-T2- CLASSIFICATION OF FIRE RESISTANCE IN ACCORDANCE WITH EN 13501-2:2016," April 29, 2020.
- [34] Eurofins Expert Services Oy, "EUF129-20000133-T4 - CLASSIFICATION OF FIRE RESISTANCE IN ACCORDANCE WITH EN 13501-2:2016," April 29, 2020.
- [35] Eurofins Expert Services Oy, "EUF129-20000133-T3 - CLASSIFICATION OF FIRE RESISTANCE IN ACCORDANCE WITH EN 13501-2:2016," April 29, 2020.
- [36] Eurofins Expert Services Oy, "Classification Report no EUFI29-19000344-T8- CLASSIFICATION OF REACTION TO FIRE IN ACCORDANCE WITH EN 13501-1:2018," 17 June 2019.